An essential histidine in bacterial cytochrome c peroxidases.

Dermot F. McGinnity

Thesis presented for the degree of Doctor of Philosophy.

Faculty of Veterinary Medicine.

University of Edinburgh.

December 1995.

Declaration

The work presented in this thesis is my own unless otherwise indicated. Part of this work is published in Gilmour, R., Prazeres, S., McGinnity, D.F., Goodhew, C.F., Moura, J.J.G., Moura, I. and Pettigrew, G.W. (1995) The binding of Ca^{++} to cytochrome c peroxidase from *Paracoccus denitrificans* - affinity and specificity of sites. *Eur.J.Biochem.* (In Press) and McGinnity, D.F., Devreese, B., Prazeres, S., Van Beeumen, J., Moura, I., Moura, J.J.G. and Pettigrew, G.W. A single histidine is required for activity of cytochrome c peroxidase from *Paracoccus denitrificans*. (Submitted *J.Biol.Chem* November 1995).

Dermot F. McGinnity

December 1995

Acknowledgements

It has all been said before so many, many thanks to Dr. Graham W. Pettigrew, Dr. Celia F. Goodhew, Dr. Ray Gilmour, Dr. Cathy Scahill, Prof. Jose J.G. Moura, Prof. Isabel Moura, Susana Prazeres, Prof. Jos van Beeumen, Dr. Bart Devresse, Dr. David Apps, Dr. Simon van Heyningen, Prof. Andrew Thomson and the staff and students of the Faculty of Veterinary Medicine, University of Edinburgh.

This work was supported by the Faculty of Veterinary Medicine Ewan McPherson Postgraduate Scholarship.

Special thanks to my mother and father for their love, generosity and good looks.

Abstract

The cytochrome c peroxidase from the bacterium *Paracoccus denitrificans* is a relative of the extensively characterised enzyme from *Pseudomonas aeruginosa*. This study investigates the role of an essential histidine residue in the enzyme mechanism of bacterial peroxidases.

Cytochrome c peroxidase from *Paracoccus denitrificans* was modified with the histidine-specific reagent diethylpyrocarbonate. The reaction can be followed spectroscopically and, at low excess of reagent, one mol of histidine was modified in the oxidised enzyme. The agreement between the spectrophotometric measurement of histidine modification and radioactive incorporation using a radiolabelled reagent indicated little modification of other amino acids. Modification of this easily modifiable histidine was associated with loss of the enzyme's ability to form the active state. With time, the modification reversed and the ability to form the active mixed valence state was recovered. However the reversal of histidine modification observed spectrophotometrically was not matched by loss of radioactivity and a slow transfer of the ethoxyformyl group to another amino acid is proposed. The presence of CN^- bound to the active peroxidatic site of the enzyme completely protected the essential histidine from modification.

In its active form cytochrome c peroxidase is a dimer, with Ca^{2+} situated at the interface between the two monomers. Under conditions where the dimer is the dominant species modification of only 0.5 mol histidine abolishes enzyme activity.

Limited subtilisin treatment of the native enzyme resulted in cleavage at a single peptide bond. Although the two fragments remain tightly associated, the cleaved enzyme is inactive. Modification with radiolabelled diethylpyrocarbonate and subsequent subtilisin treatment, followed by tryptic digestion of a 9k fragment, showed that radioactivity was located in a peptide containing a single histidine 275.

With the benefit of four homologous sequences and the use of secondary structure prediction analysis we can determine that histidine 275 is indeed conserved in

the four sequences and is preceded by a remarkably unvaried α–helical region suggestive of functional importance. It is proposed that this conserved residue acts as both a catalytic active site residue and a conduit for intermolecular electron transfer in the active mixed-valence high spin-state.

Contents

Abbreviations

CCP Cytochrome c peroxidase

DAD diaminodurol

DEPC diethylpyrocarbonate

dpm disintegrations per minute

e.p.r. electron paramagnetic resonance

EGTA ethylene glycol-bis-(β-aminoethyl ether)N,N,N'N'-tetraacetic acid

E_h redox potential

E_m midpoint redox potential

Hepes N-2-hydroxyethylpiperazine-N' 2-ethanesulphonic acid

HPLC high performance liquid chromatography

Mes 2(-N-Morpholino)ethanesulphonic acid

M_r relative molecular mass

n.m.r. nuclear magnetic resonance

P.denitrificans *Paracoccus denitrificans*

P.aeruginosa *Pseudomonas aeruginosa*

PMSF Phenylmethanesulfonyl fluoride

SDS-PAGE sodium dodecyl sulphate - polyacrylamide gel electrophoresis

Chapter I

Introduction

1.1 The toxicity and removal of hydrogen peroxide

The presence of oxygen within the cell gives rise to the production of toxic compounds such as superoxide (Figure 1.1(a)). Organisms eliminate superoxide using the ubiquitous enzyme superoxide dismutase, which produces hydrogen peroxide (Figure 1.1(b)). In more general terms hydrogen peroxide is produced as a result of the incomplete reduction of oxygen by flavoproteins or terminal oxidases (Figure 1.1(c)). The subsequent formation of the highly reactive hydroxyl radical can result in cell damage or even cell death (Figure 1.1(d)) (Halliwell and Gutteridge, 1989) and so hydrogen peroxide is removed either by catalase in a dismutation reaction (Figure 1.1(e)), or by peroxidase in a process of reduction to water (Figure 1.1(f)). Some peroxidases, such as horse radish peroxidase, are very non-specific with respect to their electron donor, while others obtain electrons from the respiratory chain via cytochrome c.

1.2 Cytochrome c Peroxidases

Cytochrome c peroxidases (CCP) are enzymes which catalyse the reduction of hydrogen peroxide using electrons donated by cytochrome c. Such a process not only results in detoxification of the hydrogen peroxide but also may allow energy conservation by the electron transport chain (Pettigrew and Moore, 1987). Cytochrome c peroxidases have been isolated and studied extensively in *Saccharomyces cerevisiae* and the *Pseudomonads aeruginosa* and *stutzeri.* In fact the bacterial enzyme was thought to be a peculiarity of the *Pseudomonads* but is now known to be more widespread than originally realised.

Paracoccus is arguably one of the most intensively studied bacteria for electron transport studies, yet the cytochrome c peroxidase remained undetected until 1990. The reason was that the enzyme is only expressed under certain specific growth conditions such as low oxygen tension (Goodhew et al.1990). This indicates that

Figure 1.1 Toxicity and removal of hydrogen peroxide
(a) Superoxide formation; (b) hydrogen peroxide formation by Superoxide dismutase (SOD); (c) hydrogen peroxide formation by incomplete reduction of oxygen; (d) hydroxyl radical formation; (e) hydrogen peroxide removal by catalase (CAT); (f) hydrogen peroxide removal by peroxidase.

(a) Cellular reduced coenzymes → Flavoproteins → ($O_2^{\cdot-}$ ⇄ O_2) *redox cyclers*

(b) $$2O_2^{\cdot-} + 2H^+ \xrightarrow[SOD]{} O_2 + H_2O_2$$

(c) $$O_2 + 2e^- + 2H^+ \longrightarrow H_2O_2$$

(d) $$H_2O_2 + e^- + H^+ \longrightarrow OH\cdot + H_2O$$

(e) $$2H_2O_2 \xrightarrow[CAT]{} 2H_2O + O_2$$

(f) $$2H_2O_2 + 2e^- + 2H^+ \xrightarrow[PEROXIDASE]{} 2H_2O$$

either more hydrogen peroxide is present under such conditions, or more likely, that some cellular constituents which only appear at low oxygen tension, such as haem d, are highly susceptible to peroxide-induced damage. Also, at low oxygen tension the electron transport system will be more reduced and there is therefore the greater possibility of single electron transfers from the flavoproteins to oxygen.

Since 1990 the enzyme has also been found in a photosynthetic bacterium *Rhodobacter* and a chemoautotroph *Nitrosomonas*. A search of sequence data banks using the BLAST algorithm (Altschul et al.1990) also revealed open reading frames homologous to the cytochrome c peroxidase in *E.coli* and two *Methylotrophs*.

Bacterial cytochrome c peroxidases are di-haem enzymes which oxidise mono-haem Class I cytochromes c and reduce hydrogen peroxide to water. The most extensively characterised example is from *Pseudomonas aeruginosa* and I will discuss the work on this enzyme before introducing the CCP used in this study from the bacterium *Paracoccus denitrificans*.

1.2.1 *Pseudomonas aeruginosa* cytochrome c peroxidase[1]

Pseudomonas aeruginosa is a gram-negative bacterium, surrounded not only by the cell membrane but also by a peptidoglycan cell wall and an outer membrane. Proteins which are secreted into the space between the cell membrane and the outer membrane are termed periplasmic. Wood (1983) proposed that all c-type cytochromes are either periplasmic or bound to the periplasmic side of the cell membrane.

P.aeruginosa cytochrome c peroxidase was first purified by Ellfolk and Soininen (1970), although Lenhoff and Kaplan (1956) first proved the enzyme's existence and using a partially purified preparation studied the characteristics of the peroxidatic reaction. Figure 1.2 shows the primary sequence of *P.aeruginosa* CCP, which has recently been revised on the basis of the gene sequence determined by Fulop et al.(1995) and contains several corrections to the original protein sequence as determined by Ronnberg et al.(1989). The sequence translates to a protein containing

[1] During preparation of this thesis the crystal structure of the cytochrome c peroxidase from *Pseudomonas aeruginosa* was published (Fulop et al. 1995). As this enzyme is homologous to the one studied from *Paracoccus denitrificans*, footnotes throughout the text refer the reader to any relevant conclusions with respect to the structure.

Figure 1.2 Amino acid sequence of *P.aeruginosa* cytochrome c peroxidase

The amino sequence is shown for the cytochrome c peroxidase from *Pseudomonas aeruginosa* which has recently been revised on the basis of the gene sequence determined by Ridout et al.(1995) and contains several corrections to the original protein sequence determined by Ronnberg et al.(1989).

```
         10         20         30         40         50
DALHDQASALFKPIPEQVTELRGQPISEQQRELGKKLFFDPRLSRSHVLS

         60         70         80         90         100
CNTCHNVGTGGADNVPTSVGHGWQKGPRNSPTVFNAVFNAAQFWDGRAKD
```

N-terminal
haem binding site

```
         110        120        130        140        150
LGEQAKGPIQNSVEMHSTPQLVEQTLGSIPEYVDAFRKAFPKAGKPVSFD

          160        170        180        190        200
NMALAIEAYEATLVTPDSPFDLYLKGDDKALDAQQKKGLKAFMDSGCSACH
```

C-terminal
haem binding site

```
        210        220        230        240        250
NGINLGGQAYFPFGLVKKPDASVLPSGDKGRFAVTKTQSDEYVFRAAPLRN

       260        270        280        290        300
VALTAPYFHSGQVWELKDAVAIMGNAQLGKQLAPDDVENIVAFLHSLSGKQP

     310        320
RVEYPLLPASTETTPRPAE
```

323 amino acids, with two haem c attachment motifs (Cys-X-Y-Cys-His, where His provides the haem iron proximal ligand), resulting in a polypeptide M_r of 36.5k.

For many years the *P.aeruginosa* enzyme was regarded as very different in nature from the well studied high-spin, protohaem IX-containing yeast cytochrome c peroxidase (YCCP) (Ellfolk et al.1973). In YCCP, a stoichiometric amount of hydrogen peroxide binds to the haem and removes two reducing equivalents to leave a ferryl (Fe IV) oxene intermediate and a tryptophan side chain radical. This intermediate is called compound I and is remarkably stable in the absence of the second substrate ferrocytochrome c or other reducing substances. Restoration of the resting ferric state requires two successive one electron transfers from cytochrome c. Figure 1.3 demonstrates that the peroxidatic centres of the two enzymes may be essentially similar, the difference being the source of the second oxidising equivalent which derives from a second haem group in the bacterial enzyme and an amino acid side chain in the yeast enzyme.

Figure 1.4 shows a model for the action of cytochrome c peroxidase from *P.aeruginosa* . The enzyme contains a high potential haem (E_m +320mV) and a low potential haem (E_m -330mV) (Ellfolk et al.1973). The high potential haem acts as a electron transferring pole and can be reduced by azurin or cytochrome c-551 or non-physiologically by ascorbate (Ronnberg et al.1981b). In the oxidised state the enzyme is inactive (Ellfolk et al.1983; Ronnberg et al.1981b), the low potential haem is low-spin and inaccessible to ligands and the high potential haem is in a spin-state equilibrium (Foote et al.1984; Foote et al.1985). This partial high spin-state was proposed to reflect the lability of a methionine ligand to the high potential haem, a lability also demonstrated by photolysis (Greenwood et al.1984). Reduction of the high potential haem creates the mixed-valence state of the enzyme and this results in the low potential haem becoming high-spin and enables binding of hydrogen peroxide. One electron is then removed from the peroxidatic iron leaving a ferryl oxene derivative and one is removed from the high potential haem to form compound I (Ronnberg et al.1981a). The addition of one electron to compound I yields compound II in which both haems are probably in the ferric state (Ellfolk et al.1983), but which is kinetically and spectroscopically distinct from the starting oxidised form.

Figure 1.3 Reaction mechanisms of cytochrome c peroxidases
The reaction mechanisms of (a) *Saccharomyces cerevisiae* CCP and (b) *Pseudomonas aeruginosa* CCP are shown. The models are based on the results of numerous workers as reviewed in Pettigrew and Moore (1987). The yeast enzyme contains a single b-type haem. The side chain radical observed in the reaction intermediate is proposed to be Tryptophan 191 (reviewed in (Bosshard et al.1991)). The bacterial enzyme contains two c-type haems, one high potential and the other low potential.

(a) *Saccharomyces cerevisiae* cytochrome c peroxidase

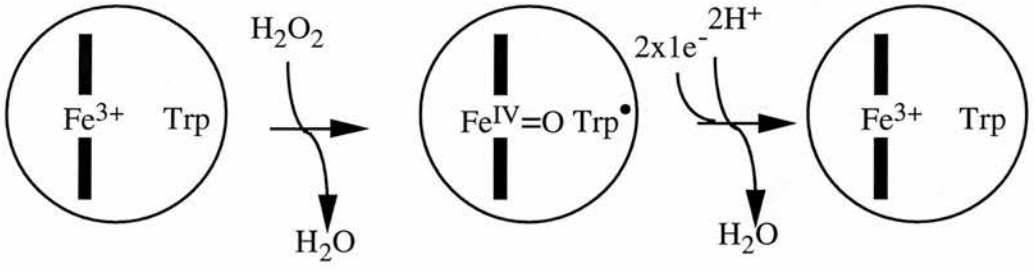

(b) *Pseudomonas aeruginosa* cytochrome c peroxidase

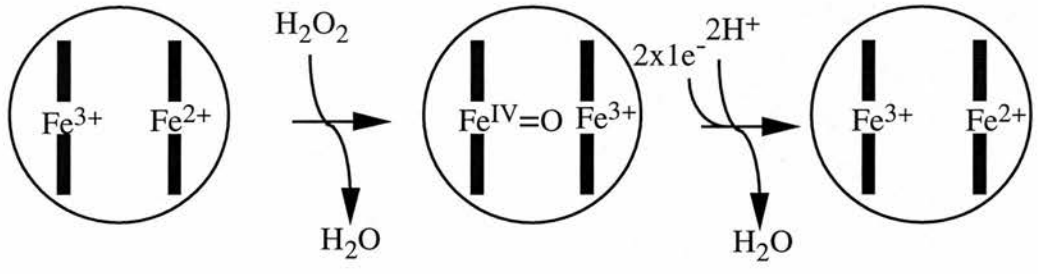

Figure 1.4 A model for the action of cytochrome c peroxidase from *P.aeruginosa*.

This diagram is a modified version of Figure 3.14 from Pettigrew and Moore (1987). The enzyme is represented as a two-domain structure with an electron transferring haem and a peroxidatic haem. M and H are the proposed methionine and histidine ligands of the two haems.[1] The redox state of the haem iron is indicated by II, ferrous; III, ferric; IV, ferryl.

1 During preparation of this text the crystal structure of the *P.aeruginosa* CCP was published (Fulop et al. 1995). The structure supports the above model with regards to the respective ligand assignments to both haems. See Discussion Chapter for detailed analysis of the X-ray structure.

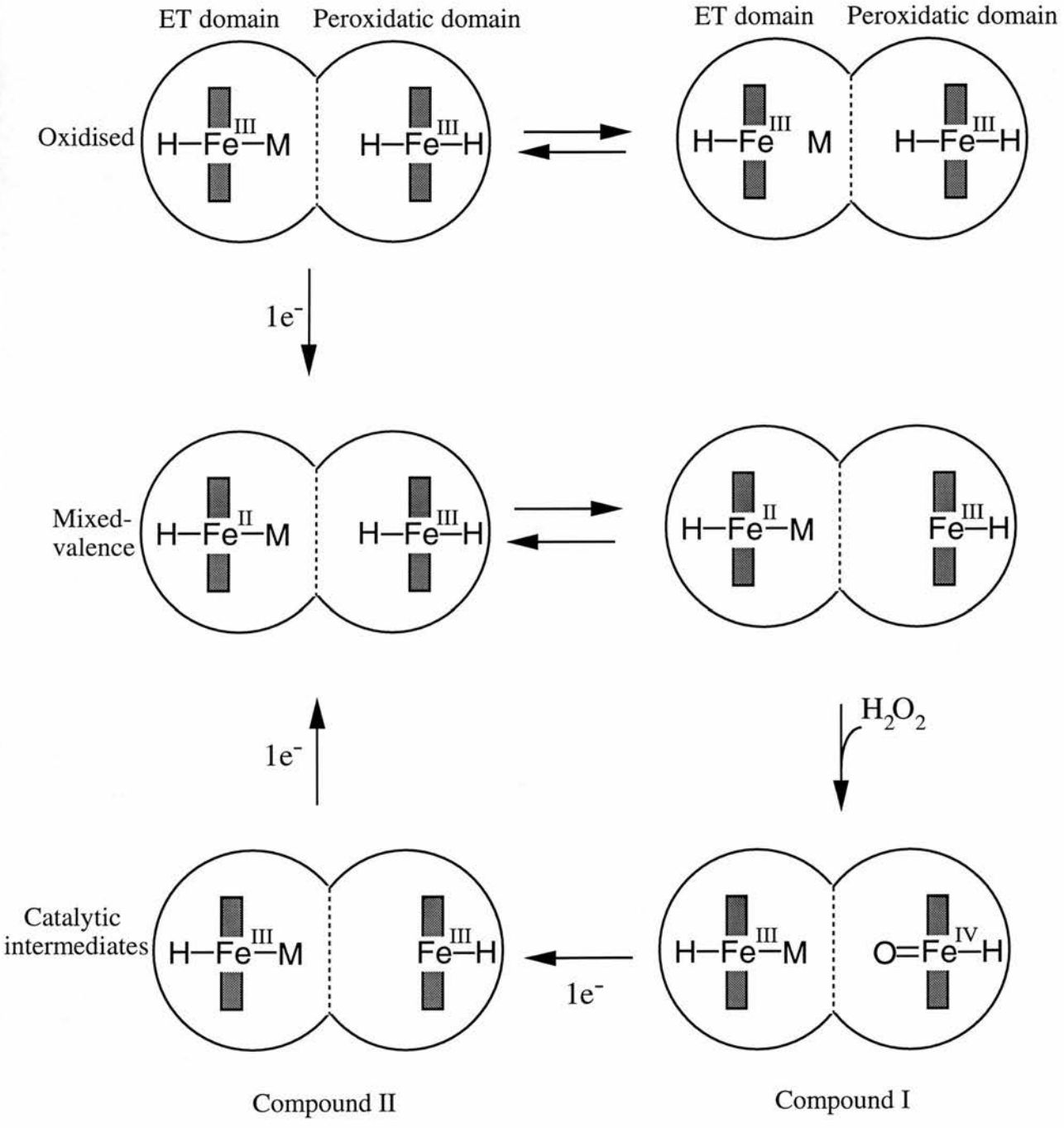
ET domain
Peroxidatic domain
ET domain
Peroxidatic domain
Oxidised
H–Fe^III–M
H–Fe^III–H
H–Fe^III
M
H–Fe^III–H
1e⁻
Mixed-valence
H–Fe^II–M
H–Fe^III–H
H–Fe^II–M
Fe^III–H
H2O2
1e⁻
Catalytic intermediates
H–Fe^III–M
Fe^III–H
1e⁻
H–Fe^III–M
O=Fe^IV–H
Compound II
Compound I

1.2.1.1 Class I cytochrome c features of *P.aeruginosa* CCP

The amino acid sequence of *P.aeruginosa* CCP suggested that the molecule was constructed in two domains, each having the general appearance of a mono-haem Class I cytochrome c (Ellfolk et al.1991). The class I cytochrome c fold, for which tuna cytochrome c is chosen as the paradigm in Figure 1.5, contains certain common elements of secondary structure and key residues. These shared features include (working from the N-terminus and using tuna cytochrome c numbering) -

(a) An N-terminal α-helix with a conserved Gly (6) and Phe (10).

(b) A haem binding site (Cys 14 - Cys 17) with a proximal His (18) as fifth iron ligand.

(c) A "right side " loop (18-38) containing Pro 30 (the carbonyl of which accepts a hydrogen bond from the back of His 18) and Arg 38 (which stabilises a buried haem propionate). This loop contains several sharp reverse turns.

(d) A "bottom loop" (39-58) which closes off the base of the haem crevice.

(e) A "left-side loop" which starts with a conserved Trp (59) and ends with the 6th haem ligand Met 80.

(f) A C-terminal α-helix (87-103) lying across the N-terminal helix at Gly 6 and carrying an aromatic partner (Tyr 97) for Phe 10.

It is not just the presence of these features but the spacing between them that is often characteristic of the Class I fold. Thus many Class I cytochromes have spacings which correspond to the 61 residues between His 18 and Met 80, the 41 residues between Arg 38 and Met 80 and the 16 residues between Met 80 and Tyr 97. However, because of the known occurrence of inserted surface loops and deletions, there are many Class I cytochromes which differ in these spacings. The most striking difference is seen in the absence of the "bottom loop" in the so-called small Class I cytochromes c such as the *Pseudomonad* cytochromes c-551.

These structural patterns can be searched for in new sequences and Ellfolk et al.(1991) proposed two Class I domains containing the two haem groups on the basis of secondary structure predictions for the *P.aeruginosa* CCP sequence. What was missing from the authors' assignment, however, was a putative methionine ligand for

Figure 1.5 The Class I fold of Tuna cytochrome c

The ribbon drawing of the main chain pathway in cytochrome c from tuna is a copy of Figure 3 from Almassy and Dickerson (1978). The haem group with its iron is represented by a cross-hatched slab with a central black ball. Covalent cysteine attachments, the methionine and histidine iron ligands, and inner and outer haem propionic acid groups (at the bottom) are also shown.

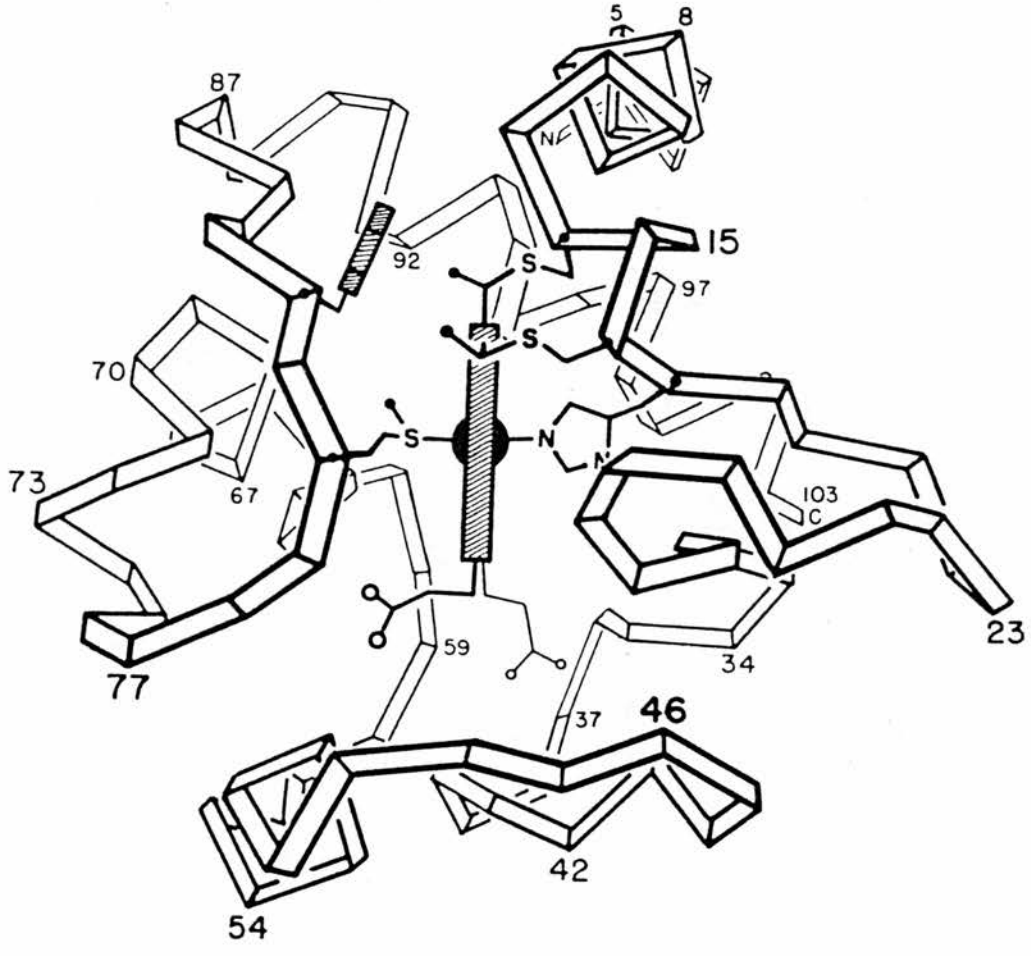
5
8
87
92
15
97
70
73
67
103
C
23
77
59
34
37
46
42
54

the N-terminal haem. This was one of the reasons why Ellfolk et al. suggested that the N-terminal domain carried out the peroxidatic function of the enzyme while the C-terminal haem domain acted as an electron-transferring partner. On the basis of the *P.aeruginosa* CCP sequence, Ellfolk et al. (1991) proposed a model for the enzyme in which His 261 from the C-terminal domain acted as the distal ligand for the N-terminal haem making it low potential in the oxidised enzyme and conferring peroxidatic activity in the activated mixed-valence form. The C-terminal haem domain was seen as being a conventional high potential Class I cytochrome c with Met 275 as the sixth iron ligand[2].

1.2.2 *Paracoccus denitrificans* cytochrome c peroxidase

In 1990 a cytochrome c peroxidase was isolated from the periplasm of the gram-negative bacterium *Paracoccus denitrificans* (Goodhew et al.1990). The enzyme is a di-haem c-type cytochrome of M_r 42000 on SDS-PAGE. The physiological electron donor to the peroxidase is probably the soluble cytochrome c550 (Pettigrew, 1991). The spectroscopic and kinetic properties of this enzyme have been characterised (Gilmour et al.1993; Gilmour et al.1994) and determined to be very similar to the one from *P.aeruginosa*, although important differences do exist. The most distinctive difference between the two enzymes is the Ca^{2+} requirement in *P.denitrificans* CCP for the low to high-spin transition at the peroxidatic haem (Gilmour et al.1995).

1.2.2.1 Spectroscopic properties of *P.denitrificans* CCP

Potentiometric redox titration of cytochrome c peroxidase established the presence of a high potential haem with a E_m of +226mV and a low potential haem with a E_m in the region -100mV (Gilmour et al.1993). By analogy with the *P.aeruginosa* enzyme the high potential haem is proposed to perform the electron transferring function while the low potential haem is the peroxidatic centre. The

[2] The crystal structure of the cytochrome c peroxidase from *Pseudomonas aeruginosa* (Fulop et al.1995) will be fully analysed in the Discussion Chapter, but the C-terminal domain does resemble a class I fold with Met 275 as the haem iron ligand. The N-terminal haem however is ligated not by His 261 but by His 71.

oxidised enzyme has a Soret maximum at 409 nm and possesses a weak absorption band at 640 nm. The 640 nm signal indicates the presence of a ferric high-spin haem (Moore and Pettigrew, 1990). The assignment of this signal to the high potential haem is in agreement with that of Foote et al.(1984) for the *P.aeruginosa* enzyme. In the *Pseudomonas* enzyme this partial high spin-state was proposed to reflect the lability of a methionine ligand to the high potential haem (Foote et al.1984). Reduction of the electron transferring haem promotes a Ca^{2+}-dependent gain of absorbance at 380 nm with concomitant loss of absorbance at 410 nm. This absorbance change represents a blue shift in the Soret of the oxidised low potential haem, which, in conjunction with the appearance of a band at 640 nm, represents a low-spin to high-spin transition in that haem.

N.m.r. spectroscopy confirms the presence of a high-spin haem in the fully oxidised and mixed-valence enzyme (Prazeres et al.1994). The fully oxidised enzyme shows two sets of resonances, one set strongly downfield-shifted, representing the electron transferring high-spin haem, and another set, less shifted and representing the peroxidatic low-spin haem. The ascorbate-reduced enzyme shows a set of strongly downfield-shifted resonances indicative of the now high-spin peroxidatic haem.

A characterisation of the oxidised and mixed-valence states of CCP was also performed by e.p.r. (Prazeres et al.1994) and Mossbauer spectroscopy (Prazeres et al.1995). The high spin-states of the enzyme are temperature dependent and can be converted to low-spin by lowering the temperature of the sample to 0°C. As e.p.r spectroscopy is carried out at 8K and Mossbauer spectroscopy between 4.2 and 200 K, very little in the way of high-spin features are observed. However both of these techniques support the model of activation as described above.

1.2.2.2 Kinetic properties of *P.denitrificans* CCP

Cytochrome c peroxidase after purification is in the fully oxidised state and is relatively inactive with a turnover number of 1920 min^{-1} (Gilmour et al.1994). In contrast, after reduction of the high potential haem in the presence of Ca^{2+} ions, activity is enhanced to generate a turnover number of 57000 min^{-1}. This increase in

activity of the enzyme is correlated with the appearance of the high spin-state of the low potential haem. This indicates that the mixed-valence high-spin form of the enzyme is the active form and that Ca^{2+} promotes this state. Also the enzyme gradually loses activity with time after dilution from stock concentrated solutions. It is proposed that the enzyme exists in a monomer-dimer equilibrium in which only the dimer is active. Dilution of the enzyme shifts the equilibrium towards the monomer and therefore activity is lost.

1.2.2.3 Ca^{2+} requirement of *P.denitrificans* CCP

An important difference between the *P.denitrificans* CCP and the *P.aeruginosa* is in the requirement for Ca^{2+} in the former to allow the crucial spin-state switch at the peroxidatic haem (Gilmour et al.1993; Gilmour et al.1994). A useful practical consequence of this is that Ca^{2+} can be withheld during the reduction process and the low-spin mixed-valence enzyme can be observed as an intermediate. When Ca^{2+} is added, an active high spin-state indicated by the gain of absorbance at 380 nm develops at the oxidised peroxidatic haem. This reflects binding of Ca^{2+} to what we will call site II, a site which is apparently empty in the oxidised form of the enzyme as isolated (Gilmour et al.1995). As turnover numbers reach more than 50000 min^{-1} it is inconceivable that this slow binding and activation of the enzyme by Ca^{2+} is part of the activation cycle. Therefore site II is proposed to exist on the oxidised enzyme also, and for high turnovers, be occupied by Ca^{2+}. The occupancy of site II can be determined by the magnitude of the spectroscopic changes that either accompany or follow reduction with ascorbate. This proportion can be assessed at a wavelength of 414 nm which is isosbestic for the oxidised and low-spin mixed-valence enzymes. Any absorbance change at such a wavelength is due to the formation of the high spin-state. Thus, for the proportion of the oxidised enzyme that contains Ca^{2+} at site II, high spin formation accompanies reduction while for the enzyme molecules that lack

Ca^{2+}, a slow binding of Ca^{2+} and formation of the high spin-state takes place in the mixed-valence form. As will be explained in the main body of the thesis and in the Discussion, each monomer is proposed to contribute one half of the Site II Ca^{2+} coordination, with the Ca^{2+} ion held at the interface of the active dimer.

If the enzyme is treated with EGTA in either the oxidised or mixed-valence state, a spectroscopic change is observed which reflects Ca^{2+} leaving a different site on the enzyme we will call site I. Although these features will be analysed in the main body of the thesis, the model of Ca^{2+} binding to the dimer is shown below.

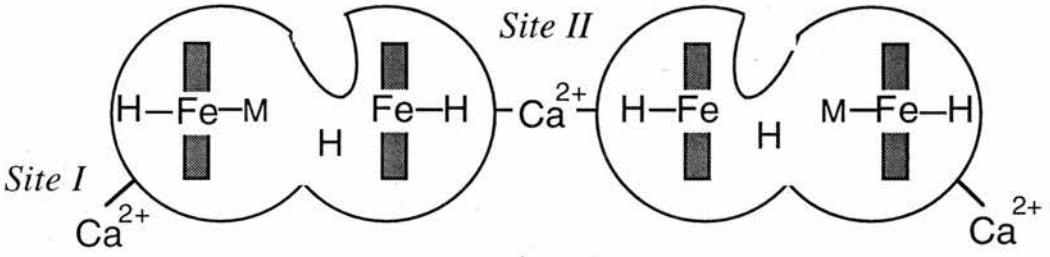

1.2.2.4 Amino acid sequence of *P.denitrificans* CCP

The amino acid sequence of *P.denitrificans* CCP has been determined (van Beeumen & Pettigrew, unpublished results) and shows 61% identity to the *P.aeruginosa* enzyme and 68 % identity to the recently sequenced CCP from *Rhodobacter capsulatus* (van Beeumen, unpublished results). Figure 1.6 aligns the sequences of the *P.aeruginosa* , *P.denitrificans* and *R.capsulatus* CCP. With the benefit of the homologous sequences, key conserved residues can be identified and general features of enzyme structure can be proposed. In some respects, for example the identification of a C-terminal Class I domain containing a conserved methionine, these confirm the structural analysis of Ellfolk et al.(1991). Also His 261 (*P.aeruginosa* CCP numbering) from the C-terminal domain, proposed to act as the distal ligand for the N-terminal haem (Ellfolk et al.1991), is indeed conserved in all three bacterial sequences and is preceded by a remarkably unvaried region suggestive of functional importance. The histidine in the *P.denitrificans* CCP corresponding to the His 261 in *P.aeruginosa* is at position 275.

Figure 1.6 Amino acid sequences of bacterial cytochrome c peroxidases
The amino sequences are shown for the cytochrome c peroxidases from (1) *Paracoccus denitrificans* (Pettigrew & van Beeumen, unpublished results), (2) *Rhodobacter capsulatus* (van Beeumen , unpublished results), (3) *Pseudomonas aeruginosa* (Ridout et al. 1995).

```
                10        20        30        40
(1)  <ETEAIDNGALREEAKGVFEAIPEKMTAIKQTEDNPEGVPLTAEKIELG
(2)        EDAALREEAKGLFEVIP      MQAPQLADNNTVTRDKIDLG
(3)          DALHDQASALFKPIP       EQVTELRGQPISEQQRELG

   50        60        70        80        90
(1)KVLFFDPRMSSSGLISCQTCHNVGLGGVDGLPTSIGHGWQKGPRNAPTMLN
(2)AMLFFDPRMSKSGVFSCQSCHNVGLGGVDGLETSIGHGWQKGPRNAPTALN
(3)KKLFFDPRLSRSHVLSCNTCHNVGTGGADNVPTSVGHGWQKGPRNSPTVFN

  100       110       120       130       140       150
(1)AIFNAAQFWDGRAADLAEQAKGPVQAGVEMSNTPDQVVKTINSMPEYVEAF
(2)AVFNVAQFWDGRAPDLAAQAKGPVQAGVEMNNTPENLVATVQSMPGYVEAF
(3)AVFNAAQFWDGRAKDLGEQAKGPIQNSVEMHSTPQLVEQTLGSIPEYVDAF

           160       170       180       190       200
(1)KAAFPEEADPVTFDNFAAAIEQFEATLITPNSAFDRFLAGDDAAMTDQEKR
(2)AKAFPGQKDPISFDNFALAVEAFEATLITPNSKFDQWLMGADGAMSADEKA
(3)RKAFPKAGKPVSFDNMALAIEAYEATLVTPDSPFDLYLKGDDKALDAQQKK

          210       220       230       240       250
(1)GLQAFMETGCTACHYGVNFGGQDYHPFGLIAKPGAEVLPAGDTGRFEVT
(2)GLKLFIDTGCAACHNGINIGGNGYYPFGVVEKPGAEVLPAGDKGRFAVT
(3)GLKAFMDSGCSACHNGINLGGQAYFPFGLVKKPDASVLPSGDKGRFAVT

           260       270       280       290
(1)RTTDDEYVFRAAPLRNVALTAPYFHSGVVWELAEAVKIMSSAQIGTELT
(2)ATADDEYVFRAGPLRNIALTAPYFHSGKVWDLREAVSVMANSQLGATLD
(3)KTQSDEYVFRAAPLRNVALTAPYFHSGQVWELKDAVAIMGNAQLGKQLA

  300       310       320       330
(1)DQQAEDITAFLGTLTGEQPVIDHPILPVRTGTTPLPTPM   P.denitrificans CCP
(2)DTQVDQITAFLGTLTGEQPEVVHPILPVRSAQTPRPEHMN  R.capsulatus CCP
(3)PDDVENIVAFLHSLSGKQPRVEYPLLPASTETTPRPAE    P.aeruginosa CCP
```

1.3 Eukaryotic peroxidases

X-ray crystallographic studies have resolved the structure of several eukaryotic peroxidases including yeast cytochrome c peroxidase (Finzel et al.1984), lignin peroxidase (Poulos et al.1993), *Arthromyces ramosus* peroxidase (Fukuyama et al.1995), *Phanerochaete chrysosporium* manganese peroxidase (Sundaramoorthy et al.1994) and pea cytosolic ascorbate peroxidase (Patterson and Poulos, 1995). Although the overall sequence identities are slight, the crystal structures of the peroxidase family reveal a remarkable similarity in the overall tertiary fold, which is especially conserved around the catalytic active site. Even in other eukaryotic peroxidases that have no resolved crystal structure, the limited similarities in the primary sequence reveals conservation within the active site region (Henrissat et al.1990).

1.3.1 Catalytic active site residues of eukaryotic peroxidases

Figure 1.7 shows the active site pattern of Yeast cytochrome c peroxidase although this structure is virtually superimposable with the other eukaryotic peroxidases. On the proximal side of the haem, the imidazole ring of histidine 175 lies perpendicular to the porphyrin plane with N[3] of the imidazole ring bonded to the haem iron. N[1] of the imidazole ring is hydrogen bonded to the side chain of asparagine 235. The indole ring of tryptophan 191 is parallel to and in van der Waals contact with the imidazole ring of histidine 175. Tryptophan 191 is the proposed site of the side chain cation radical of Compound I (Mauro et al.1988; Sivaraja et al.1989; Erman et al.1989; Fishel et al.1991).

The distal side of the single haem group is populated by key catalytic residues in a α–helical conformation. Three critical side chains, arginine 48, tryptophan 51 and histidine 52 form a ligand pocket for hydrogen peroxide. Figure 1.8 demonstrates the proposed roles of the distal histidine and arginine residues in peroxidase catalysis. The distal histidine (52 in yeast CCP) is thought to facilitate formation of the initial iron-peroxide complex by deprotonating hydrogen peroxide and subsequently promoting cleavage of the oxygen-oxygen bond by protonating the distal oxygen (Poulos and

Figure 1.7 The active site of Yeast cytochrome c peroxidase
The diagram was generated from an edited version of the 2CYP coordinate file as submitted to Brookhaven Protein Data Bank and displayed on an Evans and Sutherland computer using the application program SYBYL, developed by Tripos Associates. Residues shown in addition to the haem; on the proximal side of the haem, the proximal ligand histidine 175, asparagine 235 and tryptophan 191; on the distal side, histidine 52, arginine 48 and tryptophan 51.

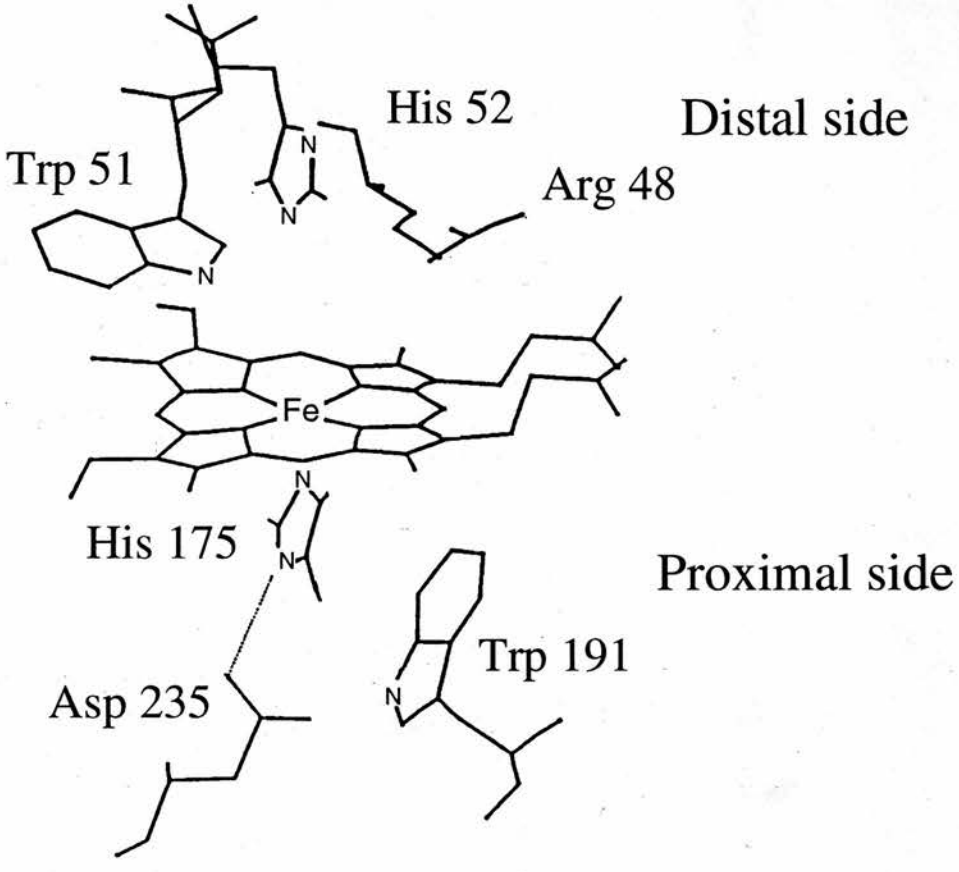
His 52
Distal side
Trp 51
Arg 48
N
N
N
Fe
N
His 175
N
Proximal side
Trp 191
N
Asp 235

Figure 1.8 Proposed roles of the distal histidine and arginine residues in peroxidase catalysis

(a) Free enzyme with active site residues, histidine (52 in yeast CCP) and arginine (48 in yeast CCP) and one water molecule. (b) A Michaelis-Menten complex forms between hydrogen peroxide and the distal side of the haem iron. (c) The distal histidine abstracts the proton from one of the oxygens. (d) The hydroperoxide O-O bond undergoes heterolytic cleavage as the distal arginine stabilises the negative charge on the oxygen. One water molecule is produced. (e) Possible intermediate transition state before (f) Compound I with an oxyferryl iron and in the case of YCCP a cationic side chain radical (Trp 191) represented by $R^{+}\cdot$. In the case of bacterial peroxidases R represents the electron transferring haem. In other eukaryotic peroxidases a π-cation porphyrin radical is formed. (g) Two one electron reduction steps with the addition of two protons bring the catalytic cycle to begin again with one water molecule in the active site.

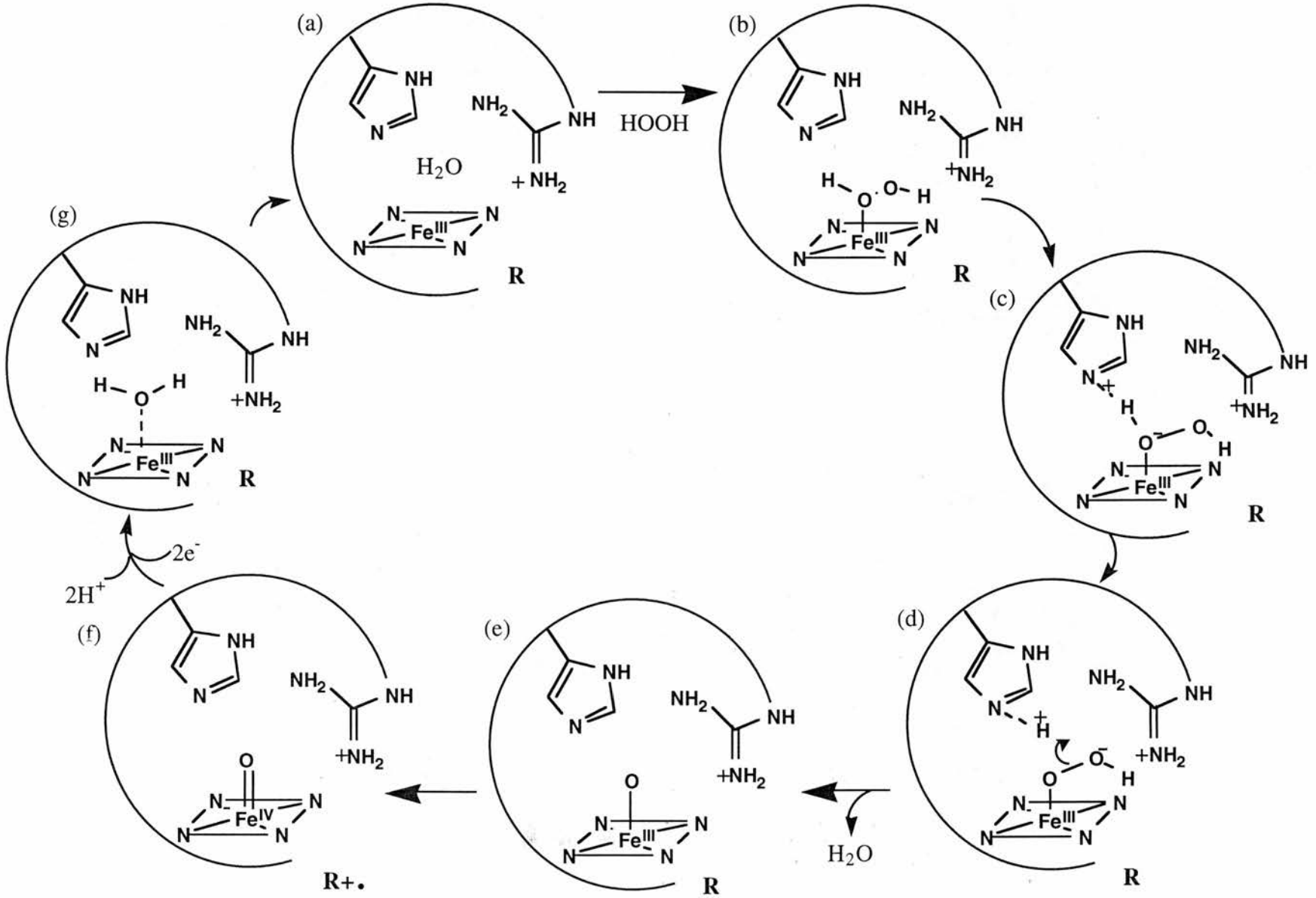
(a)
(b)
(c)
(d)
(e)
(f)
(g)
HOOH
H_2O
$2H^+$
$2e^-$
R
R+•
NH
NH_2
$+NH_2$
Fe^{III}
Fe^{IV}

Kraut, 1980). The arginine (48 in yeast CCP) is proposed to facilitate oxygen-oxygen bond scission by electrostatic stabilisation of dioxygen bond cleavage (Poulos and Kraut, 1980). Experimental support for the catalytic role of histidine in eukaryotic peroxidase comes from chemical modification studies using the histidine specific reagent diethylpyrocarbonate (Blanke and Hager, 1990; Bosshard et al.1984; Bhattacharyya et al.1992). Also site directed mutagenesis studies in YCCP demonstrates that replacement of the histidine and arginine to leucine decreases the rate of formation of Compound I by 10^5 (Erman et al.1993) or 10^2 (Vitello et al.1993). Recently, similar results have been obtained for horseradish peroxidase (Sanders et al.1994; Newmyer and Ortiz de Montellano, 1995).

Crystal structures and sequence alignments from the peroxidase family suggest that an aromatic residue is invariably adjacent to the catalytic histidine (Welinder et al.1992). However site directed mutagenesis of the distal tryptophan in yeast CCP shows this residue not to be essential for catalysis. It has been proposed that this aromatic residue adjacent to the catalytic histidine, and the histidine itself, are part of a barrier that restricts substrate access to the Compound I and II species (Newmyer and Ortiz de Montellano, 1995). This substrate barrier to the ferryl species is proposed to prevent ferryl oxygen transfer (peroxygenase) reactions in favour of electron abstraction (peroxidase) reactions.

1.3.2 Ca^{2+} requirement of eukaryotic peroxidase

A number of eukaryotic peroxidases have been shown to contain bound Ca^{2+} including horseradish peroxidase (Shiro et al.1986; Smith et al.1990), lignin peroxidase (Poulos et al.1993) and myeloperoxidase (Zeng and Fenna, 1992), but not yeast cytochrome c peroxidase. Horseradish peroxidase contains two mols of bound Ca^{2+} ions per mol of protein (Haschke and Friedhoff, 1978; Shiro et al.1986). Removal of this Ca^{2+} results in a 50% decrease in an activity and a correlating spin-state transition from a high spin-state to a state intermediate between high and low. Ca^{2+} removal also results in a shift in the n.m.r. signal of the proximal histidyl NH of

the ferrous horseradish peroxidase (Shiro et al.1986) and lowers the pK of the distal histidine by two pH units. Ca^{2+} is therefore shown to be essential for the structural integrity of the haem environment.

The crystal structure of the lignin peroxidase also indicates the presence of two bound Ca^{2+} ions (Poulos et al.1993). One Ca^{2+} lies very close to the proximal histidine ligand, whilst the other is situated on the distal side of the haem in a similar position to the Ca^{2+} found in myeloperoxidase.

The role of Ca^{2+} in peroxidases remains somewhat uncertain but the ion may play a major role in defining the structural environment in the haem crevice. More specifically Ca^{2+} may act to stabilise partial histidinate character at the proximal ligand and therefore, indirectly, the higher oxidation states of Fe (FeIII and Fe IV).

1.4 The role of histidines in the cytochrome c peroxidase of *P.denitrificans*

The general aim of this thesis is to further investigate the electron transfer processes and mode of action associated with the cytochrome c peroxidase of *Paracoccus denitrificans*. I will focus on the roles played by histidine in the enzyme, whether as a ligand to the peroxidatic haem as proposed for the *Pseudomonas* CCP and/or as a catalytic histidine by analogy with the eukaryotic peroxidases. Chemical modification of CCP by the histidine specific reagent diethylpyrocarbonate (DEPC) will be characterised and used to identify any essential histidines in the protein. The essential histidine will be identified in the sequence and conclusions drawn, regarding haem ligation and catalytic mechanism.

Chapter II

Materials and Methods

2.1 Growth of cells and enzyme purification

Paracoccus denitrificans (L.M.D. 52.44) was grown and cytochrome c peroxidase purified as described by Goodhew et al. (1990) and outlined below. Bacterial cultures were grown aerobically in 10L batches before harvesting and spheroplast formation to release the periplasmic extracts containing cytochrome c peroxidase. After spheroplasting, the periplasmic extract was partially purified on a DE52 ion-exchange column. The peroxidase fractions were pooled and further purified using a hydroxyapatite column and finally a large G75 Sephadex column. After purification the protein displayed a A_{409nm} / A_{280nm} ratio of >5 and gave a single band on SDS-PAGE (Figure 2.1). Typically 3 x 10L growths (~ 60 g wet weight of cells) were combined post DE52 for continued purification and from this, 50-100mg of purified CCP was generated. Concentrated stocks of the protein in 5mM Mes pH6, 10mM NaCl were stored at -40°C. The concentration of *P.denitrificans* CCP was routinely determined at 408 nm using $\varepsilon = 250\ mM^{-1}\ cm^{-1}$ (Goodhew et al.1990), derived from the pyridine haemochrome method (Falk, 1964). Cytochrome c peroxidase of yeast (EC 1.11.1.5) was purified by the method of Pettigrew and Seilman (1982). The concentration of yeast cytochrome c peroxidase was determined at 408 nm using $\varepsilon = 95\ mM^{-1}\ cm^{-1}$ (Coulson et al.1971). Horse heart cytochrome c (type VI) was purchased from Sigma and used without further purification.

2.2 Sodium dodecyl sulphate - polyacrylamide gel electrophoresis (SDS-PAGE)

SDS-PAGE was carried out using a slightly modified version of the method of Laemmli et al. (1970), with the loss of 2-mercaptoethanol and the gain of 2mM EDTA. The gels were typically 15% acrylamide and 0.4% bisacrylamide with dimensions

Figure 2.1 Purification profile of cytochrome peroxidase
Samples (~1nmol) after each stage of purification were taken for analysis by SDS-PAGE on a 15% polyacrylamide gel and stained for protein with Coomassie blue. M-Molecular mass markers, BSA (M_r 66k), ovalbumin (45k), carbonic anhydrase (29k), myoglobin (17k), cytochrome c (12k); P - periplasmic extract; DE- post DE52; HPT-post hydroxyapatite; G75- post Sephadex G75.

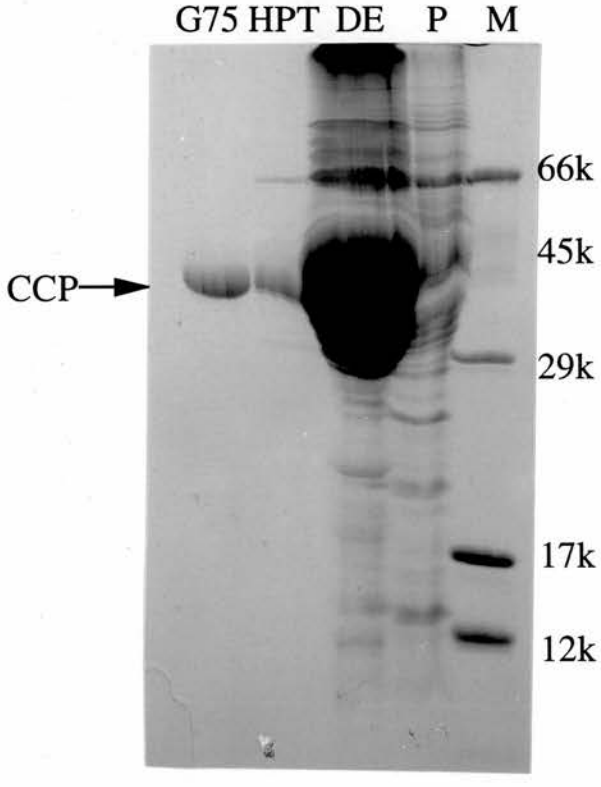
G75 HPT DE P M
66k
45k
CCP
29k
17k
12k

130mm x 150mm x 1mm. The stacking gel was 4% acrylamide and 0.1% bisacrylamide. Electrophoresis was performed at 50V for 16 hours (overnight) or at 180V for 4 hours. Samples were prepared for electrophoresis by dissolving in 62.5mM Tris / HCl pH 6.8, containing 2mM EDTA, 2% SDS and 10% glycerol. Sample denaturation was ensured by heating samples to ~100°C for 2 min immediately prior to loading onto the gel.

Gels were stained for the presence of protein or haem. For nmol amounts of protein, Coomassie Brilliant Blue R (2g/L in 45% methanol / 10% acetic acid) was used to stain gels for approximately 1 hour, before destaining in 30% methanol / 10% acetic acid. The silver staining method of Morrisey (1981) is an extremely sensitive technique, detecting pmol amounts of protein. The haem staining method of Goodhew et al. (1986) is equally sensitive. Gels were soaked in 1.25mM 3, 3' 5, 5' tetramethylbenzidine (TMBZ) in methanol / 0.25mM sodium acetate pH5 (30/70 v/v). H_2O_2 was added to a final concentration of 26mM and after staining was complete the gels were washed in propanol / 0.25M sodium acetate pH5 (30/70 v/v). Photographs were taken through a yellow filter (Cokin A.001) for haem and Coomassie blue stained gels and through a blue filter (Cokin A.020) for Silver stained gels. Densitometry scanning was carried out using a Shimadzu CS-930 scanner at 690 nm for haem stained gels, 600 nm for Coomassie blue stained gels and 500 nm for Silver stained gels.

2.2.1 Sequencing of peptides electroeluted onto polyvinylidene difluoride membrane after SDS-PAGE

Proteins which give good separation on SDS-PAGE, but are otherwise difficult to purify, can be prepared for peptide sequencing by a simple technique employing standard electrophoresis and electroblotting equipment and Immobilon polyvinylidene difluoride (PVDF) membrane purchased from Millipore. After electrophoresis as described above, gels were soaked in transfer buffer (10mM 3-[cyclohexylamino]-1-propanesulfonic acid, 10% methanol, pH11) for 5 min to reduce the amount of Tris and glycine. During this time a PVDF membrane was rinsed with 100% methanol and stored in transfer buffer. The gel sandwiched between a sheet of

PVDF membrane and several sheets of Whatman 17CHR paper, was assembled into a blotting apparatus and electroeluted for 30 min at 0.5 A. The PVDF membrane was washed in deionised water, before staining in 0.1% Coomassie blue in 50% methanol for 5 min and destaining in 50% methanol for 15 min. Finally the membrane was washed in deionised water, left to dry and stored at -20 C until ready for sequencing. Stained bands were excised with a razor blade and placed in the cartridge block of an Applied Biosystems 475A gas phase sequencer with on-line PTH analysis.

2.3 Diethylpyrocarbonate

Both DEPC and [*carbonyl*-^{14}C]DEPC were purchased from Sigma and stored desiccated at 4°C. Stock solutions were made up by dilution of DEPC into acetonitrile and assayed by reaction with 5mM Imidazole pH 7.5 ($\varepsilon_{233\ nm}$ = 3.0 $mM^{-1}\ cm^{-1}$) (Melchior and Fahrney, 1970). Although stock solutions of DEPC are quite stable in acetonitrile for several months, they did develop weak absorption in the region 250-300 nm and were then discarded. DEPC in 5mM Hepes pH 7.5 was found to hydrolyse exponentially with a half life of 20 min.

Cytochrome c peroxidase was incubated with an excess of DEPC and the stoichiometry of ethoxyformylation of histidine residues determined by following an increase of absorbance at 245 nm (ε = 3.2 $mM^{-1}\ cm^{-1}$) (Ovadi and Keleti, 1969). The reaction is complete within 20 min. Alternatively, stoichiometry of modification was determined using [^{14}C] DEPC (labelled at both carbonyl groups with overall specific activity of 2.6 mCi/mmol). Excess reagent was removed by gel filtration on a Sephadex G25 column in 5mM Hepes pH 7.5. Scintillation counting (>90% efficiency) was performed in 5ml Packard instagel with a maximum of 250µl aqueous sample in a Packard Tricarb 1900CA scintillation counter. For the calculation of moles radioactive uptake into protein, the fact that only one of the two carbonyl groups is incorporated must be taken into account (the other is lost as CO_2). 1 nmol [^{14}C] DEPC corresponds to 5838 dpm and therefore 1 nmol incorporated ethoxyformyl group corresponds to 2919 dpm.

2.4 Assay of cytochrome c peroxidase

The activity of mixed-valence cytochrome c peroxidase, in the presence of added Ca^{2+}, was measured by following the decrease in absorbance of the α band of ferrocytochrome c as it is oxidised (Gilmour et al.1994). Assays were initiated by addition of the enzyme (1nM), to a cuvette containing 5mM Hepes pH7.5 / 10mM NaCl, 7μM horse heart ferrocytochrome c, 1mM $CaCl_2$ and 18μM hydrogen peroxide. Turnover numbers were calculated using the initial gradient of cytochrome c oxidation (Gilmour et al.1994).

2.5 Spectroscopic techniques

2.5.1 Visible / UV

All spectra in the UV region were recorded on a Cary 219 spectrophotometer. Difference spectroscopy in the visible region was performed by a single beam Philips PU8700 spectrophotometer. Spectra were collected at 23°C using 1 cm pathlength quartz cuvettes.

2.5.2 Electron paramagnetic resonance

E.p.r. probes the environment of a paramagnetic centre by defining the size and shape of the magnetic moment produced by the unpaired electron of the iron atom. The factor which expresses the size of a magnetic moment of a paramagnetic species is called the g-value. The g-value specifies the position at which the e.p.r. spectrum of the paramagnetic species occurs. For mono-haem proteins e.p.r. signals can be confidently assigned to certain structural features, for example g_{max} values of ~3 represent a low-spin ferric haem whilst a g_{max} value of ~6 represents a high-spin ferric haem. Ferrous cytochromes are diamagnetic and hence do not have an e.p.r. spectrum. However as cytochrome c peroxidase is a di-haem enzyme there is the possibility of haem-haem interactions generating g-values considerably different from above (Moore and Pettigrew, 1990). An additional complication is the fact that e.p.r. spectroscopy is carried out at or near liquid helium temperatures. Care has to be taken not to draw

incorrect assumptions as the spin-state of haems are often temperature dependent (Moore and Pettigrew, 1990). E.p.r. measurements were performed using a Bruker ESP 380 spectrometer with an Oxford Instruments ESR-9 continuous flow cryostat. The relative intensities of the e.p.r. signals are determined using software which simulates the experimentally determined spectra using the values for g_{max}, g_{med} and g_{min} and integrates the resultant signals (More et al.1990).

2.5.3 Nuclear magnetic resonance

N.m.r. probes the environment of atom nuclei such as ^1H which act as small bar magnets and can interact with an external magnetic field. The external field forces the nuclear bar magnets to adopt one of two orientations; parallel and antiparallel to the direction of the applied field. Transitions between these energy levels are then induced by irradiation of the sample with radiofrequency radiation. The size of the magnetic interaction and hence the precise radiation frequency is determined by a number of factors, including the magnetic properties of surrounding electrons which act to shield the atomic nucleus from the applied field. Different hydrogens will reach resonance at different magnetic field strengths and these differences are expressed in terms of chemical shifts, defined with respect to a reference material added in the sample.

$$\text{Chemical shift (ppm)} = \frac{\text{sample frequency - reference frequency}}{\text{reference frequency}} \times 10^6$$

Samples were exchanged several times with the required buffer (prepared with 99.9% ^2H_2O) by centrifugation in a Centricon 10 microconcentrator (Amicon). The protein concentration was approximately 1mM. The mixed-valence state of CCP was achieved by addition of small amounts of a concentrated sodium ascorbate solution, in the presence of the mediator diaminodurol. High resolution ^1H-N.m.r. spectra were recorded in the Fourier transform mode on an AMX-300 spectrometer (300MHz) equipped with a temperature control unit. Temperature 303k, 2000 scans, 4k data points. When necessary, and in order to improve the signal to noise ratio, the n.m.r.

spectra were obtained by an exponential multiplication by 10Hz line broadening of free induction decays prior to Fourier transformation. All chemical shift values are quoted in parts per million (ppm) from internal 3-trimethylsilyl [2,2,3,3-$^2H_4$]-propionate, positive values referring to low field shifts.

2.6 Mass spectrometry

The mass spectrometer separates charged particles such as proteins or peptides according to their mass-to-charge ratios (m/z) on the basis of different trajectories, either in electric fields or in a combination of magnetic and electric fields (Mann and Wilm, 1995). Electrospray mass spectrometry (ES MS) of proteins is based on the formation of a mist of small, highly charged droplets containing protein molecules, under the influence of a high electric field. The small droplets evaporate rapidly and, by a process of either field desorption or residual solvent evaporation, protonated protein molecules are released into the gas phase. In contrast to all other mass spectrometric ionisation methods, the change from the liquid to the gas phase is very gentle (this property was vital in the identification of an ethoxyformyl derivative of a CCP peptide). Once the protein ions are in the gas phase, they are leaked into the vacuum of a mass spectrophotometer, where they are separated and detected according to their m/z ratio. The preparation of peptide samples in this work required consideration of the problem of ionic buffers, detergents and other involatile substances. Ionic buffers disturb the spraying process and compete with analyte molecules for charges. Other involatile substances can disturb the desorption process by forming a solid core in the evaporating droplet from which the protein molecules cannot escape. Upper limits for contaminants are about 1mM for ionic salts and 0.01% for SDS. Throughout this work peptide samples are prepared in the presence of high concentrations of ionic buffers and detergents. These problems were resolved by desalting samples using a Superdex 75 molecular exclusion column equilibrated in 0.1M ammonia solution. Alternatively some peptides were isolated and conveniently desalted by reverse phase HPLC.

2.7 Ca^{2+} titrations

Ca^{2+} concentrations in the micromolar range were set using EGTA. At the relative concentrations of protein and EGTA used, almost all the added Ca^{2+} is bound to EGTA and any removal by protein is restored from the buffer reservoir to essentially the same level of free Ca^{2+}. Thus the protein can respond to, but not significantly perturb, the levels set by EGTA. Values for free [Ca^{2+}] were calculated by taking into account the proportion of the binding form ($EGTA^{4-}$) present at the different pH values. At the pH values used, almost all the added Ca^{2+} binds to, and effectively displaces two protons from the predominant H_2EGTA^{2-} form. 2 mol NaOH were added for each mol Ca^{2+} addition to balance this proton release.

2.8 Redox Potentiometry

2.8.1 Calibration of the redox electrode

Prior to the redox titrations, the calibration of the electrode was checked using the Fe^{2+}/ Fe^{3+}-EDTA redox couple, which has a mid-point potential of +108mV at pH 5 (Kolthoff and Auerbach, 1952). By measuring the ambient potential at two different ratios of oxidised and reduced, it is possible to check the electrode generates the correct slope of 59mV and potential of 196mV (Bates, 1954).

For calibration, the electrode was placed in a stirred cuvette containing 125mM sodium acetate pH 5, 0.5mM ferric ammonium sulphate and 10mM EDTA. The solution was made anaerobic by bubbling with N_2 for 15 min. After bubbling, an anaerobic solution of ferrous ammonium sulphate was made, to give a final concentration of 0.5mM, for which the potential was recorded. A graph of E_h against log ox/red was then plotted, from which the E_m was measured and the slope determined.

2.8.2 Redox titrations

Reductive and oxidative titrations were performed in a magnetically stirred anaerobic cuvette continually flushed with nitrogen. The cuvette usually contained 3.5ml of ~6μM cytochrome c peroxidase (native, cleaved or modified) in 5mM Hepes pH 7.5,and as redox mediators,17μM diaminodurol (DAD, E_m = +220mV),phenazine methosulphate (PMS, E_m = +80mV) phenazine ethosulphate (PES, E_m = +60mV), 2-hydroxy-1,4-naphoquinone (HNQ, E_m = -140mV) ,and flavin mononucleotide (FMN, E_m = -200mV), (Wilson, 1978). Redox mediators were present to ensure rapid equilibration between the redox electrode and the buried redox centres within the enzyme.

Reductive titrations were carried out by addition of small volumes of an anaerobic solution of sodium dithionite (30mM). Sodium dithionite stocks were prepared in anaerobic 100mM Hepes pH7.5. Oxidative titrations were carried out in 30mM potassium ferricyanide in 100mM Hepes pH7.5.

The ambient redox potential (E_{obs}) was monitored by a Pt pin electrode in combination with a Ag/AgCl reference (Russell pH Ltd.) and E_m, with reference to the standard hydrogen electrode, was obtained by the addition of 196mV (Bates, 1954). Spectra were scanned in the region of the α and β bands of CCP using a Unicam SP1800 spectrophotometer, coupled to a chart recorder (BBC Servogor 120)

2.8.3 Nernst equation

The mid-point potential is calculated using the Nernst equation shown below:

$$E_h = E_m + \frac{2.3RT}{nF} \log \frac{[\text{oxidised form}]}{[\text{reduced form}]}$$

where R is the gas constant, T is the temperature, n is the number of electrons involved in the redox reaction and F is the Faraday. At 25°C this simplifies to:

$$E_h = E_m + \frac{0.059}{n} \log \frac{[\text{oxidised form}]}{[\text{reduced form}]}$$

A plot of E_h against log ox/red gives a straight line of slope 59mV for a single electron oxidation - reduction reaction. The intercept of this line with the y-axis gives the value of the mid-point potential, E_m.

2.9 Secondary structure predictions

We used a suite of eight secondary structure prediction methods contained in the package PREDICT (E. Eliopoulos, Leeds University, UK). One of the eight methods in PREDICT is that of Chou and Fasman (1974) and this accurately predicted the α-helices of the known tuna cytochrome c structure (Takano et al.1977) and was therefore used alone to predict α-helices conserved in the bacterial peroxidases.

Chapter III

Modification of cytochrome c peroxidase using diethylpyrocarbonate

3.1 Introduction

Diethylpyrocarbonate (DEPC) reacts with both free imidazole in solution and histidyl residues in proteins, yielding the ethoxyformyl derivatives. Since nucleophiles are reactive in their unprotonated state the ethoxyformyl derivative formed by Equation 1 seems most probable, the unprotonated N[3] of histidine reacting with DEPC. The derivative formed by Equation 2 seems unlikely as the reaction involves the protonated N[1] attacking DEPC. Although this reaction is reported by Miles (1972), it is perhaps only valid when the histidine is in a special environment. The diethoxyformylhistidine has been reported (Equation 3) (Miles, 1972) but is only formed when DEPC is in large excess (Morris and McKinley-McKee, 1972; Avaeva and Krasnova, 1975) or when the reaction is performed at high pH. Excess reagent is hydrolysed, giving two equivalents each of ethanol and carbon dioxide (Equation 4). The ethoxyformyl derivative is also hydrolysed (Equation 5), the rate of which can determine the feasibility of isolating modified peptides. Strong nucleophiles such as hydroxylamine or ammonia increase the rate of reversibility via Equation 6.

The reaction of DEPC with histidine residues in proteins and imidazole in solution, can be conveniently followed spectrophotometrically by an increase in absorbance, which has a maximum between 225 - 250 nm. In proteins the number of histidines modified can be determined using the extinction coefficient at 245 nm 3.2 mM^{-1} cm^{-1} (Ovadi and Keleti, 1969), or by measuring the incorporation of label from [*carbonyl*-^{14}C]DEPC. For this calculation, the fact that only one of the two carbonyl groups is incorporated must be taken into account (Equation 7, * represents radioactive carbon).

This chapter aims to thoroughly characterise DEPC and its reaction with both model compound imidazole and the protein cytochrome c peroxidase.

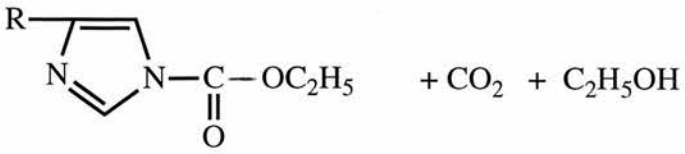

Equation 1

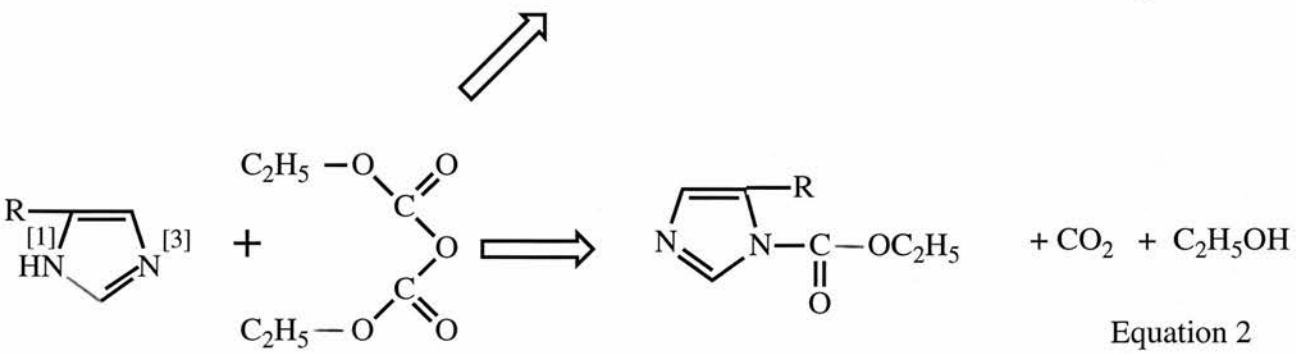

Equation 2

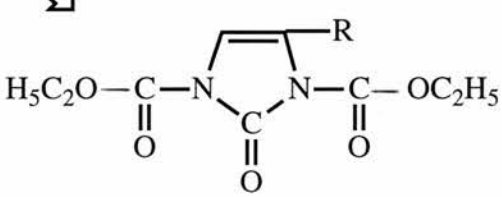

Equation 3

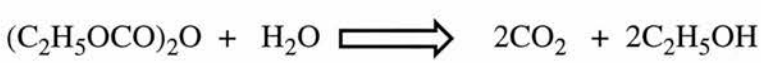

Equation 4

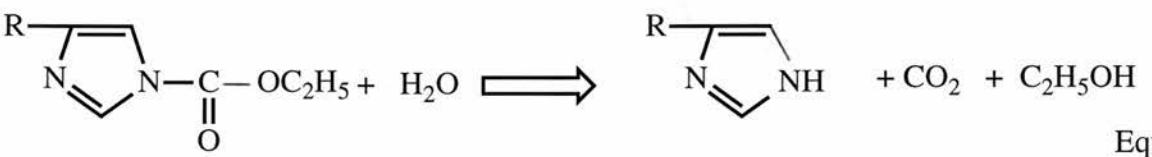

Equation 5

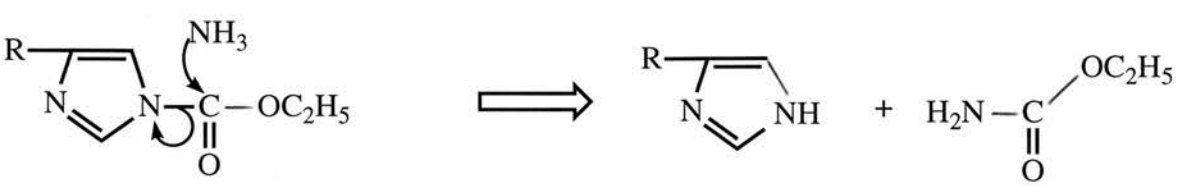

Equation 6

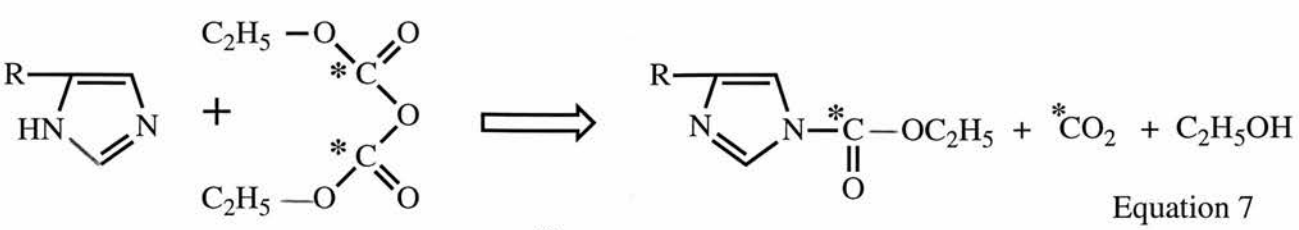

Equation 7

3.2 Results and Discussion

3.2.1 Properties of DEPC

3.2.1.1 The assay and stability of stock DEPC

Both DEPC and [*carbonyl*-^{14}C]DEPC were purchased from Sigma. Since DEPC is subject to hydrolysis [Equation 4] the vials are stored desiccated at 4°C and warmed to room temperature before dispensing. Typically, dilution of DEPC (6.9M) into acetonitrile gave stock DEPC concentrations of approximately 110mM. An aliquot of stock DEPC was added to excess imidazole and the concentration accurately determined following the rapid gain of absorbance which has a maximum at 226 nm. Figure 3.1 displays a difference spectrum (300 - 220 nm) of modification of imidazole from which a concentration of 114mM was calculated. The extinction coefficient used for this calculation is $\varepsilon = 3.0\ mM^{-1}\ cm^{-1}$ (Melchior and Fahrney, 1970).

Stock solutions of DEPC were found to be quite stable in acetonitrile for several months. In fact a slight increase in the DEPC concentration was seen over this length of time probably due to evaporation of solvent. However aged stock DEPC did develop weak absorption in the region 230 -300 nm (Figure 3.2) and for this reason fresh stocks were made up frequently.

3.2.1.2 Radioactive DEPC

[*carbonyl*-^{14}C]DEPC is labelled at 2.6 mCi / mmol. Therefore each carbonyl must be labelled at 1.3 mCi / mmol (Equation 7). [^{14}C]DEPC was diluted into acetonitrile and the concentrations of stock [^{14}C]DEPC (105mM and 10.5mM) were determined as above. As a check on radioactivity, 1µl samples of 10.5mM [^{14}C]DEPC were counted in scintillant, these generating an average of 61385 dpm. This number agreed remarkably well with 61310 dpm predicted from the quoted specific activity. This check allows confidence in subsequent calculations relating dpm to mols of

Figure 3.1 Assay of stock diethylpyrocarbonate

An aliquot of stock DEPC in acetonitrile was diluted 600 fold in 5mM Imidazole pH 7.5 in a cuvette having a 1cm light path. After 2 min a modified imidazole minus unmodified imidazole difference spectrum was taken. The stock concentration was determined following the gain of absorbance at 226 nm ($\varepsilon = 3.0 mM^{-1} cm^{-1}$).

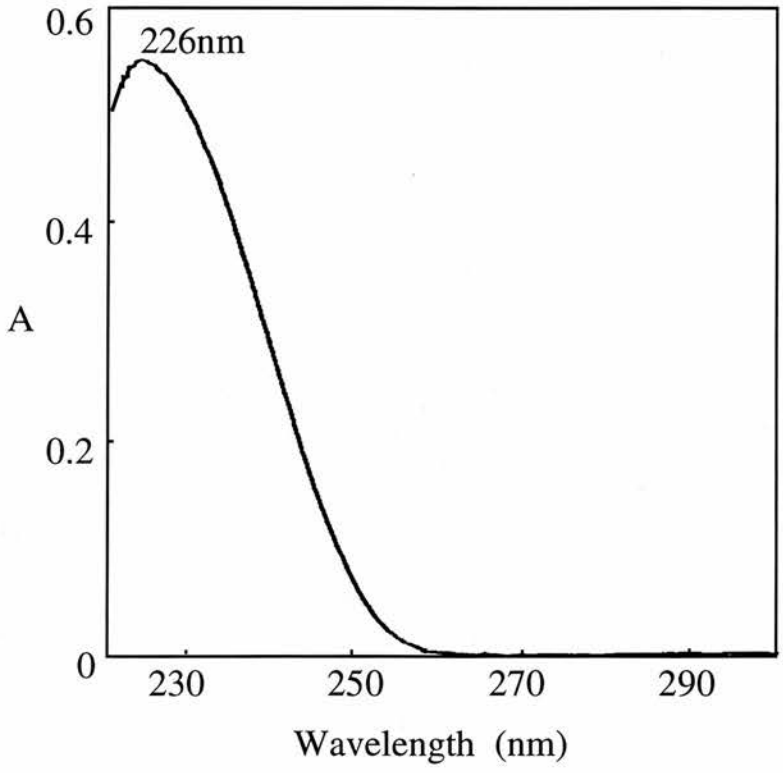
0.6
226nm
0.4
A
0.2
0
230
250
270
290
Wavelength (nm)

Figure 3.2 UV absorbance of 'old' diethylpyrocarbonate

(i) Stock DEPC (114mM) in acetonitrile, was left at 4°C for several weeks. An aliquot was diluted with H_2O to a final concentration of 240μM and the spectrum from 300 - 230 nm recorded. (ii) Fresh DEPC stock in acetonitrile (110mM) was diluted in H_2O and spectrum recorded as in (i). Spectra recorded by G.W. Pettigrew.

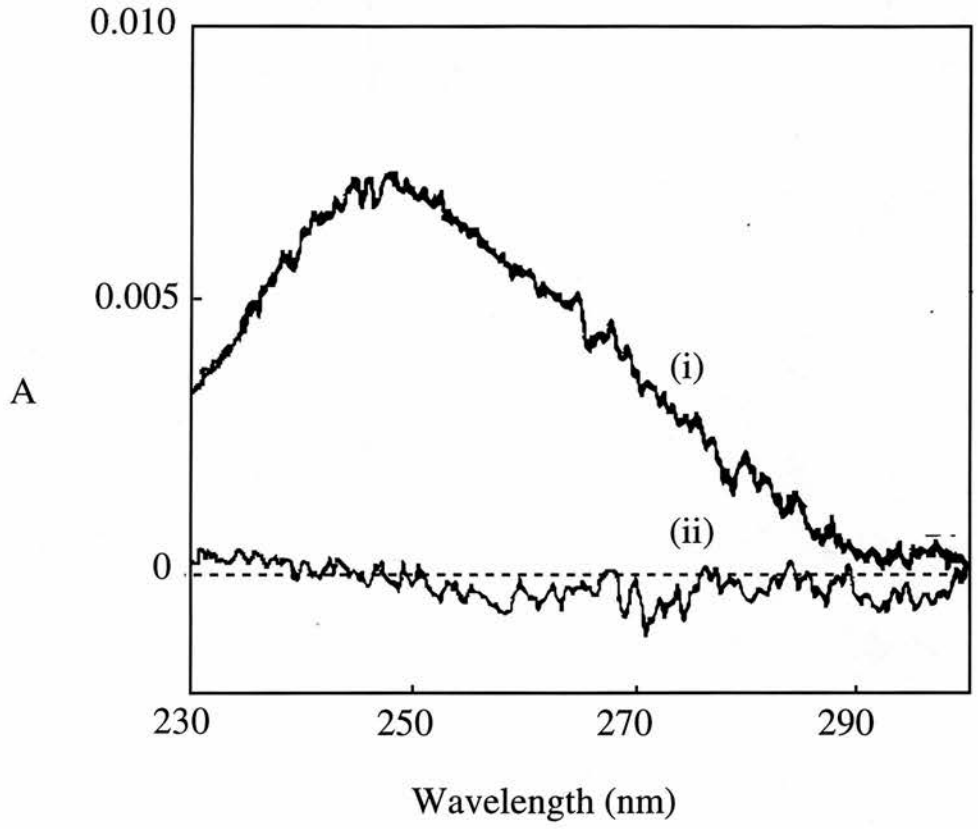
0.010
0.005
0
A
(i)
(ii)
230
250
270
290
Wavelength (nm)

radioactive compound.

The scintillation fluid, Packard Instagel, is for use with aqueous samples. To minimise quenching of radioactivity, a maximum of 5% aqueous sample in scintillant is recommended. Throughout this body of work, samples ≤1ml were counted and so a maximum of 20ml scintillant was required. To avoid waste of materials, less scintillant was routinely used for smaller sample volumes. The detection of radioactivity was unaffected by vial type (glass or plastic) or volume of scintillant. A perhaps surprising result though, was that if radioactive samples were counted, left for several days and recounted there was a significant loss of dpm. This is probably due to slow hydrolysis of [^{14}C]DEPC and escape of the product, $^{14}CO_2$ (see Equation 4). Subsequently all radioactive samples were counted (and disposed) soon after addition to scintillation fluid.

3.2.1.3 Stability of DEPC in aqueous solutions

As explained in Chapter I, the properties of cytochrome c peroxidase have been well characterised at pH7.5 (Gilmour et al.1993; Gilmour et al.1994). It had been established that at this pH value the mixed-valence low-spin form could be observed. Thus this pH was chosen for the initial studies on DEPC decomposition. The effect of incubation in 5mM Hepes pH 7.5 on the decomposition of DEPC was determined by assaying with imidazole (Figure 3.3). DEPC decayed exponentially with a half life of 20 min. This half-life compares quite favourably with the literature values of 24 min in 60mM sodium phosphate buffer pH6 and 9 min in 37mM sodium phosphate buffer pH7 (25°C) (Berger, 1975). Tris buffer accelerates the decomposition of DEPC presumably by acting as a nucleophile; the half-life of DEPC in Tris (25°C) is 1.25 min at pH7.5 and 0.37 min at pH8.2 (Miles, 1972). Hepes pH 7.5 is therefore a suitable buffer for initial DEPC modification studies.

3.2.2 Modification of imidazole with DEPC and stability of the ethoxyformyl derivative

An important consideration in the modification of CCP is the stability of the

Figure 3.3 Stability of DEPC in 5mM Hepes pH 7.5

DEPC (300μM) was incubated in 5mM Hepes pH 7.5 at 23°C. Aliquots were taken at various times and assayed with a five fold dilution into 5mM Imidazole pH 7.5. The difference spectra of modified imidazole minus imidazole displayed a gain of absorbance from which the original concentrations of DEPC were calculated (ε = $3.0mM^{-1}\ cm^{-1}$). The experimental points are fitted to a theoretical exponential decay plot with $t_{1/2}$ = 20 min.

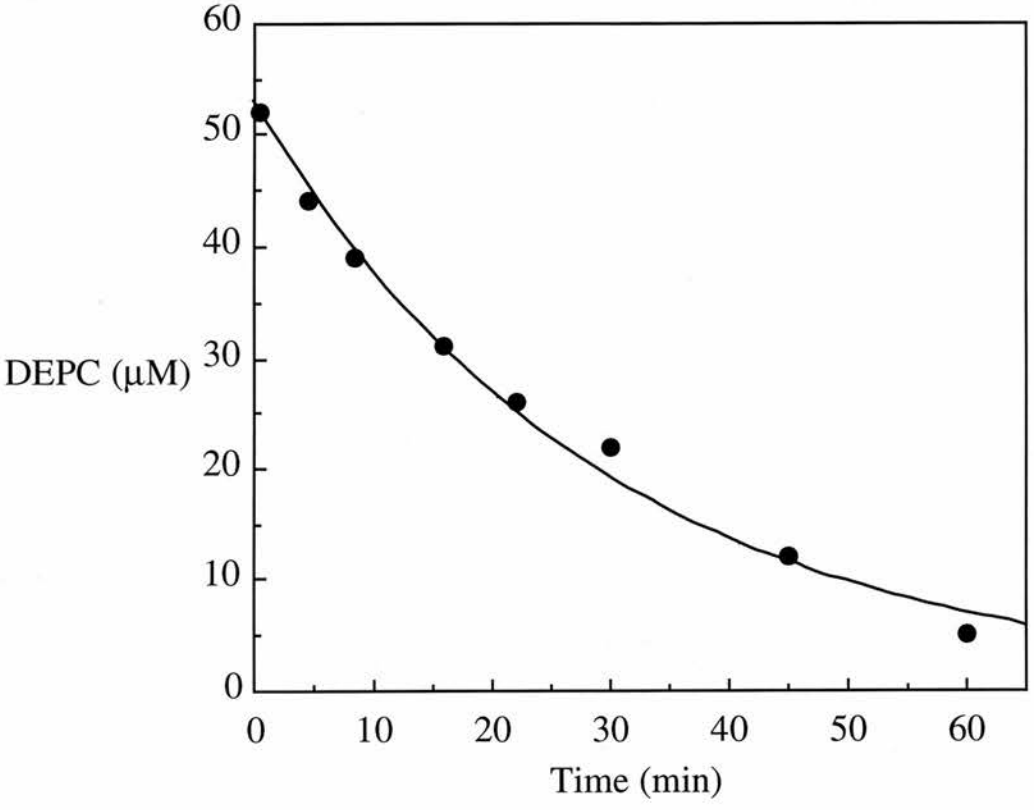
60
50
40
30
20
10
0
DEPC (μM)
0
10
20
30
40
50
60
Time (min)

ethoxyformyl derivative of DEPC. The instability of ethoxyformylhistidine has severely limited the isolation of modified peptides in previous studies (Bosshard et al.1984). Under varying conditions, the stability of ethoxyformylimidazole was determined and these results gave indications as to the stability of the ethoxyformylhistidine derivative. Both SDS and ammonia solution were to prove useful in the isolation of peptides of CCP (see Chapter V) but whether they would allow retention of the ethoxyformyl label was investigated firstly by studying the relative stability of ethoxyformylimidazole.

In 10mM Hepes pH 7.5 ethoxyformylimidazole was extremely stable with very little of the 230 nm absorbance peak lost over 24 hours (data not shown). The derivative is at least equally stable in 1% SDS, with no significant loss of label over 36 hours (Figure 3.4A). Addition of 0.1M ammonia solution to ethoxyformylimidazole causes a general rise in absorption from 200- 300 nm. In order for the reversal rate of the label to be determined the baseline was reset and the decomposition of ethoxyformylimidazole monitored by the progressive formation of an absorption trough at ~230 nm (Figure 3.4B(i)). The label is completely lost within 20 min, the loss of ethoxyformylimidazole following an exponential decay curve with a half-life of 3 min (Figure 3.4B(ii)). These data agrees well with the quoted half-life literature values of 2 hours at pH 2, 55 hours at pH 7 and 18 min at pH 10, all in water at 25°C (Melchior and Fahrney, 1970).

SDS may therefore prove useful in the isolation of modified peptides as it seems not to promote hydrolysis of ethoxyformylimidazole and is worthy of further investigation. As ammonia solution accelerates the destruction of ethoxyformylimidazole, it will probably promote similar decomposition of ethoxyformylhistidine (see later in Chapter).

3.2.3 Modification of cytochrome c peroxidase with DEPC

3.2.3.1 The extent of modification

Diethylpyrocarbonate reacts with histidine residues in proteins, yielding the ethoxyformylhistidine derivative. The reaction is followed spectrophotometrically

Figure 3.4 Stability of ethoxyformylimidazole in 1% SDS and 0.1M ammonia solution.

A DEPC (100μM) was added to 100μM Imidazole in 10mM Hepes pH 7.5. The reaction is complete within 45 min when a modified difference spectrum from 300-225 nm was recorded (0h - solid line). The solution was made to 1% SDS and after 36h another spectrum (36h - dashed line) was taken.

B (i) DEPC (100μM) was added to 100μM Imidazole in 10mM Hepes pH 7.5 and the ethoxyformylimidazole spectrum recorded as in **A**. Ammonia solution was then added (0.1M) and the baseline of the spectrophotometer immediately reset. [Ethoxyformylimidazole] at 1, 2, 4, 8 and 18 min was determined by calculating the difference in absorbance at 230 nm from the 33 min spectrum, that is when no ethoxyformylimidazole remains ($\varepsilon = 3.0 mM^{-1} cm^{-1}$).

(ii) The experimental points are fitted to a theoretical exponential decay plot with $t_{1/2} = 3$ min.

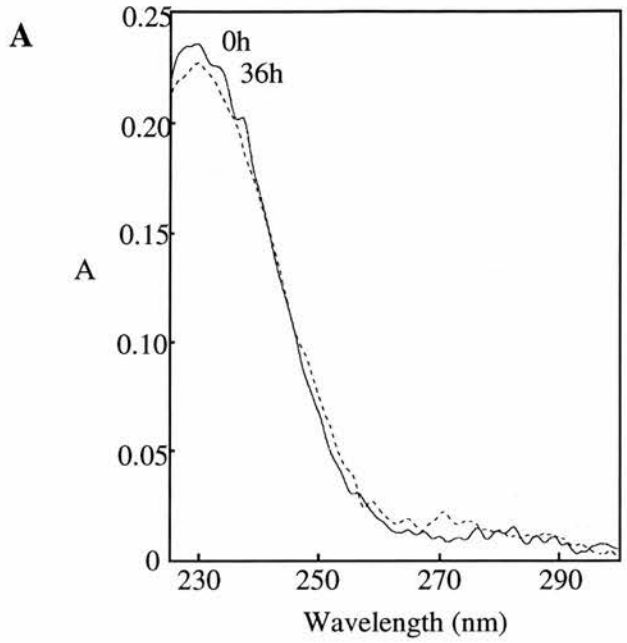

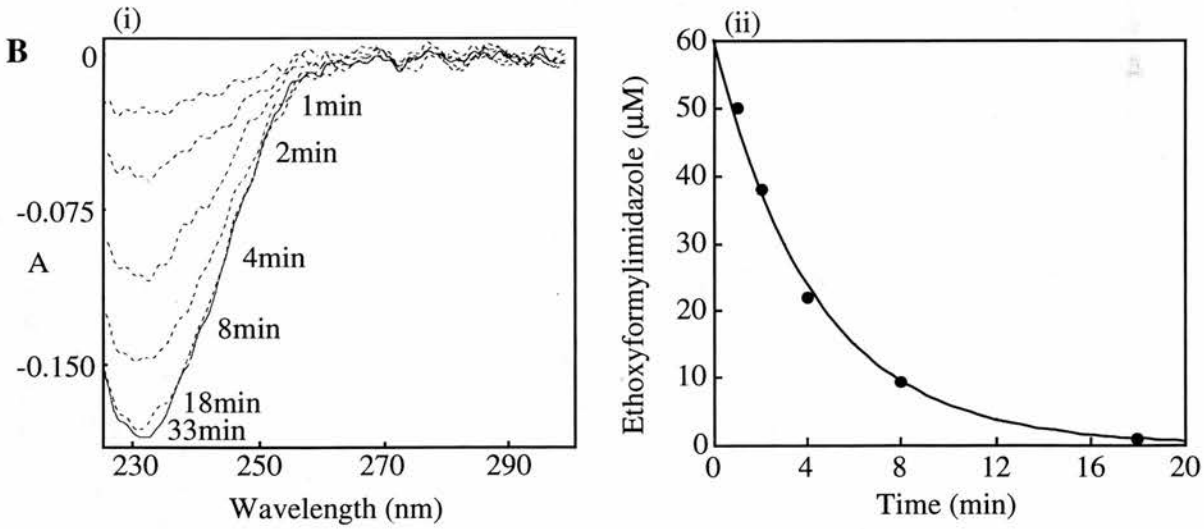

following a gain of absorbance between 240 and 250 nm. Figure 3.5 compares difference spectra (300 - 230 nm) of modification of *Paracoccus denitrificans* cytochrome c peroxidase at 2 and 20 min, Yeast cytochrome c peroxidase and the model compound imidazole.

The difference spectrum of the modified *P.denitrificans* CCP displays an initial gain of absorbance at 245 nm (Figure 3.5 **A**(i)) followed by slow formation of a trough between 265-300 nm (Figure 3.5 **A**(ii)). As described above, modification of free imidazole generated the ethoxyformylimidazole derivative which gave a peak at 233 nm but no corresponding changes at higher wavelengths (Figure 3.5 **B**). The modified YCCP difference spectrum (Figure 3.5 **C**) is very similar to the modified *P.denitrificans* CCP spectrum. For both proteins a DEPC : protein ratio of 20μM to 4μM consistently resulted in a modification of approximately 1 mol histidine per mol of protein. (Any variations were probably due to error of determining [DEPC]) The mol of histidine modified per mol of protein was determined using the extinction coefficient of ethoxyformylhistidine at 245 nm of $3.2mM^{-1}$ cm^{-1} (Ovadi and Keleti, 1969). A possible source of error for this calculation is the effect of spectral features near to the peak at 245 nm. For example the trough at 265-300 nm in the modified difference spectrum of bacterial and yeast CCP may have a 'pulling down' effect on the 245 nm peak. An independent check on the extent of modification was made by measuring the incorporation of radioactive DEPC. [^{14}C] DEPC was used to modify cytochrome c peroxidase to the extent of 1 mol of histidine modified per mol of protein, as measured by spectroscopy. Excess reagent was removed by gel filtration on a Sephadex G25 column in 5mM Hepes pH 7.5 and scintillation counting (>90% efficiency) of the desalted modified protein measures the extent of incorporation of radioactive label. These experiments have repeatedly shown that there is good agreement between the two methods of quantitation, with radioactive labelling giving slightly less (~10%) than spectroscopic measurements. This indicates firstly that ΔA_{245nm} is a reliable measurement of histidine modification and secondly that there is little uptake into amino acids other than histidine. The specificity of modification will be discussed later in this chapter.

Figure 3.5 UV difference spectra of the modification of imidazole, *P.denitrificansCCP* and YCCP with diethylpyrocarbonate.

A(i) *P.denitrificans* CCP (3.5 μM) in 5mM Hepes pH 7.5, was modified with DEPC to a final concentration of 20μM. After 2 min a modified CCP minus unmodified CCP difference spectrum was taken and showed 0.57 mol of histidine modified / mol of protein, based on ε_{245nm}= 3.2 mM^{-1} cm^{-1} for ethoxyformylhistidine.

A(ii) The reaction of DEPC with *P.denitrificans* CCP is complete within 20 min and shows 1.0 mol of histidine modified / mol of protein.

B 5 mM Imidazole in 5mM Hepes pH 7.5, was incubated with 4 μM DEPC. The difference spectrum obtained at 2 min shows 3.8 μM ethoxyformylimidazole (ε = 3.0 mM^{-1} cm^{-1}).

C YCCP (3.8 μM) in 5mM Hepes pH 7.5, was modified with DEPC to a final concentration of 20μM. After 15 min a difference spectrum was taken and showed 1.1 mol of histidine modified / mol of protein.

The wavelength of individual maxima are indicated on the respective spectra.

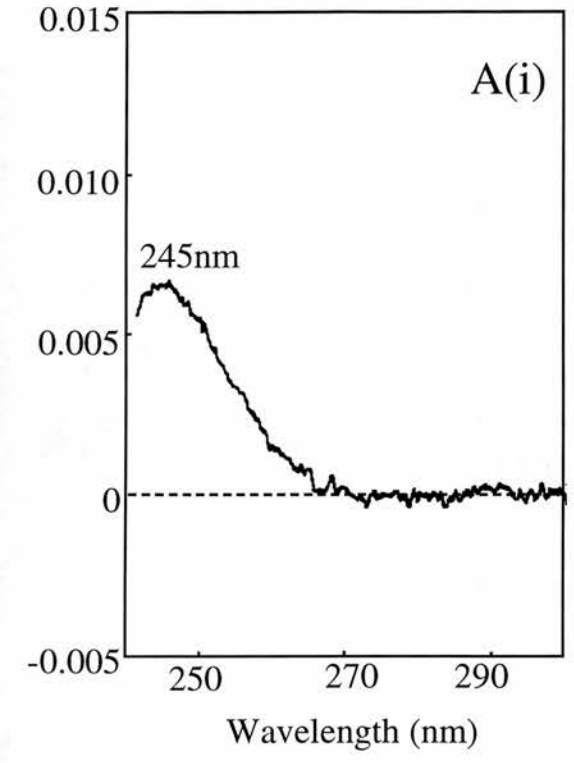
0.015
0.010
0.005
0
-0.005
A(i)
245nm
250
270
290
Wavelength (nm)

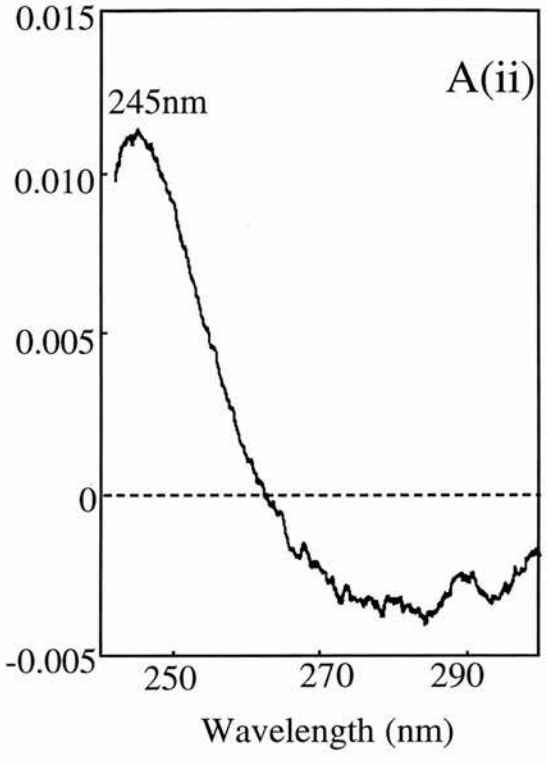
0.015
0.010
0.005
0
-0.005
A(ii)
245nm
250
270
290
Wavelength (nm)

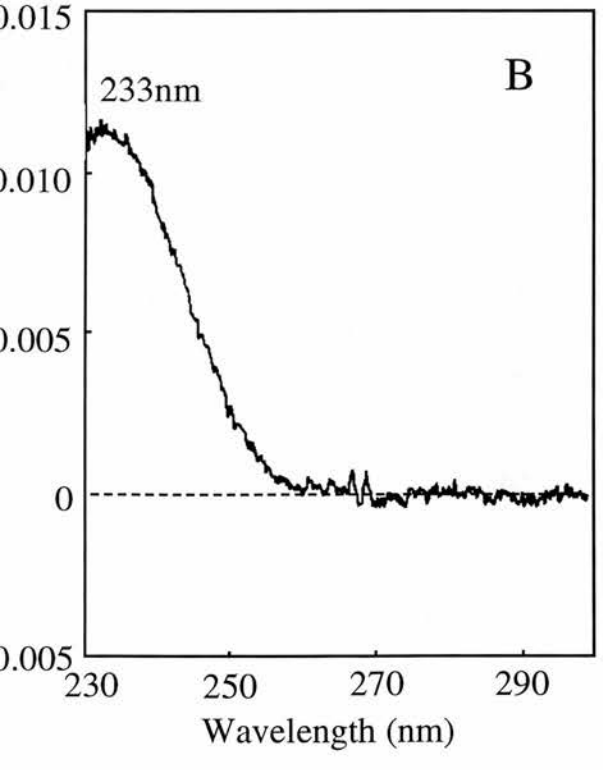
0.015
0.010
0.005
0
0.005
B
233nm
230
250
270
290
Wavelength (nm)

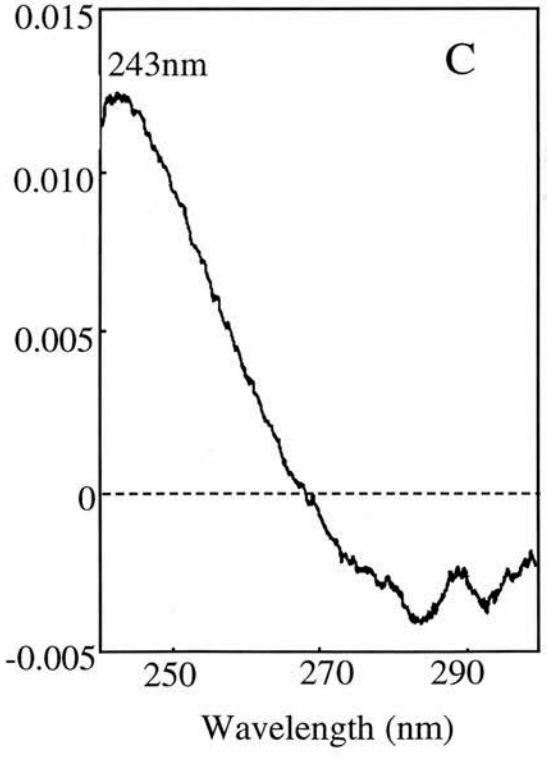
0.015
0.010
0.005
0
-0.005
C
243nm
250
270
290
Wavelength (nm)

The DEPC : protein ratio of 20μM to 4μM compares favourably to previous studies, some of which introduced mM DEPC to μM protein samples (Vincent et al.1975; Bhattacharyya et al.1992; Blanke and Hager, 1990). A large excess of DEPC is undesirable as the reagent may react to form disubstituted histidine derivative (Equation 3) (Morris and McKinley-McKee, 1972; Avaeva and Krasnova, 1975). The diethoxyformylhistidine derivative generates a higher absorbance at 245 nm and would therefore lead to overestimation of the number of histidines modified. The small excess of DEPC used to modify a single histidine in this study, predicts either a high accessibility, or an unusually reactive nature, for one histidine in cytochrome c peroxidase.

Figure 3.6(a) shows the extent of modification of CCP as DEPC concentration was raised. At each DEPC concentration the modification was allowed to proceed until the absorbance maximum at 245 nm was obtained (approx. 20 min). The biphasic nature of the reaction of DEPC with CCP demonstrates the existence of an easily modifiable histidine. Eventually at high DEPC all four available histidines are modified: the two proximal haem ligands are seemingly either not accessible or not reactive. Bosshard et al. (1984) demonstrated that modification of Yeast cytochrome c peroxidase with high [DEPC] modifies five out of the six histidines present in the protein. The authors putatively identify the unmodifiable histidine as the proximal ligand to the single haem in this enzyme.

Figure 3.6(b) compares extent of modification at pH 6 and 7.5 and it indicates that much higher DEPC concentrations are required at pH 6 to achieve modification of 1 mol of histidine, a result consistent with the requirement that histidine must be unprotonated to be modified (Holbrook and Ingram, 1973; Tudball et al.1972). Also it was determined by Gilmour et al.(1993, 1994) that at pH 7.5 the mixed-valence low-spin form of the enzyme can be observed. Therefore pH 7.5 was used for all subsequent studies.

The biphasic pattern of modification obtained by following the extent of reaction at a single high DEPC concentration also demonstrated the existence of an easily modified histidine (Figure 3.7). Upon using a relatively low DEPC : CCP ratio, a monophasic rise of absorbance at 245 nm was seen, which at its end point indicated

Figure 3.6 The extent of modification of *P.denitrificans* CCP with increasing concentrations of DEPC.

(a) *P.denitrificans* CCP (4μM) in 5mM Hepes pH 7.5 was treated with increasing concentrations of DEPC and reactions allowed to proceed to completion at each concentration.The mol histidine modified was calculated using ε_{245nm}= 3.2 mM^{-1} cm^{-1}. At a concentration of 8mM DEPC all four available histidines are modified (data not shown on figure). Boxed area indicates subset of points used in Figure 3.6(b).
(b) A comparison of histidine modification of CCP at pH 6 and 7.5. Modification of CCP (4μM) at pH 6 was carried out in 5mM Mes buffer.

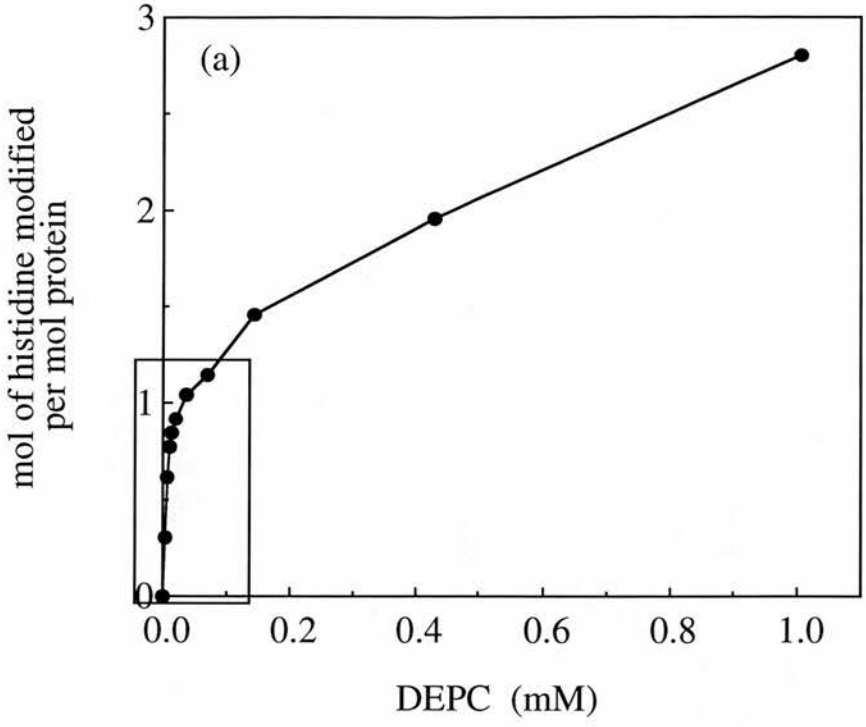
(a)
mol of histidine modified per mol protein
3
2
1
0
0.0
0.2
0.4
0.6
0.8
1.0
DEPC (mM)

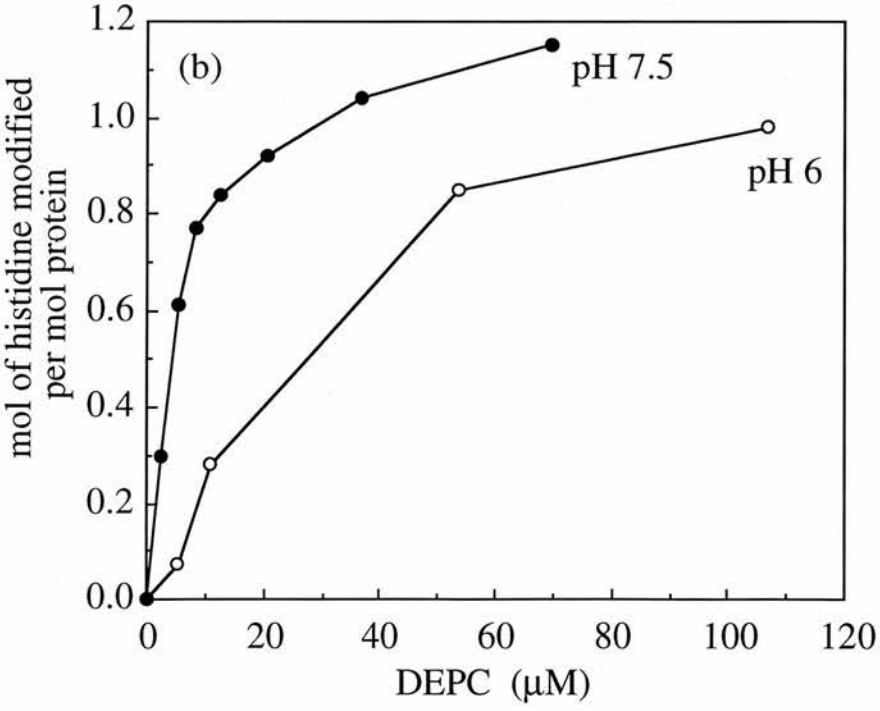
(b)
pH 7.5
pH 6
mol of histidine modified per mol protein
1.2
1.0
0.8
0.6
0.4
0.2
0.0
0
20
40
60
80
100
120
DEPC (μM)

Figure 3.7 DEPC modification of an easily modified histidine.
A CCP (4μM) in 5mM Hepes pH 7.5 was treated with DEPC (20μM). Trace **A**(i) shows the monophasic gain of absorbance at 245 nm on addition of DEPC. The end of the A_{245nm} rise was taken at 20 min and showed 0.6 mol of histidine modified per mol of protein, based on $\varepsilon = 3.2\ mM^{-1}\ cm^{-1}$. At this time a modified difference spectrum **A**(ii) from 300-240 nm was obtained (note this DEPC:protein ratio normally gave slightly higher mol of histidine modified).
B CCP (4μM) in 5mM Hepes pH 7.5 was treated with DEPC (100μM). Trace **B**(i) shows the biphasic gain of absorbance at 245 nm on addition of DEPC. The initial phase of the reaction displayed 1.0 mol of histidine modified per mol of protein. The end of the A_{245nm} rise, at 20 min, showed a total of 1.25 mol of histidine modified per mol of protein. Again a modified difference spectrum **B**(ii) from 300-240 nm was taken.

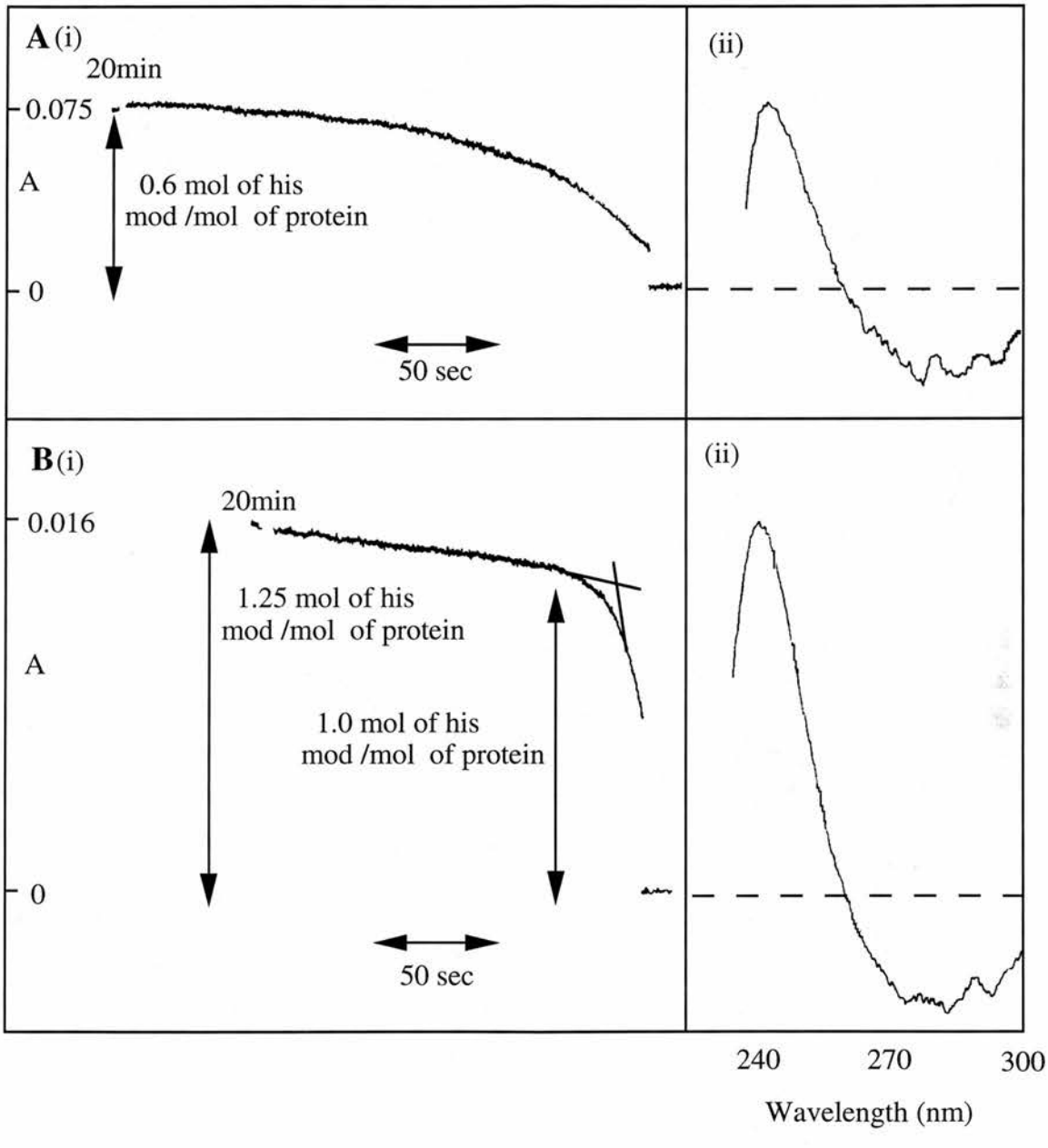
A (i)
20min
0.075
A
0.6 mol of his
mod /mol of protein
0
50 sec
(ii)
B (i)
20min
0.016
1.25 mol of his
mod /mol of protein
A
1.0 mol of his
mod /mol of protein
0
50 sec
(ii)
240
270
300
Wavelength (nm)

0.6 mol histidine modified per mol of protein (Figure 3.7 **A**(i)). A higher DEPC : CCP ratio generated a biphasic rise of absorbance at 245 nm. The initial fast phase is complete after modification of 1.0 mol of histidine, the slower phase modifying a further 0.25 mol of histidine (Figure 3.7 **B**(i)). Spectra taken from 240-300 nm confirmed the degree of modification for these two DEPC concentrations (Figure 3.7 **A , B**(ii)). A rigorous interpretation of these results is complicated by the fact that the final extent of modification is the result of the rate of modification, the rate of hydrolysis of the reagent and finally the rate of ethoxyformylhistidine reversal. However the results above show a single histidine to be more susceptible to modification by DEPC than any other histidines present in the protein.

The properties of CCP when modified at this single histidine are fully examined in Chapter IV. However it is sensible at this stage to inform the reader that modification of this susceptible histidine causes complete loss of ability to form the active state of CCP. The stability of the ethoxyformylated histidine is therefore of interest, to evaluate the feasibility of studies on the modified protein.

3.2.3.2 Stability of modification in 5mM Hepes pH 7.5

The hydrolysis of the ethoxyformylhistidine derivative of CCP in 5mM Hepes pH 7.5 does not follow a simple exponential, but 50% of the label is lost in 6 hours (Figure 3.8). The biphasic kinetics of decay seem to suggest there is more than one ethoxyformylhistidine derivative, each species with a different rate of reversal. This is not too surprising as the extent of modification was 1.1 mol histidine modified per mol of protein. This figure could represent, for example, 0.9 mol of the essential histidine modified and 0.2 mol of another histidine. Another noticeable feature of the reversal of modification spectrum, in 5mM Hepes pH 7.5, is the retention of the 265-300 nm trough as the 245 nm peak is gradually lost. This will become an important observation when correlating the loss of activity of CCP to only the 245 nm peak (Chapter IV).

A separate experiment determined that [^{14}C] DEPC labelled protein, left for 24 hours after modification, completely lost its single ethoxyformylhistidine based on

Figure 3.8 Stability of ethoxyformylhistidine in 5mM Hepes pH 7.5.
A Difference spectra of modified minus unmodified CCP were taken at different times after DEPC addition. CCP (5μM) in 5mM Hepes pH 7.5, was modified with DEPC to a final concentration of 25μM. The absorbance at 245 nm was maximal at 20 min (1.1 mol histidine modified per mol) and fell thereafter due to hydrolysis of ethoxyformylhistidine. Times shown are hours after this maximal extent of modification.
B The experimental points from **A** do not follow a simple exponential decay curve but do show 50% of the label lost in 6 hours.

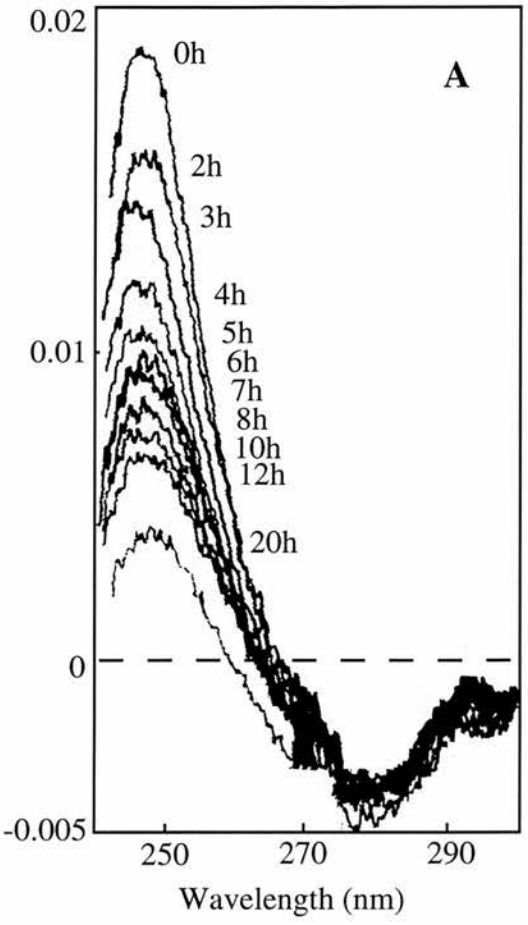
0.02
0.01
0
-0.005
0h
2h
3h
4h
5h
6h
7h
8h
10h
12h
20h
A
250
270
290
Wavelength (nm)

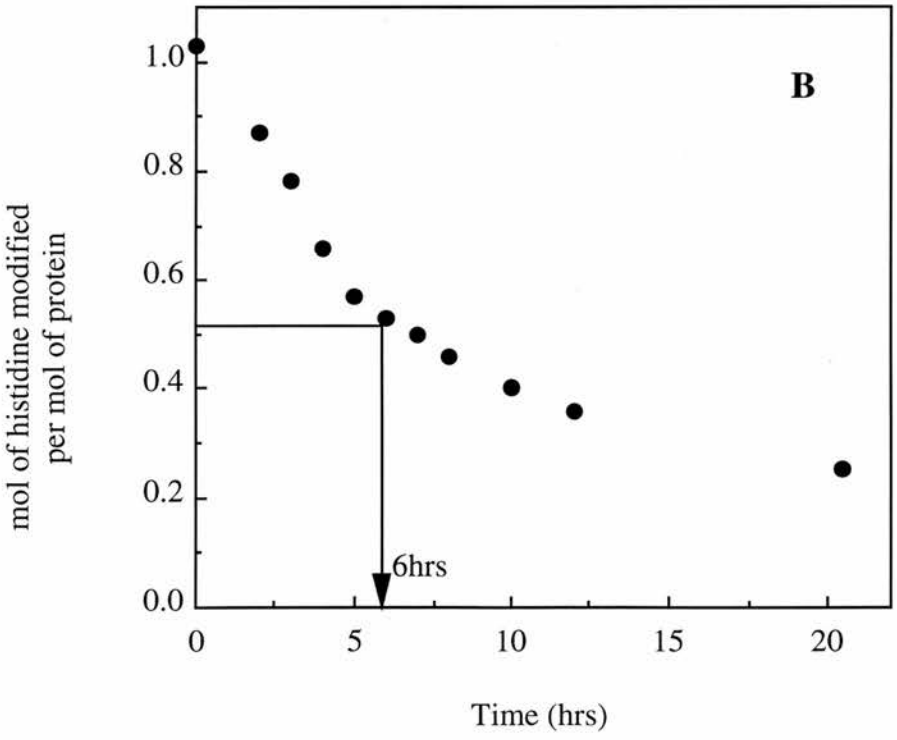
mol of histidine modified
per mol of protein
1.0
0.8
0.6
0.4
0.2
0.0
B
6hrs
0
5
10
15
20
Time (hrs)

spectrophotometric measurements at 245 nm, yet had retained almost all radioactivity. To make sense of this surprising result a slow transfer of the ethoxyformyl group to another amino acid in the protein was proposed and is demonstrated in Chapter VI.

3.2.3.3 Stability of modification in 0.1M ammonia solution

Ammonia solution was found to be useful in the separation of peptides of CCP (Chapter V) and therefore might prove useful in the isolation of modified peptides. However it was shown earlier in this chapter, that ethoxyformylimidazole rapidly decays in 0.1M ammonia solution and so it is predicted that ethoxyformylhistidine will be similarly unstable.

After modification of 1 mol of histidine from CCP, addition of ammonia solution allows excess reagent to rapidly modify an apparent total of six histidines, as calculated by the rise at 245 nm (data not shown). This is presumably due to denaturation of the protein allowing DEPC greater access and also to increased nucleophilic reactivity of the now unprotonated histidines. Although it is tempting to assume this 245 nm peak represents modification of all histidines present in CCP, quantitation of modification at this high pH is probably unreliable as disubstituted histidyl residues can form (Equation 3), thus increasing the size of the 245 nm peak. To determine the rate of reversal of a singly modified histidine in ammonia solution, excess DEPC must either be removed by gel filtration on a Sephadex G25 column or blocked with imidazole, post modification. After addition of ammonia solution the baseline was reset and the decomposition of the label monitored by the progressive formation of an absorption trough at ~245 nm (Figure 3.9 **A**). The loss of ethoxyformylhistidine follows an exponential decay curve with a half-life of 11.5 min (Figure 3.9**B**). Therefore ammonia solution is obviously unsuitable for isolation of modified peptides as the label would quickly be lost.

3.2.3.4 Stability of modification in 1% SDS

The reversal rate of ethoxyformylhistidine in 1% SDS was followed in an identical fashion to that determined in ammonia solution. Several hours after SDS addition and resetting the baseline of the modified CCP spectrum from 240-300 nm,

Figure 3.9 Stability of ethoxyformylhistidine in 0.1M ammonia solution. **A** CCP (5μM) was modified with DEPC to a final concentration of 25μM. After 20 min the modified difference spectrum showed 1.1 mol histidine modified per mol of protein. Imidazole solution pH 7.5 (2mM) was added, followed after 2 min by ammonia solution (0.1M). A new 300-240 nm baseline was immediately recorded. The absorbance at 245 nm fell thereafter due to hydrolysis of ethoxyformylhistidine. Times shown are minutes after the baseline was taken. The mol of histidine still modified at 5, 10, 13, 20, 30 and 44 min was determined by calculating the difference in absorbance at 245 nm from the 120 min spectrum when no ethoxyformylhistidine remains (ε = 3.2 mM^{-1} cm^{-1}).

B The experimental points are fitted to a theoretical exponential decay plot with $t_{1/2}$ = 11.5 min.

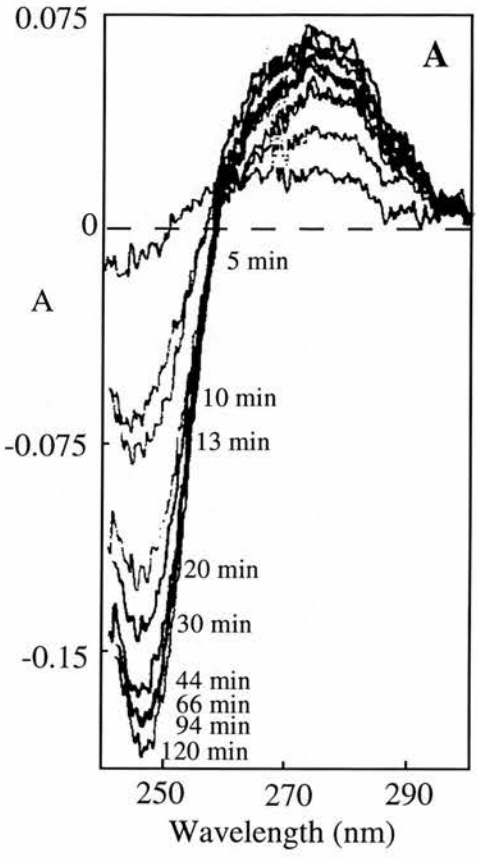
A
0.075
0
-0.075
-0.15
A
5 min
10 min
13 min
20 min
30 min
44 min
66 min
94 min
120 min
250
270
290
Wavelength (nm)

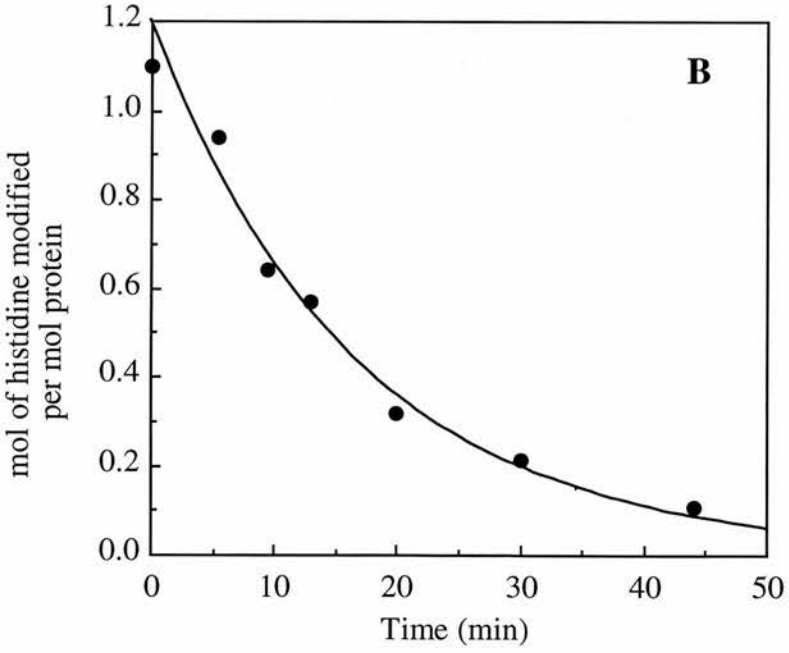
B
1.2
1.0
0.8
0.6
0.4
0.2
0.0
mol of histidine modified
per mol protein
0
10
20
30
40
50
Time (min)

there was no significant trough at 245 nm (data not shown). The reversal rate in SDS is dramatically increased, however, by addition of ammonia solution (0.1M) but is still slower than modified CCP in ammonia solution alone. This may be due to a hydrophobic coating of the protein preventing ammonia and/or water gaining access to the label. The fact that the rate of ethoxyformylhistidine reversal in 1% SDS is actually slower than in Hepes buffer proved extremely useful in the isolation of modified peptides.

3.2.3.5 Specificity of modification

In this type of study it is important to be confident of the specificity of modification and this is why the different features of the modified CCP spectrum were thoroughly examined. Of most concern were the features between 265 and 300 nm which are not present in the spectrum of ethoxyformylimidazole. Possible explanations that have been considered include: confirmational alterations in the protein structure, most likely within the haem environment, caused by modification of either the essential histidine or for example of the haem itself; modification of the essential histidine which then distorts the environment of nearby residues such as tyrosine or tryptophan; modification of susceptible residues such as tyrosine or tryptophan.

Both tyrosine and tryptophan modifications are known to result in an absorbance trough around 280 nm. Tryptophan modification by DEPC has been reported only rarely (Rosen et al.1970) as N-ethoxyformylation of Trp only occurs in extremely hydrophobic environments. O-ethoxyformylation of tyrosine is more common (Burstein et al.1974) and the extent of the absorbance change commonly seen in CCP would imply modification of at least one mol of tyrosine per mol of protein (E_{278nm} = 1.3 mM^{-1} cm^{-1}). Figure 3.8 shows that during reversal of modification in 5mM Hepes pH 7.5 the 245 nm peak is gradually lost but the 265-300 nm trough remains. However during reversal of modification in 0.1M ammonia solution the 265-300 nm trough reverses along with the 245 nm peak (Figure 3.9). This evidence seems to indicate the trough corresponds to modification of a tyrosine, or perhaps

tryptophan, which reverses only in ammonia solution. The strong evidence against such an explanation includes the mol of radioactive label per mol of protein determined from [^{14}C]DEPC incorporation, which correlates well with the figure determined from ΔA_{245nm}. The correspondence between the two types of measurement also holds good over short time periods of modification when no development of the trough between 265 and 300 nm has yet occurred (see Chapter VI, Figure 6.1). Thus despite the lack of a satisfactory explanation for the origin of the 265-300 nm features we conclude that they cannot be due to modification of another amino acid. The feature is also present in the spectra of modified yeast CCP and similar features have been observed in other proteins modified with DEPC (Burstein et al.1974; Bhattacharyya et al.1992)

In the following chapter it will be shown that the loss of ability to form the active state of *P.denitrificans* CCP is correlated with the absorbance gain at 245 nm and not with the presence of the 265-300 nm trough. The properties of the enzyme modified at a single histidine will be thoroughly characterised.

Chapter IV

An essential histidine in cytochrome c peroxidase

4.1 Introduction

The previous chapter introduced the histidine-specific reagent diethylpyrocarbonate and its reaction both with model compounds and cytochrome c peroxidase from *P.denitrificans*. An easily modified histidine in cytochrome c peroxidase was identified, which upon modification was relatively stable. The properties of the enzyme modified at this histidine are investigated in this chapter. As ethoxyformylation of the easily modified histidine causes fundamental changes to cytochrome c peroxidase the model of action for the enzyme is described once more.

Cytochrome c peroxidase contains a high potential, electron transferring haem and a low potential, peroxidatic haem. In the oxidised state the enzyme is inactive (Ronnberg et al.1981a; Ellfolk et al.1983; Gilmour et al.1994). The high potential haem shows partial high-spin character (Foote et al.1984) and is thought to be coordinated by His and Met. The low potential haem is also low-spin, inaccessible to ligands and thought to be coordinated by two His (Aasa et al.1981). Reduction of the electron transferring haem causes coordination by the distal histidine to be lost and access of hydrogen peroxide to the pentacoordinate haem is permitted (Ellfolk et al.1984; Foote et al.1985). Ca^{2+}, bound at the dimer interface, is required for this low to high spin-state transition at the peroxidatic haem (Gilmour et al.1993; Gilmour et al.1995).

This chapter describes the properties of cytochrome c peroxidase ethoxyformylated at a single histidine with DEPC. Our original expectation was that a distal ligand to the peroxidatic haem would only become accessible to modification in the active mixed-valence state when no longer coordinated to the haem. Although susceptibility of the different states of the enzyme to modification was not as predicted, modification of one histidine completely abolished activity.

4.2 Results and Discussion

4.2.1 The most easily modified histidine is essential for activity

It is worth re-emphasising that the active form of the enzyme is achieved by reduction of the electron transferring haem and the Ca^{2+}-dependent appearance of the high spin-state at the peroxidatic haem. Thus to fully assess the effect of modification of a single histidine on the oxidised enzyme, the protein must be reduced with ascorbate and the appearance of either activity or the high-spin band at 380 nm monitored on addition of Ca^{2+}. The gain of absorbance at 380, 500 and ~630 nm is diagnostic of a low to high spin-state transition of the haem iron in this ferrihaemprotein (see Chapter I, section 1.2.2.1).

Figure 4.1(a) demonstrates the loss of ability to form the high-spin 380nm band in the mixed-valence enzyme, after modification of one histidine in the oxidised state. These data are plotted in Figure 4.1(b) along with loss of catalytic activity upon modification of histidine. Thus modification of a single histidine in cytochrome c peroxidase abolishes both the ability to form the high spin-state and activity. In yeast cytochrome c peroxidase one mol of histidine is also readily modifiable at low concentrations of DEPC but in this case modification was not associated with loss of activity. This is consistent with the results of Bosshard et al. (1984) who found modification of only the fourth histidine to be modified resulted in loss of activity. This histidine was putatively identified as histidine 52 positioned distal to the haem and involved in promoting acid-base catalysis of hydrogen peroxide (see Chapter I, section 1.3.1). Similarly in horseradish peroxidase two histidines were modified by DEPC but it is the more slowly modified that is essential (Bhattacharyya et al.1992).

The good agreement between the proportional loss of activity and the modification of 1 mol of histidine (Figure 4.1) indicates that a single histidine is being modified, rather than, for example, two residues each at a level of 50%. There have been cases in enzymes (acidic proteases like pepsin) of an active site containing two key residues of the same type and the modification of either results in loss of activity. This is supported by the plots of Figure 3.6(a) and Figure 3.7 which indicate that one

Figure 4.1 Modification of a single histidine from *P.denitrificans* CCP abolishes catalytic activity and the ability of the enzyme to form the high spin mixed-valence state.

(a) shows the loss of ability to form the characteristic high-spin 380 nm band on modification of a single histidine. CCP (4μM) in 5mM Hepes pH 7.5 was modified for 20 min with DEPC at the following concentrations : 0μM, 1.5μM, 2.8μM, 5.6μM, 8.4μM, 12.2μM, 16.4μM, 24.6μM. The extent of modification for each DEPC concentration was calculated to be: 0, 0.12, 0.27, 0.46, 0.58, 0.68, 0.86, 1.0 mol of histidine modified per mol of protein respectively. The samples were then reduced with 1mM ascorbate pH 7 and 10μM DAD and the ability of the modified enzyme to form the active high spin-state was tested after addition of 1mM $CaCl_2$ (Gilmour et al.1993). The results are represented by difference spectra of the mixed-valence enzyme after Ca^{2+} treatment minus the mixed-valence enzyme. Each difference spectrum with decreasing ΔA_{380nm} correlates to the increased extent of modification as listed above. (b) Loss of ability to form the 380 nm band in the mixed-valence enzyme and loss of catalytic activity as histidine modification increases. The % high-spin of each sample was calculated from the changes at 380 nm in Figure 4.2a. Aliquots of each sample were assayed and activity determined (see Chapter II - Materials and Methods).

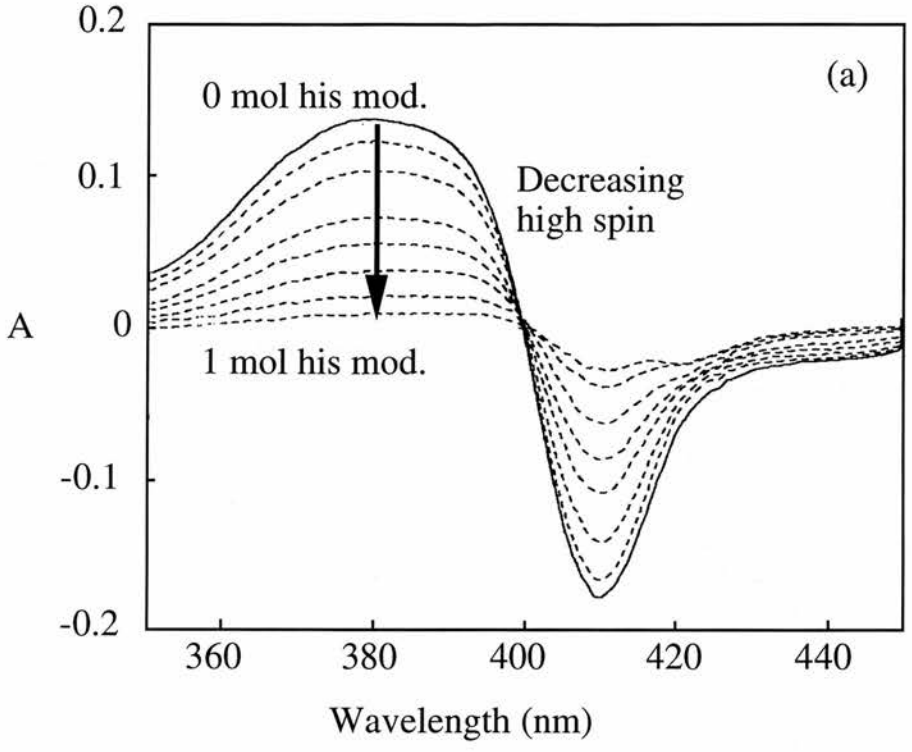
0.2
0.1
0
-0.1
-0.2
A
(a)
0 mol his mod.
Decreasing
high spin
1 mol his mod.
360
380
400
420
440
Wavelength (nm)

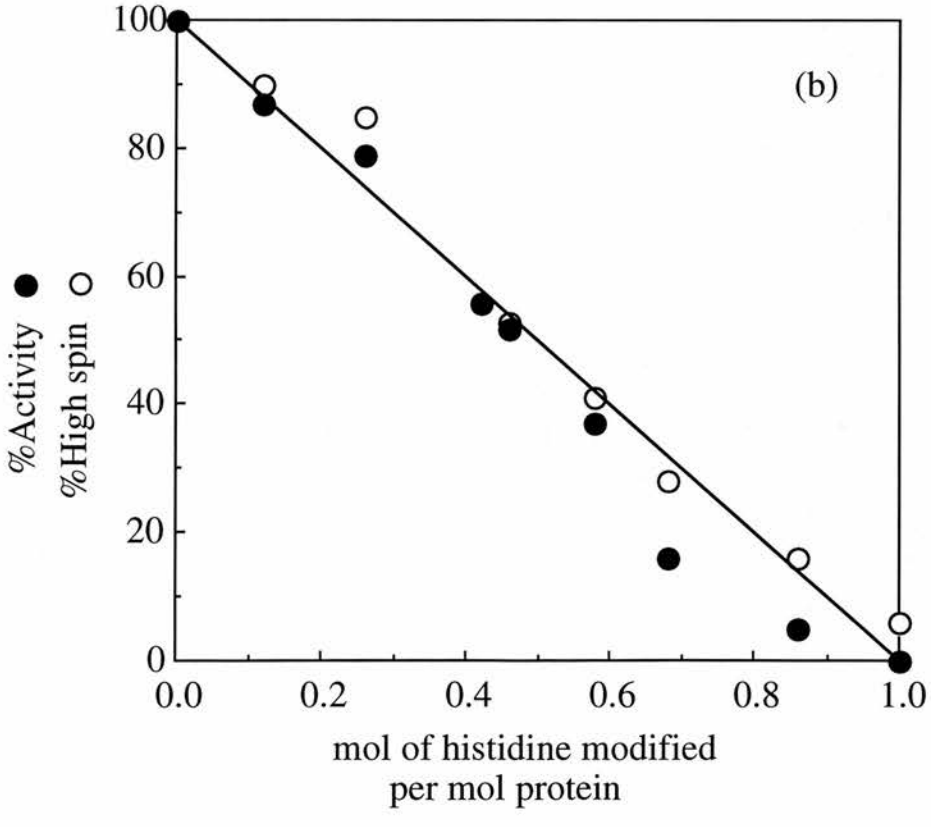
100
80
60
40
20
0
(b)
%Activity ●
%High spin ○
0.0
0.2
0.4
0.6
0.8
1.0
mol of histidine modified
per mol protein

histidine is particularly susceptible to modification. Beyond 20 min of reaction the slow loss of the ethoxyformyl groups from histidine exceeds further modification by residual reagent.

4.2.2 Modification of 0.5 mol histidine abolishes activity in dimeric enzyme

Under conditions where dimeric cytochrome c peroxidase is the dominant species (such as high [salt]), modification of only 0.5 mol histidine per mol of protein results in complete inactivation of the enzyme. Figure 4.2 compares the results of modifying dimeric enzyme to the results from Figure 4.1 where enzyme in the monomeric state requires modification of 1 mol histidine for inactivation of the enzyme. It should be remembered that the monomer : dimer equilibrium is reflected in the kinetics of high-spin formation as measured at 414 nm (see Chapter I, section 1.2.2.3). Thus the relative predominance of monomer or dimer can be quantified under different conditions .

As modification of only 0.5 mol histidine per mol results in complete inactivation of the dimeric enzyme, the molecules of the dimer must show strong cooperativity, a feature already found for the binding of Ca^{2+} to calcium binding site II (see Chapter I, section 1.2.2.3). As a result of this experiment the standard conditions of modification throughout these studies are under conditions where the monomeric species predominates.

4.2.3 Electron paramagnetic resonance spectroscopy of native and modified cytochrome c peroxidase

E.p.r. spectra of native (Gilmour et al.1993; Prazeres et al.1994) and modified cytochrome c peroxidase are shown and interpreted below. Figure 4.3(a) displays the e.p.r. spectrum of the native oxidised peroxidase and shows two resonances at g_{max} 3.4 and 3.0. The presence of these two signals, characteristic for low-spin ferric haems, reflect the separate environments of the two haems. The fact that the relative intensity of the 3.4 signal, assigned to the high potential haem, is less than the 3.0

Figure 4.2 Modification of only 0.5 mol histidine per mol abolishes activity in dimeric cytochrome c peroxidase

Cytochrome c peroxidase solutions (4μM) in 5mM Hepes pH 7.5, 50mM NaCl, 2mM $CaCl_2$ (closed circles) were treated with increasing concentrations of DEPC for 20 min (0-25μM). The amount of ethoxyformylhistidine was calculated from the increase in absorbance at 245 nm. Modified samples were then reduced with ascorbate (1mM) and DAD (10μM) in the presence of $CaCl_2$ (2mM). Samples were assayed (see Chapter I - Materials and Methods) and activity expressed as a percentage of that for unmodified CCP. The data is compared to that from Figure 4.1(b) where solutions of cytochrome c peroxidase were modified in 5mM Hepes pH 7.5 alone (open circles).

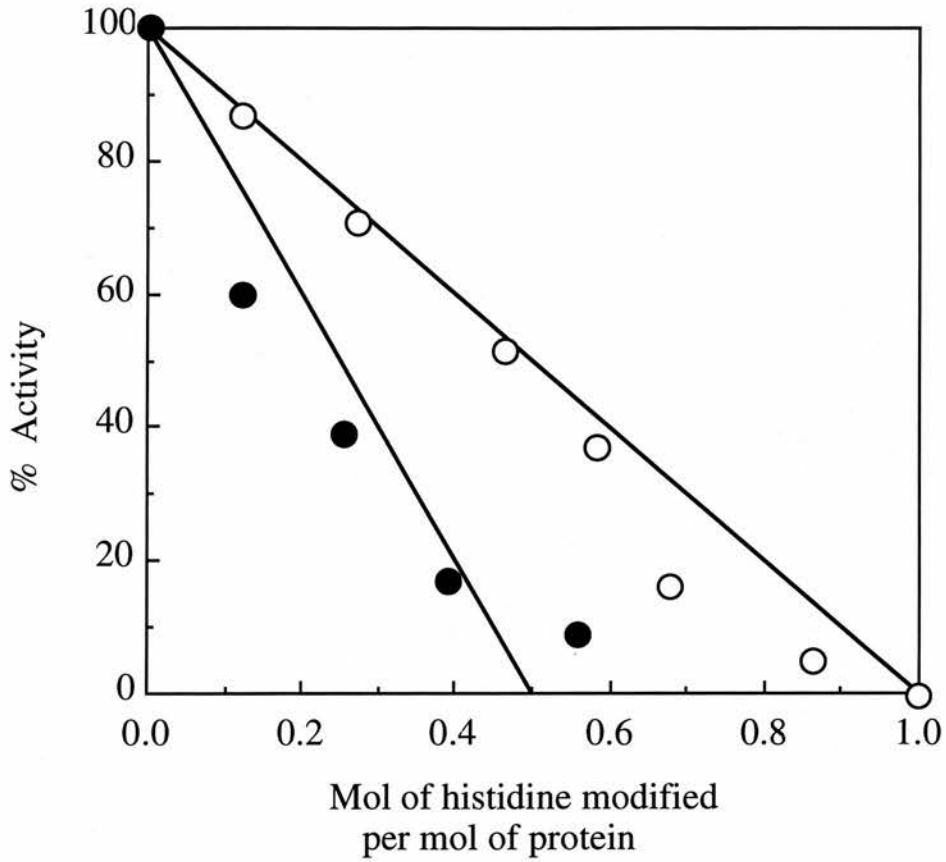
100
80
60
40
20
0
% Activity
0.0
0.2
0.4
0.6
0.8
1.0
Mol of histidine modified
per mol of protein

Figure 4.3 E.p.r. spectroscopy of native and modified cytochrome c peroxidase

(a) E.p.r. spectra of native cytochrome c peroxidase in oxidised, mixed-valence and mixed-valence + Ca^{2+} states. 9ml of cytochrome c peroxidase (4μM) in 5mM Hepes pH7.5 was concentrated to 180μl and spectra recorded from this 200μM sample (oxidised), after reduction with 1mM ascorbate and 10μM DAD (mixed-valence - Ca^{2+}) and after addition of 1mM $CaCl_2$ (mixed-valence + Ca^{2+}).

(b) E.p.r. spectra of modified cytochrome c peroxidase in oxidised, mixed-valence and mixed-valence + Ca^{2+} states. To 9ml of CCP (4μM) in 5mM Hepes pH7.5 was added DEPC to a final concentration of 20μM which resulted in 1.1 mol of histidine modified per mol of protein. The solution was concentrated and spectra recorded as for the native sample. Experimental conditions :- temperature 8K; microwave frequency 9.45GHz; microwave power 2mW; modulation 10.39; gain 1.6×10^5. g values for selected resonances are shown.

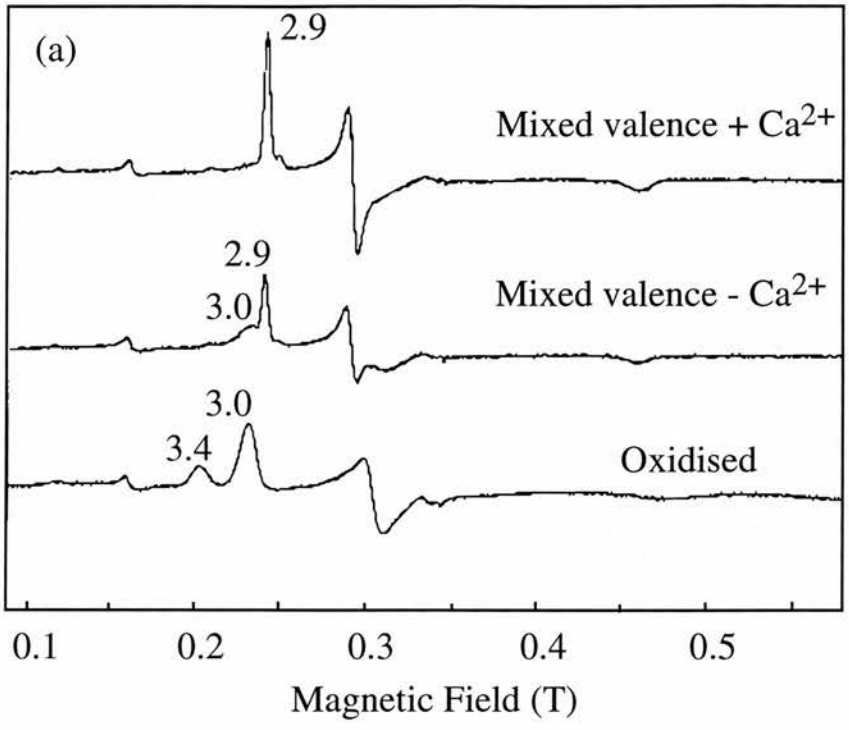
(a)
2.9
Mixed valence + Ca2+
2.9
3.0
Mixed valence - Ca2+
3.0
3.4
Oxidised
0.1
0.2
0.3
0.4
0.5
Magnetic Field (T)

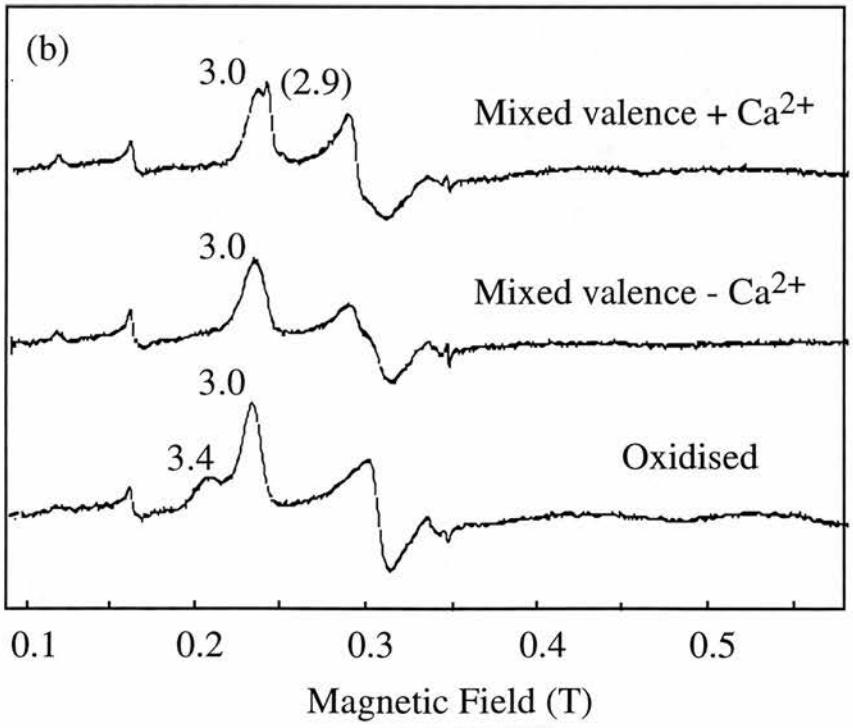
(b)
3.0
(2.9)
Mixed valence + Ca2+
3.0
Mixed valence - Ca2+
3.0
3.4
Oxidised
0.1
0.2
0.3
0.4
0.5
Magnetic Field (T)

signal, assigned to the low potential haem, results from the fact that the intensity of an e.p.r. line depends on the other accompanying g-values. A mathematical expression relating the intensities (I) of the e.p.r. lines was deduced by Aasa et al. (1981).

$$Ig_{max} \propto \sqrt{(g_{min}^2 + g_{med}^2)} \,/\, (1 - g_{min}^2/g_{max}^2)\,(1 - g_{med}^2/g_{max}^2)$$

This means that if the set of g-values are 3.4, 2.0 and 0.6 for the high potential haem and 3.0, 2.3 and 1.4 for the low potential haem, this factor will be 5.5 for the high potential haem and 12.6 for the low potential haem. So if we assume equal amounts of each haem, the intensity of the e.p.r. signal of the low potential haem will be between 2 and 3 times that of the high potential haem.

The g_{max} 3.4 signal disappears upon reduction of the high potential haem, (ferrous haems are diamagnetic and therefore e.p.r. silent) and this was the basis of the signal assignment to the high potential haem. In the e.p.r. spectrum of the mixed-valence enzyme, the transition of the g_{max} 3.0 signal to the Ca^{2+} dependent g_{max} 2.9 signal was equated with the low to high spin-state transition at the peroxidatic haem, at room temperature (Figure 4.3(a)). Because of the high protein concentrations needed for e.p.r. spectroscopy, endogenous Ca^{2+} allows partial appearance of this 2.9 signal in the mixed-valence spectrum in the absence of added Ca^{2+}. The modified enzyme cannot undergo the transition to the active form (Figure 4.3(b)) and is mostly trapped in a low-spin mixed-valence form with g_{max} 3.0. Therefore in the modified enzyme, both e.p.r. and visible spectroscopy reflect the inability of the peroxidatic haem to go high-spin upon reduction of the electron transferring haem in the presence of Ca^{2+}.

4.2.4 Nuclear magnetic resonance spectroscopy of native and modified cytochrome c peroxidase

The process of enzyme activation and the effect of histidine modification on the enzyme can also be followed by n.m.r.

Figure 4.4(a) shows the low-field region of the n.m.r. spectra of native cytochrome c peroxidase. Because iron in ferric haems is paramagnetic, protons from

Figure 4.4 300 MHz ^{1}H n.m.r. spectroscopy of native and DEPC-treated cytochrome c peroxidase

(a)(i) The low-field region of the 300 MHz n.m.r. spectra of oxidised cytochrome c peroxidase (1mM) in 50mM Hepes pH 7.5. (ii) The sample was reduced with DAD (5μM) and ascorbate (5mM) to generate the mixed-valence state. (iii) $CaCl_2$ (5mM) was then added to give the mixed-valence state plus Ca^{2+}.

(b) N.m.r. spectra of DEPC-treated cytochrome c peroxidase in (i) oxidised, (ii) mixed-valence and (iii) mixed-valence + Ca^{2+} states. Cytochrome c peroxidase (4μM) in 5mM Hepes pH 7.5 was modified with DEPC (20μM) to the extent of 1.0 mol histidine per mol. The protein solution was exchanged with D_2O before being concentrated to 1mM and spectra recorded as for the native sample.

Experimental conditions:- temperature 303 K; 2000 scans; 4K data points. Spectra recorded by S. Prazeres, Universidade Nova de Lisboa.

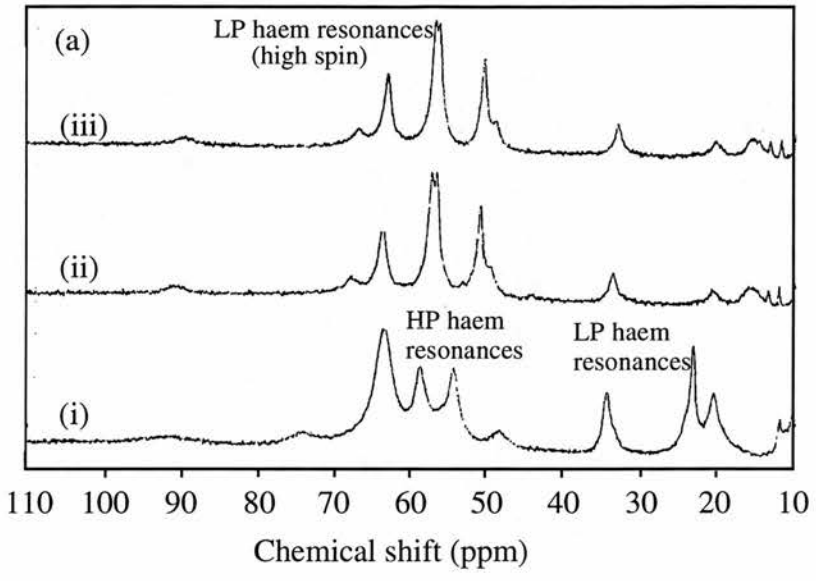
(a)
LP haem resonances
(high spin)
(iii)
(ii)
HP haem
resonances
LP haem
resonances
(i)
110 100 90 80 70 60 50 40 30 20 10
Chemical shift (ppm)

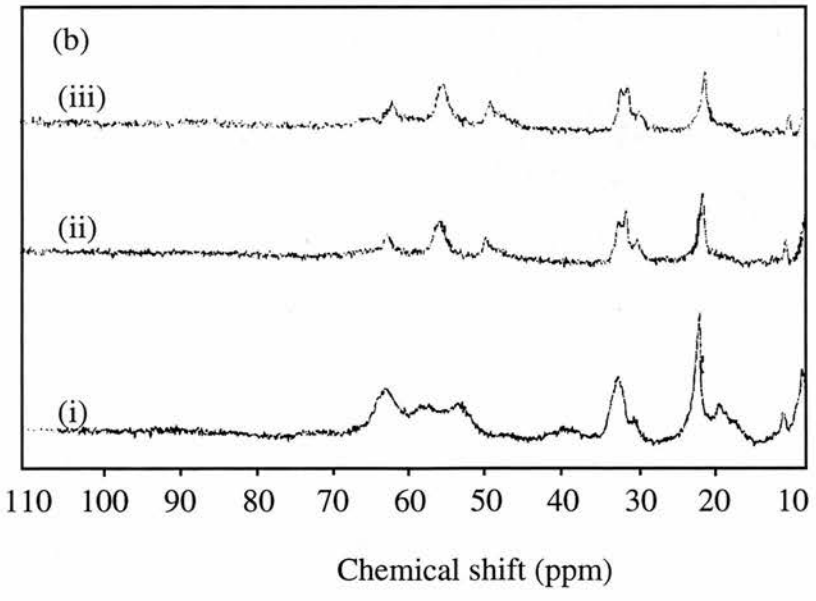
(b)
(iii)
(ii)
(i)
110 100 90 80 70 60 50 40 30 20 10
Chemical shift (ppm)

the haem methyl groups are detected, shifted from the main diamagnetic envelope region. N.m.r. spectroscopy confirms the presence of a high-spin haem in both oxidised and mixed-valence haems (Gilmour et al.1993; Prazeres et al.1993; Prazeres et al.1994). In the spectrum of the oxidised enzyme (Figure 4.4a(i)) there are two sets of resonances, one between 54 and 65 ppm and another set between 22 and 34 ppm. The resonances between 54 and 65 ppm were assigned to the partially high-spin, high potential electron transferring haem. The chemical shifts of the resonances between 54 and 65 ppm are very sensitive to experimental conditions (for example compare Figure 4.4a(i) to Figure 3 from Gilmour et al.(1993)). This sensitivity probably reflects some small change in the spin-state equilibrium. The broad resonance around 90 ppm is assigned to the γ-CH_3 group of a methionine axial to the high potential haem. The two methyl resonances at 22 and 34 ppm are assigned to the fully low-spin, low potential haem. In the spectrum of the mixed-valence enzyme (Figure 4.4a(ii)) the resonances previously observed are replaced by four new haem methyl resonances located between 50 and 65 ppm and assigned to the fully high-spin, low potential haem. Because of the high protein concentrations needed for n.m.r. spectroscopy, endogenous Ca^{2+} allows conversion of the low potential haem to the high spin-state upon reduction of the high potential haem; thus the addition of Ca^{2+} has no effect on the n.m.r. spectrum (Figure 4.4a(iii)).

After modifying a 4μM solution of cytochrome c peroxidase with DEPC to the extent of 1 mol of histidine per mol of protein, the solution was concentrated to approximately 1mM for n.m.r. spectroscopy. Also as preparation of the protein sample required exchange with ^2H_2O and these procedures took several hours, reversal of modification complicated the resultant spectrum. The n.m.r. spectrum of the modified oxidised peroxidase shows important differences in both haems. Comparing the n.m.r. spectrum from oxidised native (Figure 4.4a(i)) and modified (Figure 4.4b(i)) protein, the sets of resonances between 54 and 65 ppm (associated with the high potential haem) are very much diminished, as are some but not all of the resonances between 22 and 34 ppm (associated with the low potential haem). Similarly upon

reduction of the high potential haem, all the high-spin resonances arising from the low potential haem are significantly smaller than in the native enzyme. It is clear though that none of the resonances have been totally lost and this is probably due to reversal of modification.

To overcome the problem of reversal and thus achieve definitive n.m.r. spectra of modified protein, 1mM of oxidised cytochrome c peroxidase was titrated with DEPC. At a final concentration of 2.01mM the haem methyl resonances between 54 and 65 ppm, originating from the partial high-spin, high potential haem, were abolished (Figure 4.5). One of the resonances at 19 ppm, originating from the low potential haem methyl was similarly abolished. At a [DEPC] of 2.01mM the modified protein was reduced with ascorbate and DAD, and spectra taken in the absence and presence of added Ca^{2+}. No high-spin resonances from the low potential haem methyls were observable in the region 50 to 65 ppm.

The ratio of 1 CCP : 2 DEPC required to abolish high-spin signals in both oxidised and mixed-valence forms is smaller than the ratio 1 CCP : 5 DEPC needed at μM [protein]. However it should be remembered that at mM [protein] the dimeric form of the enzyme will predominate and so modification of only 0.5 mol of histidine per mol would be expected to abolish the high-spin signals. Also the kinetics of reaction will be much faster at the high protein concentrations required for n.m.r.

Therefore in the modified oxidised enzyme, n.m.r. spectroscopy reflects the fully low spin-state of the electron transferring haem and the inability of the peroxidatic haem to go high-spin upon reduction of the electron transferring haem, in the presence of Ca^{2+}.

4.2.5 Potentiometric redox titration of modified cytochrome c peroxidase

After modifying the essential histidine in cytochrome c peroxidase, oxidative and reductive titrations of the high potential haem in the presence of Ca^{2+} were performed. The respective reductive and oxidative titrations are shown in Figures 4.6A(i) and 4.6A(ii). The data from both titrations are fitted to Nernst plots with

Figure 4.5 ^{1}H N.m.r. spectroscopy of cytochrome c peroxidase titrated with DEPC

Cytochrome c peroxidase (1mM) in 50mM Hepes pH 7.5 was exchanged with D_2O and then treated with DEPC to give final concentrations of 0mM, 0.76mM and 2.01mM. The low-field region of the 300 MHz n.m.r. spectrum at each concentration was recorded. To the sample with 2.01 mM DEPC was added DAD (5μM) and ascorbate (10mM) to generate the mixed-valence form. Excess $CaCl_2$ (10mM) was then added to give the mixed-valence state plus Ca^{2+}. Spectra recorded by S.Prazeres, Universidade Nova de Lisboa.

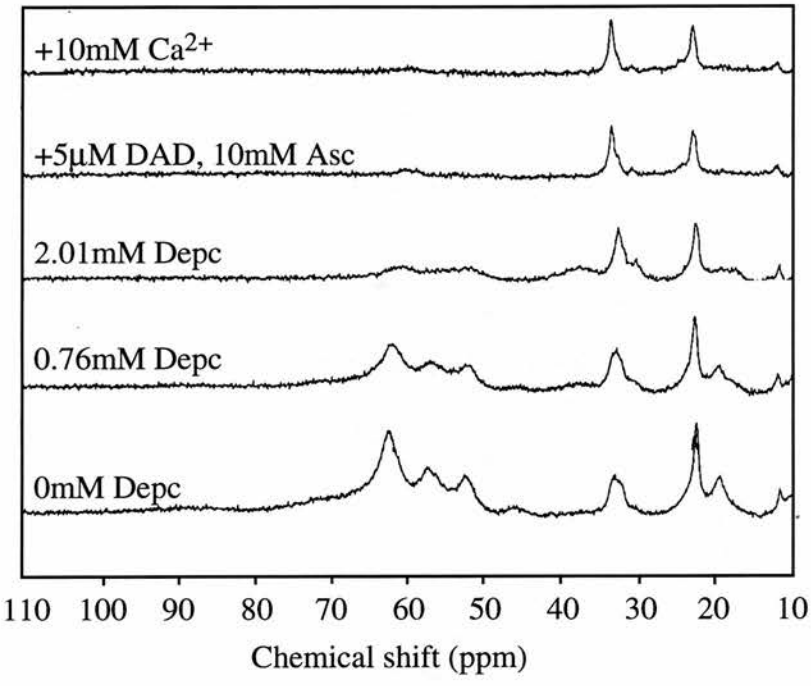
+10mM Ca2+
+5μM DAD, 10mM Asc
2.01mM Depc
0.76mM Depc
0mM Depc
110 100 90 80 70 60 50 40 30 20 10
Chemical shift (ppm)

Figure 4.6 Potentiometric redox titration of cytochrome c peroxidase modified at a single histidine

Cytochrome c peroxidase (5μM) in 5mM Hepes pH 7.5 was modified to an extent of 1.0 mol of histidine per mol. The redox titration of the modified protein was performed as described in Chapter II- Materials and Methods. A(i) and A(ii) show the reductive and oxidative titrations of the high potential haem only, as followed in the region of the α and β bands. A(iii) is a Nernst analysis of the redox titration of the high potential haem with reductive (open circles) and oxidative (closed circles) arms. The midpoint potential (E_m) is +222mV.

B is a Nernst plot of both the reductive titration (open circles) of the high potential haem and the oxidative titration of the same haem after the low potential haem had undergone reduction and oxidation (closed circles).

The data are fitted to theoretical plots with slopes of 59mV (25°C) derived from the Nernst equation (see Chapter II- Materials and Methods).

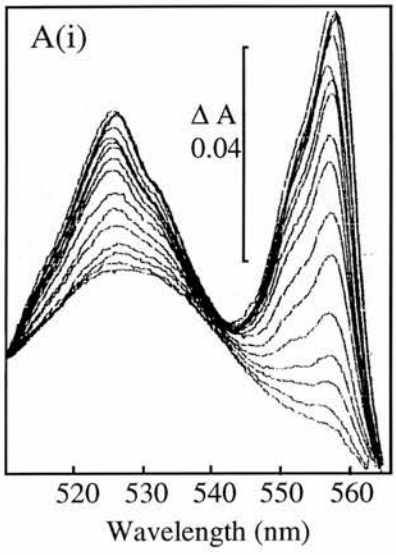
A(i)
Δ A
0.04
520 530 540 550 560
Wavelength (nm)

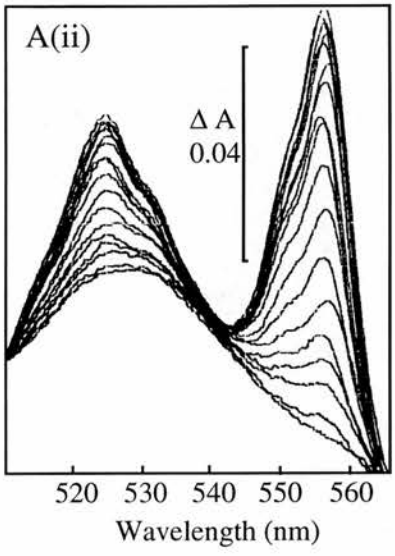
A(ii)
Δ A
0.04
520 530 540 550 560
Wavelength (nm)

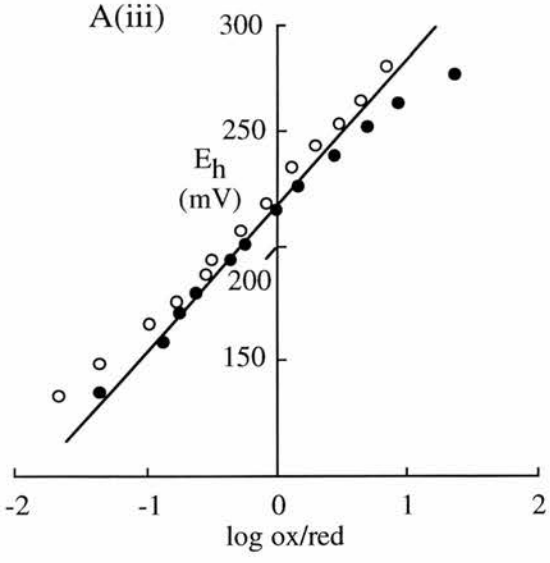
A(iii)
300
250
E_h
(mV)
200
150
-2 -1 0 1 2
log ox/red

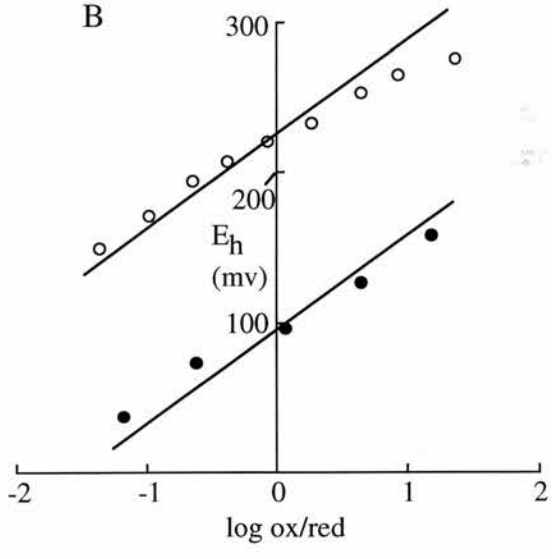
B
300
200
E_h
(mv)
100
-2 -1 0 1 2
log ox/red

slopes of 59mV (25°C) (Figure 4.6A(iii)). The high potential haem of the modified protein (in the absence or presence of Ca^{2+}) has a midpoint potential of 222mV. This compares with the midpoint potential of the high potential haem of the native enzyme, in the presence of Ca^{2+}, 226mV and in the absence of Ca^{2+}, 176mV (Gilmour et al.1993). Non-concordance of the mid-point potential of the high potential haem in the absence and presence of Ca^{2+} was proposed by the authors to reflect the influence of the spin-state of the low potential haem. When the high potential haem is titrated in the presence of Ca^{2+}, the low potential haem is high-spin, but in the absence of Ca^{2+} remains low-spin.

In either the absence or presence of Ca^{2+}, modification of the essential histidine abolishes the ability of the low potential haem to form the high spin-state upon reduction of the high potential haem. Therefore we might have expected a midpoint potential for the high potential haem of ~176 mV, that of the native CCP in the absence of Ca^{2+}. The fact that the potential is ~222mV shows other factors are involved. Later in this Chapter it will be shown that modification of the essential histidine in the oxidised enzyme causes a high to low spin-state transition at the high potential haem. This spin-state transition would be predicted to have an affect on the midpoint potential. Both redox states prefer a six coordinate octahedral geometry, and therefore it might be predicted that the high to low spin-state transition of the high potential haem would stabilise the oxidised form and therefore lower the redox potential. However the factors influencing redox potentials are numerous and to a large degree not well understood, at least on a quantitative basis.

The redox potential of both high and low potential haems are determined in the native protein by successive reduction of both haems with sodium dithionite followed by oxidation of both haems with potassium ferricyanide. Although the low potential haem is difficult to titrate accurately, a midpoint potential of -100 to -200mV has been calculated (Gilmour et al.1993). Reduction of the low potential haem of the modified cytochrome c peroxidase causes a permanent change in the protein, so that the following oxidative titration of both haems show hysteresis relative to the respective

reductive titrations. Figure 4.6B is a Nernst plot displaying this hysteresis of oxidative and reductive titrations of the high potential haem, the oxidative titration performed after reduction and reoxidation of the low potential haem. There is no satisfactory explanation for this hysteresis of midpoint potentials and no record of such a phenomenon in the literature.

4.2.6 Specificity of modification

The difference spectrum due to modification at pH 7.5 showed the presence of a shallow trough between 265-300 nm (Figure 3.5A(ii)). We wanted to be certain that this was not an indicator of modification of aromatic acids such as tyrosine or tryptophan which may affect the activity of the protein. A difference spectrum (Figure 3.5A(i)) obtained after modification for 2 min showed no trough between 265-300 nm and yet the histidine modified correlated well with the proportion of protein unable to form the high spin-state. Approximately 0.6 mol of histidine per mol of protein was modified, resulting in 40% of the enzyme retaining the ability to go to its active form in the mixed-valence plus Ca^{2+} state.

Also during reversal of modification the 245 nm peak is gradually lost but the 265-300 nm trough remains (Figure 4.7(a)). This loss of the ethoxyformyl group is associated with proportional recovery of the ability to form the active state of the enzyme (Figure 4.7(b)). The broad trough between 265 and 300 nm persists and therefore, whatever its origin, it cannot be associated with active state changes. In a separate experiment it was further determined that regain of catalytic activity also correlated with the loss of a single ethoxyformylhistidine. Therefore the appearance of the trough between 265 and 300 nm is not associated with changes in the activity of the enzyme and those changes we observe are due to histidine modification.

4.2.7 Modification of the different redox states of cytochrome c peroxidase and the protective effect of CN^-

The susceptibilities to modification of the three redox states of the enzyme are very different and not as we originally predicted. For the two mixed-valence forms of

Figure 4.7 Loss of ethoxyformylhistidine with time correlates with regain of the high spin state

(a) Difference spectra of modified minus unmodified CCP were taken at different times after DEPC addition. CCP (12μM) in 5mM Hepes pH7.5, was modified with DEPC to a final concentration of 45μM. The absorbance at 245 nm was maximal at 20 min (1.0 mol histidine modified per mol) and fell thereafter due to slow hydrolysis of ethoxyformylhistidine. Times shown are hours after this maximal extent of modification.

(b) The mol of ethoxyformylhistidine remaining at a given time was obtained from measurements at 245 nm. The extent of the ability to form the high spin-state was measured. 2μM aliquots were taken at each time point after modification. These were reduced with ascorbate (1mM) and DAD (10μM) and the amount of high-spin formed by the enzyme after addition of $CaCl_2$ (1mM) was measured at 380 nm (as described in the legend to Figure 4.1) and expressed as a percentage of an unmodified sample.

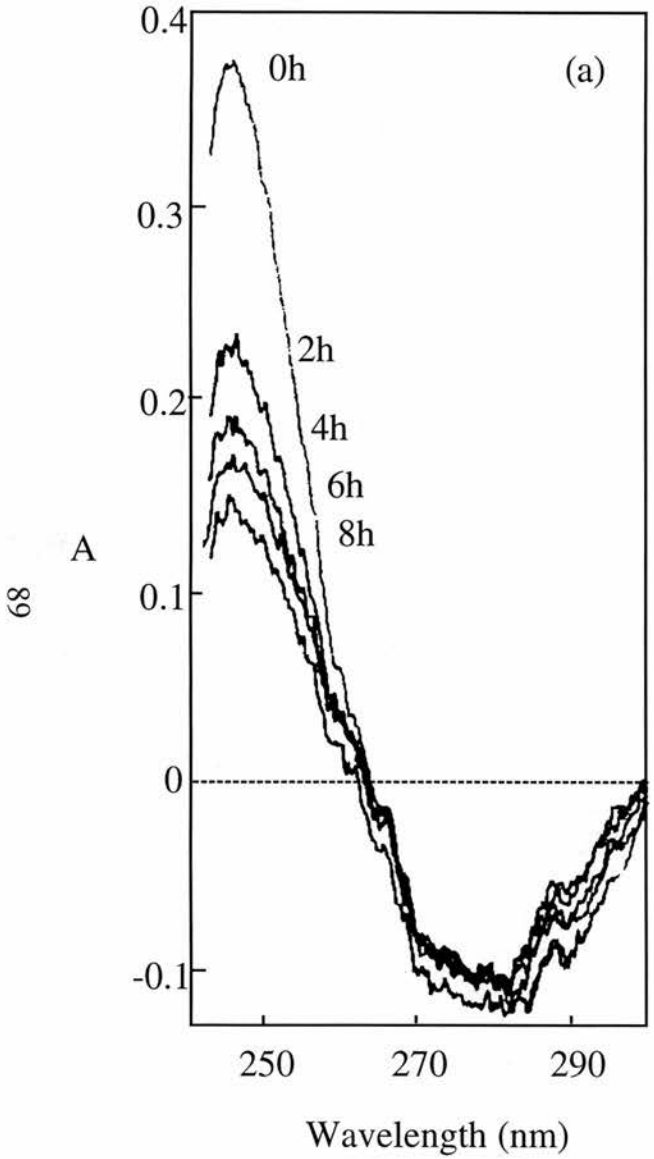
0.4
0.3
0.2
0.1
0
-0.1
A
0h
2h
4h
6h
8h
(a)
250
270
290
Wavelength (nm)

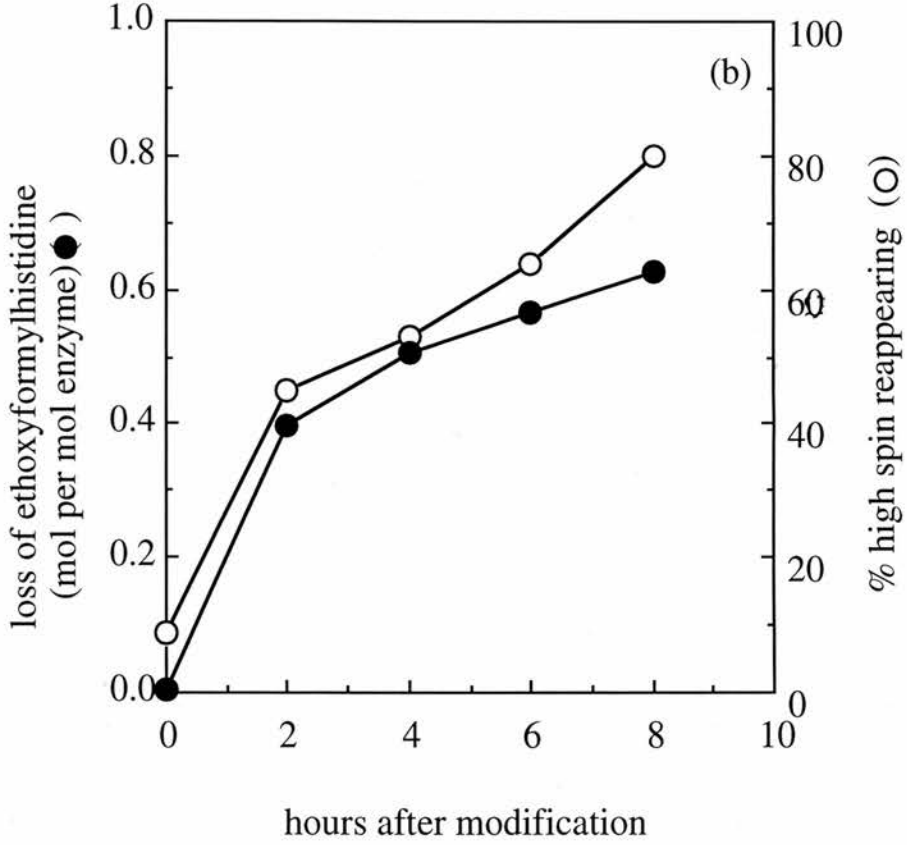
1.0
0.8
0.6
0.4
0.2
0.0
loss of ethoxyformylhistidine
(mol per mol enzyme) (●)
(b)
100
80
60
40
20
0
% high spin reappearing (○)
0
2
4
6
8
10
hours after modification

because ascorbate interferes with UV measurements. [^{14}C] DEPC was used to determine the extent of modification in the oxidised and mixed-valence high spin-states (Table 4.1). The result indicates that the histidine modified in the oxidised enzyme at low levels of DEPC is not modified in the mixed-valence high spin-state until higher levels of reagent are used. Figure 4.8 shows that the oxidised enzyme at 4μM loses all ability to form the active spin-state at 20μM DEPC, whilst this only occurs with the mixed-valence low-spin and mixed-valence high spin-states, at much higher concentrations of reagent. These results show that in the oxidised enzyme the essential histidine is more susceptible to modification than in the mixed-valence low spin-state. Similarly the essential histidine in the mixed-valence low spin-state of the enzyme is more susceptible to modification than in the mixed-valence high spin-state.

We originally proposed that histidine 275, the putative distal ligand to the peroxidatic haem (Aasa et al.1981), would not be modifiable in either the oxidised or mixed-valence low spin-state of the enzyme because of coordination to the iron. In the mixed-valence high spin-state, histidine 275 would dissociate from the iron and become accessible and therefore modifiable. However the results clearly show a histidine that is easily modified in the fully oxidised state of the enzyme but is progressively more difficult to modify in the mixed-valence low and high spin-states. The initial conclusion was that the essential histidine could not be the distal ligand to the peroxidatic haem but this was tempered by the result of the next experiment.

The continuation of the experiment in Figure 4.8 shows that modification of the CN^- adduct of the mixed-valence high-spin enzyme, with levels of DEPC that completely inactivate the same state in the absence of CN^-, yields an enzyme which retains almost all activity. When CN^- is removed by molecular exclusion (a process that also reoxidises the enzyme) the modified protein, at 4μM, can be further modified with a 5x excess of DEPC to give complete loss of the ability to form the high spin-state. Addition of CN^- to the oxidised and mixed-valence low spin-states has no effect on the modifiability of the enzyme. These results show that CN^-, when bound to the peroxidatic haem, protects an essential histidine from modification and imply that this

Table 4.1 Extent of modification of oxidised and mixed-valence high-spin forms of cytochrome c peroxidase using [^{14}C] DEPC.

Cytochrome c peroxidase (4μM) in 5mM Hepes pH 7.5 was treated with [^{14}C] DEPC to final concentrations of 20μM (5 DEPC : 1 CCP) and 1.2 mM (300 DEPC : 1 CCP). After 20 min these two solutions were desalted on G25 Sephadex columns equilibrated in 5mM Hepes pH 7.5 and 200μl aliquots of the desalted material added to 4ml scintillation fluid. To a further two solutions of cytochrome c peroxidase (4μM) in 5mM Hepes pH 7.5 was added ascorbate (1mM), DAD (10μM) and $CaCl_2$ (1mM) and then similarly treated. Mol of histidine modified per mol protein was calculated on the basis that 1nmol [^{14}C]-ethoxyformylhistidine gave 2919 dpm (see Chapter III). Experiment performed by Dr. G.W. Pettigrew.

		mol ethoxyformylhistidine per mol of protein
5 : 1 DEPC : CCP	Oxidised CCP	1.0
	Mixed valence, high spin CCP	0.2
300 : 1 DEPC : CCP	Oxidised CCP	3.3
	Mixed valence, high spin CCP	3.5

Figure 4.8 Relative susceptibility to modification by DEPC of the different states of cytochrome c peroxidase

Solutions of cytochrome c peroxidase were treated as follows to generate the four different redox / spin-state forms of the enzyme. Cytochrome c peroxidase (4μM) in 5mM Hepes pH 7.5 (**Oxidised CCP**) was reduced with ascorbate (1mM) and DAD (10μM) (**Mixed-valence low-spin CCP**). Addition of $CaCl_2$ (1mM) initiates the low to high spin-state transition (**Mixed-valence high spin CCP**). NaCN (100μM) pH7 binds to the pentacoordinate high-spin haem (**Cyano mixed-valence CCP**). CN^- was removed and the enzyme reoxidised by molecular exclusion on a G25 Sephadex column equilibrated with calcium free 5mM Hepes pH 7.5. DEPC was added to each form of CCP until the enzymes ability to form the high spin-state was abolished. This property is measured in each form by generating the mixed-valence low spin-state after modification and monitoring the changes in A_{380nm} upon addition of $CaCl_2$ (1mM). The DEPC : CCP ratio required to abolish the ability to form the high spin-state is noted next to each form of the enzyme.

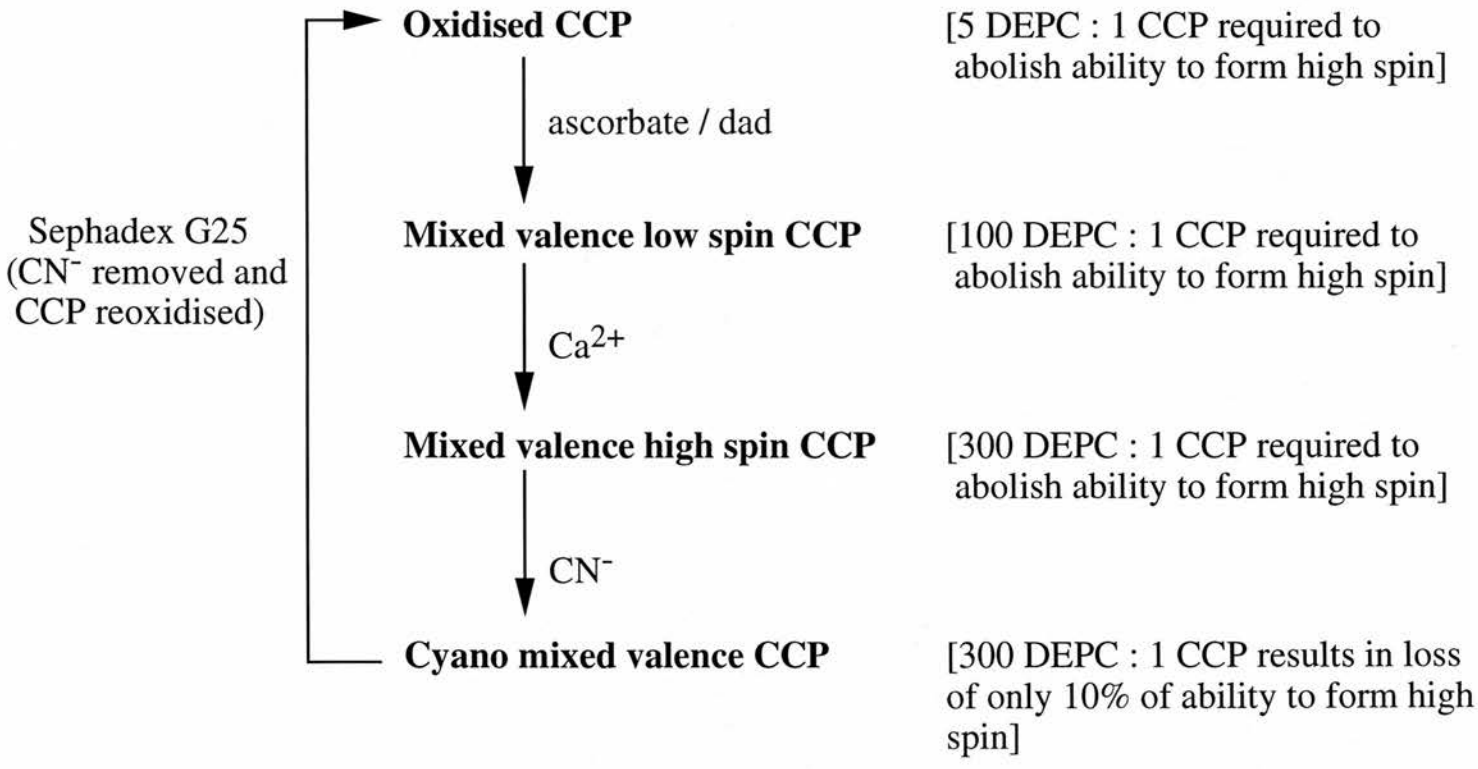
Oxidised CCP
[5 DEPC : 1 CCP required to abolish ability to form high spin]
ascorbate / dad
Mixed valence low spin CCP
[100 DEPC : 1 CCP required to abolish ability to form high spin]
Sephadex G25
(CN- removed and
CCP reoxidised)
Ca2+
Mixed valence high spin CCP
[300 DEPC : 1 CCP required to abolish ability to form high spin]
CN-
Cyano mixed valence CCP
[300 DEPC : 1 CCP results in loss of only 10% of ability to form high spin]

histidine is located close to the iron at the distal side of the haem.

4.2.8 Modification of CCP in oxidised state causes a high to low spin-state transition of the high potential haem

Difference spectra of modified cytochrome c peroxidase were routinely obtained in the ultra-violet region of the spectrum to quantify ethoxyformylhistidine. These difference spectra may also be useful, if observed at longer wavelengths, to determine haem-linked changes in the enzyme subsequent to ethoxyformylation of a single histidine residue. Figure 4.9(a) shows difference spectra from 350 to 700 nm of cytochrome c peroxidase modified with DEPC at pH 7.5 minus corresponding spectra from native enzyme. At both pH 7.5 (Figure 4.9(a)) and pH 6 (Figure 4.9(b)) the progressive decrease in absorbance at 380, 500 and 630 nm and gain at 410nm and 530 nm (diagnostic of a high to low spin-state transition of a ferrihaem) is complete upon modification of 1 mol of histidine per mol of protein. At pH 6 the total loss of 380 nm absorbance is approximately half that at pH 7.5.

This study suggests that modification of a single histidine in oxidised CCP converts the partial high spin-state of the high potential haem to low-spin. The spin-state of the high potential haem in the native oxidised enzyme is seemingly dependent on pH with approximately twice as much high-spin present at pH 7.5 than at pH 6.

4.2.9 Effect of Ca^{2+} on native and modified cytochrome c peroxidase

The following body of work was predominantly but not exclusively concerned with investigating the differences in Ca^{2+} binding between the native and modified protein. A more general analysis of the specificity, affinity and proposed function of Ca^{2+} binding sites in cytochrome c peroxidase is described in Chapter I, section 1.2.2.3 and for further detail see Gilmour et al.(1995). The following results supply some of the evidence for the presence of at least two and possibly three Ca^{2+} binding sites in cytochrome c peroxidase. One, which is occupied by Ca^{2+} in the isolated form of the enzyme, we call site I: the second is unoccupied in the dilute isolated enzyme

Figure 4.9 Modification of one histidine from cytochrome c peroxidase causes a high to low spin-state transition

(a) Cytochrome c peroxidase (4μM) in 5mM Hepes pH 7.5 was modified for 20 min with the following concentrations of DEPC- 1.4, 2.7, 5.4, 11, 16, 32, 54 and 86μM. The extent of modification for each DEPC concentration was calculated from the increase absorbance at 245 nm to be 0.2, 0.4, 0.5, 0.8, 0.9, 1.2, 1.3 and 1.7 mol histidine modified per mol.The difference between the spectra from 350-700 nm of modified and unmodified enzyme at varying amounts of modification is shown.

(b) Cytochrome c peroxidase (4μM) in 5mM Mes pH 6 was modified for 20 min with the following concentrations of DEPC- 2, 21, 54 and 214μM. The extent of modification for each DEPC concentration was calculated to be 0.1, 0.3, 0.9 and 1.3 mol histidine modified per mol. The difference between the spectra of modified and unmodified enzyme at varying amounts of modification is shown.

(a)

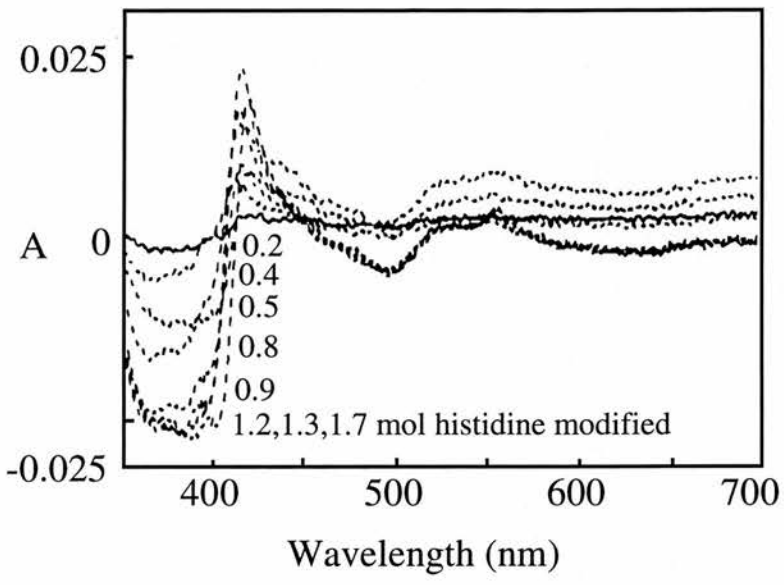
0.025
A 0
-0.025
0.2
0.4
0.5
0.8
0.9
1.2,1.3,1.7 mol histidine modified
400
500
600
700
Wavelength (nm)

(b)

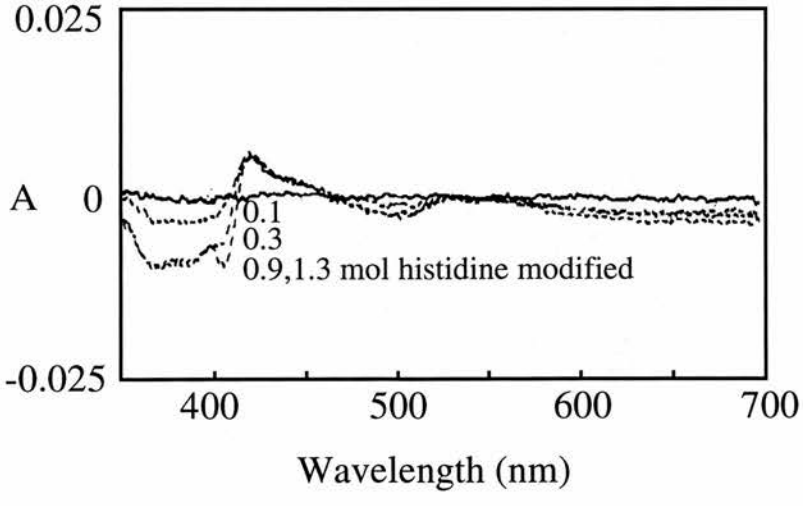
0.025
A 0
-0.025
0.1
0.3
0.9,1.3 mol histidine modified
400
500
600
700
Wavelength (nm)

and we call this site II; the putative third Ca^{2+} binding site is occupied in the isolated form of the enzyme and has properties similar to but distinguishable from site I, we call this site III. As will be explained it has been difficult to conclusively prove the existence of site III. The results will be rationalised for both 'two site' and 'three site' models.

The model identifying two Ca^{2+} binding sites for cytochrome c peroxidase (Figure 4.10) was also shown in Chapter I,section 1.2.2.3. Figure 4.11 shows a model identifying three Ca^{2+} binding sites for cytochrome c peroxidase The results described below involve investigation of different components of the separate models. Both the 'two site' and 'three site' models are referred to throughout the chapter to assist the reader's interpretation of the system being studied.

4.2.9.1 Binding of Ca^{2+} to the oxidised enzyme

Treatment of cytochrome c peroxidase with EGTA (1mM) in 5-10mM Mes pH 6 results in rapid loss of absorbance at 412 nm and gain at 398 nm. This is followed by a slower broad loss in absorbance at 380 nm and gain at 410 nm (Figure 4.12a (i) and (ii)). The former represents the 'fast' EGTA effect and the latter the 'slow' EGTA effect. Treatment of cytochrome c peroxidase with EGTA in 10mM Hepes pH 7.5 results in a smaller proportion of the 'fast' EGTA effect and a higher proportion of the 'slow' EGTA effect (Figure 4.12 (b)). When EGTA treatment is performed in the presence of 50mM NaCl, no second (slow) spectral phase is observed and the first (fast) phase itself is slower (Figure 4.12 (c)). All these EGTA changes are reversible by titration with Ca^{2+}. Figure 4.13(a) shows the back titration of EGTA treated enzyme in 5mM Mes pH6, with Ca^{2+}, which gave a K_D for binding of 1.6μM (Figure 4.13(b)). Note the proportion of the protein present with bound Ca^{2+}, and therefore the K_D, was calculated from the size of the absorbance change at 398 nm relative to the total change.

Foote et al. (1985) determined in oxidised *P. aeruginosa* CCP, that high-spin

Figure 4.10 Two site Ca^{2+} binding model for cytochrome c peroxidase. The enzyme is represented as a two domain structure with a haem in each domain. The electron transferring domain is shown as a smaller circle for diagrammatic purposes. The left column contains species which are fully oxidised; the right contains species which have a reduced electron transferring domain. Ca^{2+} binding site II is shown at the interface of two monomers. The mixed-valence enzyme at level A is the active form and is shown as having a substrate access channel to the peroxidatic haem group. The enzyme is isolated as a mixture of the oxidised forms at levels A and C.

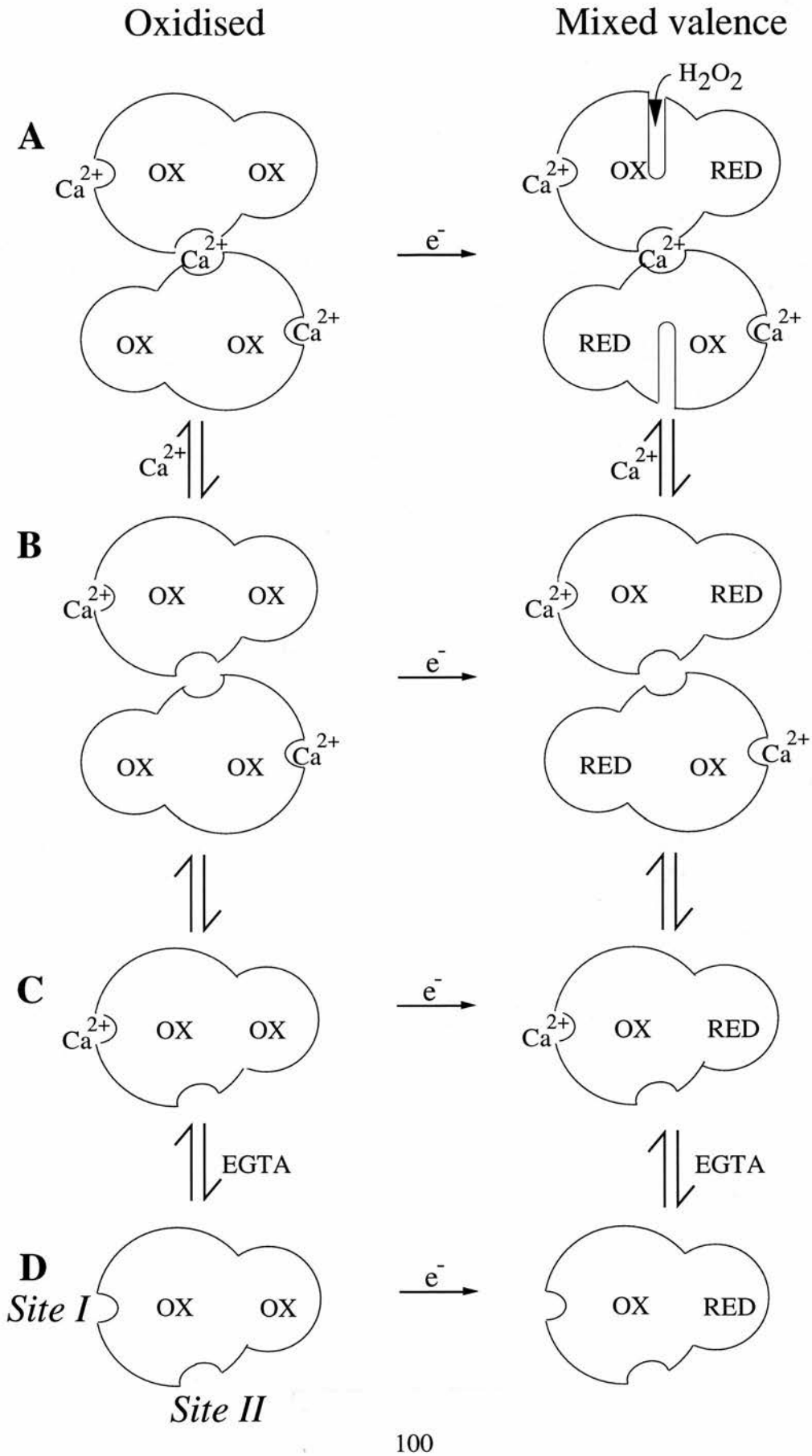
Oxidised
Mixed valence
A
B
C
D
Site I
Site II
OX
RED
Ca^{2+}
H_2O_2
e^-
EGTA

Figure 4.11 Three site Ca^{2+} binding model for cytochrome c peroxidase. The enzyme is represented as a two domain structure with a haem in each domain. The electron transferring domain is shown as a smaller circle for diagrammatic purposes. The left column contains species which are fully oxidised; the right contains species which have a reduced electron transferring domain. The mixed-valence enzyme at level A is the active form and is shown as having a substrate access channel to the peroxidatic haem group. Ca^{2+} binding site II is shown at the interface of two monomers. Ca^{2+} binding site I is shown as part of the peroxidatic domain. Ca^{2+} binding site III is shown as part of the electron transferring domain.

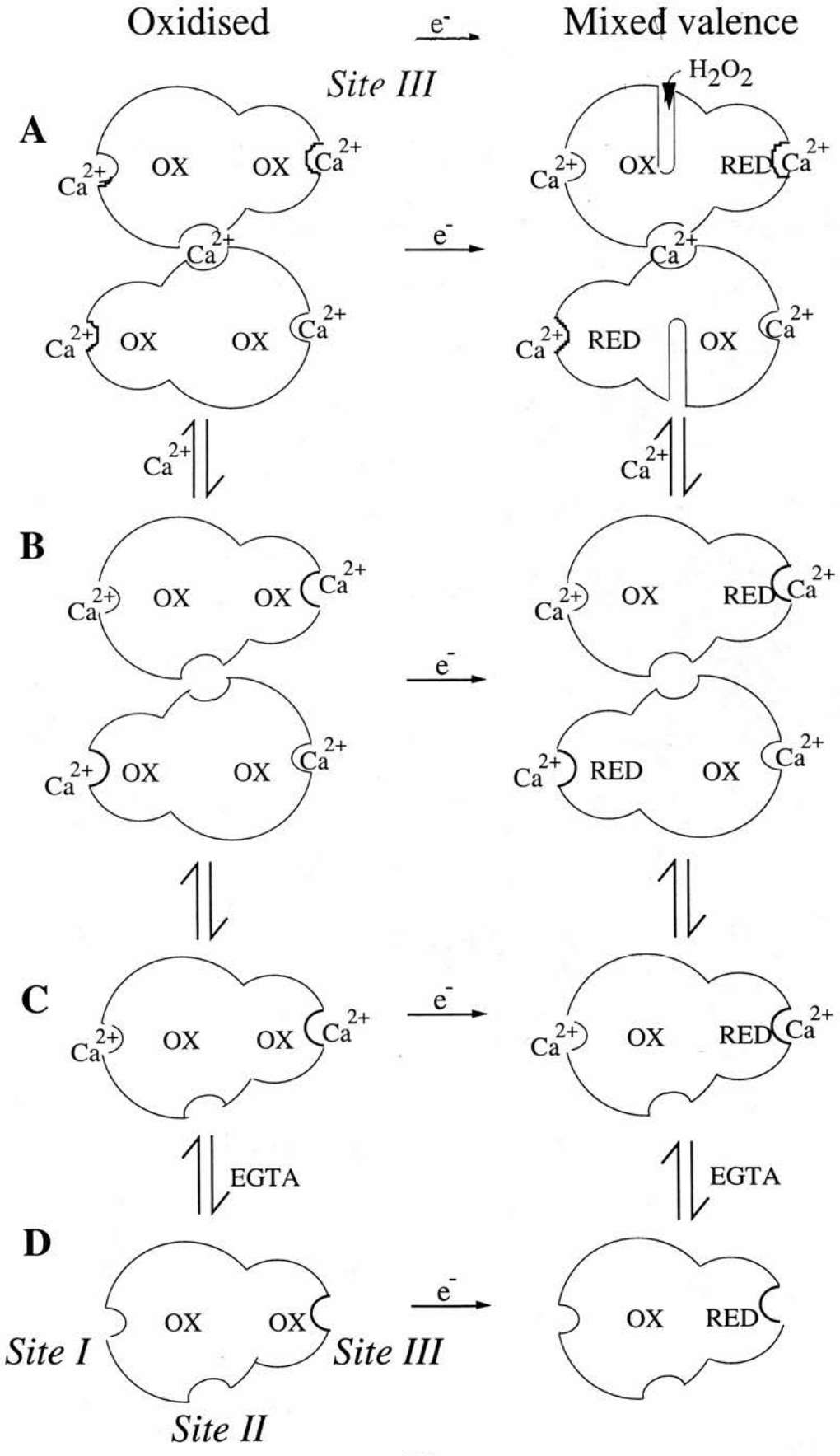
Oxidised
e-
Mixed valence
Site III
H2O2
A
Ca2+
OX
OX
Ca2+
Ca2+
Ca2+
OX
OX
Ca2+
Ca2+
OX
RED
Ca2+
Ca2+
Ca2+
RED
OX
Ca2+
Ca2+
Ca2+
B
Ca2+
OX
OX
Ca2+
Ca2+
Ca2+
OX
OX
Ca2+
Ca2+
OX
RED
Ca2+
Ca2+
Ca2+
RED
OX
Ca2+
C
Ca2+
OX
OX
Ca2+
Ca2+
OX
RED
Ca2+
EGTA
EGTA
D
OX
OX
OX
RED
Site I
Site III
Site II

Figure 4.12 Treatment of cytochrome c peroxidase with EGTA
(a) Cytochrome c peroxidase (4μM) in 10mM Mes pH6 was aged for 20 min to allow any changes to occur due to dilution and then treated with EGTA (1mM). (i) The time course of spectral changes was followed by difference spectroscopy against a reference of the oxidised protein. The upper spectrum at 398 nm is that obtained after 30 s and subsequent spectra were at 2, 4, 8, 16 and 24 min after EGTA addition and follow a progressive fall at 398 nm. (ii) The difference spectrum 30 s after EGTA addition from (i) (dashed line) is compared with the difference between a spectrum 24 min after EGTA treatment and that 30 s after EGTA treatment (solid line). The former represents the "fast" EGTA effect and the latter the "slow" EGTA effect.
(b) Cytochrome c peroxidase (4μM) in 10mM Hepes pH7.5 was aged for 20 min and then treated with EGTA (1mM). The spectral change was obtained 24 min after EGTA addition by difference spectroscopy against a reference of the oxidised protein.
(c) Cytochrome c peroxidase (4μM) in 10mM Mes pH6, 50mM NaCl was aged for 20 min and then treated with EGTA (1mM). The time course of spectral changes was followed by difference spectroscopy against a reference of the oxidised protein. The lower spectrum at 398 nm is that obtained after 30 s and subsequent spectra were at 2, 4, 8, 16 and 24 min after EGTA addition and follow a progressive rise at 398 nm.

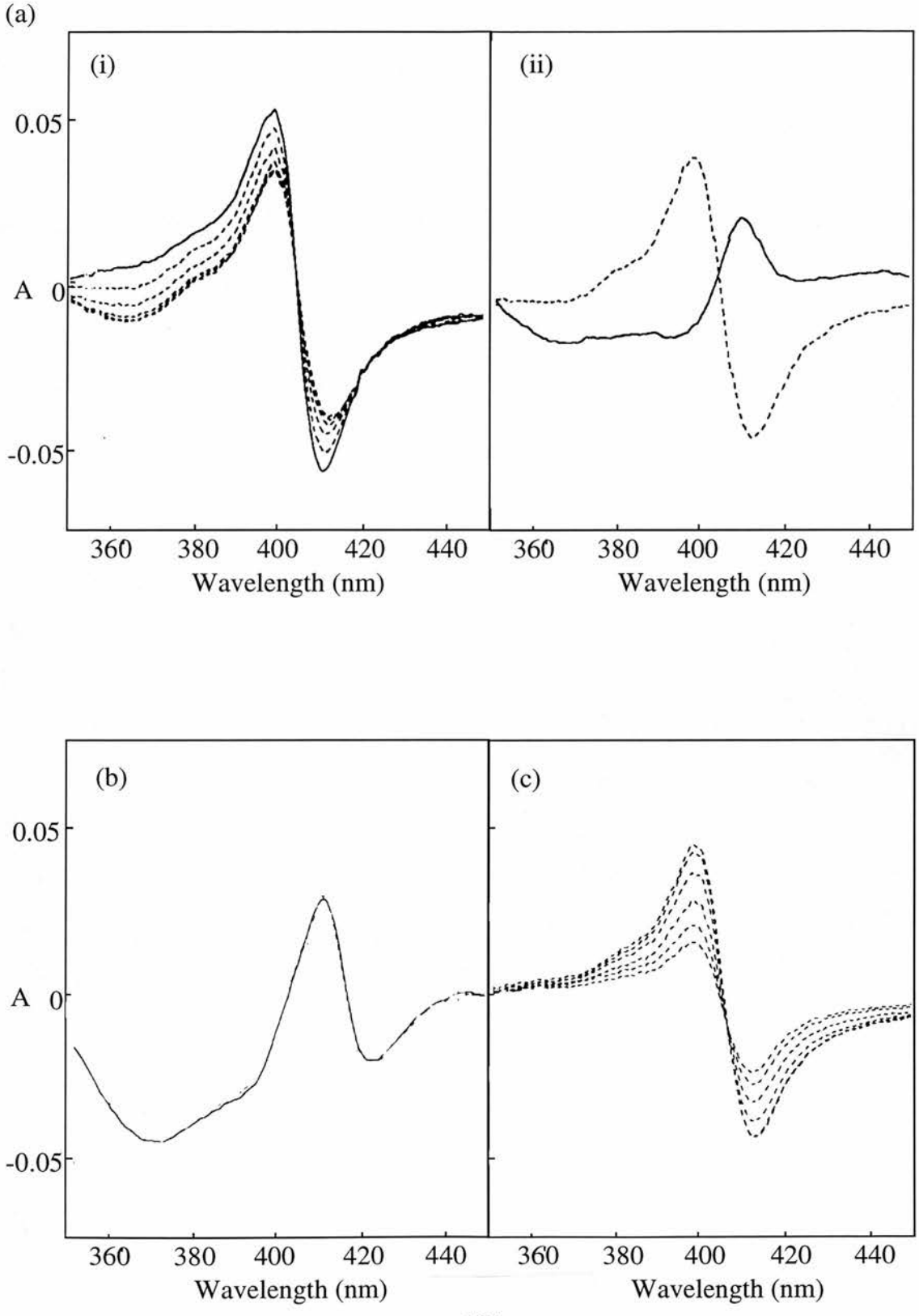
(a)
(i)
(ii)
0.05
A 0
-0.05
360 380 400 420 440
Wavelength (nm)
360 380 400 420 440
Wavelength (nm)
(b)
(c)
0.05
A 0
-0.05
360 380 400 420 440
Wavelength (nm)
360 380 400 420 440
Wavelength (nm)

Figure 4.13 Back titration of EGTA treated cytochrome c peroxidase with Ca^{2+}

(a) Cytochrome c peroxidase (4μM) in 5mM Mes pH 6 was treated with EGTA as in Figure 4.12(a) and, after the completion of the EGTA-induced changes, Ca^{2+} was titrated back into the solution. Free Ca^{2+} concentrations at this pH were calculated from considerations of the binding constant of the $EGTA^{4-}$ form and its concentration at this pH (see Chapter II-Materials and Methods). 2 moles of NaOH were added for each mole of Ca^{2+} to balance the effect of the proton release from the predominant H_2EGTA^{2-} form. The difference between the spectra after Ca^{2+} additions and the spectrum after completion of the EGTA induced changes are shown. At 398 nm the spectra in descending order are after additions of Ca^{2+} to free concentrations of 0.09, 0.18, 0.27, 0.36, 0.54, 0.73, 0.92, 1.11, 1.49, 1.88, 2.89, 5.07, 16.6, 70.5 and 253 μM.

(b) The proportion of the protein present with bound Ca^{2+} was calculated from the size of the absorbance change at 398 nm relative to the total change. Log $[Ca^{2+}]$ is the log of the calculated free $[Ca^{2+}]$. The experimental data from (a) are fitted to a theoretical curve for a single Ca^{2+}-binding site with a K_D of 1.6μM.

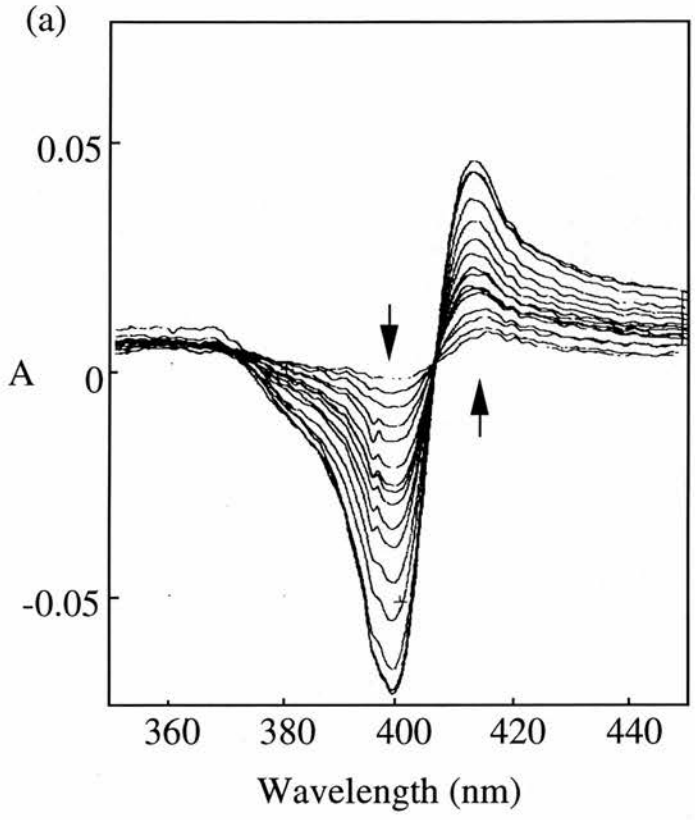
(a)
0.05
A
0
-0.05
360
380
400
420
440
Wavelength (nm)

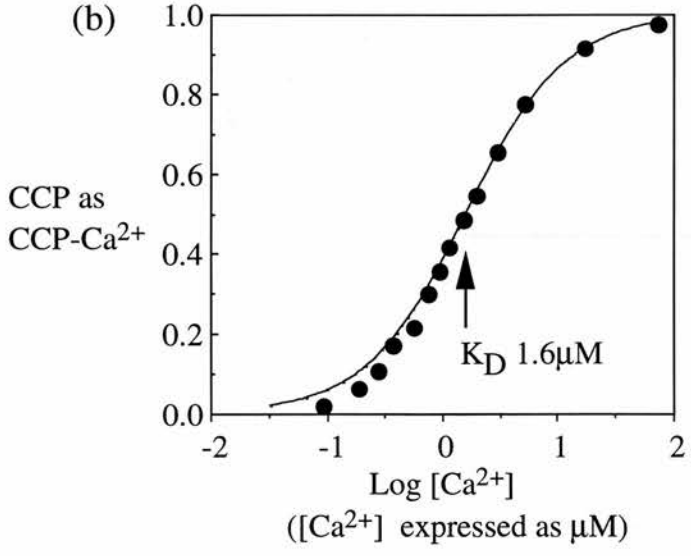
(b)
1.0
0.8
0.6
0.4
0.2
0.0
CCP as
CCP-Ca2+
K_D 1.6µM
-2
-1
0
1
2
Log [Ca2+]
([Ca2+] expressed as µM)

signals arose due to a labile methionine coordination of the high potential haem. Subsequently Gilmour et al. (1993) reached the same conclusion for oxidised *P.denitrificans* cytochrome c peroxidase.

It can be proposed that the EGTA treatment of oxidised cytochrome c peroxidase shifts the high potential haem to a fully low spin-state, with the loss of absorbance at 380 nm and gain at 410 nm. This effect is what is known as the 'slow' EGTA effect and follows the 'fast' EGTA effect which results in a loss of absorbance at 412 nm and gain at 398 nm. Consequently this must represent a spin-state change at the low potential haem and the absorbance shift to lower wavelengths indicates a low to high spin-state transition of this haem. Note these effects can not be influenced by Ca^{2+} binding to site II as this site is unoccupied in the dilute oxidised enzyme (Gilmour et al.1995) (also see Chapter I, section 1.2.2.3). These results establish the interconversion of forms C and D in the oxidised form with a K_D for binding of 1.6μM ('two site' Figure 4.10 and 'three site' Figure 4.11).

4.2.9.2 Data interpreted as a 'two Ca^{2+} binding site' model:-

One interpretation of these changes is a reflection of Ca^{2+} binding to a single site on the oxidised enzyme as isolated, which influences the spin-states of the two haem groups. This site will be called site I. Within the 'two site' model definition there are two possible models which reflect the different rates of the two haem linked spin-state transitions upon addition of EGTA (see below).

'Two Ca^{2+} binding site' model

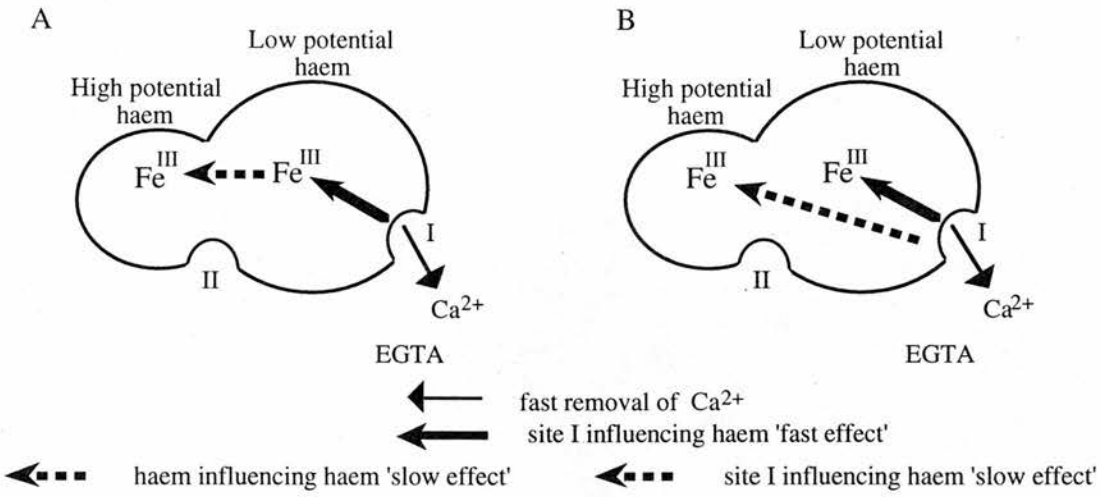

Model A represents EGTA removing Ca^{2+} from site I which rapidly causes a low to high spin-state change at the low potential haem ('fast' EGTA change). This new protein conformation subsequently causes a high to low spin-state transition at the high potential haem ('slow' EGTA change).

Model B represents EGTA removing Ca^{2+} from site I which similarly causes a rapid low to high spin-state change at the low potential haem ('fast' EGTA change). However in this model, the absence of Ca^{2+} from site I directly, but slowly, generates the high to low spin-state transition at the high potential haem.

4.2.9.3 Data interpreted as a 'three Ca^{2+} binding site' model:-

A second interpretation of these changes is a reflection of Ca^{2+} binding to two separate sites on the oxidised enzyme as isolated, each site influencing the spin-state of one of the two haem groups. These sites will be called site I and site III. In this model (see below) EGTA removes Ca^{2+} from site I which rapidly causes a low to high spin-state change at the low potential haem ('fast' EGTA change). EGTA subsequently removes Ca^{2+} from site III causing a high to low spin-state change at the high potential haem ('slow' EGTA change).

'Three Ca^{2+} binding site' model

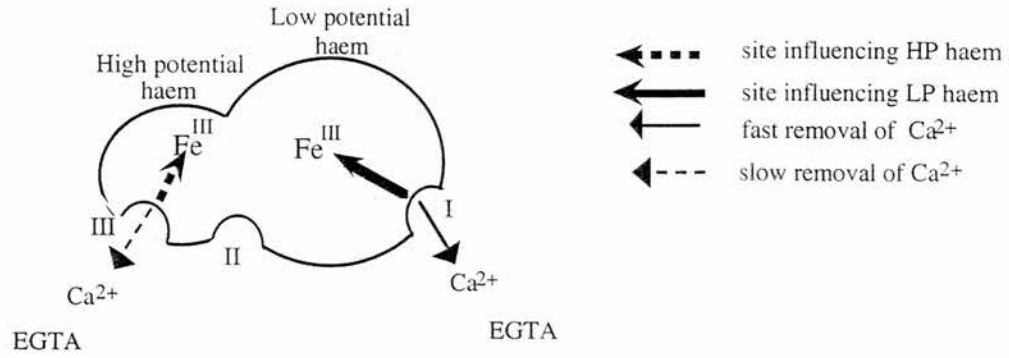

The high to low spin-state transition at the high potential haem is lost upon ethoxyformylation of one histidine (see section 4.2.8). The results of modification of CCP at pH 7.5 and pH 6 on the decrease of absorbance at 380 nm (see Figure 4.9) suggests that there is approximately twice as much high-spin present at the high potential haem at pH 7.5 relative to pH 6. The relative trough sizes at 380 nm upon treatment of CCP with EGTA at pH 7.5 and pH 6 (see Figure 4.12a(i) and b(i)) are also consistent with the presence of a greater proportion of high spin-state at pH7.5.

4.2.9.4 Binding of Ca^{2+} to the oxidised modified enzyme

Section 4.2.8 described the loss of absorbance at 380 nm upon modification of a histidine residue in the oxidised enzyme. This reflects the high to low spin-state transition at the high potential haem and is consistent with no further loss of absorbance at 380 nm, upon subsequent treatment with EGTA (Figure 4.14). The reversal of the 'fast' EGTA change with Ca^{2+}, corresponding to changes at the low potential haem, (Figure 4.15(a)) gave a K_D for binding of 1.7μM (Figure 4.15(b)), similar to that for the unmodified enzyme.

According to the 'two site' model, modification of a single histidine must directly influence the spin-state of the high potential haem, causing a high to low spin-state transition, rather than disrupting Ca^{2+} binding to site I. This is because the spin-state transition at the low potential haem is entirely unaffected upon modification of the histidine.

Figure 4.14 Treatment with EGTA of cytochrome c peroxidase modified at a single histidine.

Cytochrome c peroxidase (4μM) in 5mM Mes pH6, modified to the extent of 1.2 mol of histidine per mol of protein, was treated with EGTA as described in the legend to Figure 4.12(a). The time course of spectral changes was followed by difference spectroscopy against a reference of the oxidised protein. The spectra were at 30 s, 2, 4, 8, 16, 24 min after EGTA addition and are almost coincident.

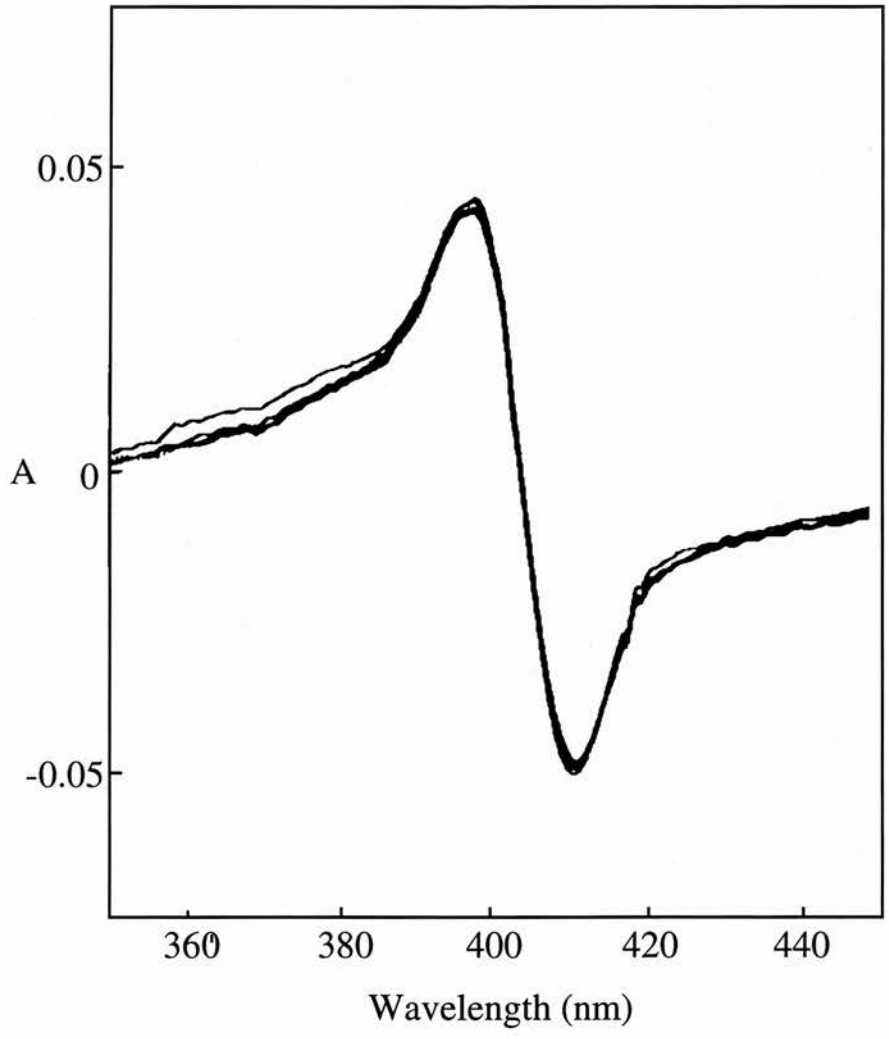
0.05
A 0
-0.05
360
380
400
420
440
Wavelength (nm)

Figure 4.15 Back titration of EGTA treated cytochrome c peroxidase modified at a single histidine, with Ca^{2+}

(a) Modified cytochrome c peroxidase (4μM) in 5mM Mes pH6 was treated with EGTA as in Figure 4.12(a) and, after the completion of the EGTA-induced changes, Ca^{2+} was titrated back into the solution. Free [Ca^{2+}] were calculated and proton release balanced as described in the legend Figure 4.13(a). The difference between the spectra after Ca^{2+} additions and the spectrum after completion of the EGTA induced changes are shown. The arrows show the direction of absorbance change at 398 and 412 nm. At 398 nm the spectra in descending order are after additions of Ca^{2+} to free concentrations of 0.09, 0.18, 0.27, 0.36, 0.55, 0.73, 0.92, 1.11, 1.49, 1.88, 2.89, 5.07, 16.6, 70.5 and 138 μM.

(b) The proportion of the protein present with bound Ca^{2+} was calculated from the size of the absorbance change at 398 nm relative to the total change. Log [Ca^{2+}] is the log of the calculated free [Ca^{2+}]. The line is a theoretical curve for a single Ca^{2+}-binding site with a K_D of 1.7μM.

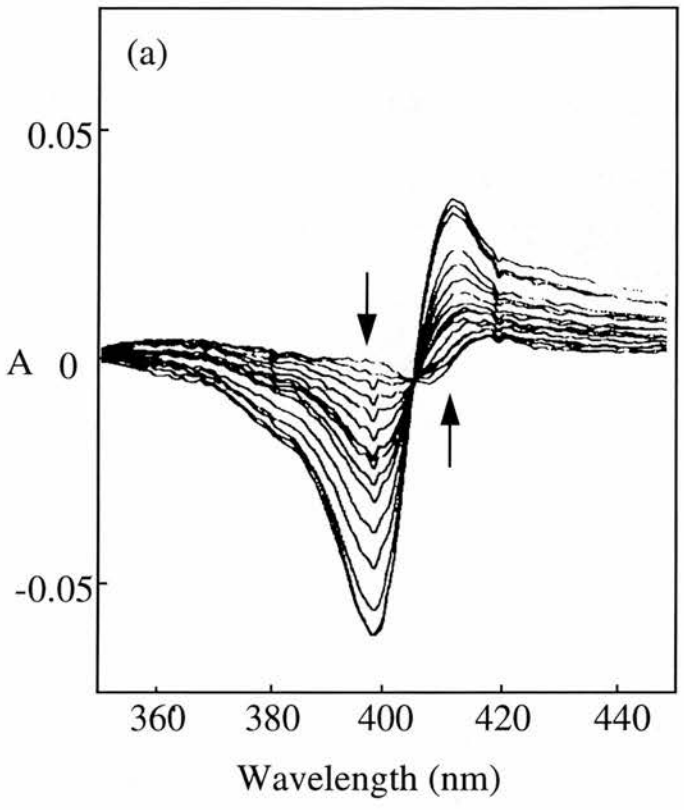
(a)
0.05
A 0
-0.05
360
380
400
420
440
Wavelength (nm)

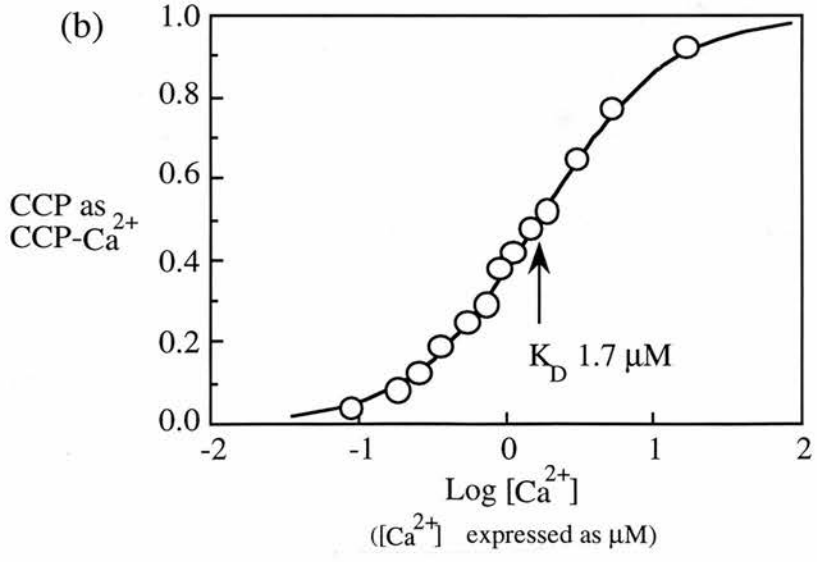
(b)
1.0
0.8
0.6
0.4
0.2
0.0
CCP as
CCP-Ca2+
K_D 1.7 µM
-2
-1
0
1
2
Log [Ca2+]
([Ca2+] expressed as µM)

According to the 'three site' model, site I influences the spin-state change at the low potential haem and site III influences the spin-state change at the high potential haem. Modification of a single histidine disrupts Ca^{2+} binding to site III but not site I therefore causing the spin-state transition (high to low) at the high potential haem only.

4.2.9.5 Binding of Ca^{2+} to the native mixed-valence enzyme

In the mixed-valence enzyme only two Ca^{2+} binding sites are of interest. Site I which for this purpose is defined as the site which influences the low potential haem in the oxidised enzyme and site II which is empty in the oxidised form of the enzyme. If site III exists it has no role in the following analysis. Binding of Ca^{2+} to the mixed-valence enzyme is complicated by the presence of both sites I and II, indicated by two distinct spectroscopic changes. However Ca^{2+} binds more rapidly to site I. Thus the properties of both sites in the mixed-valence form can be investigated. One way to do this is to treat the oxidised enzyme (refer to Figures 4.10 and 4.11 -oxidised C) with EGTA (oxidised D) and then reduce it with ascorbate. Under these conditions, both sites I and II are empty in the mixed-valence enzyme (mixed-valence D). Ca^{2+} can then be titrated back into the sample and the filling of both Ca^{2+} binding sites can be observed separated in time (mixed-valence C then A). Difference spectra obtained 30 min after each Ca^{2+} addition are shown in Figure 4.16a. These are composite spectra which include the components of two distinct spectral changes. One, which is complete 1 min after Ca^{2+} addition, involves loss of absorption at 398 nm and gain at 412 nm (Figure 4.16b) and reflects Ca^{2+} returning to site I (compare with Figure 4.13a). The data fit a similar binding curve and K_D of 0.9 μM that was observed for the oxidised enzyme (Figure 4.16d). The second change occurs on a slower time scale and can be displayed after subtraction of the contribution of the fast change (Figure 4.16c). It involves an increase in absorbance at 380 nm and reflects Ca^{2+} returning to site II. The slow increase in the 380 nm band observed in Figure 4.16c reflects Ca^{2+}

Figure 4.16 Ca^{2+} titration of cytochrome c peroxidase treated with EGTA and then reduced with ascorbate.

(a) Cytochrome c peroxidase (4μM) in 5mM Mes pH6 was aged for 20 min to allow any changes to occur due to dilution and then treated with EGTA (1mM) for 30 min. The enzyme was then reduced with ascorbate (1mM) and DAD (10μM). After reduction was complete, Ca^{2+} was titrated back into the solution. Free [Ca^{2+}] were calculated and proton release balanced as described in the legend to 4.13(a). The difference between the spectra 30 min after Ca^{2+} additions and the spectrum after completion of the EGTA induced changes are shown. At 380 nm the spectra in ascending order are after additions of Ca^{2+} to free concentrations of 0.18, 0.36, 0.73, 1.11, 1.88, 5.07, 35.7 and 138 μM.

(b) In addition to the spectra taken 30 min after Ca^{2+} additions, spectra were also taken 1 min after Ca^{2+} additions. Ca^{2+} re-entering site I was followed by the rapid change in spectrum after a Ca^{2+} addition. That rapid change for an individual Ca^{2+} addition was obtained as the difference between the spectrum 1 min after a Ca^{2+} addition and the preceding spectrum 30 min after the previous Ca^{2+} addition. These differences were progressively summed to give the set of difference spectra shown. They represent the site I changes after additions of Ca^{2+} to free concentrations of 0.18, 0.36, 0.73, 1.11, 1.88, 5.07, 35.7 and 138 μM and are in descending order at 398 nm. The spectrum obtained for free [Ca^{2+}] of 138 μM was coincident with that for 35.7 μM. Analysis of this Ca^{2+} binding appears in (d).

(c) The slow phase of spectral change following Ca^{2+} addition represents Ca^{2+} entering site II and was obtained as the difference between the spectrum 30 min after a Ca^{2+} addition and the spectrum 1 min after the Ca^{2+} addition. These differences were progressively summed to give the set of difference spectra shown. They represent the site II changes after additions of Ca^{2+} to free concentrations of 0.18, 0.36, 0.73, 1.11, 1.88, 5.07, 35.7 and 138 μM and are in ascending order at 380 nm.

(d) The proportion of protein present with bound Ca^{2+} at site I was calculated from the size of the absorbance change at 398 nm in (c) relative to the total change. Log [Ca^{2+}] is the log of the calculated free [Ca^{2+}]. The line is a theoretical curve for a single Ca^{2+}-binding site with a K_D of 0.9 μM.

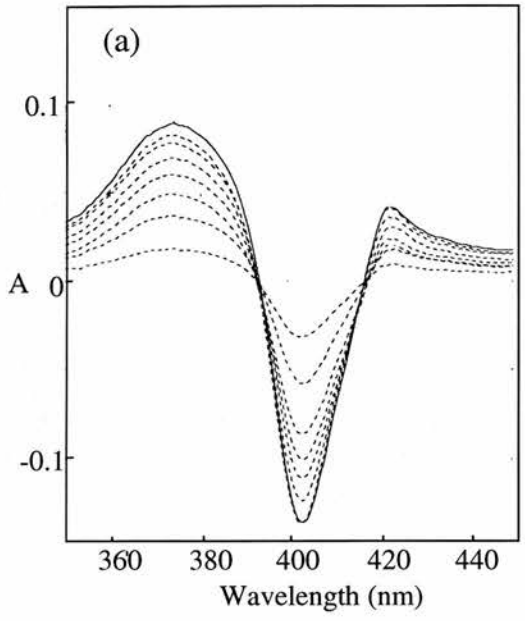
(a)
0.1
A 0
-0.1
360
380
400
420
440
Wavelength (nm)

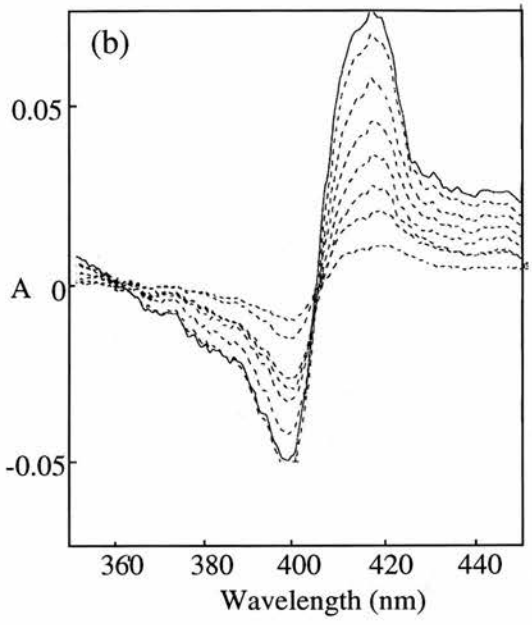
(b)
0.05
A 0
-0.05
360
380
400
420
440
Wavelength (nm)

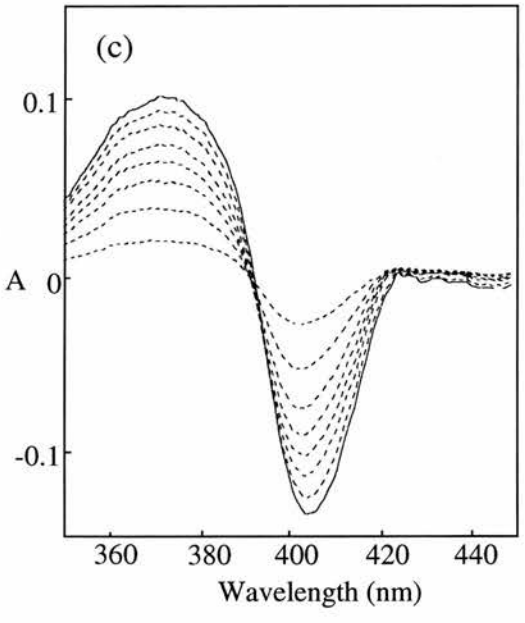
(c)
0.1
A 0
-0.1
360
380
400
420
440
Wavelength (nm)

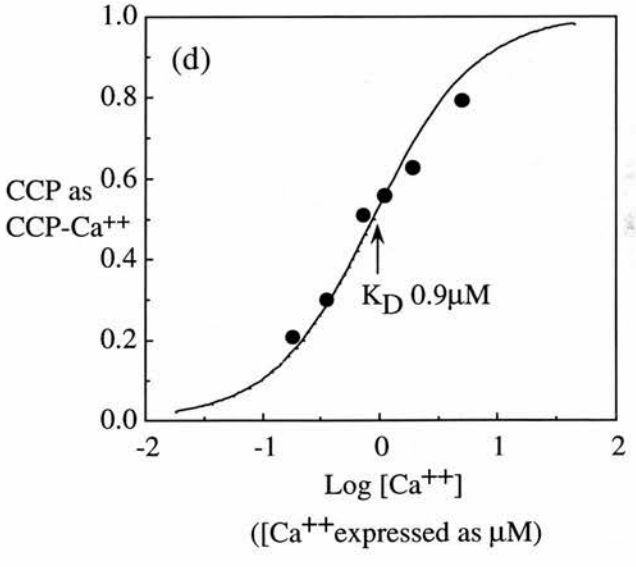
(d)
1.0
0.8
0.6
0.4
0.2
0.0
CCP as
CCP-Ca++
K_D 0.9μM
-2
-1
0
1
2
Log [Ca++]
([Ca++expressed as μM)

binding to a second site on the enzyme - site II. Gilmour et al. (1994) showed that the entry of Ca^{2+} into this site is correlated with the appearance of active enzyme. Because of the very slow rate of attainment of equilibrium, it is difficult to obtain good titrations for this site, but the K_D is similar to that for site I. This equilibrium may be complex and involve the dimerisation of the mixed-valence form B before subsequent Ca^{2+} binding (Gilmour et al.1995).

4.2.9.6 Binding of Ca^{2+} to the modified mixed-valence enzyme

The effect of Ca^{2+} binding to cytochrome c peroxidase modified at a single histidine, was analysed in an identical way to the native mixed-valence enzyme. The modified enzyme was treated with EGTA, reduced with ascorbate and then titrated with Ca^{2+}. In the native enzyme two spectroscopic signals are isolated by time, reflecting Ca^{2+} entering site I then site II (Figure 4.16 b and c). However the composite difference spectra (Figure 4.17a) for Ca^{2+} binding to the modified protein, reflects only the site I spectral change. The isolated site I spectral changes are very similar to that of the native enzyme (compare Figure 4.16b to 4.17b). The data fit a similar binding curve and the K_D of 1.4 μM compares with the native enzyme in both redox states and the modified oxidised enzyme (Figure 4.17d).

The absence of the second (site II) spectral change, a slow increase in 380nm absorbance, reflects (compare Figure 4.16c to 4.17c) the inability of the modified enzyme to form the high spin-state at the low potential haem which is essential for activity. Either the modified enzyme cannot bind Ca^{2+} at site II or the enzyme with bound Ca^{2+} can no longer promote the spectral transition to the high spin-state.

4.2.9.7 Alternative Ca^{2+} binding site models

The results above comparing the effect of Ca^{2+} on native and modified protein support models reflecting the presence of either two or three Ca^{2+} binding sites which

Figure 4.17 Ca^{2+} titration of modified cytochrome c peroxidase treated with EGTA and then reduced with ascorbate

(a) Cytochrome c peroxidase (4μM) was allowed to age for 20 min to allow any changes to occur due to dilution before being modified with DEPC (100μM) to an extent of 1.1 mol of ethoxyformylhistidine per mol. The modified enzyme was then treated with EGTA (1mM) for 30 min and reduced with ascorbate (1mM) and DAD (10μM). Ca^{2+} was titrated back into the solution. Free [Ca^{2+}] were calculated and proton release balanced as described in the legend to Figure 4.13(a). The difference between the spectra 30 min after Ca^{2+} additions and the spectrum after completion of the EGTA induced changes are shown. At 380 nm the spectra in ascending order are after additions of Ca^{2+} to free concentrations of 0.18, 0.36, 0.73, 1.11, 1.88, 5.07, 35.7 and 138 μM.

(b) As in Figure 4.16, spectra were also taken at 1 min after Ca^{2+} addition. The progressively summed difference spectra between the spectrum 1 min after a Ca^{2+}addition and the preceding spectrum 30 min after the previous Ca^{2+} addition are shown. They represent the site I changes after additions of Ca^{2+} to free concentrations of 0.18, 0.36, 0.73, 1.11, 1.88, 5.07, 35.7 and 138 μM and are in descending order at 398 nm. The spectrum obtained for free [Ca^{2+}] of 138 μM was coincident with that for 35.7 μM. Analysis of this Ca^{2+} binding appears in (d).

(c) Any slow phase of spectral change following Ca^{2+} addition was obtained as the difference between the spectrum 30 min after a Ca^{2+} addition and the spectrum 1 min after the Ca^{2+} addition. These differences were progressively summed to give the set of difference spectra shown. They represent relatively small changes (compared to Figure 4.16(c)) after additions of Ca^{2+} to free concentrations of 0.18, 0.36, 0.73, 1.11, 1.88, 5.07, 35.7 and 138 μM and are in descending order at 420 nm.

(d) The proportion of the modified protein present with bound Ca^{2+} at site I was calculated from the size of the absorbance change at 398 nm in (c) relative to the total change. Log [Ca^{2+}] is the log of the calculated free [Ca^{2+}]. The line is a theoretical curve for a single Ca^{2+}-binding site with a K_D of 1.4μM.

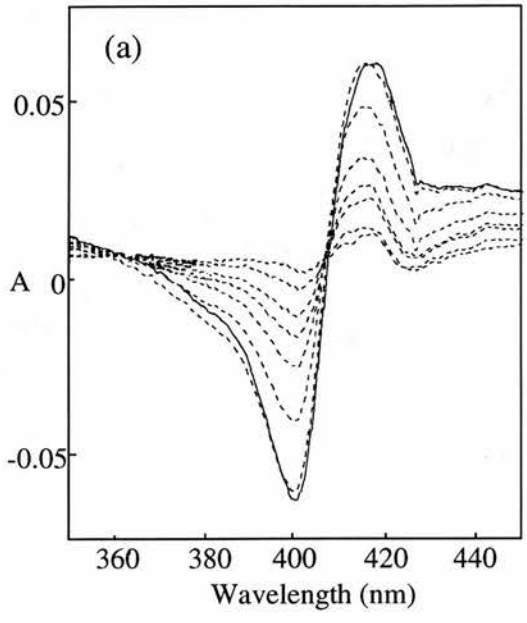
(a)
0.05
A 0
-0.05
360
380
400
420
440
Wavelength (nm)

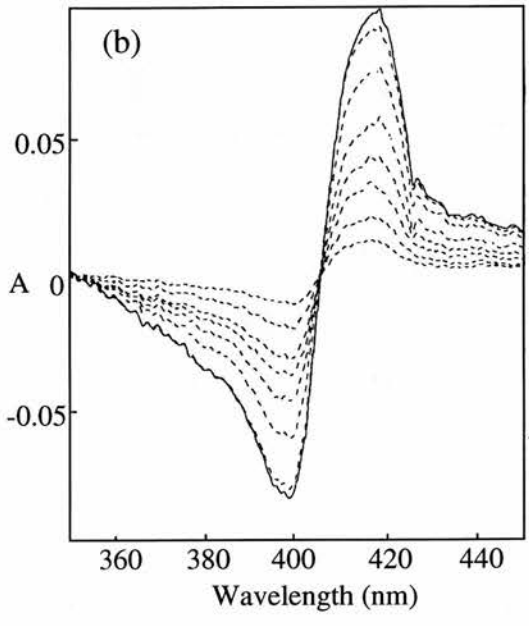
(b)
0.05
A 0
-0.05
360
380
400
420
440
Wavelength (nm)

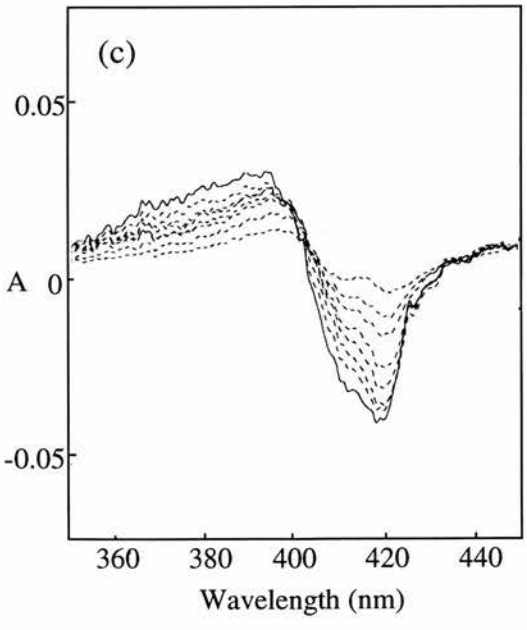
(c)
0.05
A 0
-0.05
360
380
400
420
440
Wavelength (nm)

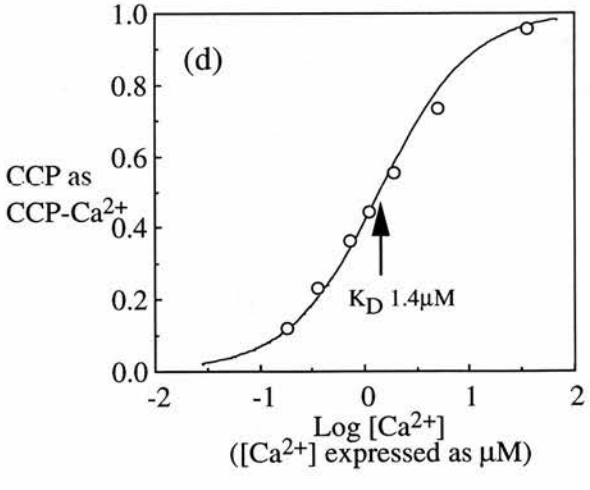
(d)
1.0
0.8
0.6
0.4
0.2
0.0
CCP as
CCP-Ca2+
KD 1.4μM
-2
-1
0
1
2
Log [Ca2+]
([Ca2+] expressed as μM)

influence haem spin-states in cytochrome c peroxidase.

The 'two Ca^{2+} binding site' model involves a direct influence of histidine modification on the spin-states of haems : modification of one histidine in the oxidised enzyme may not affect Ca^{2+} binding to site I as such, but rather directly cause a spin-state change only at the high potential haem. The modified enzyme reduced with ascorbate would similarly be unable to go to its active high spin-state at the low potential haem.

The 'three Ca^{2+} binding site' model (Figure 4.11), which involves an indirect influence of histidine modification on spin-states by selective disruption of Ca^{2+} binding sites. In the oxidised enzyme this model proposes separate Ca^{2+} binding sites influencing different haems. Ca^{2+} binding site I influences the spin-state of the low potential haem whilst a separate Ca^{2+} binding site that will be called site III influences the spin-state of the high potential haem. In the mixed-valence state Ca^{2+} binding site II influences the spin-state of the low potential haem to generate the active enzyme. In this model modification of one histidine residue would disrupt Ca^{2+} binding to both site II and site III but not site I. This might indicate a close proximity of site II and III.

It is extremely difficult to distinguish between all the possible models presented above. The results can support both models and they probably cannot be resolved until further information on protein structure or stoichiometry of Ca^{2+} binding is gained.

Chapter V

Cleavage of CCP with subtilisin

5.1 Introduction

The previous two chapters described the presence of an essential histidine in *P.denitrificans* CCP, easily ethoxyformylated by the reagent DEPC. The aim of the work described in this chapter was to identify this essential histidine in the sequence, but because of the relatively rapid loss of the ethoxyformyl group, few studies have attempted location of a modified histidine in a peptide digest, although there is one exception (Hegyi et al.1974). In our case, there was the additional problem that c-type cytochromes tend to be resistant to proteolysis unless the haem is removed, but this procedure requires conditions (0.1M HCl, 8M urea) which would be likely to accelerate loss of ethoxyformyl groups.

Trial experiments were initiated in an attempt to exploit any specific sites in the protein that were susceptible to proteolysis. A susceptible region in the homologous CCP from *P.aeruginosa* was identified using a single bond cleavage by *P.aeruginosa* elastase (Soininen and Ellfolk, 1975). The cleavage rendered the peroxidase inactive by preventing conformational changes necessary for the function of the native enzyme. The separation of the two *P.aeruginosa* CCP peptides required 1% SDS and consisted of a 28k di-haem peptide and a 11k non-haem peptide (Ronnberg, 1987).

Attempts at locating equally susceptible cleavage sites in *P.denitrificans* CCP were carried out using *P.aeruginosa* elastase extract, thermolysin and subtilisin. Although identification of the modified essential histidine was the primary reason for this work, the characterisation of cleaved CCP and the isolated peptides may enhance our understanding of the peroxidase mode of action. A desired goal from this perspective is the cleavage and purification of the two domains of CCP. Perhaps more realistically a fragment of the enzyme which contains for example, a proposed haem ligand, can be removed from CCP and the properties of the cleaved enzyme studied. This type of study may lead to conclusively identifying the function of the N and C-

terminal haems.

5.2 Results and Discussion

5.2.1 Cleavage of CCP with *P.aeruginosa* elastase extract and thermolysin

Incubation of P.*aeruginosa* elastase with *P.aeruginosa* CCP generates two peptides of CCP, one of M_r 28k and the second 11k, with a well defined single cleavage site between Ser 223 and Val 224 (*P.aeruginosa* CCP numbering) (Ronnberg, 1987; Soininen and Ellfolk, 1975; Ridout et al.1995). SDS-PAGE densitometry scans of products from the incubation mixture of *P.aeruginosa* elastase extract and *P.denitrificans* CCP are shown in Figure 5.1(a). The scans demonstrate that even at very low enzyme : substrate ratios, cleavage is not restricted to one site, but instead a quantity of low molecular mass peptides are generated. (Figure 5.1(a) i) to iii) respectively). Thus *P.aeruginosa* elastase seems unable to restrict cleavage to a limited number of sites in *P.denitrificans* CCP and is therefore of little use in the preparation of peptides for either identification of the modified essential histidine or for more general structural studies. An alternative explanation of course, is that the crude extract used may contain other proteases.

Other non-specific proteases such as thermolysin and subtilisin were therefore used in an attempt to cleave CCP at a naturally susceptible location. SDS-PAGE densitometry scans of products from the incubation mixture of thermolysin and CCP are shown in Figure 5.1(b). Haem staining was used so non-haem peptides are not detectable. The scans demonstrate that at low enzyme : substrate ratios, a quantity of low molecular mass haem peptides are generated along with a haem peptide of M_r~30k, which is similar in size to the haem peptide generated by cleavage of *P.aeruginosa* CCP with elastase. The possibility remains therefore of a site susceptible to proteolysis which is common to both bacterial peroxidases.

5.2.2 Cleavage of CCP with subtilisin

As *P.denitrificans* CCP is proposed to consist of two class I cytochrome c

Figure 5.1 Trial cleavage of *P.denitrificans* CCP using *P.aeruginosa* elastase extract and thermolysin

(a) *Pseudomonas aeruginosa* (N.C.T.C 10332) was grown aerobically in a medium containing trisodium citrate (5 g/l), KH_2PO_4 (1 g/l), $MgSO_4$ (0.5 g/l) and yeast extract (4 g/l) adjusted to pH 7 with NaOH, at 37°C in 100 ml culture flasks on an orbital shaker for 2 days (Pettigrew and Brown, 1988). *P.aeruginosa* elastase extract was prepared according to a modified method of Morihara et al. (1965). The culture broth was centrifuged (5000g 20 min), the resulting supernatant brought to 0.6 saturation with solid ammonium sulphate and allowed to stand overnight at 4°C. The precipitate was collected by centrifugation (10000g, 20 min), dissolved in water and desalted down a small G25 Sephadex column equilibrated in 10mM phosphate buffer pH 7. 100 pmol (0.5µl) *P.denitrificans* CCP was incubated with diluted *P.aeruginosa* elastase extract (20µl) for 60 min at 40°C. The reaction was stopped by inactivating protease at 100°C for 5 min and SDS-PAGE (15% polyacrylamide) was performed on the samples. The traces are absorbance scans at 690 nm following haem staining using the method of Goodhew et al. (1986). (i) CCP, (ii) CCP + elastase extract (diluted x100), (iii) CCP + elastase extract (diluted x40).

(b) Thermolysin purified from *Bacillus thermoproteolyticus rokko* was purchased from Sigma (Type X). *P.denitrificans* CCP was incubated with thermolysin in 10mM Hepes pH 7.5, 10mM $CaCl_2$, for 30 min at 30°C and the reaction stopped with EDTA (10mM) and SDS-PAGE performed on the samples. The traces are absorbance scans at 690 nm following haem staining. (i) CCP, (ii) enzyme : substrate ratio of 1:40 (w/w), (iii) enzyme : substrate ratio of 1:10 (w/w).

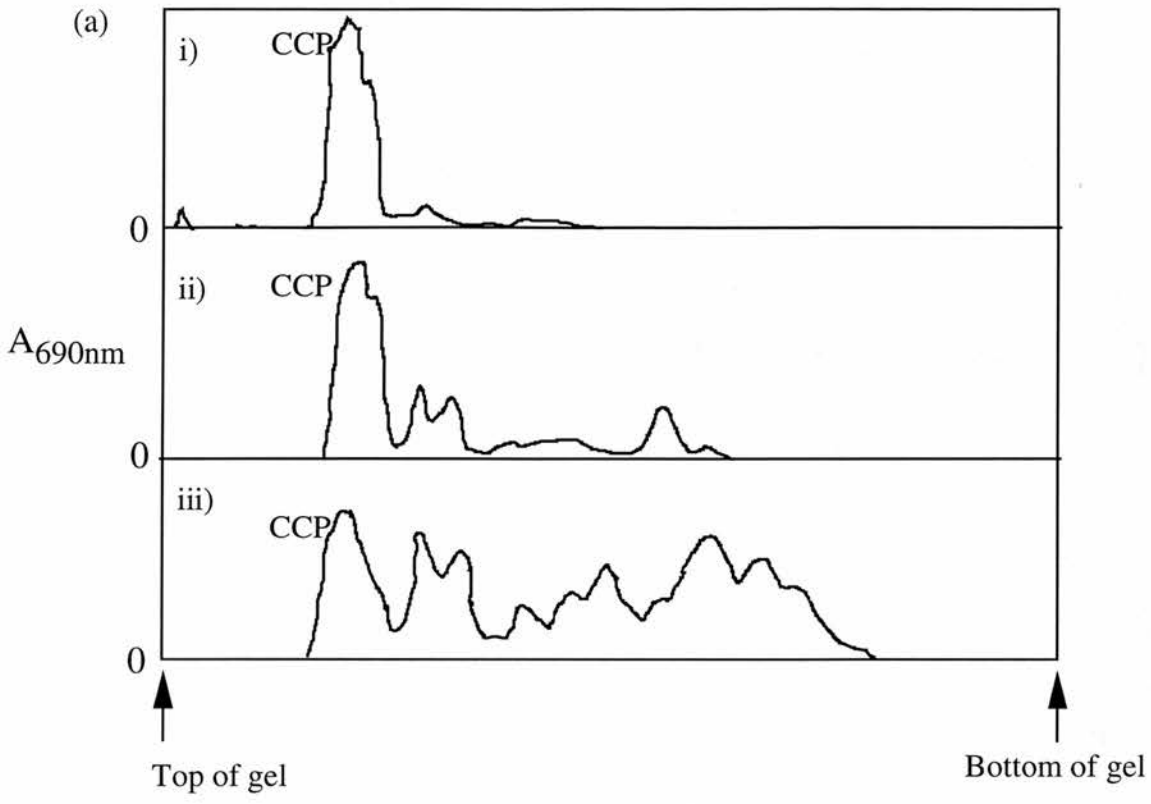
(a)
i)
CCP
0
ii)
CCP
A690nm
0
iii)
CCP
0
Top of gel
Bottom of gel

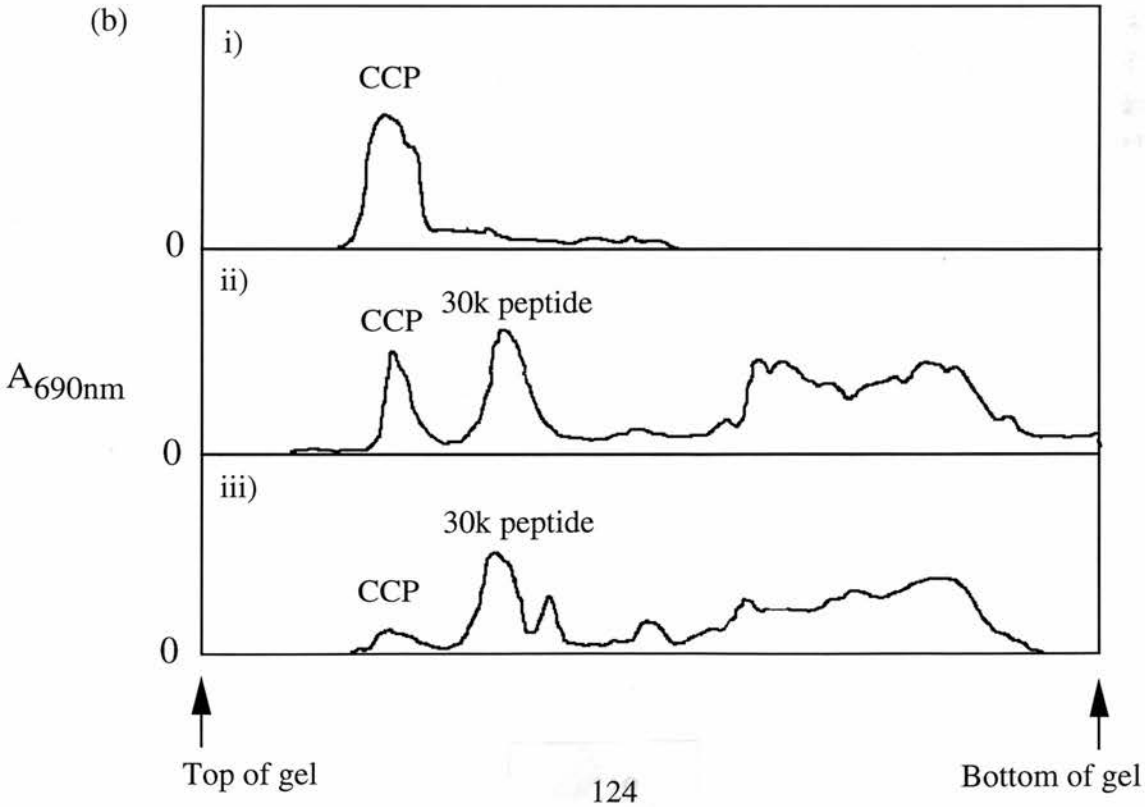
(b)
i)
CCP
0
ii)
CCP
30k peptide
A690nm
0
iii)
30k peptide
CCP
0
Top of gel
Bottom of gel

domains (to be discussed thoroughly in Chapter VII), the susceptibility to proteolysis of a class I cytochrome such as mitochondrial cytochrome c was of interest. In light of the knowledge that mitochondrial ferricytochrome c is digested by subtilisin whilst ferrocytochrome c is completely resistant to subtilisin (Yamanaka et al.1959; Nozaki et al.1958; Hantgan and Taniuchi, 1977; Endo et al.1985), the cleavage of CCP with subtilisin was performed using the mixed-valence form of the enzyme. This was in an attempt to restrict cleavage to a single susceptible bond in the protein. Extent of cleavage was easily controlled using a suitable enzyme : substrate ratio for a full 60 min at the set temperature of 0°C.

Figure 5.2(a) shows SDS-PAGE of products from the incubation mixture of subtilisin and *P.denitrificans* CCP and demonstrates a much cleaner cleavage pattern than with elastase or thermolysin. Gels stained for protein (Figure 5.2a i)) and haem (Figure 5.2a ii)) show cleavage of CCP into a haem containing peptide and a non-haem fragment at low intensities of digestion. Figure 5.2 (b) shows densitometry scans of selected lanes from Figure 5.2a i). Compared to the action of elastase and thermolysin (Figure 5.1) these scans demonstrate the defined nature of the subtilisin cleavage.

Approximate M_r values for the peptides generated by subtilisin were determined by migration on SDS-PAGE, relative to proteins with predefined molecular masses (Figure 5.3). The apparent M_r of whole CCP is 42.2k, of the haem peptide 29.5k and of the non-haem peptide 8.7k. Figure 5.2a i) appears to show a small haem peptide is generated subsequent to the other peptides, probably as a result of subdigestion of the larger haem peptide. Although cleavage was limited to reduce the amount of these smaller haem fragments, this tended to leave some undigested CCP (see for example Figure 5.4).

The M_r of the peptides, as determined from their relative mobility on SDS-PAGE, can only be viewed as an estimation of their true molecular mass. From the primary sequence of whole CCP with both haems attached, a M_r of 39.5k is calculated, yet a value of 42k is consistently generated by SDS-PAGE. Discrepancies of this sort are common for cytochrome c-type proteins and are probably due to the

Figure 5.2 Cleavage of *P.denitrificans* CCP using subtilisin

Bacterial subtilisin (Carlsberg) was purchased from Sigma (Type XXIV). To aliquots of CCP (5μM) in 10mM Hepes pH 7.5 was added ascorbate (1mM), DAD (10μM) and 1mM $CaCl_2$. Subtilisin was added to give enzyme : substrate ratios of 1: 2100, 1050, 700, 525, 420, 350, 300 and 233 (w/w) respectively. After 60 min at 0°C, subtilisin was inhibited by PMSF (1mM), EGTA (10mM).

(a)i) 1.25 nmol of each digest was loaded on a gel (15% polyacrylamide) for SDS-PAGE which was subsequently stained for protein with Coomassie Brilliant Blue R. Lane A Molecular weight standards, BSA (M_r 66k), ovalbumin (45k), carbonic anhydrase (29k), myoglobin (17k) and cytochrome c (12k); Lane B CCP (1.25 nmol); Lane C to K cleaved CCP with enzyme : substrate ratios of 1: 2100, 1050, 700, 525, 420, 350, 300 and 233 (w/w) respectively.

(a)ii) 300 pmol of each digest was loaded on a second gel for SDS-PAGE which was subsequently stained for haem using the method of Goodhew et al. (1986). Lane A Molecular weight standard cytochrome c (M_r 12k); Lane B CCP (1.25 nmol); Lane C to K cleaved CCP with enzyme : substrate ratios of 1: 2100, 1050, 700, 525, 420, 350, 300 and 233 (w/w) respectively.

(b) The traces are absorbance scans at 600 nm following protein staining for samples (i) CCP only, (ii) enzyme: substrate ratio of 1: 525 and (iii) enzyme : substrate ratio of 1: 300 (w/w).

(a)

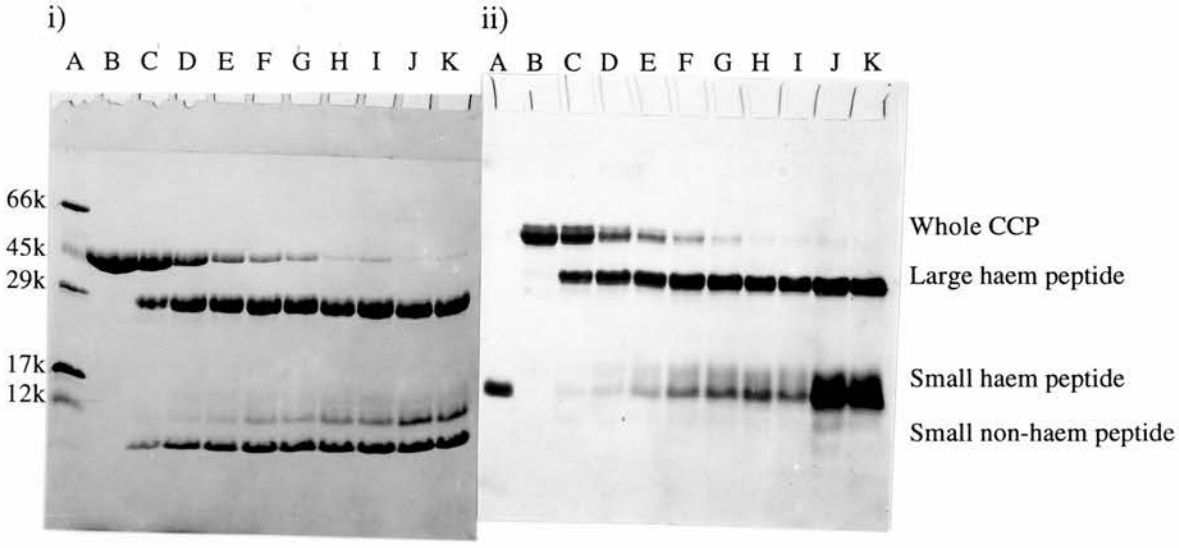
i)
ii)
A B C D E F G H I J K
A B C D E F G H I J K
66k
45k
29k
17k
12k
Whole CCP
Large haem peptide
Small haem peptide
Small non-haem peptide

(b)

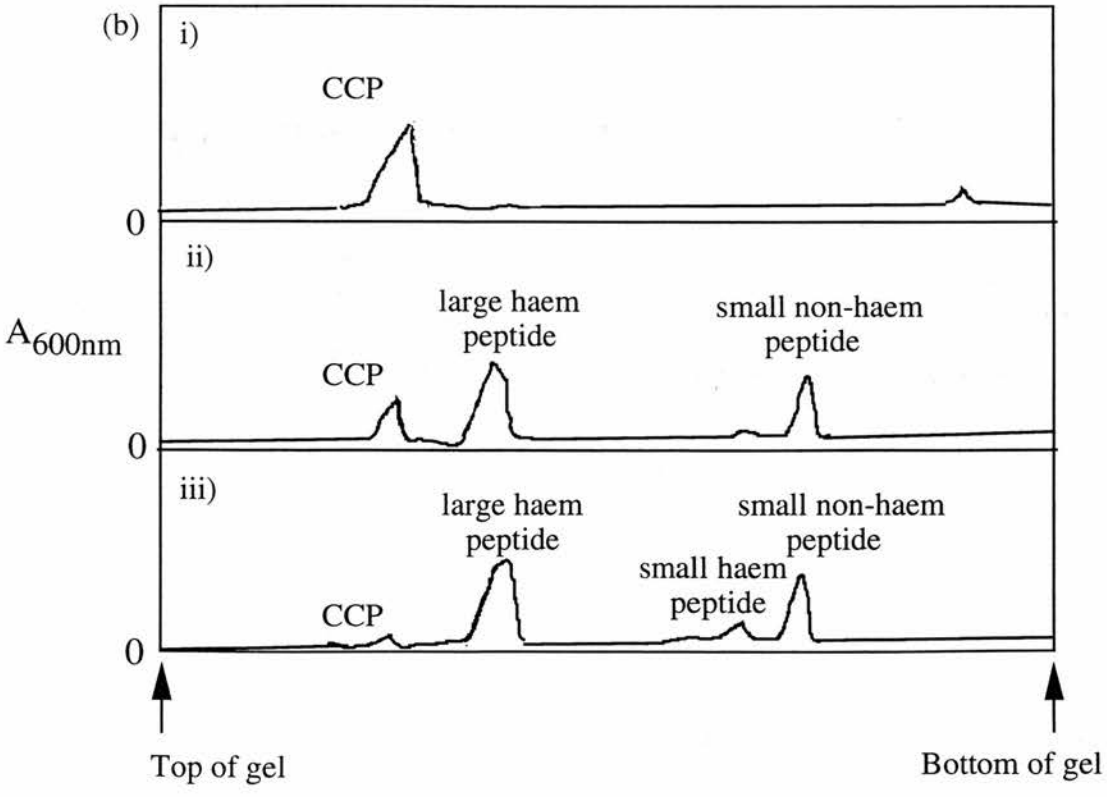
i)
CCP
0
ii)
large haem peptide
small non-haem peptide
CCP
A600nm
0
iii)
large haem peptide
small non-haem peptide
small haem peptide
CCP
0
Top of gel
Bottom of gel

Figure 5.3 Molecular weight estimation of peptides from subtilisin-cleaved CCP

The approximate molecular weight of peptides from CCP cleaved with subtilisin was determined from the Coomassie blue stained gel of Figure 5.2 (a)i). The closed circles represent the relative mobility of molecular weight standards BSA (M_r 66k), ovalbumin (45k), carbonic anhydrase (29k), myoglobin (17k) and cytochrome c (12k). From the relative mobility of the standards, peptides of CCP were interpolated to have an M_r of 8.7k (small non-haem peptide), 10.6k (small haem peptide) and 29.5k (large haem peptide) respectively. The M_r of undigested CCP was 42.2k.

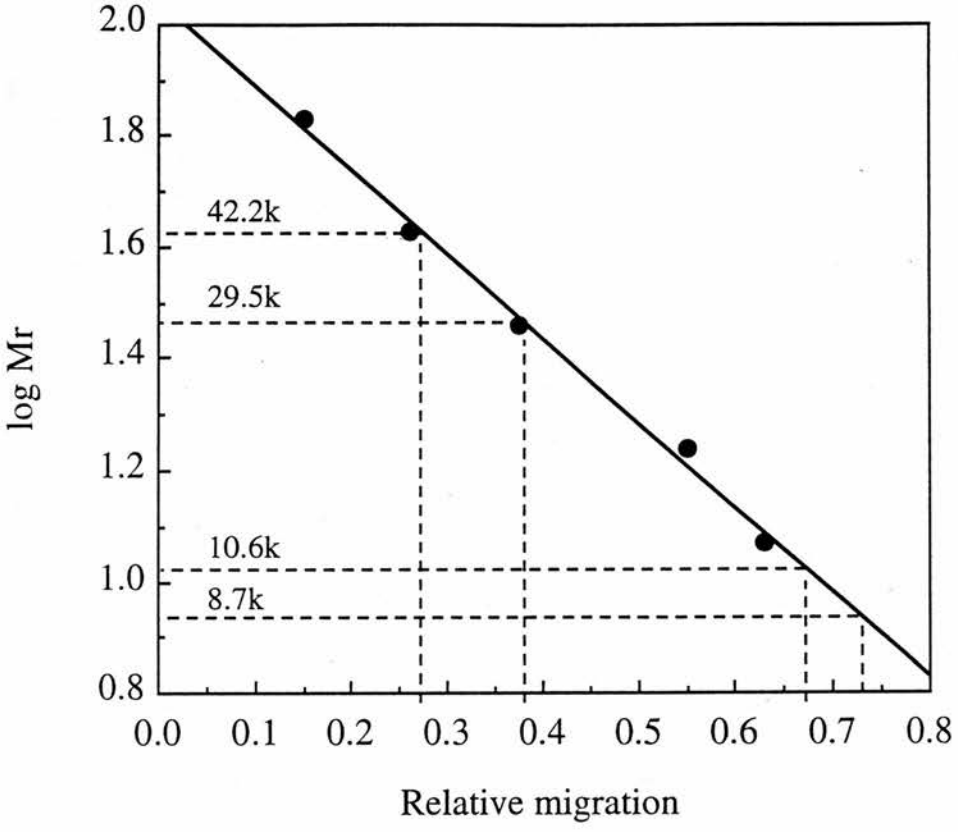
2.0
1.8
1.6
1.4
1.2
1.0
0.8
log Mr
42.2k
29.5k
10.6k
8.7k
0.0
0.1
0.2
0.3
0.4
0.5
0.6
0.7
0.8
Relative migration

Figure 5.4 Optimum extent of CCP cleavage with subtilisin
To CCP (5μM) in 10mM Hepes pH 7.5 was added ascorbate (1mM), DAD (10μM) and $CaCl_2$ (1mM). Subtilisin was added to give an enzyme : substrate ratio of 1: 500 (w/w). After 60 min at 0°C subtilisin was inhibited by PMSF (1mM), EGTA (10mM). The digest (1nmol) was loaded on a gel (15% polyacrylamide) for SDS-PAGE which was subsequently stained for protein with Coomassie blue. Lane A- Molecular weight standards, BSA (M_r 66k), ovalbumin (45k), carbonic anhydrase (29k), myoglobin (17k) and cytochrome c (12k); Lane B- CCP (1 nmol); Lane C- digested CCP (1nmol).

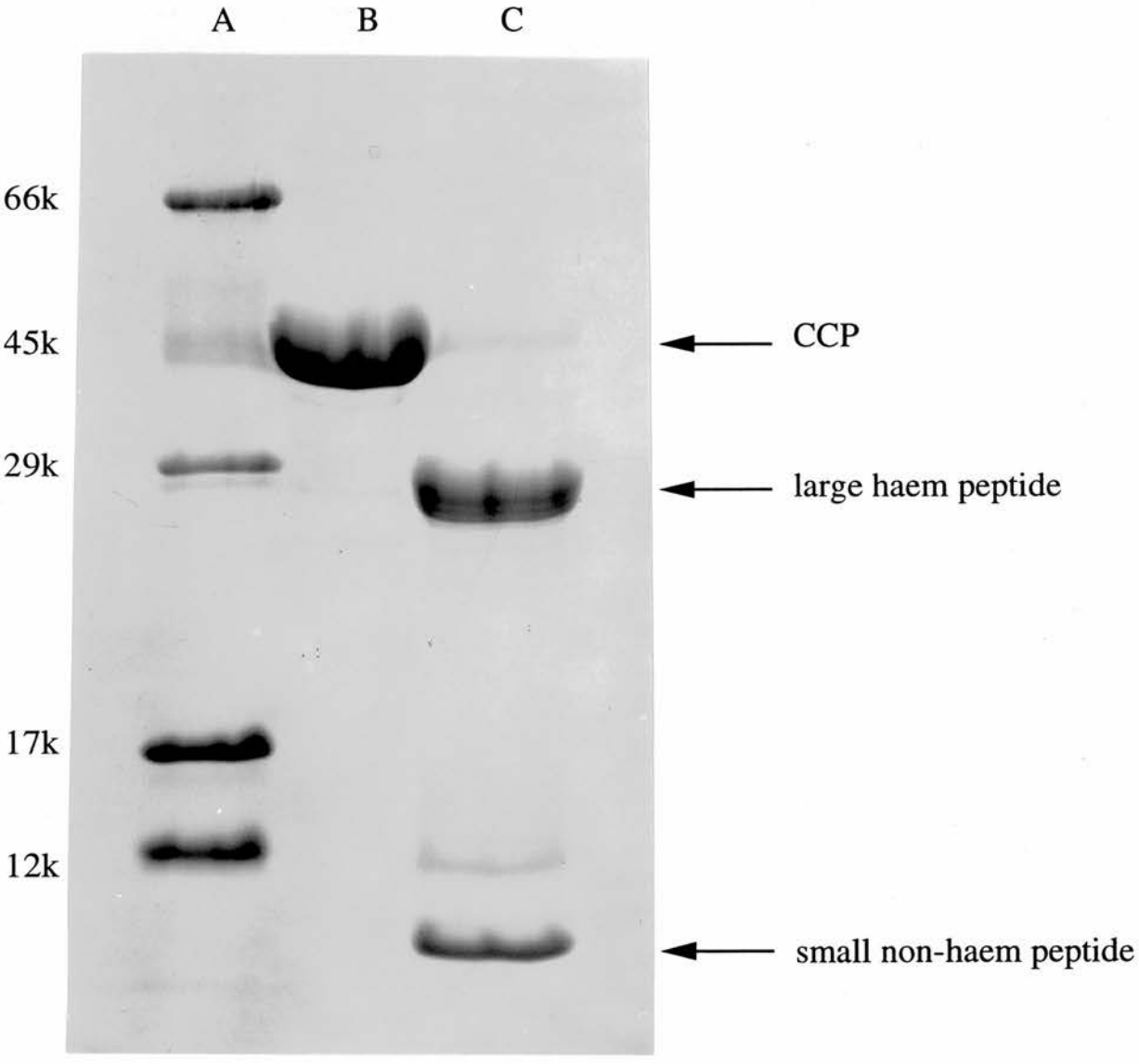
A
B
C
66k
45k
29k
17k
12k
CCP
large haem peptide
small non-haem peptide

haem group preventing complete protein denaturation upon incubation with SDS. Lack of an accurate M_r for the peptides make it impossible to predict whether the large haem peptide (~29.5k) and the small non-haem peptide (~8.7k) represent cleavage at one or more than one bond of the whole protein. It is possible though to predict the approximate location of the cleavage(s). The ~9k non-haem peptide can only arise from the C-terminal region of CCP as a ~9k N-terminal fragment would have a single haem attached. Interestingly release of the ~9k C-terminal fragment predicts a cleavage in the sequence region from *P.denitrificans* CCP analogous to the susceptible sequence region from *P.aeruginosa* CCP.

The cleavage pattern of the modified protein (up to 2 mol ethoxyformylhistidine per mol) with subtilisin was demonstrated to be identical to that of the native protein (Figure 5.5). Thus subtilisin seemed to be of possible use in the task of identifying the essential histidine in CCP and so a protocol was devised for purifying the cleaved peptides with the intention of identifying the precise cleavage location.

Complete separation of the two peptides resulting from cleavage of *P.aeruginosa* CCP with elastase required 1% SDS in the equilibration buffer of a molecular exclusion column (Soininen and Ellfolk, 1975). This requirement reflects the strength of attraction between the two fragments. It was envisaged that cleaved *P.denitrificans* CCP and the resultant separated fragments would lend themselves to general protein studies as well as for identification of the modified histidine. Because of the denaturing action of SDS, these conditions were thought to be less than ideal for use in these types of studies and so initial attempts used non-denaturing conditions for attempts at separating the two fragments.

5.2.3 Separation of CCP peptides using:-

(1) G75 Sephadex equilibrated in 20mM Tris pH 8, 100mM NaCl

Figure 5.6 shows the attempted separation of peptides from a subtilisin digest of CCP using a G75 Sephadex column equilibrated in 20mM Tris pH8, 100mM NaCl. Eluate fractions were collected and monitored at 280 and 410 nm. Only one

Figure 5.5 The relative susceptibility to cleavage of modified and native CCP

To aliquots of CCP (5μM) in 10mM Hepes pH 7.5 was added DEPC to final concentrations of 0, 5, 25, 100 and 400μM. This generated protein modified to the extent of 0, 0.5, 1.0, 1.5 and 2.0 mol ethoxyformylhistidine per mol respectively. After 20 min imidazole pH7.5 (2x respective [DEPC]) was added to each sample to quench any remaining DEPC. To each sample was added ascorbate (1mM), DAD (10μM) and $CaCl_2$ (1mM). Subtilisin was added to give enzyme : substrate ratioS of 1: 500 (w/w). After 60 min at 0°C, subtilisin was inhibited by PMSF (1mM), EGTA (10mM). The digests (1nmol) were loaded on a gel (15% polyacrylamide) for SDS-PAGE which was subsequently stained for protein with Coomassie blue . Lane A - Molecular weight standards, BSA (M_r 66k), ovalbumin (45k), carbonic anhydrase (29k), myoglobin (17k) and cytochrome c (12k); Lane B, C, D, E and F- digested CCP modified to the extent of 0, 0.5, 1.0, 1.5 and 2.0 mol per mol respectively.

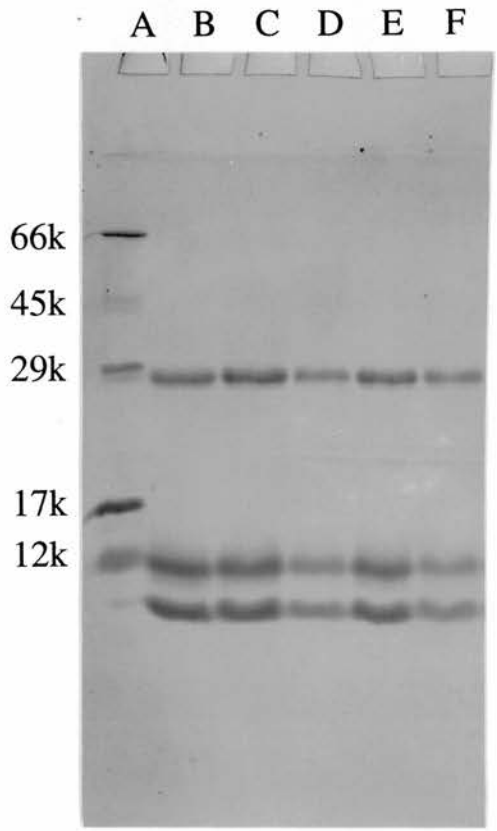
A B C D E F
66k
45k
29k
17k
12k

main peak was observed, which upon determining its protein and haem composition by SDS-PAGE (Figure 5.6 (i) and (ii) respectively), was found to contain both large and small haem peptides, the small non-haem peptide and any remaining undigested CCP. The stained bands appear very diffuse due to the high [salt] loaded onto the polyacrylamide gel. Obviously the peptides within the cleaved protein remain strongly attracted to one another.

(2) G75 Sephadex equilibrated in 0.1M ammonia solution

The failure of G75 Sephadex equilibrated in Tris / NaCl to separate the CCP peptides led to the use of 0.1M ammonia solution. As well as being potentially useful in separating strongly attracting peptides, ammonia itself is volatile and can be easily removed from the resulting sample. Figure 5.7 shows the attempted separation of peptides from a subtilisin digest of CCP using a G75 Sephadex column equilibrated in 0.1M ammonia solution. Eluate fractions were collected and monitored at 280 and 410 nm. The protein and haem composition of the two main peaks detected showed only partial separation of the high molecular mass peptides from the low molecular mass peptides.

5% formic acid was also used as an equilibration solution for Sephadex G75 in attempting to purify the subtilisin-cleaved CCP peptides and the degree of separation was slightly poorer than the 0.1M ammonia solution (results not shown).

(3) Reverse phase high performance liquid chromatography

As the first objective of this separation exercise was to purify and consequently identify the CCP fragments, reverse phase HPLC was performed in an attempt to prepare analytical amounts of the large haem peptide and the small non-haem peptide for amino acid composition, Edman degradation and mass spectrometry. Figure 5.8 shows the elution profile (monitored at 214 nm) from the reverse phase column and the respective SDS-PAGE analysis of the peak composition. The polyacrylamide gel stained for protein clearly shows the resolution of both undigested CCP and the lower molecular mass haem peptide, but the larger haem peptide and the small non-haem peptide coelute in the same fraction. This provides more evidence of the strength of

Figure 5.6 Attempted separation of peptides from subtilisin digest of CCP using G75 Sephadex equilibrated in 20mM Tris pH8, 100mM NaCl
To CCP (10-20μM) in 10mM Hepes pH 7.5 was added ascorbate (1mM), DAD (10μM) and $CaCl_2$ (1mM). Subtilisin was added to give an enzyme : substrate ratio of approximately 1: 400 (w/w). After 60 min at 0°C subtilisin was inhibited by PMSF (1mM), EGTA (10mM). The digest (20 nmol) was loaded onto a G75 Sephadex column (2 x 80 cm) pre-equilibrated in 20mM Tris pH 8, 100mM NaCl at 4°C. Fractions (3ml) were collected and both A_{280nm} (open circles) and A_{410nm} (closed circles) recorded. The protein and haem composition of freeze dried fractions was determined by both (i) Coomassie blue and (ii) haem staining (Goodhew et al. 1986), after SDS-PAGE, on a 15% polyacrylamide gel.
(i) Lane A- molecular weight standards BSA (M_r 66k), ovalbumin (45k), carbonic anhydrase (29k), myoglobin (17k) and cytochrome c (12k): Lane B Undigested CCP: Lane C to G- Fractions 34 to 38 respectively: Lane H to K- Fractions 46 to 49 respectively.
(ii) Lane A and K- molecular weight standard cytochrome c (M_r 12k): Lane B Undigested CCP: Lane C to G - Fractions 34 to 38 respectively: Lane H to J - Fractions 47 to 49 respectively.

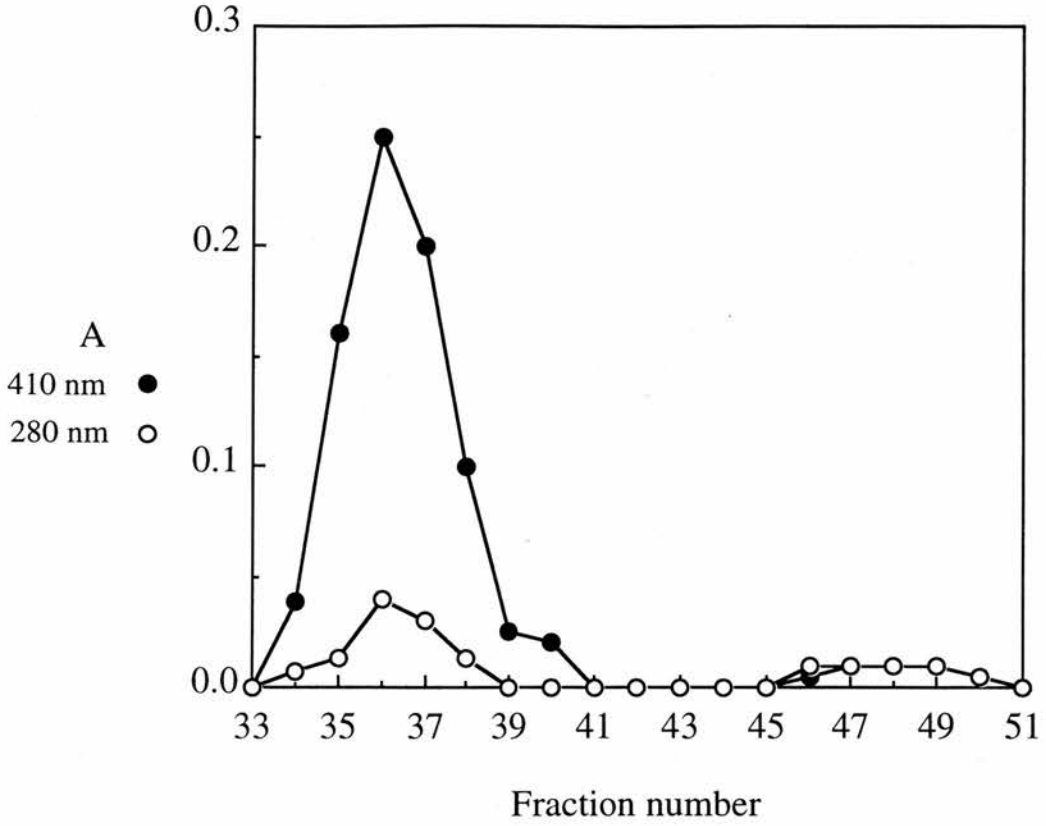
0.3
0.2
0.1
0.0
A
410 nm
280 nm
33 35 37 39 41 43 45 47 49 51
Fraction number

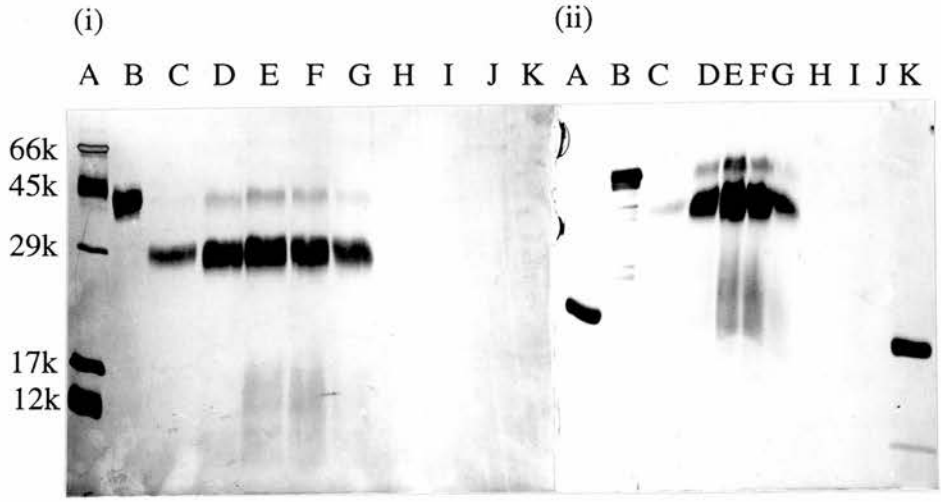
(i)
(ii)
A B C D E F G H I J K A B C DEFG H I J K
66k
45k
29k
17k
12k

Figure 5.7 Attempted separation of peptides from subtilisin digest of CCP using G75 Sephadex equilibrated in 0.1M ammonia solution
Subtilisin digested CCP was prepared as in the legend to Figure 5.4 and loaded (20 nmol) onto a G75 Sephadex column (2 x 80 cm) pre-equilibrated in 0.1M ammonia solution at 4°C. Fractions (3ml) were collected and both A_{280nm} (open circles) and A_{410nm} (closed circles) recorded. The protein and haem composition of eluate was determined by (i) silver staining (Morrisey, 1981) and (ii) haem staining (Goodhew et al.1986), after SDS-PAGE, on a 15% polyacrylamide gel.
(i) Lane A and I - molecular weight standards BSA (M_r 66k), ovalbumin (45k), carbonic anhydrase (29k), myoglobin (17k) and cytochrome c (12k): Lane B Undigested CCP: Lane C to G - Fractions 30 to 34 respectively: Lane H - Fraction 38.
(ii) Lane A and I- molecular weight standard cytochrome c (M_r 12k): Lane B Undigested CCP: Lane C to G - Fractions 30 to 34 respectively: Lane H - Fraction 38.

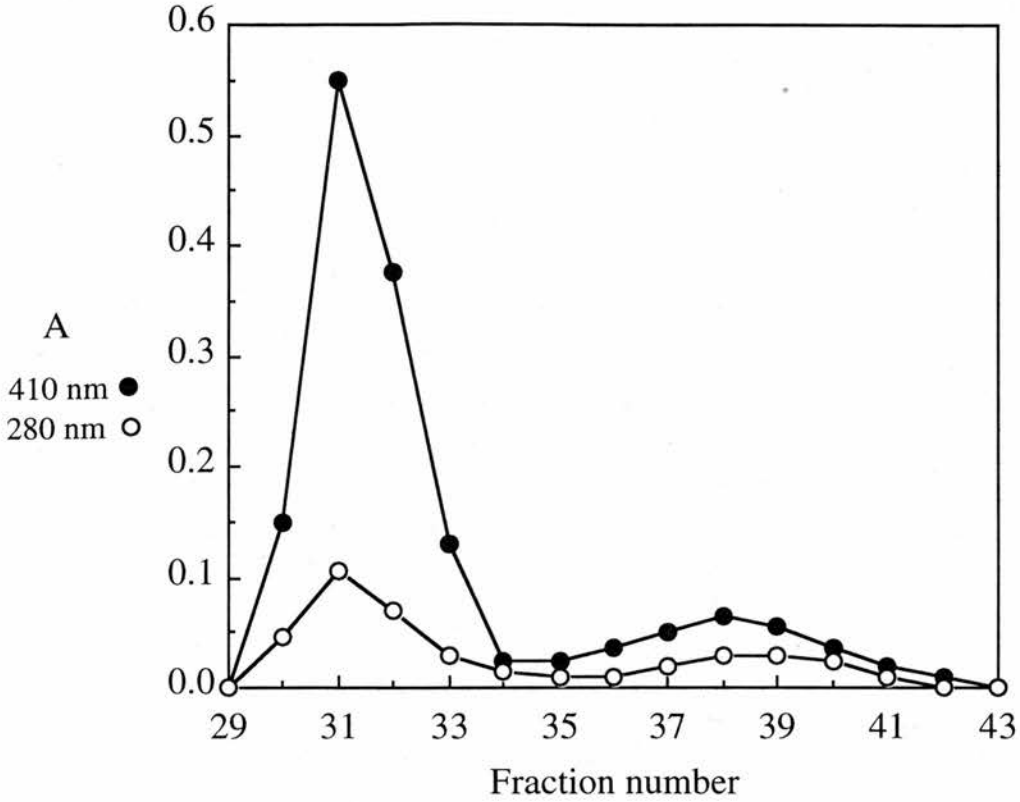
A
410 nm ●
280 nm ○
0.6
0.5
0.4
0.3
0.2
0.1
0.0
29
31
33
35
37
39
41
43
Fraction number

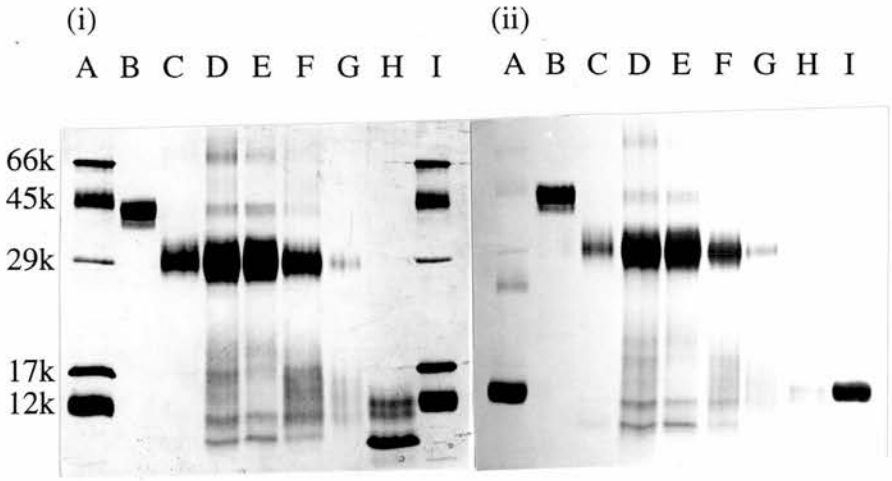
(i)
A B C D E F G H I
(ii)
A B C D E F G H I
66k
45k
29k
17k
12k

Figure 5.8 Attempted separation of peptides from subtilisin digest of CCP using reverse phase HPLC

Subtilisin digested CCP was prepared as in the legend to Figure 5.4 and loaded (2 nmol) onto an aquapore RP300 reverse phase C8 cartridge (30 x 2.1 mm). A gradient of 0-70% acetonitrile in 0.1% trifluoroacetic acid was used and the eluate continuously monitored at 214 nm. The protein and haem composition of peaks 1-3 was determined by silver staining (Morrisey, 1981), after SDS-PAGE on a 15% polyacrylamide gel. (i) Lane A and G - molecular weight standards BSA (M_r 66k), ovalbumin (45k), carbonic anhydrase (29k), myoglobin (17k) and cytochrome c (12k): Lane B - Undigested CCP: Lane C - Digested CCP: Lane D,E, F - peak 1, 2, 3 respectively.

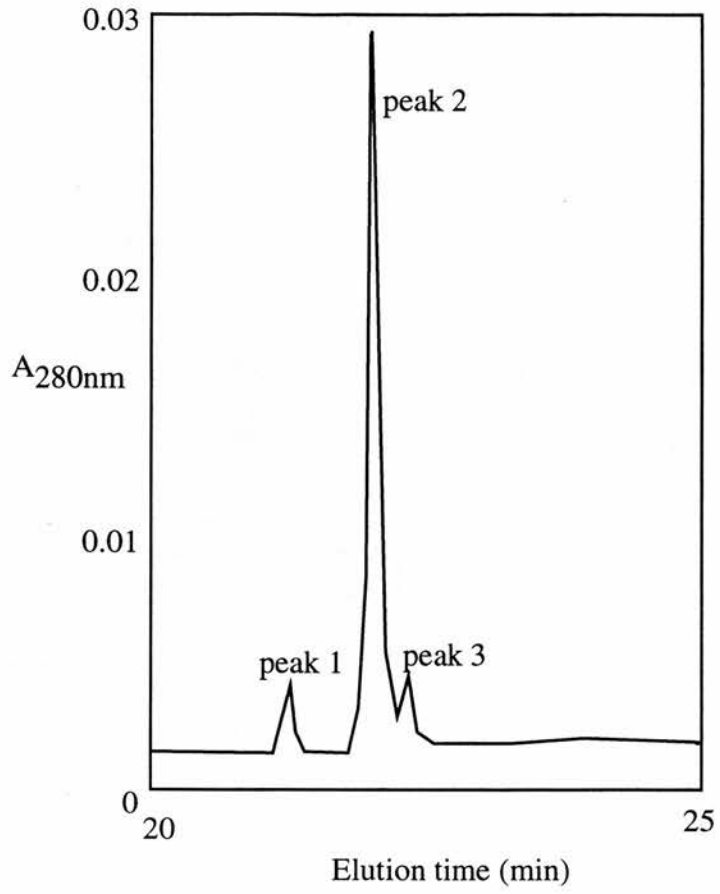
0.03
0.02
A_{280nm}
0.01
0
peak 1
peak 2
peak 3
20
25
Elution time (min)

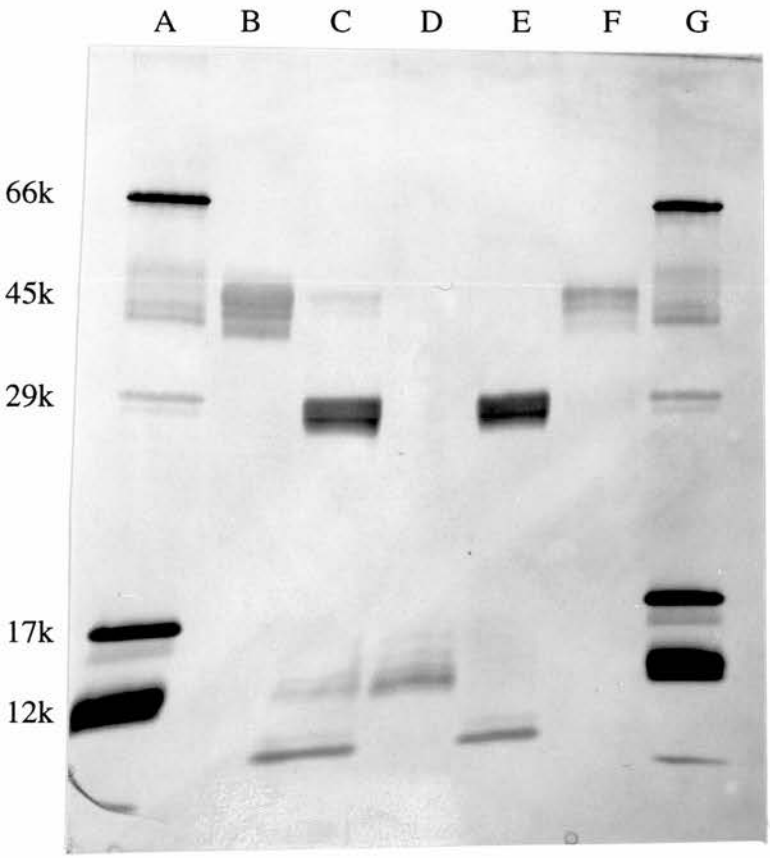
A
B
C
D
E
F
G
66k
45k
29k
17k
12k

attraction between these two peptides in particular.

From the evidence of these trial separations and from the need for SDS to separate the two fragments of *P.aeruginosa* CCP (Soininen and Ellfolk, 1975; Ronnberg, 1987), it was thought necessary to use SDS in the separation of the two fragments from *P.denitrificans* CCP.

(4) G75 Sephadex equilibrated, at 4°C, in 20mM Tris pH 8, 100mM NaCl and 0.1% SDS

Figure 5.9 shows the attempted separation of peptides from a subtilisin digest of CCP (digestion has progressed more than usual in this experiment) using G75 Sephadex equilibrated, at 4°C, in 20mM Tris pH 8, 100mM NaCl and 0.1% SDS. Eluate fractions were collected and monitored at 280 and 410 nm. Despite the presence of SDS, the protein and haem composition of the two main peaks still displayed only partial separation of the high molecular mass peptides from the low molecular mass peptides. Again the large haem peptide and the smaller non-haem peptide coelute in the same fraction. Therefore the SDS concentration was increased to 1% and the temperature raised to 23°C.

(5) G75 Sephadex equilibrated, at 23°C, in 20mM Tris pH 8, 100mM NaCl and 1% SDS

Figure 5.10 shows the separation of peptides from a subtilisin digest of CCP using G75 Sephadex equilibrated, at 23°C, in 20mM Tris pH 8, 100mM NaCl and 1% SDS. Eluate fractions were collected and monitored at 280 and 410 nm. Protein and haem staining, subsequent to SDS-PAGE of the two main peaks determined the larger haem peptide to be separated from the other small peptides. To achieve purification of the smaller non-haem peptide, the level of subtilisin digestion of CCP had to be decreased so no smaller haem peptides were generated. This lowering of digestion however left an amount of undigested CCP which would now coelute with the larger haem peptide. Therefore to fully purify both the large haem peptide and the smaller non-haem fragment two levels of digestion were required in two separate experiments.

The similarity of the properties of cleaved *P.aeruginosa* and *P.denitrificans*

Figure 5.9 Attempted separation of peptides from subtilisin digest of CCP using G75 Sephadex equilibrated in 20mM Tris pH8, 100mM NaCl, 0.1% SDS

Subtilisin digested CCP was prepared as in the legend to Figure 5.4 and loaded (20 nmol) onto a G75 Sephadex column (2 x 80 cm) pre-equilibrated in 20mM Tris pH8, 100mM NaCl, 0.1% SDS at 4°C. Fractions (3ml) were collected and both A_{280nm} (open circles) and A_{410nm} (closed circles) recorded. The protein and haem composition of freeze-dried fractions was determined by (i) silver staining (Morrisey, 1981) and (ii) haem staining (Goodhew et al.1986), after SDS-PAGE, on a 15% polyacrylamide gel.
(i) Lane A - molecular weight standards BSA (M_r 66k), ovalbumin (45k), carbonic anhydrase (29k), myoglobin (17k) and cytochrome c (12k): Lane B- Digested CCP: Lane C to G - Fractions 79 to 83 respectively: Lane H to K - Fractions 93 to 96.
(ii) Lane A - molecular weight standard cytochrome c (M_r 12k): Lane B to F - Fractions 79 to 83 respectively: Lane G to J - Fraction 93-96.

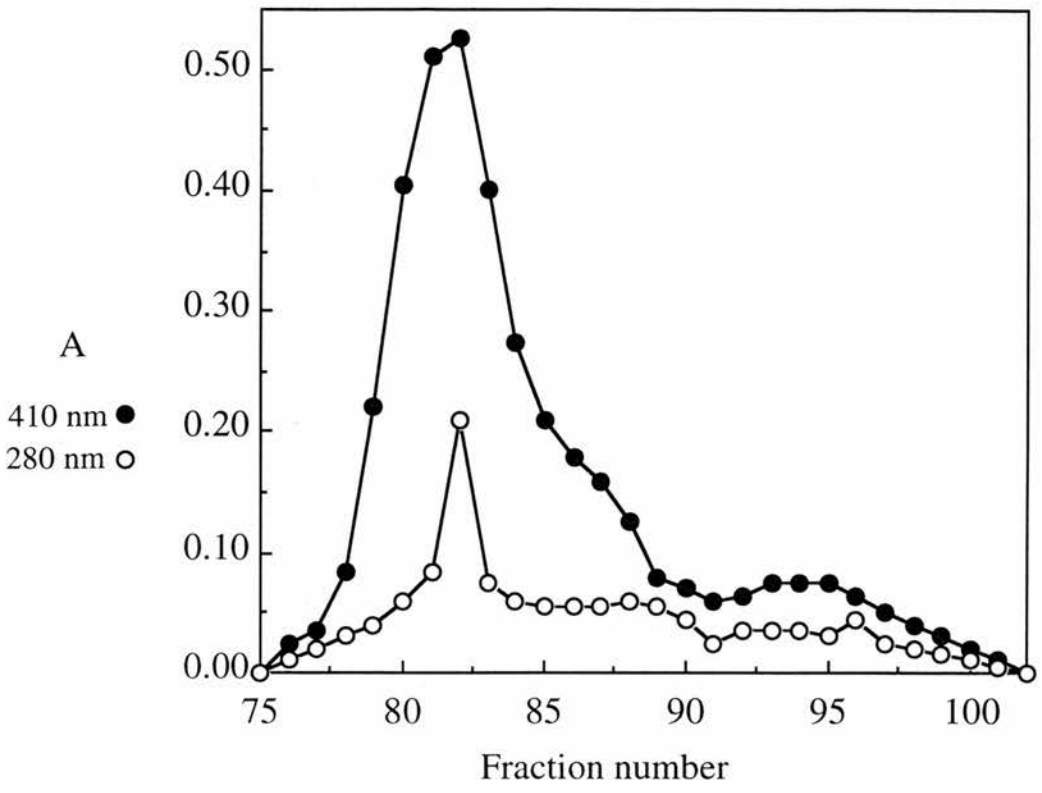
A
410 nm ●
280 nm ○
0.50
0.40
0.30
0.20
0.10
0.00
75
80
85
90
95
100
Fraction number

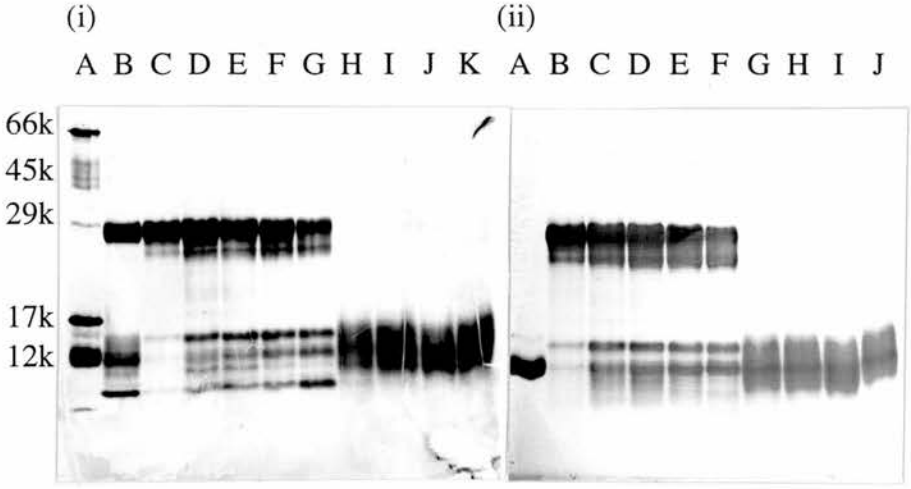
(i)
(ii)
A B C D E F G H I J K A B C D E F G H I J
66k
45k
29k
17k
12k

Figure 5.10 Separation of peptides from subtilisin digest of CCP using G75 Sephadex equilibrated in 20mM Tris pH8, 100mM NaCl, 1% SDS
Subtilisin digested CCP was prepared as in the legend to Figure 5.4 and made to 1% SDS before being loaded (20 nmol) onto a G75 Sephadex column (2 x 80 cm) pre-equilibrated in 20mM Tris pH8, 100mM NaCl, 1% SDS at 23°C. Fractions (3ml) were collected and both A_{280nm} (open circles) and A_{410nm} (closed circles) recorded. The protein and haem composition of eluate was determined by (i) silver staining (Morrisey, 1981) and (ii) haem staining (Goodhew et al.1986), after SDS-PAGE, on a 15% polyacrylamide gel.
(i) Lane A - molecular weight standards BSA (M_r 66k), ovalbumin (45k), carbonic anhydrase (29k), myoglobin (17k) and cytochrome c (12k): Lane B - Digested CCP: Lane C to F - Fractions 50 to 53 respectively: Lane G to J - Fractions 69 to 72.
(ii) Lane A - molecular weight standard cytochrome c (M_r 12k): Lane B - Digested CCP: Lane C to F - Fractions 50 to 53 respectively: Lane G to J - Fractions 69 to 72 respectively.

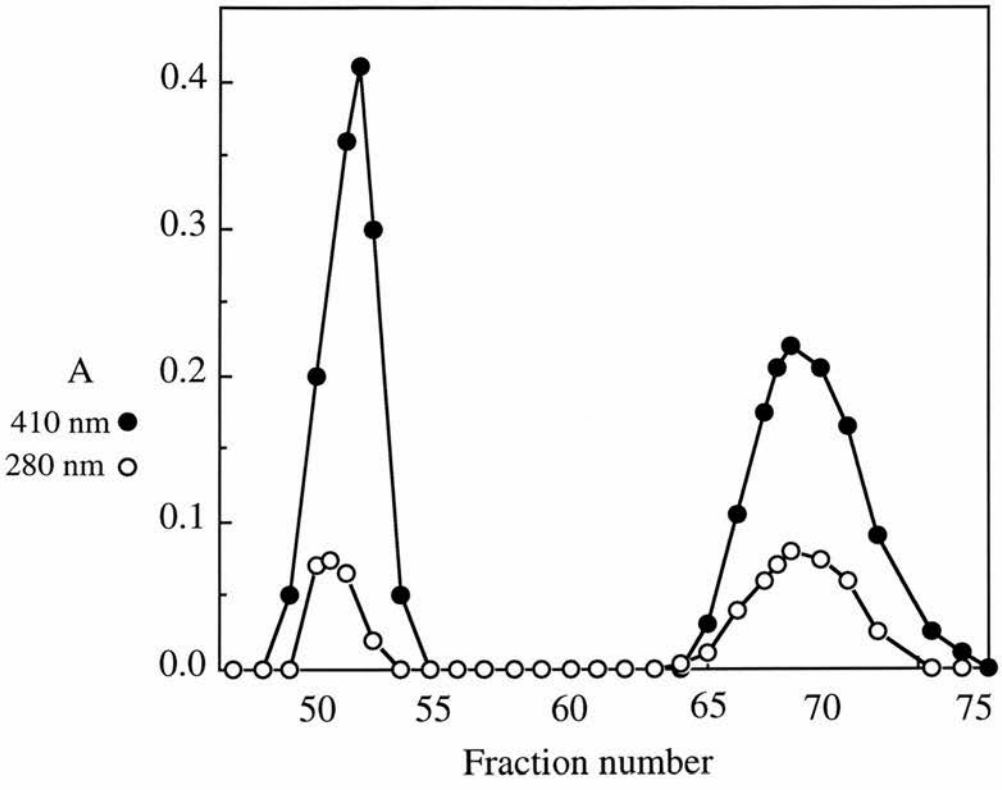
A
410 nm ●
280 nm ○
0.4
0.3
0.2
0.1
0.0
50
55
60
65
70
75
Fraction number

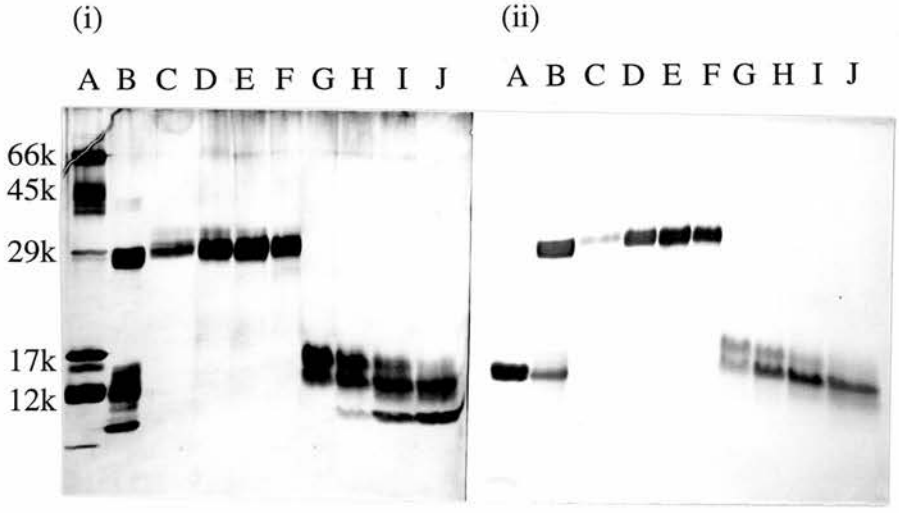
(i)
A B C D E F G H I J
66k
45k
29k
17k
12k
(ii)
A B C D E F G H I J

peroxidases are striking. Both proteins, upon cleavage with different non-specific proteases, generate a large haem peptide (M_r~30k) and a small non-haem peptide (M_r~10k). The denaturing action of 1% SDS is required to promote separation and therefore purification of the two fragments from both proteins.

The technique described above was suitable for purifying preparative amounts of both the large haem peptide and the small non-haem peptide from CCP. However it became obvious that a semi-analytical method was also required, in order to achieve rapid separations during the identification of labelled essential histidine (see Chapter VI). The technique developed involved use of a Superdex 75 molecular exclusion column in an Fast Protein Liquid Chromatography set up, with eluate monitoring at 280 nm. Whereas the CCP peptides are eluted from a large G75 Sephadex column approximately 24 h after loading, peptides are eluted from a Superdex 75 column within 20 min.

(6) Superdex 75 equilibrated in 0.1M ammonia solution

As Sephadex G75 equilibrated in 0.1M ammonia solution permitted partial separation of the cleaved CCP peptides the same conditions were used for the Superdex 75 column. Figure 5.11 shows the 280 nm profile of the attempted separation of cleaved CCP through a Superdex 75 column equilibrated in 0.1M ammonia solution. The protein composition of the eluted peak was determined by Coomassie blue staining following SDS-PAGE and clearly shows no separation of the peptides. However these column conditions were subsequently determined to be useful for desalting purified peptides. This was especially useful for preparing peptides for mass spectrometry.

(7) Superdex 75 equilibrated in 20mM Tris pH8, 100mM NaCl and 1% SDS

Figure 5.12 shows the separation of peptides from a subtilisin digest of CCP using Superdex 75 equilibrated, at 23°C, in 20mM Tris pH 8, 100mM NaCl and 1% SDS. Staining for protein following SDS-PAGE showed the larger haem peptide to be separated from the smaller non-haem peptide. However it was determined by using

Figure 5.11 Attempted separation of peptides from subtilisin digest of CCP using Superdex 75 equilibrated in 0.1M ammonia solution

Subtilisin digested CCP was prepared as in the legend to Figure 5.4. The digest (~3 nmol) was loaded onto a Pharmacia Superdex 75 column equilibrated in 0.1M ammonia solution at 23°C; flow rate 0.75 ml/min. The eluate was continuously monitored at 280 nm and the protein composition of the resultant peak determined by Coomassie blue staining after SDS-PAGE, on a 15% polyacrylamide gel.

Lane A - molecular weight standards BSA (M_r 66k), ovalbumin (45k), carbonic anhydrase (29k), myoglobin (17k) and cytochrome c (12k): Lane B - Digested CCP: Lane C - Main peak.

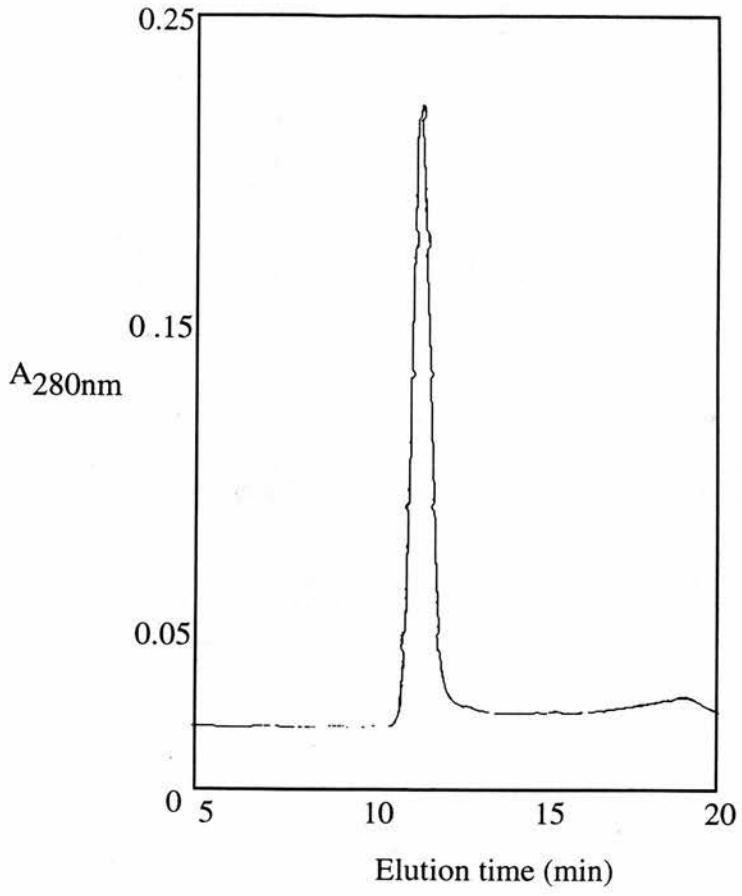
0.25
0 .15
A_{280nm}
0.05
0
5
10
15
20
Elution time (min)

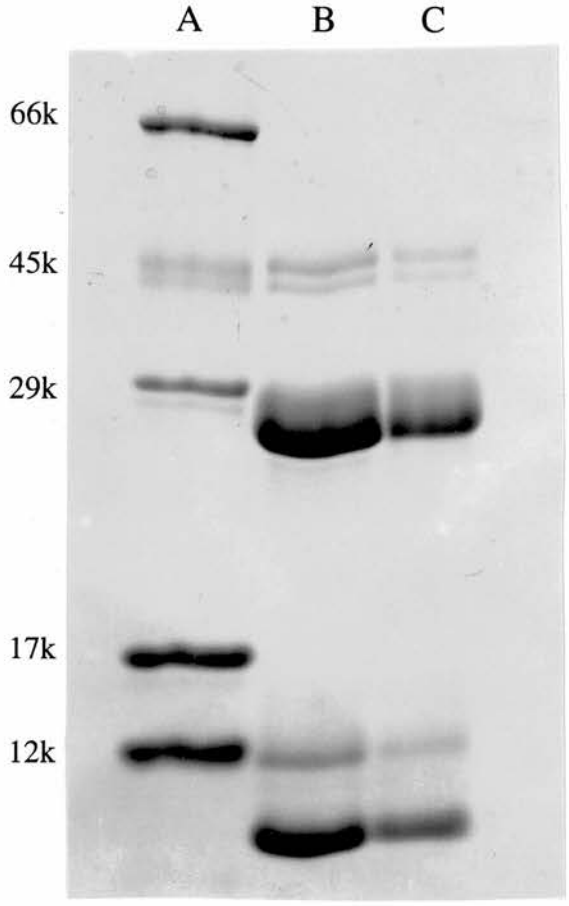
A
B
C
66k
45k
29k
17k
12k

149

Figure 5.12 Separation of peptides from subtilisin digest of CCP using Superdex 75 equilibrated in 20mM Tris pH8, 100mM NaCl, 1% SDS

Subtilisin digested CCP was prepared as in the legend to Figure 5.4. The digest (~3 nmol) was made to 1% SDS and loaded onto a Pharmacia Superdex 75 column equilibrated in 20mM Tris pH 8, 100mM NaCl, 1% SDS at 23°C; flow rate 0.75 ml/min. The eluate was continuously monitored at 280 nm and the protein composition of the resultant freeze-dried fractions determined by Coomassie blue staining after SDS-PAGE, on a 15% polyacrylamide gel.

Lane A - molecular weight standards BSA (M_r 66k), ovalbumin (45k), carbonic anhydrase (29k), myoglobin (17k) and cytochrome c (12k): Lane B - Digested CCP pre-Superdex: Lane C, D, E - fractions 1, 2, 3 respectively.

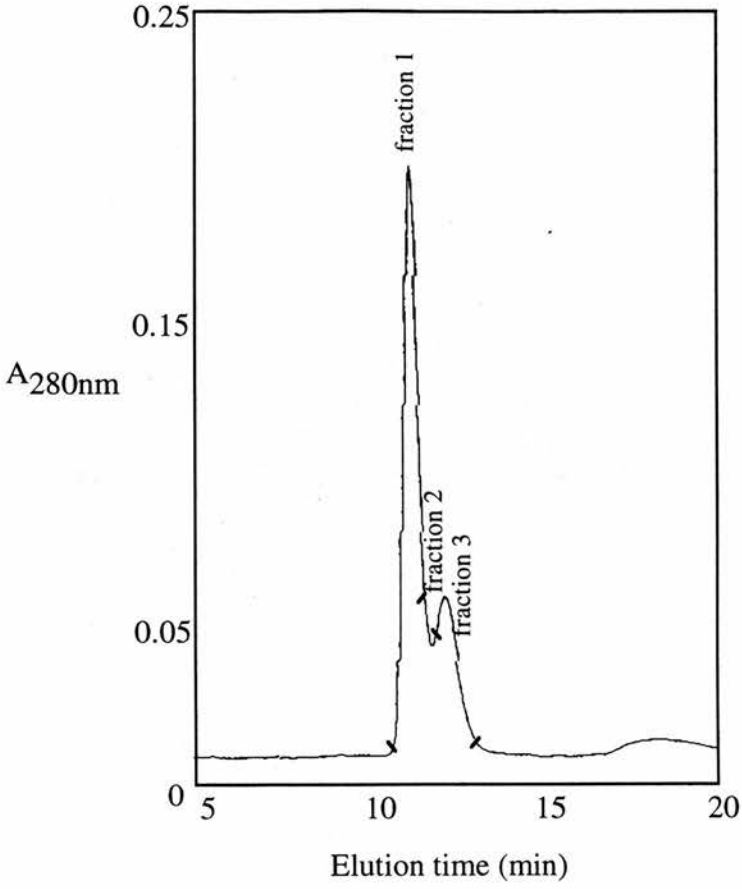
0.25
0.15
0.05
0
A280nm
fraction 1
fraction 2
fraction 3
5
10
15
20
Elution time (min)

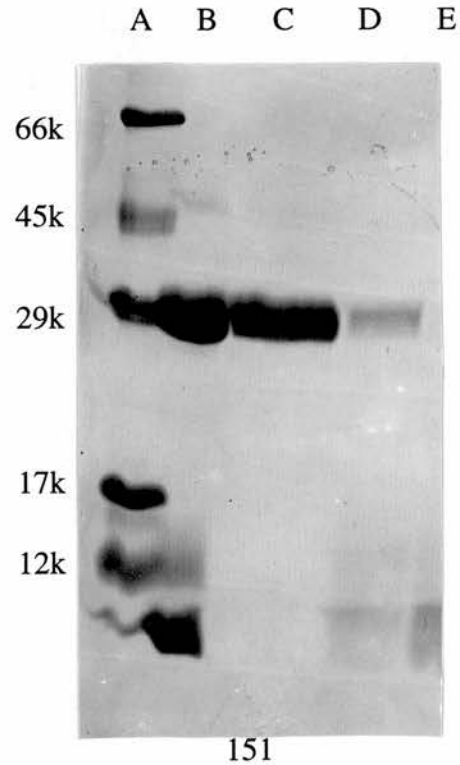
A
B
C
D
E
66k
45k
29k
17k
12k

molecular weight standards, that the resolution capability of Superdex 75 is significantly decreased upon using SDS in the equilibration buffer. This could be due to either SDS coating the inside or outside of the dextran beads and/or to the column's inability to resolve the SDS:protein aggregates. SDS was added to the cleaved protein sample, to a final concentration of 1%, prior to loading on the Superdex 75 column equilibrated in 20mM Tris pH8, 100mM NaCl.

(8) Superdex 75 equilibrated in 20mM Tris pH8, 100mM NaCl

Figure 5.13 shows the separation of peptides from a subtilisin digest of CCP, in 1% SDS, using Superdex 75 equilibrated, at 23°C, in 20mM Tris pH 8, 100mM NaCl. The resolution of the two main peaks is greater than in the column equilibrated in 1% SDS. Again staining for protein subsequent to SDS-PAGE showed the larger haem peptide to be well separated from the smaller non-haem peptide. The limitation to this method was the amount of material able to be purified; 3-4 nmols of cleaved CCP in 200µl of 1% SDS was the maximum that could be loaded to ensure separation of the peptides. At higher protein concentrations SDS must not be able to denature cleaved CCP sufficiently to allow separation of the peptides. Increasing the concentration of SDS did not improve resolution.

Both preparative and analytical methods have been developed for purification of subtilisin-cleaved peptides from CCP. The next section of work will use the preparative and analytical purification techniques described above, as well as a separate method, to identify both the large haem peptide and the small non-haem peptide of CCP.

5.2.4 Edman degradation of peptides from subtilisin-cleaved CCP

While the above methods for purifying CCP peptides were being developed, a relatively new technique for isolating peptides specifically for sequencing by Edman degradation was performed. subtilisin-cleaved samples of CCP were prepared as described in the legend to Figure 5.4 and separated by SDS-PAGE. Electrophoretic transfer of the separated peptides to an inert support polyvinylidenediflouride (PVDF)

Figure 5.13 Separation of peptides from subtilisin digest of CCP, in 1% SDS, using Superdex 75 equilibrated in 20mM Tris pH 8, 100mM NaCl
Subtilisin digested CCP was prepared as in the legend to Figure 5.4. The digest (~3 nmol) was made to 1% SDS and loaded onto a Pharmacia Superdex 75 column equilibrated in 20mM Tris pH8, 100mM NaCl at 23°C. The eluate was continuously monitored at 280 nm and the protein composition of the resultant freeze-dried fractions determined by Coomassie blue staining after SDS-PAGE, on a 15% polyacrylamide gel.
Lane A - molecular weight standards BSA (M_r 66k), ovalbumin (45k), carbonic anhydrase (29k), myoglobin (17k) and cytochrome c (12k): Lane B - Subtilisin digested CCP: Lane C to G - fractions 1 to 5 respectively.

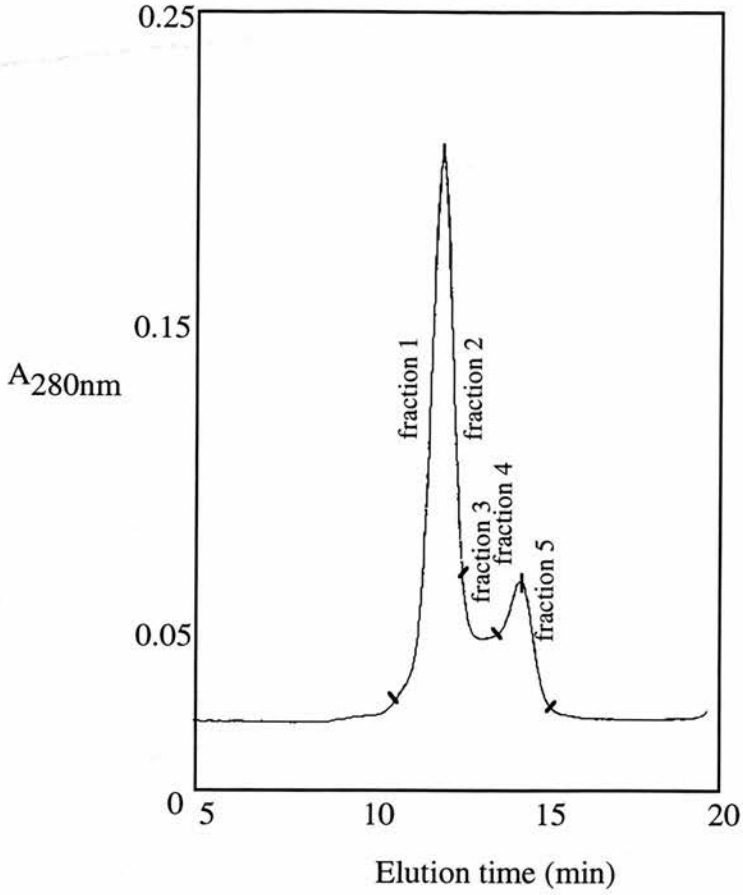
0.25
0.15
0.05
0
A_{280nm}
fraction 1
fraction 2
fraction 3
fraction 4
fraction 5
5
10
15
20
Elution time (min)

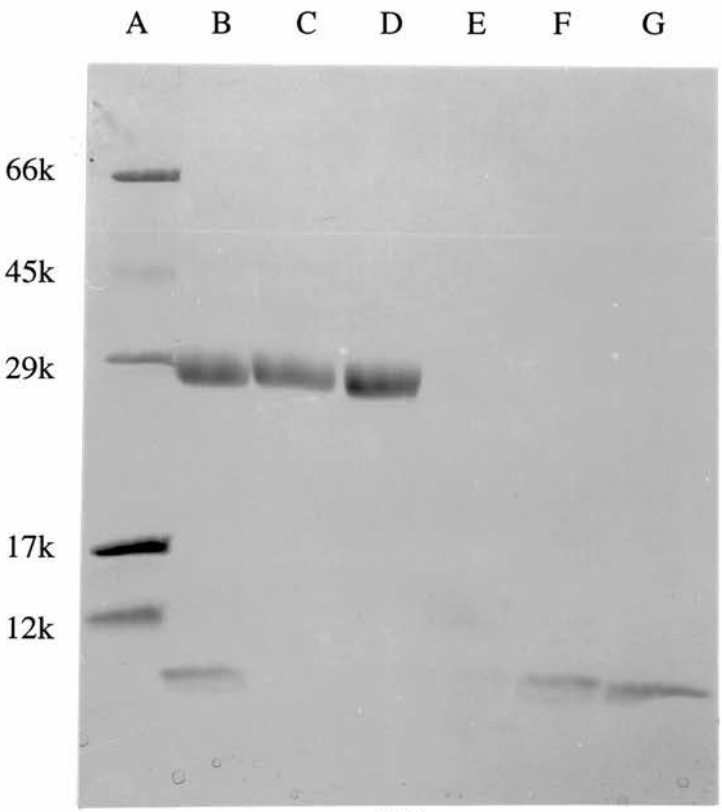
A
B
C
D
E
F
G
66k
45k
29k
17k
12k

membrane (ProBlott) was then initiated . The membrane was stained for protein with Coomassie blue and the location of the large haem peptide and the small non-haem peptide identified. Each band was excised from the membrane, placed in the standard reaction cartridge block and sequenced using an Applied Biosystems 477A instrument with a 120A on-line phenylthiohydantoin analyser (see Materials and Methods, section 2.2.1 for detailed protocol). For the small non-haem peptide, five cycles of Edman degradation released the amino acids R T T D D respectively. For the large haem peptide no amino acids were released suggesting a blocked N-terminus to the fragment.

From this small amount of sequence information, the specific subtilisin cleavage site was tentatively identified (Figure 5.14). Assuming only one cleavage site, it is proposed that subtilisin-cleaved CCP between T250 and R251 generating a C-terminal non-haem fragment from R251 to M338, the first five residues of this fragment being R T T D D and a N-terminal fragment from pE1 (pyroglutamate) to T250 which contains both haem binding sites. The M_r of both these peptides, as estimated from SDS-PAGE (see Figure 5.3), correlate to their proposed sequences.

5.2.5 Amino acid composition of the large haem peptide

As no N-terminal sequence information for the large haem peptide was available, amino acid composition analysis was carried out and the results shown in Table 5.1. The table compares the experimental analysis of purified large haem peptide with the actual values derived from the sequence pE1 to T250. These values compare quite well and lead to the conclusion that the large haem peptide is indeed pE1-T250. However the identity of both peptides were confirmed by mass spectrometry.

5.2.6 Mass spectrometry of peptides from subtilisin-cleaved CCP

Figure 5.15 shows mass spectra of the large haem peptide and the small non-haem peptide. The spectrum of the large haem peptide actually shows the presence of three peptides of M_r 27950.90, 27622.64 and 26986.18. The spectrum of the small non-haem peptide shows the presence of only one peptide of M_r 9581.38, with several sodium adduct derivatives of the same peptide. Table 5.2 compares the experimentally

Figure 5.14 Amino acid sequence of *P.denitrificans* CCP and proposed subtilisin cleavage site

The recently determined amino acid sequence of CCP from *P.denitrificans* is shown (Goodhew, Pettigrew and van Beeumen unpublished results). (1) This arrow indicates the proposed single cleavage location (between T250 and R251) of *P.denitrificans* CCP upon incubation with subtilisin. (2) This arrow indicates the analogous position in *P.denitrificans* CCP of the *Pseudomonas* CCP elastase cleavage site.
<E represents the N-terminal residue pyroglutamate of *P.denitrificans* CCP.

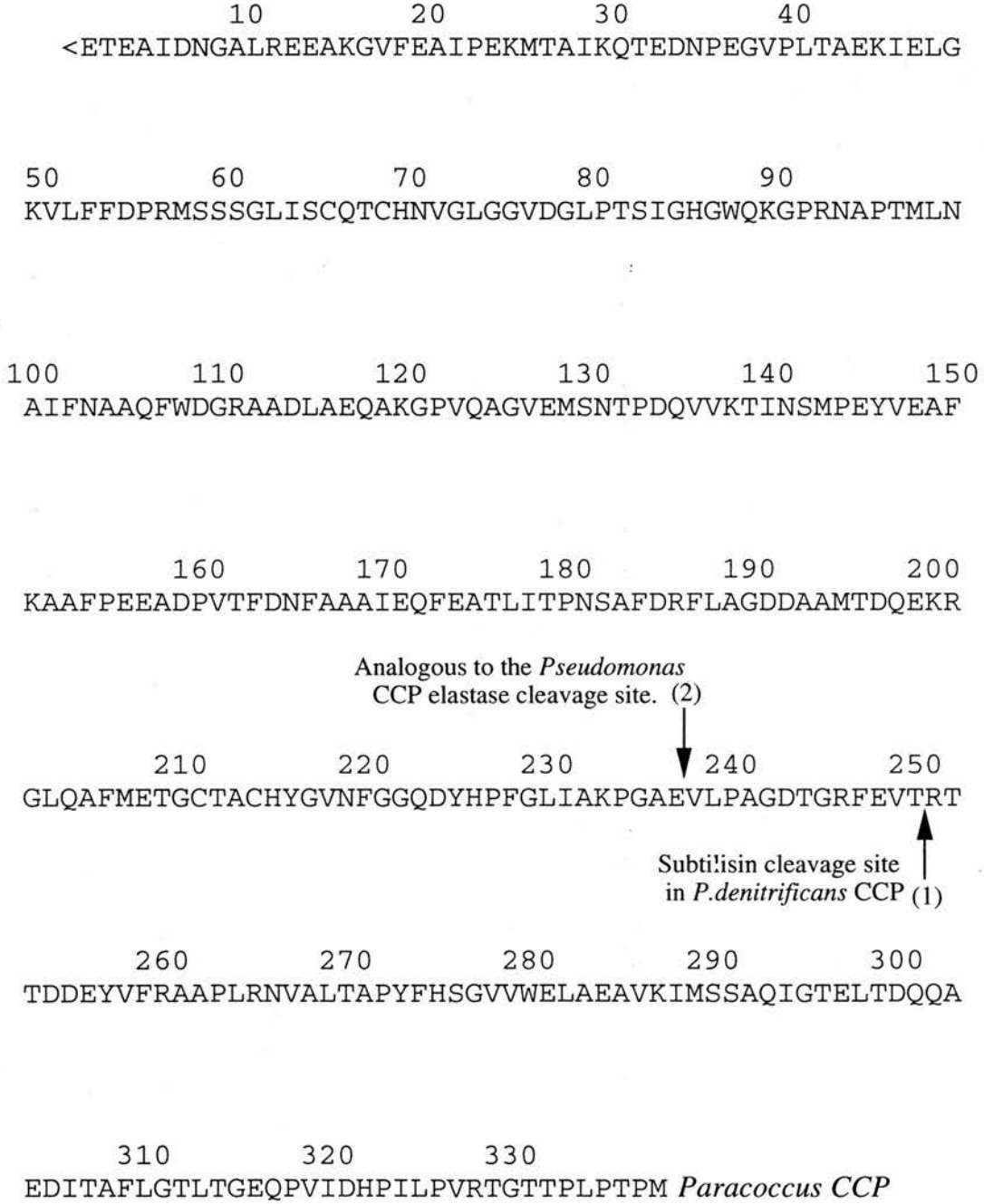
10 20 30 40
<ETEAIDNGALREEAKGVFEAIPEKMTAIKQTEDNPEGVPLTAEKIELG
50 60 70 80 90
KVLFFDPRMSSSGLISCQTCHNVGLGGVDGLPTSIGHGWQKGPRNAPTMLN
100 110 120 130 140 150
AIFNAAQFWDGRAADLAEQAKGPVQAGVEMSNTPDQVVKTINSMPEYVEAF
160 170 180 190 200
KAAFPEEADPVTFDNFAAAIEQFEATLITPNSAFDRFLAGDDAAMTDQEKR
Analogous to the *Pseudomonas* CCP elastase cleavage site. (2)
210 220 230 240 250
GLQAFMETGCTACHYGVNFGGQDYHPFGLIAKPGAEVLPAGDTGRFEVTRT
Subtilisin cleavage site in *P.denitrificans* CCP (1)
260 270 280 290 300
TDDEYVFRAAPLRNVALTAPYFHSGVVWELAEAVKIMSSAQIGTELTDQQA
310 320 330
EDITAFLGTLTGEQPVIDHPILPVRTGTTPLPTPM *Paracoccus CCP*

Table 5.1 Amino acid composition of large haem peptide from CCP
Composition was obtained with a ~1 nmol sample of the large haem peptide generated and purified as described in the legends to Figure 5.4 and Figure 5.10 respectively. Hydrolysis and analysis were performed using an Applied Biosystems A420 derivatizer. Cysteine and tryptophan were not determined. The lower values for methionine probably represents oxidative damage during acid hydrolysis, and the product methionine sulphone may account for the larger than expected value for serine.

Composition (mol of residue/mol)

Amino acid	Hydrolysis and analysis of large haem peptide	Sequence of pE1-T250
Glycine	31	25
Alanine	32	32
Valine	12	14
Leucine	15	14
Isoleucine	10	11
Serine	12	8
Threonine	18	17
Aspartic acid Asparagine	28	26
Glutamic acid Glutamine	34	33
Phenylalanine	14	16
Tyrosine	2	3
Methionine	3	7
Lysine	9	11
Histidine	3	4
Arginine	9	7
Proline	16	16
Tryptophan	-	2
Cysteine	-	4

Figure 5.15 Mass spectrometry of subtilisin generated peptides of CCP
The large haem peptide and the small non-haem peptide (1nmol of each) were generated by subtilisin treatment of CCP as described in the legend to Figure 5.4 and purified as described in the legend to Figure 5.13. Samples were desalted through a Superdex 75 column equilibrated in 0.1M ammonia solution and freeze-dried before use. Mass spectroscopy was performed using a BioQ triple quadrupole mass spectrometer equipped with a pneumatically assisted electrospray source (Fisons, Altrincham,UK) operating in positive ion mode.
(a) Mass spectrum of large haem peptide - the spectrum shows the presence of three peptides (A, B, C) with M_r of A - 27622.64, B - 27950.90 and C - 26986.18. The mass spectrum represents the relative abundance of peptide plotted against the mass / charge ratio of each peptide. Each peak of the spectrum is letter coded with the number of charges on the ionised species.
(b) Mass spectrum of small non-haem peptide - the spectrum shows the presence of a singly charged peptide with a M_r of 9581.38. Peaks A-D all differ from 9581.38 by approximately 23 (which is the mass of sodium) and therefore represent Na-adducts of the 9581.38 peptide. The results are tabulated in Table 5.2.
Spectra recorded by Bart Devreese, Univ. of Gent, Belgium.

(a)

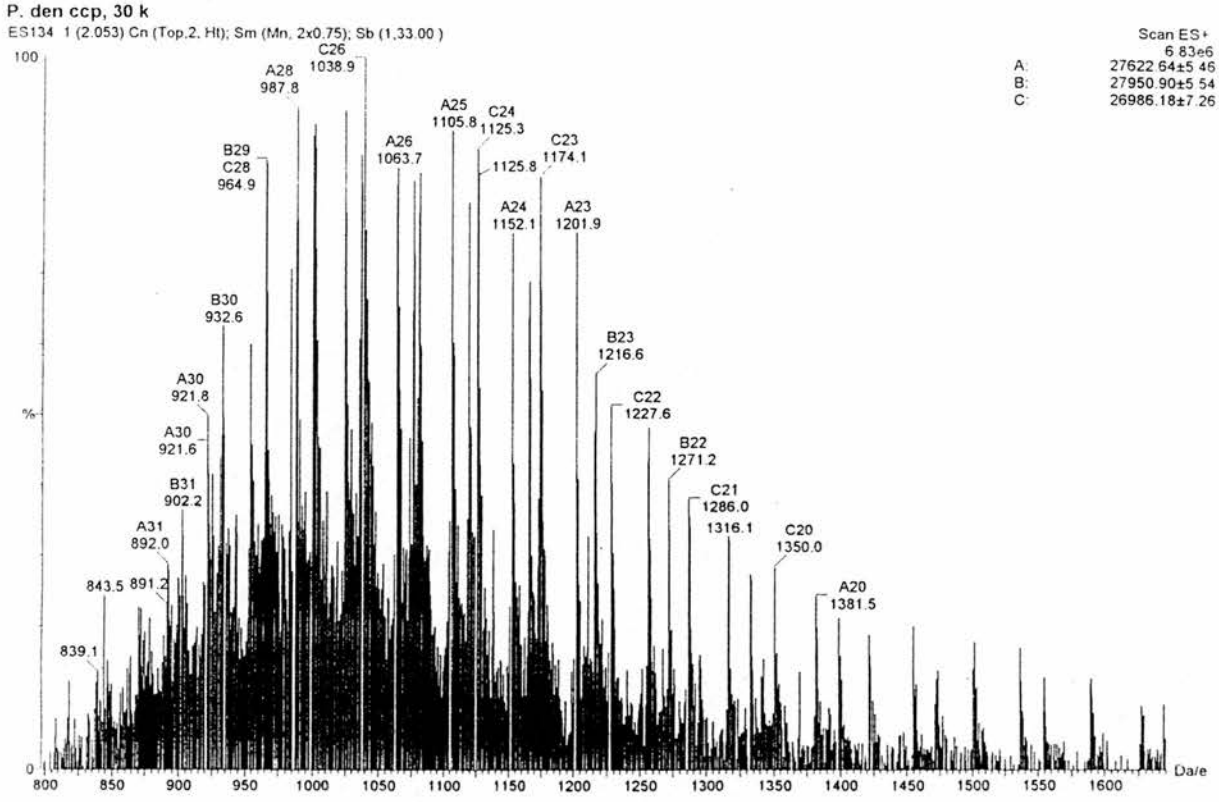
P. den ccp, 30 k
ES134 1 (2.053) Cn (Top,2, Ht); Sm (Mn, 2x0.75); Sb (1,33.00)
Scan ES+
6.83e6
A: 27622.64±5.46
B: 27950.90±5.54
C: 26986.18±7.26
A28 987.8
C26 1038.9
A25 1105.8
C24 1125.3
A26 1063.7
C23 1174.1
1125.8
B29 C28 964.9
A24 1152.1
A23 1201.9
B30 932.6
B23 1216.6
A30 921.8
C22 1227.6
A30 921.6
B22 1271.2
C21 1286.0
B31 902.2
1316.1
A31 892.0
C20 1350.0
843.5
891.2
A20 1381.5
839.1
%
Da/e

(b)

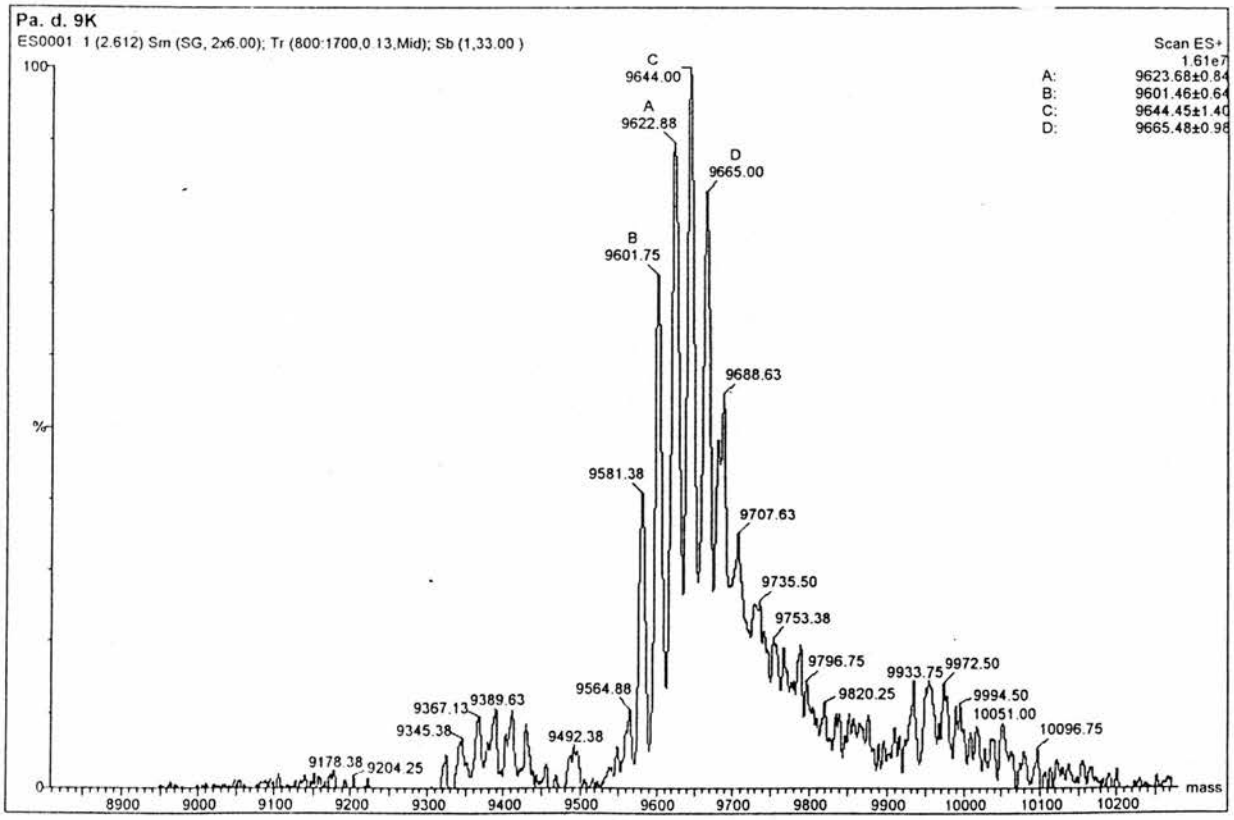
Pa. d. 9K
ES0001 1 (2.612) Sm (SG, 2x6.00); Tr (800:1700,0.13,Mid); Sb (1,33.00)
Scan ES+
1.61e7
A: 9623.68±0.84
B: 9601.46±0.64
C: 9644.45±1.40
D: 9665.48±0.98
C 9644.00
A 9622.88
D 9665.00
B 9601.75
9688.63
9581.38
9707.63
9735.50
9753.38
9796.75
9933.75
9972.50
9564.88
9820.25
9994.50
9367.13
9389.63
10051.00
9345.38
9492.38
10096.75
9178.38
9204.25
%
mass

Table 5.2 M_r of subtilisin generated peptides of CCP

Mass spectra of the large haem peptide and small non-haem peptide were performed as described in the legend to Figure 5.14. Whole CCP represents the holoprotein with two haem groups attached. The first and last residue of each peptide is indicated (pE1 represents the N-terminal pyroglutamate). Note the sum of the M_r of the large haem peptide and small non-haem peptide (minus one H_2O = 18) generate a M_r which is within 7 of whole CCP. The resolution of the mass spectrometer allows for isotopic resolution of peptides under approximately M_r 3000. By averaging the mass of elemental isotopes according to their natural distribution, and thus determining the average mass of individual residues, the theoretical M_r of peptides over 3000 were calculated.

Peptide	M_r determined by sequence	M_r determined by electrospray mass spectrometry
Peptide pE1-T250	27950.940	27950.9
Peptide R251-M338	9579.878	9581.38
Whole CCP pE1-M338	37512.803	37508.0

determined M_r values of the two isolated peptides with their theoretical M_r values and conclusively establishes that the larger fragment contains both haems and the residues pE1-T250, while the smaller fragment contained residues R251-M338. The two other fragments in the mass spectrum of the larger peptide are pE1-F247 and pE1-A241 and these fragments represent a degree of heterogeneous cleavage of the parent pE1-T250 peptide. As explained above purification of the pE1-T250 peptide required the level of subtilisin digestion of CCP to be slightly raised, so no CCP remains to coelute with the pE1-T250 peptide. This increased level of digestion probably generated the heterogeneous cleavage of the pE1-T250 peptide.

Subtilisin cleavage between T250 and R251 does not reflect limitations in the action of subtilisin but rather the limited access of protease to the native substrate. Note that this subtilisin cleavage site is only 13 residues away from the elastase cleavage site in *P.aeruginosa* (see Figure 5.14). The cleavage of a single bond in the same region of two homologous proteins implies the presence of a structural segment that is susceptible to proteolytic attack and common to both peroxidases. This structural feature is probably located on the surface of both proteins and may consist of a loop of residues, easily cleaved at different positions depending on the protease used. The heterogeneous cleavage of the *P.denitrificans* pE1-T250 peptide by subtilisin probably indicates further clipping to the exposed tail.

After the subtilisin-cleaved peptides of CCP were isolated and the site of cleavage positively identified, the usefulness of the cleaved protein and the separated peptides could be evaluated. Chapter VI describes the use of subtilisin-cleaved CCP peptides in the identification of the modified essential histidine. The remainder of this chapter concentrates on determining the spectroscopic and kinetic properties of the cleaved protein.

5.2.7 Subtilisin cleavage of CCP causes a spin state transition at low potential haem with resulting loss of activity

It is worth re-emphasising that the active form of the enzyme is achieved by reduction of the electron transferring haem and the Ca^{2+}-dependent appearance of the

high spin-state at the peroxidatic haem. As described above, cleavage of *P.denitrificans* CCP with the protease subtilisin is carried out with the peroxidase in this mixed-valence + Ca^{2+} state. The formation of the high spin-state can be easily monitored by a broad gain in absorbance at 380 nm. Figure 5.16 (a)i) shows the progressive loss of 380 nm absorbance over the time of subtilisin cleavage of CCP. Loss of the 380 nm absorbance peak represents the high to low spin-state transition at the peroxidatic haem. Assaying the peroxidase (protocol in Chapter II, section 2.4), after incubation with subtilisin, determined the cleaved enzyme to be catalytically inactive. Thus cleavage of a single bond between T250 and R251 in CCP abolishes both the high spin-state and activity. Figure 5.16(a)ii) demonstrates that after 60 min partial reoxidation of the high potential haem begins to occur, as monitored by loss in absorbance at 420, 525 and 550 nm.

The fact that cleavage of a single T250 - R251 bond in CCP causes complete abolishment of catalytic activity is quite remarkable. In the intact enzyme, reduction of the high potential haem causes a Ca^{2+} dependent low to high spin-state transition at the low potential haem. The cleavage of the T250 - R251 prevents the interaction between the two haems resulting in the conformational change at the low potential haem. Similarly the proteolytic cleavage of the S223 - V224 (*P.aeruginosa* CCP numbering) bond in *P.aeruginosa* CCP renders the peroxidase catalytically inactive by preventing the same spin-state transition at the peroxidatic haem.

5.2.8 Electron paramagnetic resonance spectroscopy of native and subtilisin-cleaved CCP

E.p.r. spectra of native (Gilmour et al.1993; Prazeres et al.1994) and subtilisin-cleaved CCP are shown and interpreted below. Figure 5.17(a) displays the e.p.r. spectrum of the native oxidised peroxidase and shows two resonances at g_{max} 3.4 and 3.0 representing the high and low potential haems respectively. A spectroscopic indicator of the active enzyme is the Ca^{2+} dependent appearance of a g_{max} 2.9 signal in the e.p.r. spectrum of the mixed-valence enzyme, which can be equated with the high-spin peroxidatic haem at room temperature (Figure 5.17(a)).

Figure 5.16 Spin-state transition at the peroxidatic haem as CCP is cleaved with subtilisin

To CCP (5μM) in 10mM Hepes pH7.5 was added ascorbate (1mM) and DAD (10μM) and the spectrum from 350-600 nm recorded and stored. $CaCl_2$ (1mM) was added and after 20 min the difference spectrum of mixed-valence+ Ca^{2+} minus mixed-valence - Ca^{2+} was generated. Subtilisin was added to give an enzyme : substrate ratio of 1: 3300 (w/w). Spectra (350-600 nm) were recorded at 0, 1, 3, 6, 10, 20, 30, 40, 50, 60, 70, 90, 120, 140, 160 and 180 min (at 30°C) after subtilisin addition. Subtilisin was inhibited by PMSF (1mM), EGTA (10mM) at each time point.
Digests (1nmol) 1, 3, 6, 10, 20, 30, 40, 50 and 60 min after subtilisin addition were subsequently loaded on a gel (15% polyacrylamide) for SDS-PAGE and stained for protein with Coomassie blue.

(a) Shown are difference spectra from 350-600 nm of mixed-valence + Ca^{2+} minus mixed-valence - Ca^{2+}, 0 to 180 min after subtilisin addition. (i) each difference spectra with decreasing ΔA_{380nm} correlates to increasing time after subtilisin addition (from 0 to 40 min). (ii) each difference spectra with increasing ΔA_{408nm} correlates to increasing time after subtilisin addition (from 40 to 180 min).
(b) Lane A Molecular weight standards, BSA (M_r 66k), ovalbumin (45k), carbonic anhydrase (29k), myoglobin (17k) and cytochrome c (12k); Lanes B-J CCP after subtilisin addition at time 1, 3, 6, 10, 20, 30, 40, 50 and 60 min respectively.

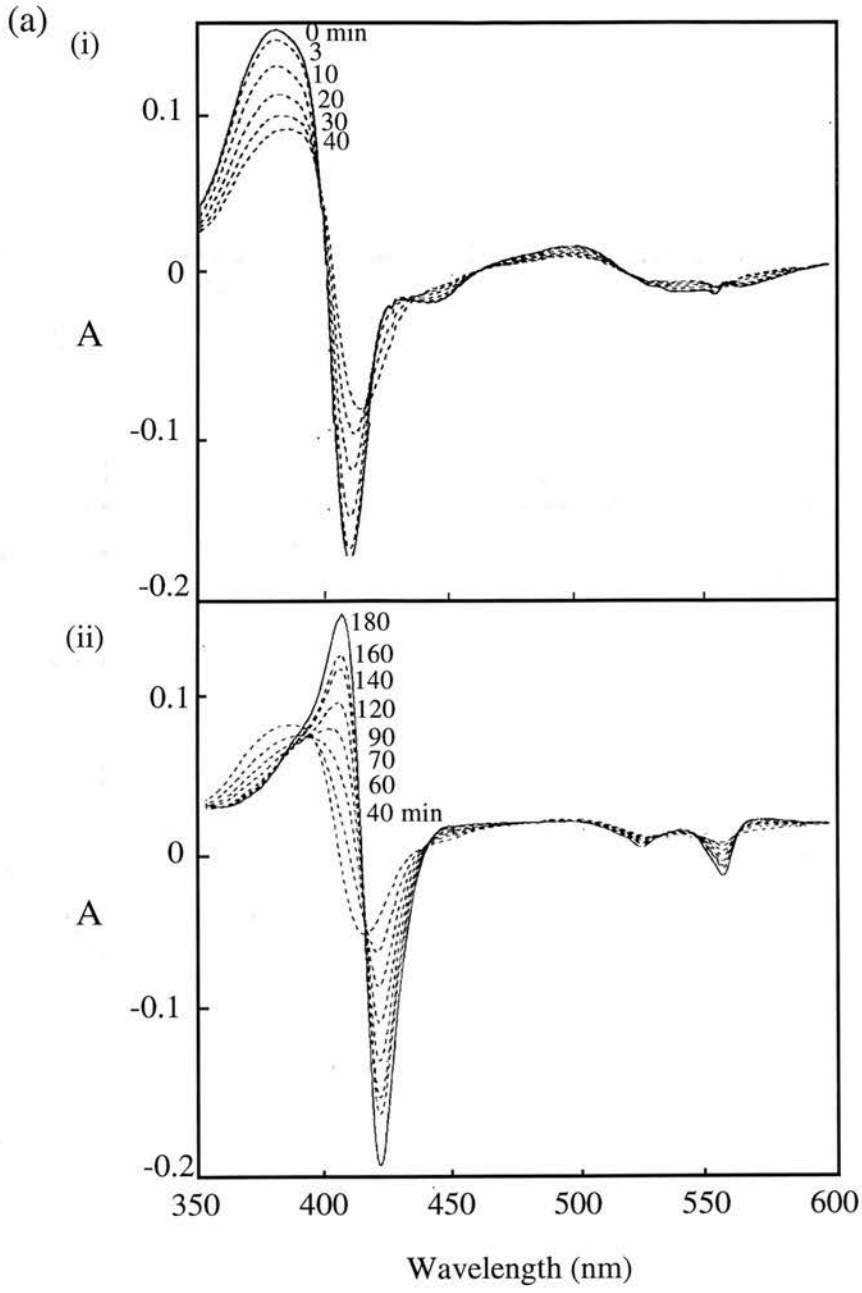
(a)
(i)
0 min
3
10
20
30
40
0.1
0
A
-0.1
-0.2
(ii)
180
160
140
120
90
70
60
40 min
0.1
0
A
-0.1
-0.2
350
400
450
500
550
600
Wavelength (nm)

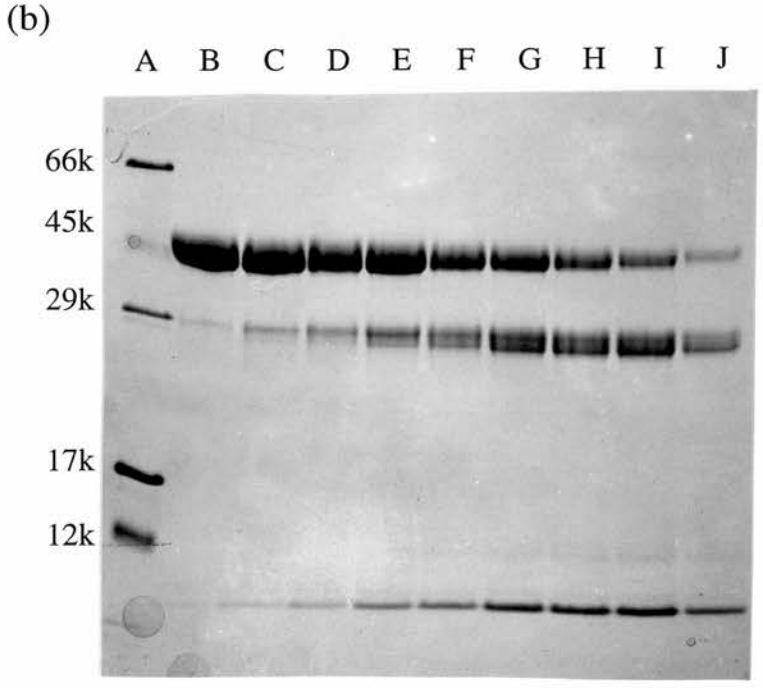
(b)
A
B
C
D
E
F
G
H
I
J
66k
45k
29k
17k
12k

Figure 5.17 E.p.r. spectroscopy of native and cleaved CCP

(a) E.p.r. spectra of native CCP in oxidised, mixed-valence -$Ca^{2+}$and mixed-valence + Ca^{2+} states. 9ml of CCP (4μM) in 5mM Hepes pH7.5 was concentrated to 180μl and spectra recorded from this 200μM sample (oxidised), after reduction with 1mM ascorbate and 10μM DAD (mixed valence -Ca^{2+}) and after addition of 1mM $CaCl_2$ (mixed-valence + Ca^{2+}).

(b) E.p.r. spectra of subtilisin-cleaved CCP in oxidised, mixed-valence -$Ca^{2+}$and mixed-valence + Ca^{2+} states.To CCP (4μM) in 5mM Hepes pH7.5 was added ascorbate (1mM), DAD (10μM) and $CaCl_2$ (1mM). Subtilisin was added to give an enzyme : substrate ratio of 1: 500 (w/w). After 60 min at 0°C subtilisin was inhibited by PMSF (1mM), EGTA (10mM). The sample was exchanged with 5mM Hepes pH 7.5 and concentrated to 200μM. Spectra were recorded from this reoxidised sample as for the native enzyme. Experimental conditions :- temperature 8K; microwave frequency 9.45GHz; microwave power 2mW; modulation 10.39; gain 1.6 x 10^5. g values for selected resonances are shown.

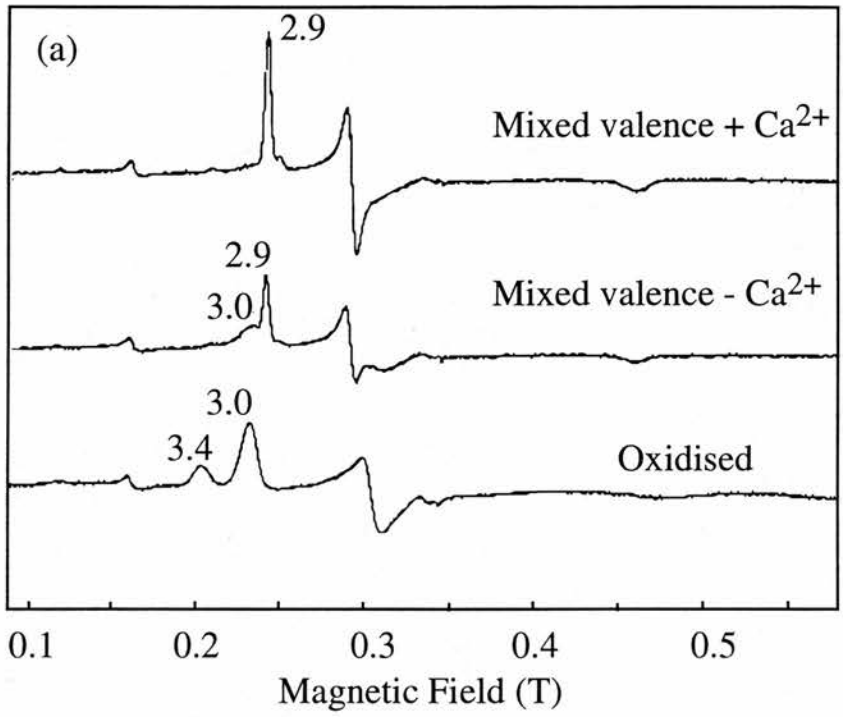
(a)
2.9
Mixed valence + Ca2+
2.9
3.0
Mixed valence - Ca2+
3.0
3.4
Oxidised
0.1
0.2
0.3
0.4
0.5
Magnetic Field (T)

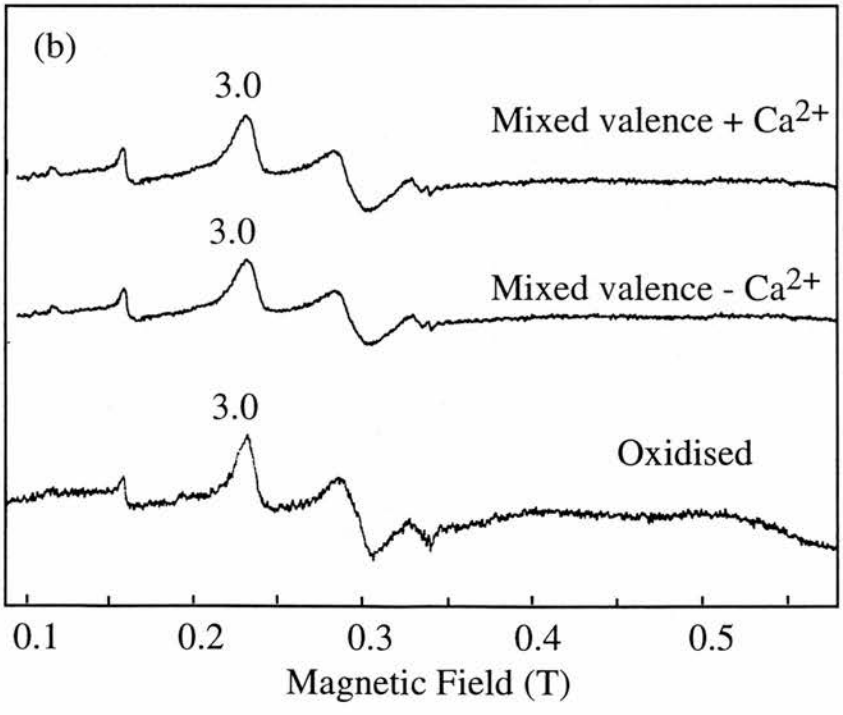
(b)
3.0
Mixed valence + Ca2+
3.0
Mixed valence - Ca2+
3.0
Oxidised
0.1
0.2
0.3
0.4
0.5
Magnetic Field (T)

Because of the high protein concentrations needed for e.p.r. spectroscopy, endogenous Ca^{2+} allows partial appearance of this g_{max} 2.9 signal in the spectrum of the mixed-valence enzyme (Gilmour et al.1995). Subtilisin cleavage must influence the high potential haem of oxidised CCP to cause the disappearance of the g_{max} 3.4 signal. The cleaved enzyme also cannot undergo the transition to the active form (Figure 5.17(b)) and is trapped in a low-spin mixed-valence form with g_{max} 3.0. Therefore in the cleaved enzyme, both e.p.r. and visible spectroscopy reflect the inability of the peroxidatic haem to go high-spin upon reduction of the electron transferring haem in the presence of Ca^{2+}.

5.2.9 Nuclear magnetic resonance spectroscopy of native and subtilisin-cleaved CCP

The effect of subtilisin cleavage on CCP can also be followed by n.m.r. Figure 5.18(a) shows the low-field region of the ^1H n.m.r. spectra of native CCP. As reported in Gilmour et al.(1993), Prazeres et al.(1993) and Prazeres et al.(1994) and already explained in Chapter IV, section 4.2.4, n.m.r. confirms the presence of a high-spin haem in both oxidised and mixed-valence haems. Figure 5.18a(i) shows the n.m.r. spectrum of oxidised CCP. The resonances between 54 and 65 ppm are assigned to the partially high-spin, high potential electron transferring haem and the two methyl resonances at 22 and 34 ppm are assigned to the fully low-spin, low potential haem. In the spectrum of the mixed-valence enzyme (Figure 5.18a(ii)) the four new haem methyl resonances located between 50 and 65 ppm are assigned to the fully high-spin, low potential haem. Because of the high [protein] needed for n.m.r., endogenous Ca^{2+} allows conversion of the low potential haem to the high spin-state upon reduction of the high potential haem; thus the addition of Ca^{2+} has no effect on the n.m.r. spectrum (Figure 5.18a(iii)).

The n.m.r. spectrum of the subtilisin-cleaved, reoxidised CCP shows important differences to the native enzyme in both haems. Comparing the n.m.r. spectrum from oxidised native (Figure 5.18a(i)) and cleaved (Figure 5.18b(i)) protein,

Figure 5.18 300 MHz ^{1}H n.m.r. spectroscopy of native and subtilisin-cleaved CCP

(a)(i) The low-field region of the 300 MHz n.m.r. spectra of oxidised CCP (1mM) in 50mM Hepes pH 7.5. (ii) The sample was reduced with DAD (5μM) and ascorbate (5mM) to generate the mixed-valence state. (iii) $CaCl_2$ (5mM) was then added to give the mixed-valence state plus Ca^{2+}.

(b) N.m.r. spectra of subtilisin-cleaved CCP in (i) oxidised, (ii) mixed-valence and (iii) mixed-valence + Ca^{2+} states. To CCP (4μM) in 5mM Hepes pH7.5 was added ascorbate (1mM), DAD (10μM) and 1mM $CaCl_2$. Subtilisin was added to give an enzyme : substrate ratio of 1: 500 (w/w). After 60 min at 0°C, subtilisin was inhibited by PMSF (1mM), EGTA (10mM). The protein solution was exchanged with D_20 before being concentrated to 1mM and spectra of the reoxidised enzyme recorded as for the native sample.

Experimental conditions:- temperature 303 K; 2000 scans; 4K data points. Spectra recorded by S. Prazeres, Universidade Nova de Lisboa.

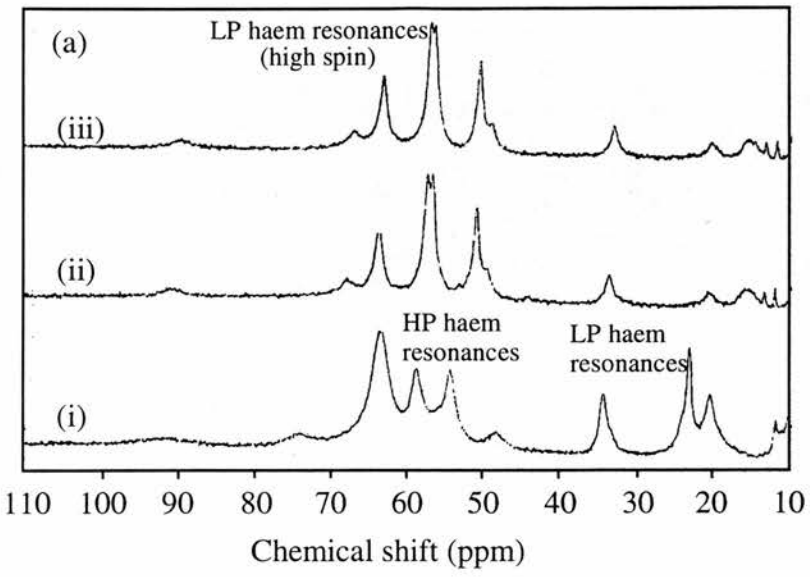
(a)
LP haem resonances
(high spin)
(iii)
(ii)
HP haem
resonances
LP haem
resonances
(i)
110 100 90 80 70 60 50 40 30 20 10
Chemical shift (ppm)

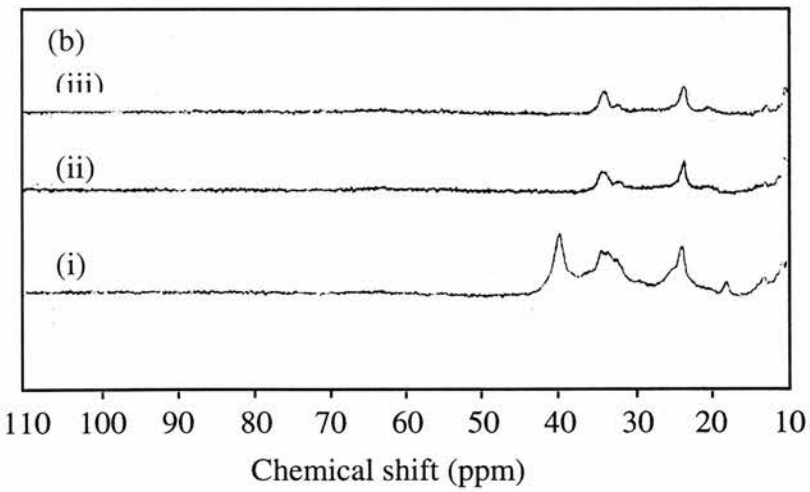
(b)
(iii)
(ii)
(i)
110 100 90 80 70 60 50 40 30 20 10
Chemical shift (ppm)

the sets of resonances between 54 and 65 ppm (associated with the high potential haem) are abolished, as are some of the resonances between 22 and 34 ppm (associated with the low potential haem). Upon reduction of the high potential haem, no high-spin resonances in the region 50 to 65 ppm, arising from the low potential haem, were observable (Figure 5.18b(ii)) even after the addition of excess Ca^{2+} (Figure 5.18b(iii)).

For CCP, cleaved at a single site with subtilisin, n.m.r. also reflects the fully low spin-state of the oxidised electron transferring haem and the inability of the peroxidatic haem to go high-spin upon reduction of the electron transferring haem, in the presence of Ca^{2+}.

5.2.10 Potentiometric redox titration of CCP cleaved at a single bond with subtilisin

After subtilisin-cleaved CCP was prepared as described in the legend to Figure 5.4, oxidative and reductive titrations of the high potential haem in the presence of Ca^{2+} were performed. The respective reductive and oxidative titrations are shown in Figures 5.19A(i) and 5.19A(ii). The data from both titrations are fitted to Nernst plots with slopes of 59mV (25°C) (Figure 5.19A(iii)). The high potential haem of the cleaved protein (in the absence or presence of Ca^{2+}) has a midpoint potential of 240mV. This is only slightly raised from the midpoint potential of the high potential haem of the native enzyme in the presence of Ca^{2+}, 226mV. In the absence of Ca^{2+} the high potential haem of native CCP has a midpoint potential of 176mV (Gilmour et al.1993).

In either the absence or presence of Ca^{2+}, subtilisin cleavage of CCP abolished the ability of the low potential haem to form the high spin-state upon reduction of the high potential haem. We may have expected a midpoint potential for the high potential haem of ~176 mV, that of the native CCP in the absence of Ca^{2+}. As concluded for the peroxidase modified at a single histidine, other undefined influences must be

Figure 5.19 Potentiometric redox titration of CCP cleaved at a single bond with subtilisin

To CCP (5μM) in 10mM Hepes pH 7.5 was added ascorbate (1mM), DAD (10μM) and $CaCl_2$ (1mM). Subtilisin was added to give an enzyme : substrate ratio of approximately 1: 500 (w/w). After 60 min at 0°C subtilisin was inhibited by PMSF (1mM), EGTA (10mM). The sample was desalted through potassium ferricyanide (1mM) on a G25 Sephadex column. The redox titration of reoxidised cleaved protein was performed as described in Chapter II- Materials and Methods. **A**(i) and **A**(ii) show the reductive and oxidative titrations of the high potential haem only, as followed in the region of the α and β bands. **A**(iii) is a Nernst analysis of the redox titration of the high potential haem with reductive (open circles) and oxidative (closed circles) arms. The midpoint potential (E_m) is +240mV.

B is a Nernst plot of both the reductive titration (open circles) of the high potential haem and the oxidative titration of the same haem after the low potential haem had undergone reduction and oxidation (closed circles).

The data are fitted to theoretical plots with slopes of 59mV (25°C) derived from the Nernst equation (see Chapter II- Materials and Methods).

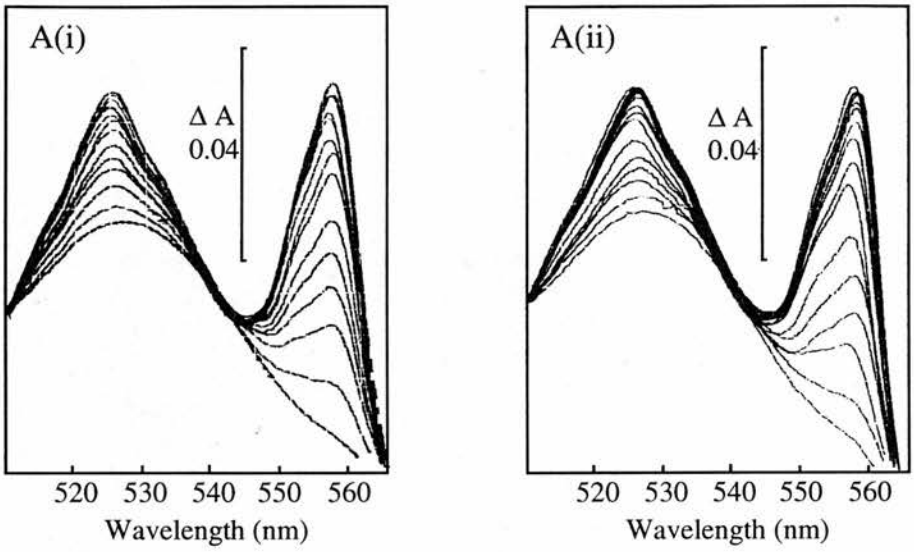
A(i)
Δ A
0.04
520 530 540 550 560
Wavelength (nm)
A(ii)
Δ A
0.04
520 530 540 550 560
Wavelength (nm)

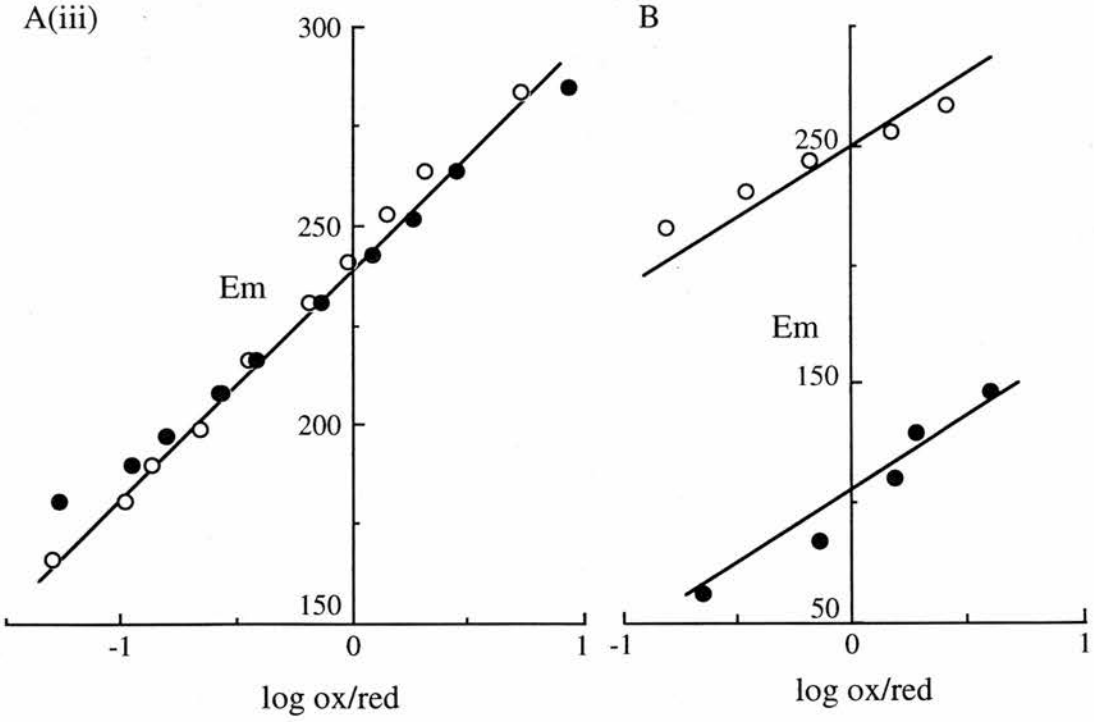
A(iii)
300
250
200
150
Em
-1
0
1
log ox/red
B
250
150
50
Em
-1
0
1
log ox/red

responsible for the resulting redox potential of the high potential haem of the cleaved enzyme (Chapter IV, section 4.2.5).

Figure 5.19B is a Nernst plot from a redox titration of cleaved CCP and shows hysteresis between the oxidative and reductive titrations of the high potential haem when the oxidative titration of this haem was performed after reduction of the low potential haem. This phenomenon was first observed in the modified enzyme and remains difficult to interpret (see Chapter IV, section 4.2.5).

The similarities between the properties of CCP modified at a single histidine and the enzyme cleaved at a single site with subtilisin are striking leading to the conclusion that modification and cleavage are affecting the internal mechanisms which allows the enzyme to progress from the inactive oxidised form to the active mixed-valence state.

Chapter VI

Identification of the essential histidine in cytochrome c peroxidase

6.1 Introduction

The excellent agreement between the proportional loss of activity and the modification of 1 mol of histidine (See Chapter IV, section 4.2.1) indicates that a single histidine is being modified. If we assume that the two histidines which remain unmodified at high [DEPC] are the conserved proximal ligands to the two haem groups, His 85 and His 275 are the only remaining conserved histidines and therefore one or the other (or both) was likely to be essential for activity. Because of the relatively rapid loss of the ethoxyformyl group, few studies have attempted location of a modified histidine in a peptide digest, although there is one exception (Hegyi et al.1974). After modification of the native enzyme with [^{14}C]DEPC we were able to exploit a remarkable single bond cleavage by subtilisin in the native state, which releases a C-terminal fragment containing the conserved His 275 and one other non-conserved histidine and an N-terminal fragment containing the conserved His 85 and one other non-conserved His. The location of the radiolabel was followed by both autoradiography and radioactive counting of the separated peptides. Further subdigestion of the modified peptide led to isolation of a radiolabelled fragment containing a single histidine and therefore identification of that histidine as essential for the activity of cytochrome c peroxidase.

6.2 Results and Discussion

6.2.1 Spectrophotometric and radioactive measurement of CCP modification

In Chapter III, section 3.2.3.1, it was determined that there is a fair agreement between the two methods of quantifying the extent of DEPC modification , with radioactive labelling giving slightly less (~10%) than spectroscopic measurements. This indicates firstly that ΔA_{245nm} is a quite reliable measurement of histidine modification although perhaps generating slight overestimates, and secondly that there is little uptake into amino acids other than histidine. The difference spectrum due to modification showed the presence of a trough between 265-300 nm (Figure 6.1 (a) (i). We wanted to be certain that this was not an indicator of modification of aromatic acids such as tyrosine or tryptophan which may be responsible for part or all of the radioactive labelling with [^{14}C]DEPC. A difference spectrum (Figure 6.1 (a) (ii) obtained after modification for 2.5 min showed no trough between 265-300 nm and yet the histidine modified correlated fairly well with the proportion of protein labelled with [^{14}C]DEPC (Figure 6.1 (b)). Therefore whatever the origin of the 265-300 nm trough, it cannot represent direct radiolabel uptake in the protein. The essential histidine is now confirmed as the site of radiolabel incorporation and can be identified as such.

Although the features of the trough between 265 and 300 nm resemble that expected for O-ethoxyformylation of tyrosine (Burstein et al.1974), the extent of the absorbance change would imply a modification of at least one mol tyrosine per mol protein (ε_{278nm} = 1.3 mM^{-1} cm^{-1}) and this is certainly not supported by measurement of radiolabelling. Therefore the conclusion is that the 265-300 nm trough may not be associated with tyrosine modification. The feature is also present in the spectra of modified yeast CCP and similar features have been observed in other proteins modified with DEPC (Burstein et al.1974; Bhattacharyya et al.1992).

Figure 6.1 Correspondence between spectrophotometric and radioactive DEPC labelling of CCP

To CCP (10μM) in 5mM Hepes pH 7.5 was added [^{14}C]DEPC to a final concentration of 40μM. After 2.5 min a modified minus unmodified difference spectra was taken while simultaneously desalting a second aliquot of modified CCP through G25 Sephadex equilibrated in 5mM Hepes pH 7.5 and subsequently counting the sample for radioactive label. After 25 min another modified minus unmodified difference spectra was taken while desalting a second aliquot of modified CCP and again counting for radioactive label. (a) Difference spectrum of modification 2.5 min ii) and 25 min i) after DEPC addition. (b) Table comparing mol of ethoxyformylhistidine as measured by ΔA_{245nm} in (a) and mol of radioactive label incorporated, 2.5 and 25 min after DEPC addition.

(a)

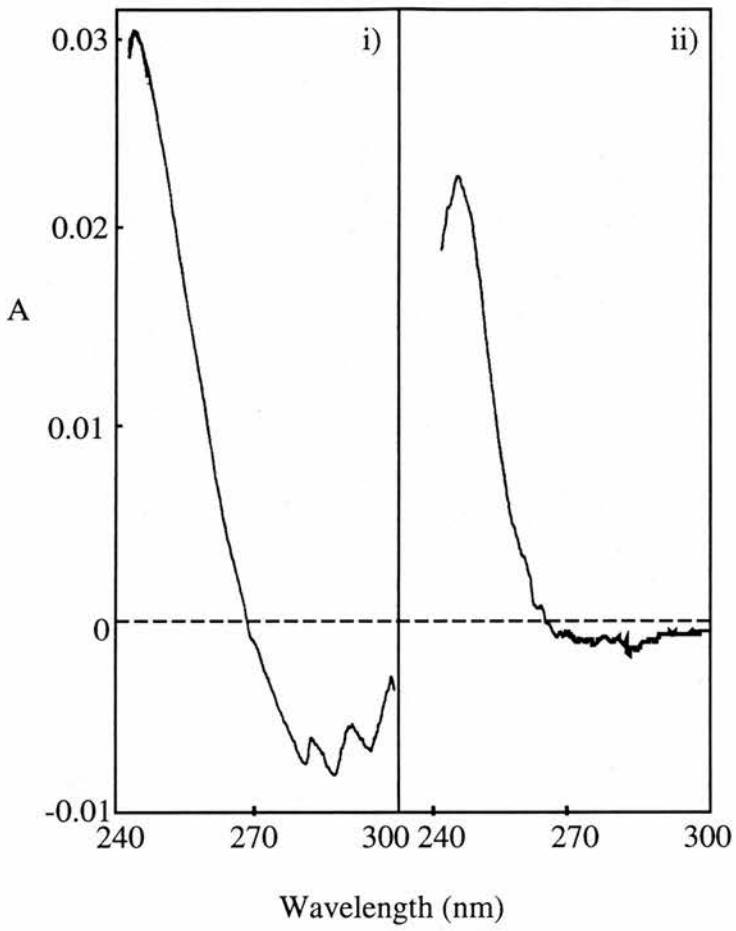

(b)

Time after DEPC addition (min)	mol ethoxyformylhistidine / mol	mol radioactive label / mol
2.5	0.68	0.54
25	0.93	0.80

6.2.2 The distribution of histidines in cytochrome c peroxidase

Mass spectrometry had established that the larger fragment contained both haems and the residues pE1-T250 while the smaller fragment contained residues R251-M338 (see Chapter V, section 5.2.6). A schematic representation of the CCP sequence with the subtilisin cleavage site and the position of all six histidines is shown in Figure 6.2. The only two conserved histidine, apart from the proximal ligands, are His 85 and 275 and these are located in peptides pE1-T250 and R251-M338 respectively. The conserved nature of these residue make them equally strong candidates for the site of modification[3].

6.2.3 Identification of the site of modification in the amino acid sequence by autoradiography

Samples of oxidised holoenzyme were radiolabelled with ^{14}C[DEPC] to the extent of 0.5, 1.0, 1.5 and 2.5 mol histidine per mol and subsequently digested with subtilisin. The protein composition of modified whole and cleaved CCP was determined by Coomassie blue staining following SDS-PAGE on a 15% polyacrylamide gel (Figure 6.3 (a) i)). The dried gel was exposed to autoradiograph film for one month at -40°C before development (Figure 6.3 (a) ii)). The ratio of label in the two CCP peptides, at different levels of modification, was determined by densitometry scans of the autoradiograph film at 550 nm (Figure 6.3 (b)). At low levels of modification (0.5 and 1.0 mol histidine per mol), the ratio of radiolabelled (R251-M338) : (pE1-T250) indicated peptide (R251-M338) to be the site of ethoxyformylation (Figure 6.3 (b) i) and ii)). At higher levels of modification (1.5 and 2.5 mol histidine per mol) the majority of label was located in peptide pE1-T250 (Figure 6.3 (b) iii) and iv)).

The close correlation between modification of a single histidine and loss of activity (see Chapter IV, section 4.2.1) had led us to expect a much cleaner pattern of label distribution. The reason for the equivocal distribution of radioactivity was

[3] The crystal structure of *P.aeruginosa* CCP has recently been reported (Fulop et al. 1995). This shows His 85 to be the distal ligand to the N-terminal haem while His 275 is located at the interface between the two domains (see Discussion Chapter). Therefore His 275 is likely to be the site of modification.

Figure 6.2 The distribution of histidines in *P.denitrificans* CCP and the position of subtilisin cleavage.

The single cleavage location in the native mixed-valence enzyme between residues T250 and R251 was confirmed by mass spectrometry (Tables 5.2 and 6.2) of the resultant CCP peptides. The identity of the C-terminal fragment was confirmed by five cycles of Edman degradation (Chapter V, section 5.2.4). The six histidines in *P.denitrificans* CCP are numbered. His 85 and 275 are the only non-proximal histidines conserved in the three bacterial cytochrome c peroxidases.

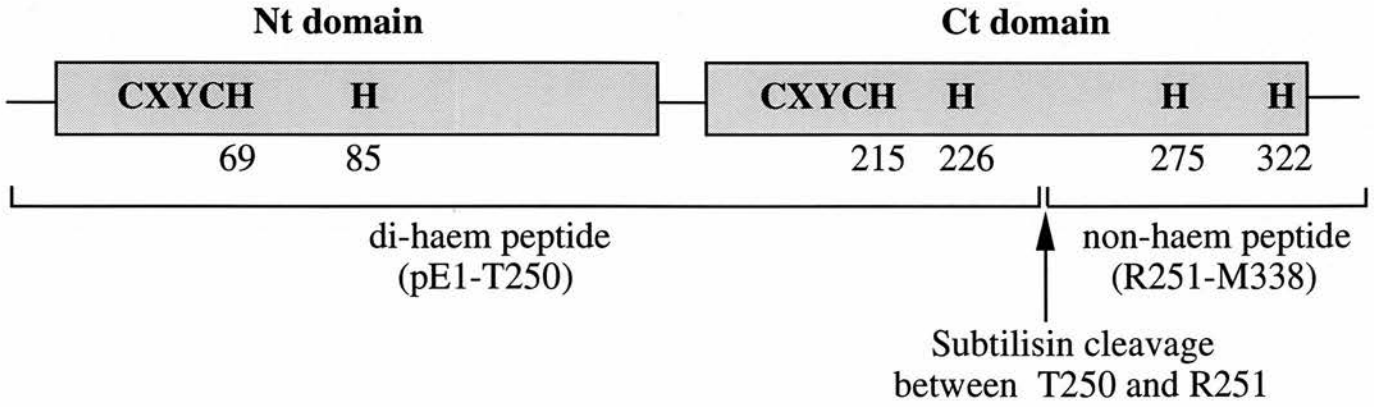
Nt domain
Ct domain
CXYCH
H
CXYCH
H
H
H
69
85
215
226
275
322
di-haem peptide
(pE1-T250)
non-haem peptide
(R251-M338)
Subtilisin cleavage
between T250 and R251

Figure 6.3 Identification of peptide R251-M338 as site of modification by autoradiography

Aliquots of CCP (5μM) in 10mM Hepes pH 7.5 were ethoxyformylated to an extent of 0.5, 1.0, 1.5 and 2.5 mol histidine per mol, with different concentrations of [^{14}C]DEPC (5, 25, 110 and 400 μM respectively). The modified samples were desalted through a small G25 Sephadex column, equilibrated in 10mM Hepes pH7.5, before being digested with subtilisin. To modified CCP solutions (~3μM) in 10mM Hepes pH7.5, was added ascorbate (1mM), DAD (10μM) and $CaCl_2$ (1mM). Subtilisin was added to give a substrate : enzyme ratio of 500:1 (w/w). After 60 min at 0°C, subtilisin was inhibited by PMSF (1mM), EGTA (10mM). SDS-PAGE (15% polyacrylamide) on both modified whole CCP and modified cleaved CCP (1nmol of each) was performed and the protein composition determined by staining with Coomassie blue. The gel was subsequently soaked in 1M salicylic acid pH7 for 30 min and dried for 3 hours at 80°C. The autoradiograph Hyperfilm-βmax was exposed to the dried gel for 4 weeks at -40°C and the film developed using Kodak D19 according to the manufacturers instructions.

(a) i) Coomassie blue stained SDS-PAGE; Lane A - Molecular mass markers, BSA (Mr 66k), Ovalbumin (45k), Carbonic anhydrase (29k), Myoglobin (17k), Cytochrome c (12k); Lanes B, D, F, H - whole CCP modified to an extent of 0.5, 1.0, 1.5 and 2.5 mol histidine / mol respectively. Lanes C, E, G, I - cleaved CCP modified to an extent of 0.5, 1.0, 1.5 and 2.5 mol histidine / mol respectively. (ii) Autoradiograph of Coomassie blue stained gel; Lanes A-I, autoradiographs of A-I from (i).

(b) Densitometry scans at A_{550nm} of modified, cleaved CCP autoradiographs. (i) Scan of lane C from (a)ii), 0.5 mol histidine / mol; (ii) Scan of lane E from (a)ii), 1.0 mol histidine / mol; (iii) Scan of lane G from (a)ii), 1.5 mol histidine / mol; (iv) Scan of lane I from (a)ii), 2.5 mol histidine / mol. Numbers shown next to peak represent arbitrary area units for the respective peaks. The ratio of labelled R251-M338 : pE1-T250 for the different levels of modification are given.

(a) (i) (ii)

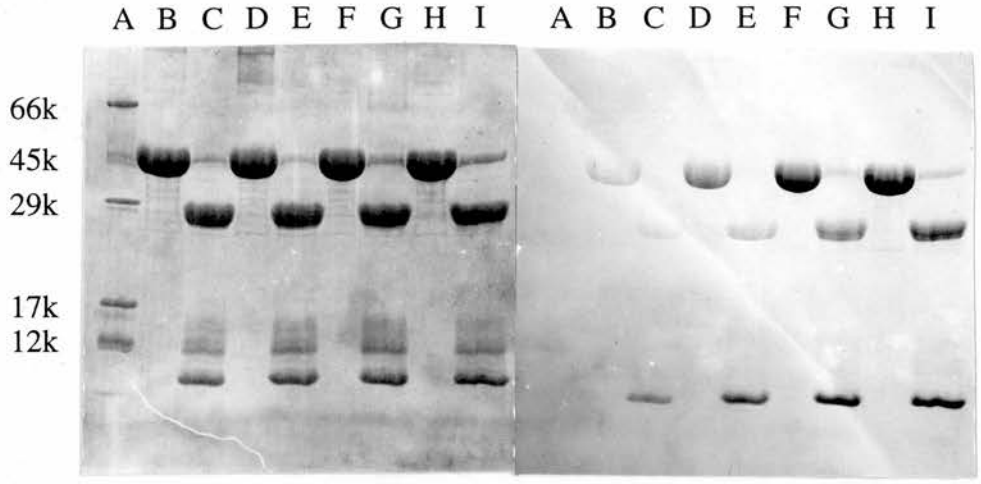

(b)

Ratio of labelled (R251-M338):(pE1-T250)

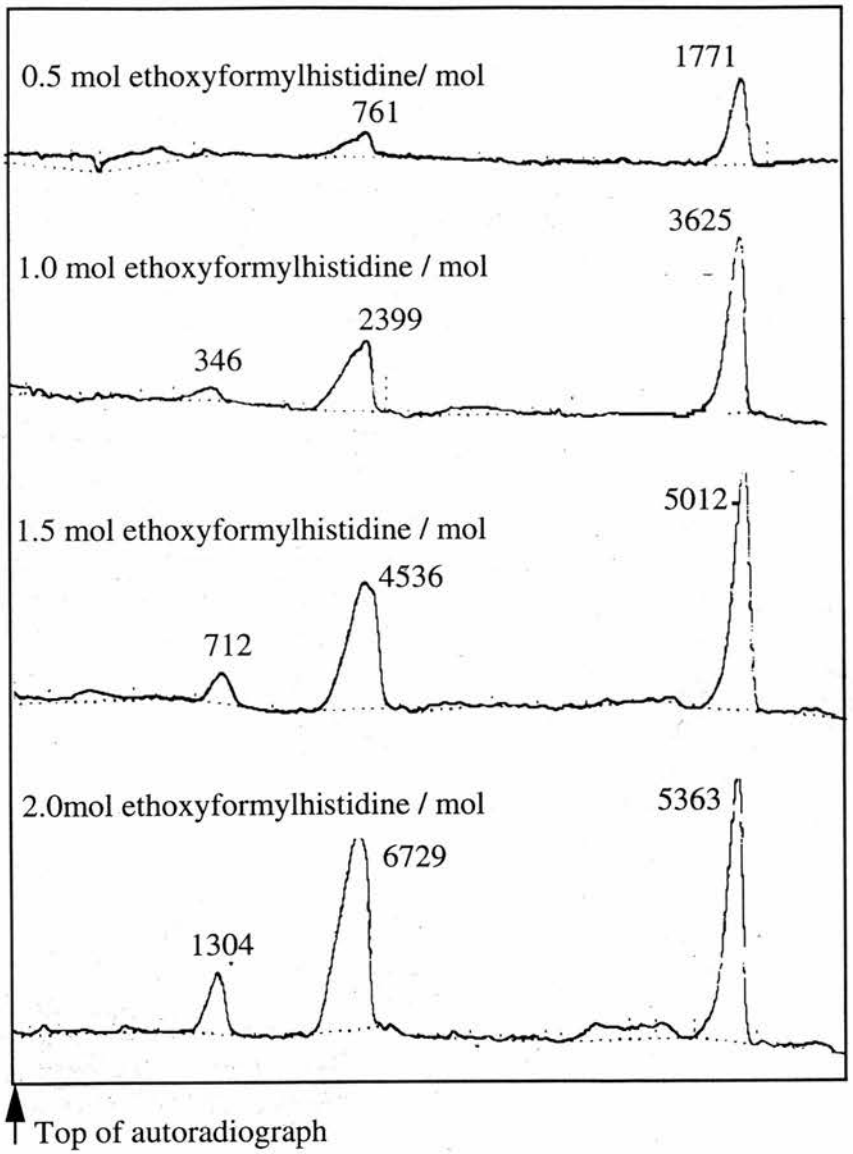

eventually resolved and is detailed below. Firstly, a separate method of determining the site of CCP modification with [^{14}C]DEPC by isolating the two peptides and counting them for radiolabel, is described.

6.2.4 Identification of site of modification in the amino acid sequence by radioactive counting

6.2.4.1 Peptide pE1-T250 or R251-M338 as the site of modification

Subtilisin digestion of the native mixed-valence holoenzyme released two fragments which are separable by molecular exclusion after dissociation in SDS (Figure 6.4) (also see Chapter V, section 5.2.3). SDS-PAGE analysis of the elution profile of the molecular exclusion column showed complete resolution of the larger from the smaller peptide (Figure 6.4). However, the remaining undigested whole protein, which accounted for 7% of the total protein by densitometry of the Coomassie blue stained gel, coeluted with the larger peptide. As mentioned in Chapter V, although the level of undigested protein could be lowered by more intense digestion, this tended to increase the amount of fragments of the larger peptide and these coeluted with the smaller peptide.

Subtilisin digestion of the mixed-valence holoenzyme which had been radiolabelled in the oxidised state to the extent of one mol histidine per mol gave the same peptide pattern as shown in Figure 6.4. A ratio of 2.2:1 for radioactive disintegrations in the peptide (R251-M338) relative to the peptide (pE1-T250) was obtained and if the contribution of undigested protein to the (pE1-T250) fraction was allowed for, this ratio became 2.9:1. This ratio is a strong indication that the single essential histidine resides in the (R251-M338) fragment. Similar ratios of label distribution were also determined by autoradiography (Figure 6.3), but the close correlation between modification of a single histidine and loss of activity had led us to expect a much cleaner pattern of label distribution.

Figure 6.4 Identification of peptide (R251-M338) as the site of modification by radioactive counting

CCP (20μM) in 10mM Hepes pH 7.5 was modified to an extent of 0.9 mol histidine per mol, with [^{14}C] DEPC (100μM). The modified sample (15μM) was desalted through a small G25 Sephadex column, equilibrated in 10mM Hepes pH7.5, before being digested with subtilisin as described in the legend to Figure 6.3. The digest was made to 1% in SDS and loaded onto a Pharmacia Superdex 75 column equilibrated in 20mM Tris pH7.3, 100mM NaCl. The eluate was monitored at 280 nm and the resultant two main peaks collected. The protein composition of the two peaks was determined by Coomassie blue stain after SDS electrophoresis on a 15% polyacrylamide gel. The remainder (2/3) of the two peaks were used for radioactive counting. The distribution of label between the two fractions is shown in the histogram. The contribution of labelled undigested protein to the fraction containing peptide (pE1-T250) was deducted to give a corrected dpm. Lane 1 - M_r standards; Lane 2 - undigested CCP; Lane 3 - subtilisin digest; Lane 4 - peak 1 from Superdex column; Lane 5 - peak 2.

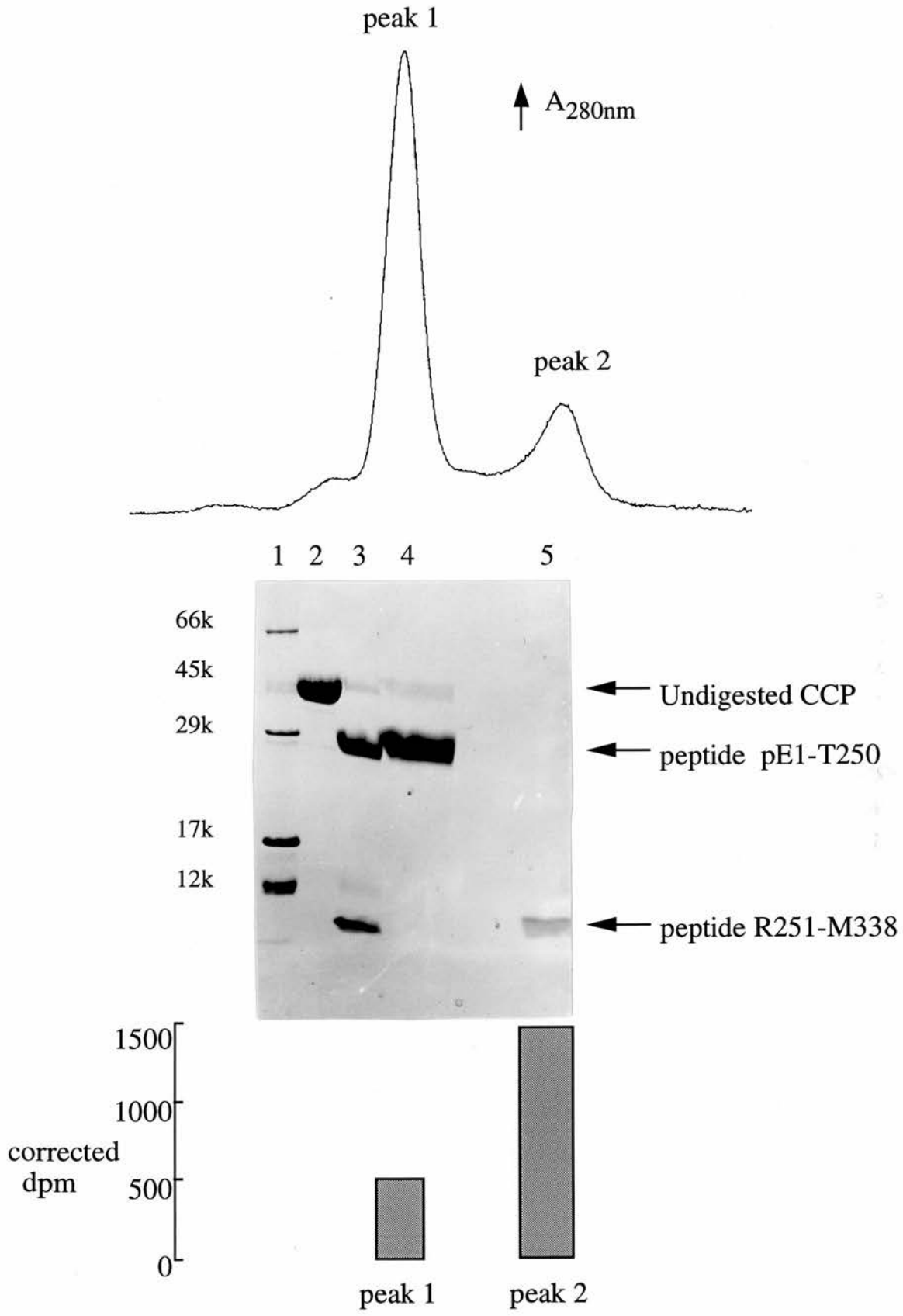
peak 1
A280nm
peak 2
1 2 3 4 5
66k
45k
29k
17k
12k
Undigested CCP
peptide pE1-T250
peptide R251-M338
1500
1000
corrected dpm
500
0
peak 1
peak 2

6.2.4.2 Transfer of radioactivity from R251-M338 to pE1-T250

An experimental observation which allowed us to explain the pattern of label distribution was that a [^{14}C] DEPC-labelled protein sample left for 24h after modification has completely lost its ethoxyformylhistidine based on spectroscopic measurements at 245 nm, yet had retained almost all radioactivity (Table 6.1). Cleavage and separation of the two subtilisin fragments yielded a (R251-M338):(pE1-T250) radiolabel ratio of ~ 1:5 (Figure 6.5). Therefore, over the 24 hours, label has transferred from a specific site on the peptide (R251-M338) to the peptide (pE1-T250). It is proposed that a partial transfer of this type is the reason for the ratio of 2.9:1, rather than higher, that we observed for an analysis completed within approximately 2h. This retention of label on the protein no longer blocked enzyme activity but did generate some resistance to subtilisin proteolysis (Figure 6.6). This was a surprising result as native CCP and the ethoxyformylhistidine derivative of CCP are equally susceptible to subtilisin (see Chapter V, section 5.2.2). Therefore the enzyme:substrate ratio had to be slightly increased to achieve similar levels of digestion.

We are unaware of a precedent for such an intramolecular transfer of an ethoxyformyl group but propose it to be consistent with attack on the ethoxyformylhistidine 275 by a lysine that is adjacent in the folded protein but resides in the N-terminal (pE1-T250) sequence. Ethoxyformyllysine itself is not susceptible to nucleophilic attack and is therefore stable (Melchior and Fahrney, 1970). This proposal will be tested by identification of the labelled residue in the peptide (pE1-T250).

6.2.4.3 Identification of His 275 as the essential modified histidine

As the peptide (R251-M338) contains both His 275 and His 322, unequivocal identification of the essential histidine in CCP required isolation of a fragment containing a single histidine. Therefore the peptide (R251-M338) was subdigested with trypsin generating six smaller fragments (labelled A-F) (Figure 6.7) which were isolated by reverse phase HPLC and identified by mass spectrometry (Table 6.2). His

Table 6.1 Loss of ethoxyformylhistidine does not correlate with loss of radioactive label

CCP (10μM) in 5mM Hepes pH 7.5 was modified with [^{14}C]DEPC to a final concentration of 40μM. Difference spectra of modified minus unmodified CCP were taken at different times after DEPC addition. The absorbance at 245 nm was maximal at 20 min. The times 0, 3 and 6h shown are hours after this maximal extent of modification. Aliquots of modified CCP were also taken at 0, 3 and 6 hours, desalted and counted for radioactivity.

Time after modification (hours)	mol ethoxyformylhistidine / mol	mol radioactive label / mol
0	0.96	0.93
3	0.54	0.90
6	0.25	0.83

Figure 6.5 Transfer of radioactive label from peptide R251-M338 to peptide pE1-T250

CCP (10μM) in 10mM Hepes pH 7.5 was modified to an extent of 1.0 mol histidine modified per mol protein with [^{14}C]DEPC (40μM). After 20 min, modified CCP was desalted through G25 Sephadex equilibrated in 5mM Hepes pH 7.5. Times shown are hours after desalting modified CCP.

(a) t 0h, an aliquot of modified CCP was digested with subtilisin as described in the legend to Figure 6.3. The digest was made to 1% in SDS and loaded onto a Pharmacia Superdex 75 column equilibrated in 20mM Tris pH 7.3, 100mM NaCl. The resultant two main peaks containing peptides pE1-T250 and R251-M338 were collected and used for radioactive counting.

(b) t 24h, a second aliquot of DEPC-treated CCP was taken after 24 hours, digested and separated as in (a) (a slight difference was the raised substrate : enzyme ratio of 400:1 (w/w) see Figure 6.6). Again the radioactive distribution between the two peptides was determined.

The distribution of label between the two peptides at t=0h and t=24h is shown in the respective histograms.

(a) Time 0

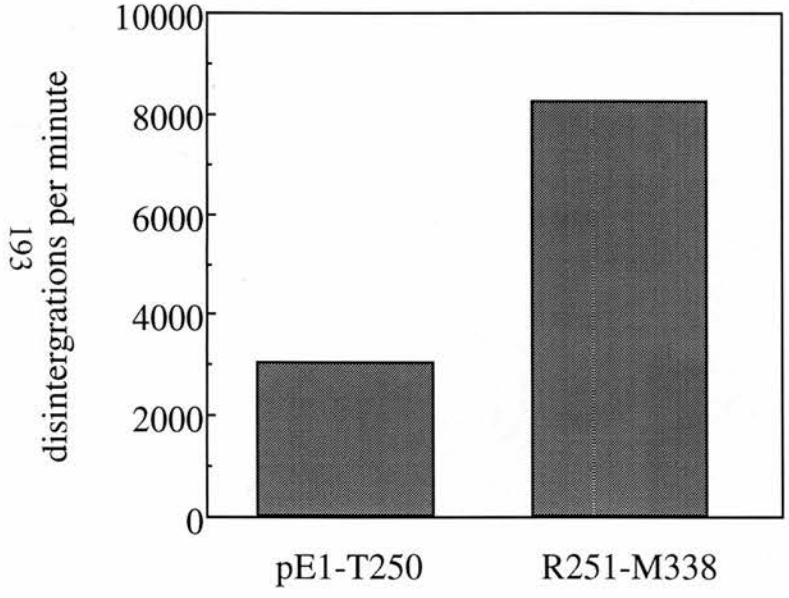

(b) Time 24 hrs

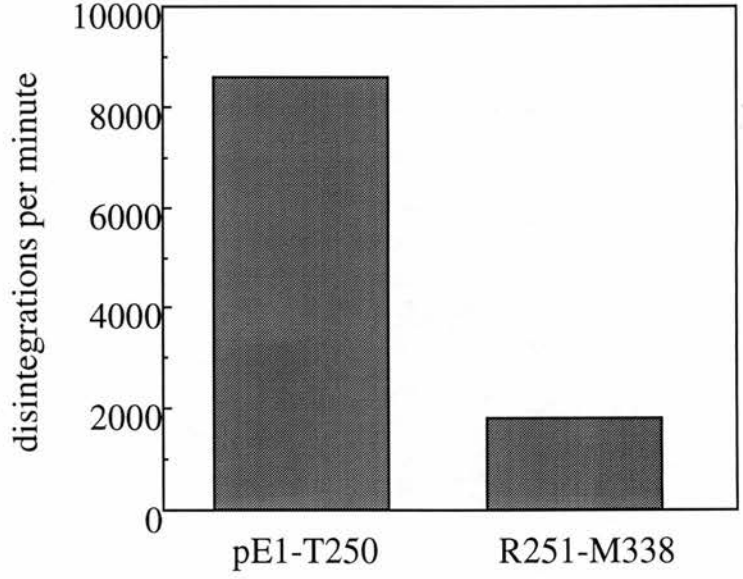

Figure 6.6 Cleavability of CCP, 0h and 24h after modification with DEPC

CCP (10μM) in 10mM Hepes pH 7.5 was modified to an extent of 1.1 mol histidine per mol, with DEPC (40μM). The modified sample was desalted through G25 Sephadex equilibrated in 10mM Hepes pH7.5. At 0h and 24h after ethoxyformylation, aliquots of modified CCP were digested with subtilisin as described in the legend to Figure 6.3. The protein composition of both whole and cleaved CCP, 0h and 24h after modification was determined by Coomassie blue stain after SDS electrophoresis on a 15% polyacrylamide gel. Lane A - Molecular mass markers, BSA (M_r 66k), Ovalbumin (45k), Carbonic anhydrase (29k), Myoglobin (17k), Cytochrome c (12k); Lane B - undigested CCP, 0h after modification; Lane C - digested CCP, 0h after modification; Lane D - undigested CCP, 24h after modification; Lane E - digested CCP, 24h after modification.

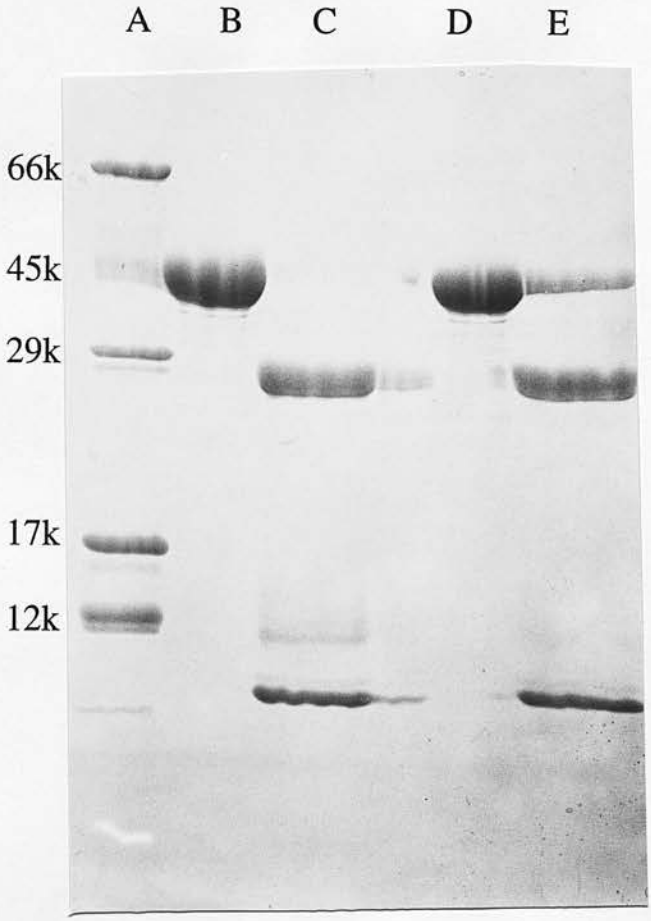
A
B
C
D
E
66k
45k
29k
17k
12k

Figure 6.7 Identification of His 275 as radiolabelled amino acid.
Unmodified purified peptide (R251-M338) was prepared as in Figure 6.4. Trypsin was added to give a substrate : enzyme ratio of 50:1 (w/w). After 10 min at 23°C, trypsin was inhibited with 0.5mM PMSF. The resultant peptides were separated by HPLC on a reverse phase Techsphere 50DS (25cm x 4.6mm) column, using a gradient of 0 - 70% acetonitrile in 0.1% trifluoroacetic acid and gave rise to the 214 nm profile labelled 'Unmodified'. Six peptides were collected (A-F), and identified by mass spectrometry (Table 6.2).

CCP modified to an extent of 0.9 mol histidine per mol of with [^{14}C] DEPC, was cleaved with subtilisin and the resultant radiolabelled peptide (R251-M338) purified as in Figure 6.4. The digestion of this peptide with trypsin yielded the HPLC profile labelled 'Modified'. The unmodified peptide is labelled E1 whilst the modified peptide is labelled E2. The distribution of radiolabel was determined by radioactive counting and shown in the histogram below each peak.

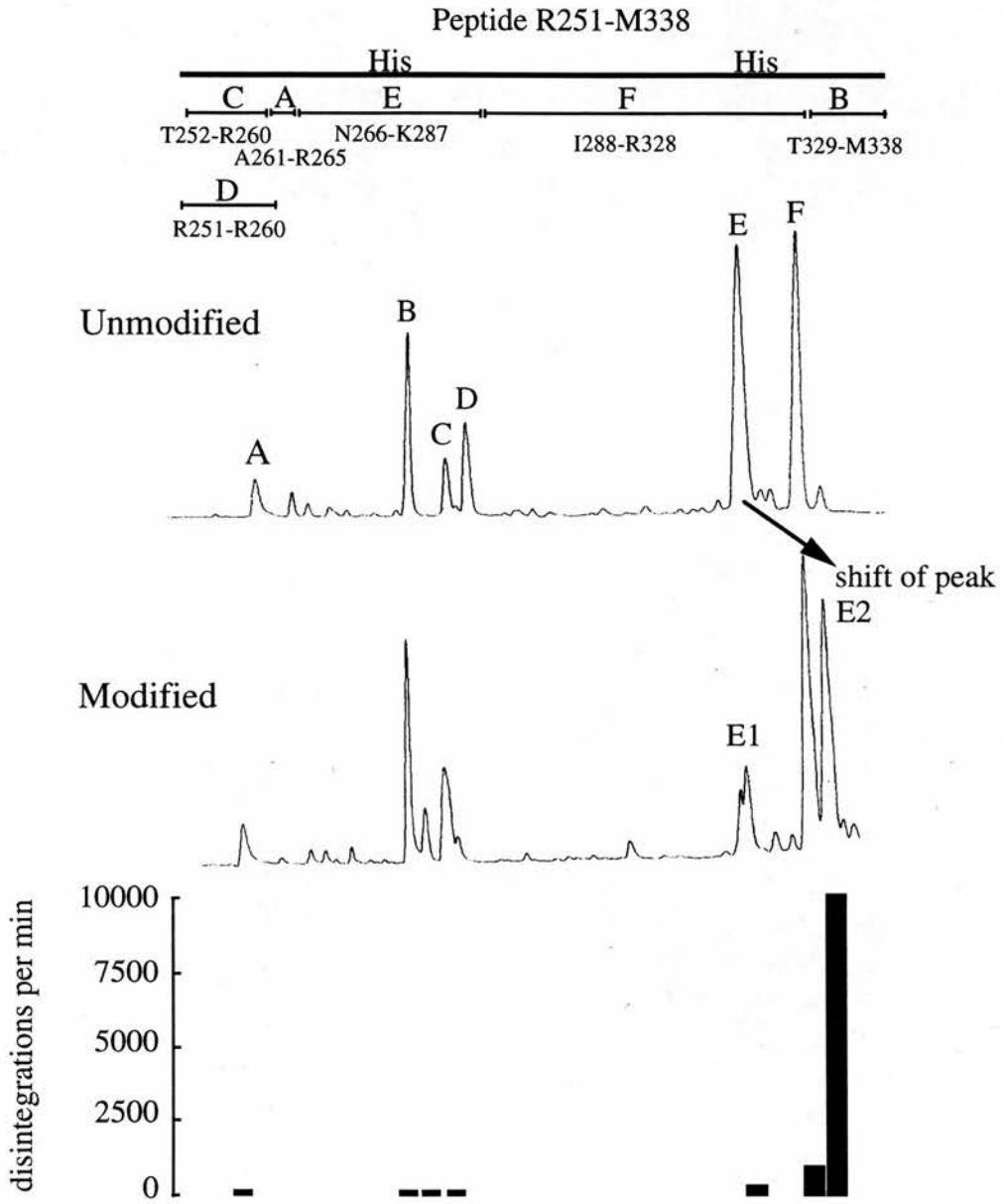
Peptide R251-M338
His
His
C
A
E
F
B
T252-R260
A261-R265
N266-K287
I288-R328
T329-M338
D
R251-R260
Unmodified
A
B
C
D
E
F
shift of peak
E2
Modified
E1
disintegrations per min
10000
7500
5000
2500
0

Table 6.2 Electrospray Mass Spectrometry of peptides from *P.denitrificans* CCP

Whole CCP represents the holoprotein with two haem groups attached. The first and last residue of each peptide is indicated (pE1 represents the N-terminal pyroglutamate). Peptides (pE1-T250) and (R251-M338) (1nmol of each) were generated by subtilisin treatment of CCP as described in the legend to Figure 6.4. The masses of these two peptides correspond well with those calculated from the amino acid sequence. The tryptic peptides of the (R251-M338) fragment were generated and purified as described in the legend to Figure 6.7. Samples were desalted through a Superdex 75 column equilibrated in 0.1M ammonia solution and freeze-dried before mass spectrometry. The masses again correspond well with those calculated from the amino acid sequence. The resolution of the mass spectrometer allows for isotopic resolution of peptides under approximately M_r 3000. By averaging the mass of elemental isotopes according to their natural distribution, and thus determine the average mass of individual residues, the theoretical M_r of peptides over 3000 were calculated. The theoretical M_r of peptides under 3000 was calculated using monoisotopic mass values. Mass spectrometry was performed using a BioQ triple quadrupole mass spectrometer equipped with a pneumatically assisted electrospray source (Fisons, Altrincham,UK) operating in positive ion mode.

Peptide	M_r determined by sequence	M_r determined by electrospray mass spectrometry
Whole CCP pE1-M338	37512.80	37507.97
peptide pE1-T250	27950.93	27950.90
peptide R251-M338	9579.87	9581.38
A A261-R265	526.32	526.30
B T329-M338	1014.51	1014.54
C T252-R260	1144.47	1144.65
D R251-R260	1300.57	1300.05
E N266-K287	2400.12	2400.25
F I288-R328	4406.98	4406.84
E2 R251-R260	2472.12	2472.62

275 and His 322 were located in peptides E and F respectively.

The essential histidine of CCP was radiolabelled with [^{14}C] DEPC and the modified peptide (R251-M338) isolated, digested and the resultant tryptic peptides separated as for the native protein. The HPLC profile for the modified tryptic digest displayed an extra peak E2, the appearance of which correlated with the diminution of the original peak E1. Almost all the label was contained in peptide E2 (Figure 6.7). Thus we conclude that peptide E contains the essential histidine, which, when ethoxyformylated, increases the retention time of the peptide. This was confirmed by obtaining an elution profile which matched that of the unmodified protein after reversal of the modification in 0.2M ammonia solution. As peptide E was the only tryptic fragment of R251-M338 to contain a tryptophan residue, E1 and E2 were easily distinguished from the other fragments by specific staining for Trp (Figure 6.8 (a)) and the high 280 nm absorbance (Figure 6.8 (b)) . Also the M_r of peptide E2 was determined to be 2472.62, by mass spectrometry (Table 6.2). This corresponds well with the theoretical mass of 2400.12 for peptide E (N266-K287) plus 72 for an ethoxyformyl group. Thus, as confirmed by both autoradiography and radioactive counting, His 275 is the single histidine modified at low DEPC:CCP ratios which is essential for activity.

The success of these experiments relied on the retention of a large proportion of the ethoxyformyl label throughout the peptide cleavage and isolation procedures. The utilisation of rapid chromatographic techniques and the careful choosing of separation conditions, led to detection of the majority of the radiolabel. Fortunately the requirement to use 1% SDS in separating the peptides R251-M338 and pE1-T250 (see Chapter V, section 5.2.3) established a stable ethoxyformylhistidine derivative (see Chapter III, section 3.2.3.4). Conversely 0.1M ammonia solution would have been unusable in the separation of radiolabelled peptides, as the ethoxyformyl group would have been lost within minutes.

Figure 6.8 Peptide E from tryptic digest of R251-M338 contains tryptophan

(a) Peptides A-F (~100pmol) from a tryptic digest of peptide R251-M338 were spotted out on a TLC plate, left to dry and sprayed with 2% p-dimethylaminobenzaldehyde in 5% HCl. The presence of tryptophan generates a purple colour. Shown is the densitometry scan at 550 nm of the TLC plate. Lanes A-F represent tryptic fragments A to F. (b) i) Reverse phase HPLC profile recorded at 214 nm, from tryptic digest of peptide R251-M338. ii) HPLC profile recorded at 280 nm of i).

(a)

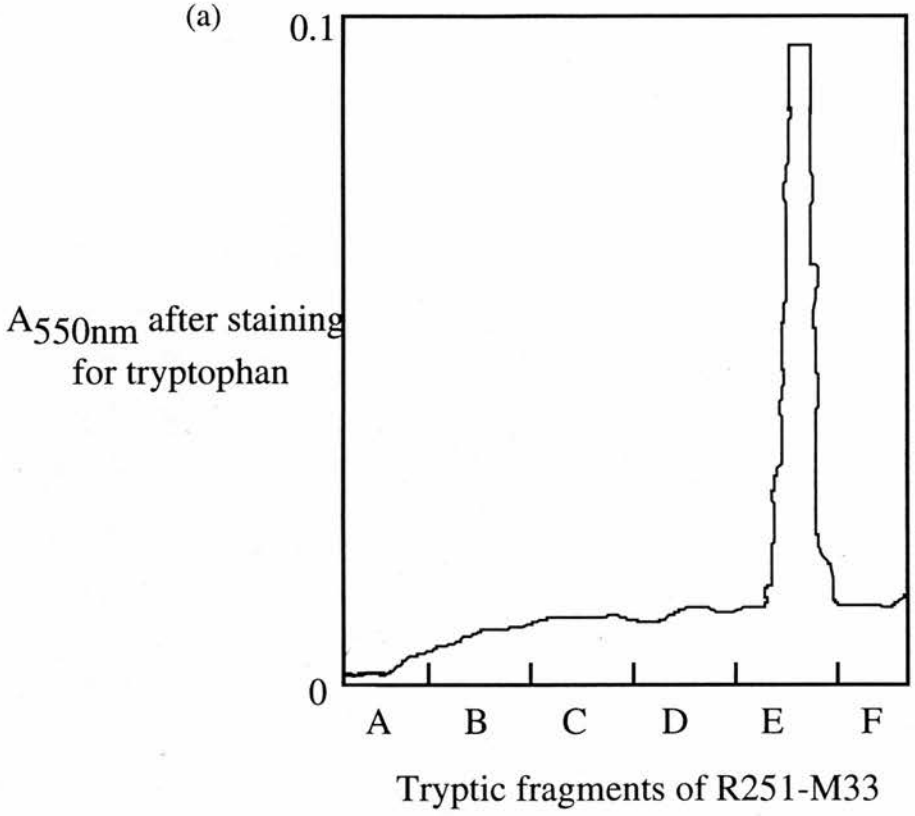
0.1
0
A_{550nm} after staining for tryptophan
A
B
C
D
E
F
Tryptic fragments of R251-M33

(b)

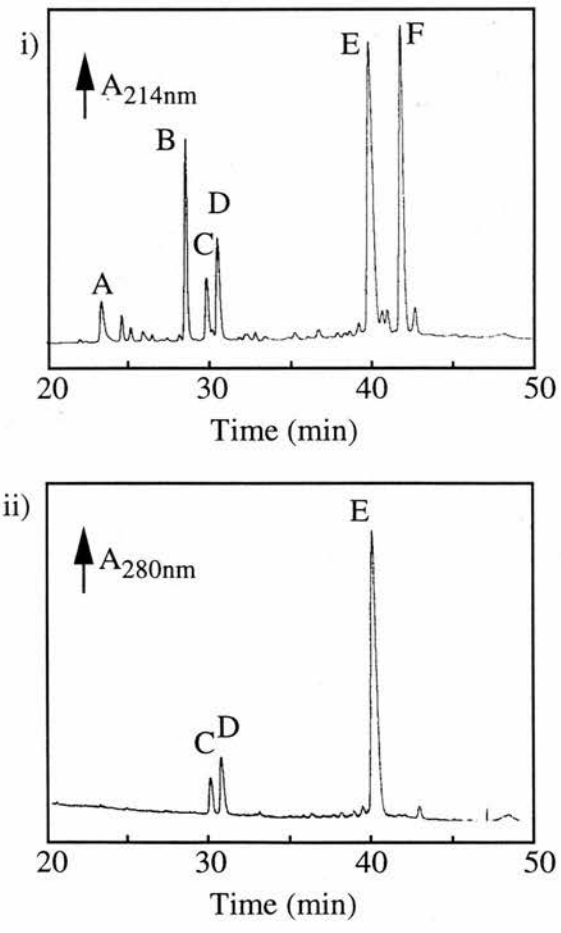
i)
A_{214nm}
A
B
C
D
E
F
20
30
40
50
Time (min)
ii)
A_{280nm}
C
D
E
20
30
40
50
Time (min)

Chapter VII

Discussion

7.1 Introduction

This thesis has focused on investigating the role of histidines in the mode of action of cytochrome c peroxidase from the bacterium *Paracoccus denitrificans* . The CCP from *P.denitrificans* is a relative of the extensively characterised enzyme from *Pseudomonas aeruginosa*. During the preparation of this thesis, the crystal structure of the oxidised form of *P.aeruginosa* cytochrome c peroxidase was published (Fulop et al.1995). I will introduce the structure of *P.aeruginosa* cytochrome c peroxidase as determined by Fulop et al. (1995) and with the benefit of amino acid sequences from homologous bacterial peroxidases, discuss certain features of the structure. The work presented in this thesis, including the modification and identification of an essential histidine in the cytochrome c peroxidase of *P.denitrificans* , will then be discussed.

7.2 Crystal structure of the oxidised form of cytochrome c peroxidase from *Pseudomonas aeruginosa*

The primary sequence of *P.denitrificans* cytochrome c peroxidase has been determined (Goodhew, van Beeumen and Pettigrew, unpublished results) and is aligned in Figure 7.1 with the CCP from *P.aeruginosa* . The *P.aeruginosa* CCP sequence is based on the recently determined gene sequence (Ridout et al.1995) and contains several corrections to the original protein sequence as determined by Ronnberg et al.(1989). The 61% identity between the *P.aeruginosa* CCP and the *P.denitrificans* CCP sequence allow confidence that the overall structure of the two molecules will be retained.

The X-ray structure of the *P.aeruginosa* CCP determined to 2.4Å resolution showed the molecules formed dimers in the crystal. The monomer is a fascinating structure, clearly divided into two domains, each domain containing a haem c group and reminiscent of class I cytochromes c such as tuna cytochrome c and *Pseudomonas* cytochrome c 551. However, as the coordinates of the *P.aeruginosa*

Figure 7.1 Amino acid sequence and α–helices of cytochrome c peroxidase from *P.aeruginosa* aligned with CCP sequence from *P.denitrificans*

This is a modified version of Figure 2 from Fulop et al. (1995). The amino acid sequences are for the cytochrome c peroxidases from (1)*Pseudomonas aeruginosa* (Ridout et al.1995); shown beneath are the α–helices as determined from the crystal structure and represented by α . (2)*Paracoccus denitrificans* (Goodhew, van Beeumen and Pettigrew, unpublished work). Both sequences are numbered from their respective N-termini.

```
                      10                  20        30
(1)           DALHDQASALFKPIP         EQVTELRGQPISEQQRELG
                  ααααααα                          αααααα
                     α1                                 α2
(2)  <ETEAIDNGALREEAKGVFEAIPEKMTAIKQTEDNPEGVPLTAEKIELG
                 10         20        30        40

        40         50         60         70         80
(1)KKLFFDPRLSRSHVLSCNTCHNVGTGGADNVPTSVGHGWQKGPRNSPTVFN
   ααααα            ααα
                    α3
(2)KVLFFDPRMSSSGLISCQTCHNVGLGGVDGLPTSIGHGWQKGPRNAPTMLN
   50         60         70         80         90

       90         100        110        120        130
(1)AVFNAAQFWDGRAKDLGEQAKGPIQNSVEMHSTPQLVEQTLGSIPEYVDAF
                            αααααααα   αααααααα   αααααα
                                 α4         α5         α6
(2)AIFNAAQFWDGRAADLAEQAKGPVQAGVEMSNTPDQVVKTINSMPEYVEAF
  100        110        120        130        140        150

     140        150        160        170        180
(1)RKAFPKAGKPVSFDNMALAIEAYEATLVTPDSPFDLYLKGDDKALDAQQKK
   αα           ααααααααααααα          αααααα         ααααα
                      α7                    α8
(2)KAAFPEEADPVTFDNFAAAIEQFEATLITPNSAFDRFLAGDDAAMTDQEKR
            160        170        180        190        200

    190        200        210        220        230
(1)GLKAFMDSGCSACHNGINLGGQAYFPFGLVKKPDASVLPSGDKGRFAVT
   ααααααα
     α9
(2)GLQAFMETGCTACHYGVNFGGQDYHPFGLIAKPGAEVLPAGDTGRFEVT
           210        220        230        240        250

     240        250        260        270        280
(1)KTQSDEYVFRAAPLRNVALTAPYFHSGQVWELKDAVAIMGNAQLGKQLAPDD
                                      ααααααα          αα
                                         α10
(2)RTTDDEYVFRAAPLRNVALTAPYFHSGVVWELAEAVKIMSSAQIGTELTDQQ
            260        270        280        290        300

   290        300        310        320
(1)VENIVAFLHSLSGKQPRVEYPLLPASTETTPRPAE  P.aeruginosa CCP
    ααααααα
      α11
(2)AEDITAFLGTLTGEQPVIDHPILPVRTGTTPLPTPM P.denitrificans CCP
           310        320        330
```

enzyme are as yet unavailable, the interpretation of the structure relies heavily on the figures from Fulop et al. (1995). The α-helices of *P.aeruginosa* CCP, as determined from the crystal structure are also shown in Figure 7.1, which is a modified version of Figure 2 from Fulop et al. (1995).

Figure 7.2 shows the crystal structure of the cytochrome c peroxidase from *P.aeruginosa* and is a reprint of Figure 3 from Fulop et al. (1995). As explained in Chapter I, section 1.2.1.1, Ellfolk et al. (1991) discerned a class I pattern for both domains based on secondary structure predictions and sequence patterns. The class I cytochrome c fold, for which tuna cytochrome c and *Pseudomonas* c551 are chosen as paradigms (Figure 7.3), contains certain common elements of secondary structure and key residues. From the structure of *P.aeruginosa* CCP it can be seen that both domains retain to a degree the class I fold, yet contain additional secondary structure features and unexpected differences. The folds of the two domains are compared with the fold of two typical class I cytochromes in Figure 7.3, which is a reprint of Figure 5 from Fulop et al. (1995). The two domains are connected by the N and C-terminal tails as well as the interconnecting stretch of residues from 160-169.

7.2.1 N-terminal haem domain of *P.aeruginosa* CCP

The N-terminal domain is comprised of residues 17-164. As a result of the bis-histidyl coordination of the N-terminal haem iron, Fulop et al. (1995) have assigned the function of this domain as the low potential peroxidatic centre. The helices α2 and α7 correspond to the class I N and C-terminal helices respectively. The N-terminal helix (α2) contains the characteristic Gly (34) and Phe (38) and the C-terminal α-helix (α7) lies across the N-terminal helix at Gly 34 and contains an aromatic partner (Tyr 159) for Phe 38. The haem binding site is Cys 51-Cys 54 with His 55 providing the proximal ligand to the haem. After the haem binding site the structure differs markedly from a class I type fold. Instead of a 'right side loop', an extended stretch of chain, described as a flexible loop in Fulop et al. (1995), reaches round to the distal side of the haem and His 71 coordinates the haem iron at the sixth position. The chain then

Figure 7.2 Structure of the oxidised form of cytochrome c peroxidase from *P.aeruginosa*

This figure is a reprint of Figure 3 from Fulop et al. (1995). The ribbon diagram is colour-ramped blue to red from the N to the C terminus. The small grey sphere shows the location of the calcium ion and the haems are in the ball-and-stick representation. LP and HP denote the proposed low-potential and high-potential haem domains respectively.

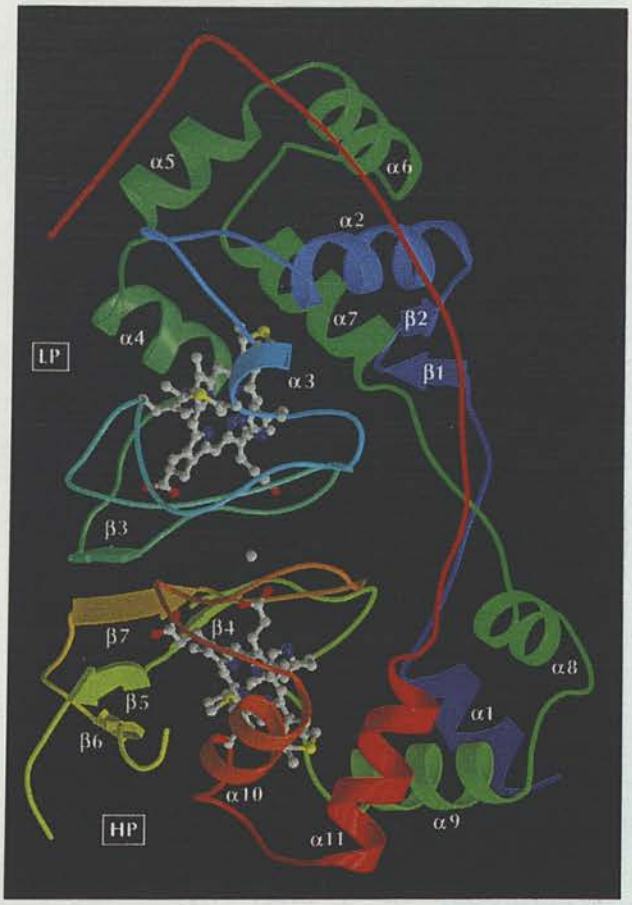
α5
α6
α2
α7
β2
α4
LP
α3
β1
β3
β7
β4
α8
β5
α1
β6
α10
HP
α11
α9

Figure 7.3 Comparison of the class I cytochrome c fold with the *P.aeruginosa* CCP domains

This figure is a reprint of Figure 5 from Fulop et al. (1995). (a) N-terminal haem domain of CCP, (b) C-terminal haem domain of CCP, (c) Cytochrome c_{551} from *P.aeruginosa* . (d) Tuna cytochrome c. The cytochromes are colour-ramped dark blue to light blue from the N to the C-terminus. The CCP domains are coloured similarly. The haems are shown in ball-and-stick representation.

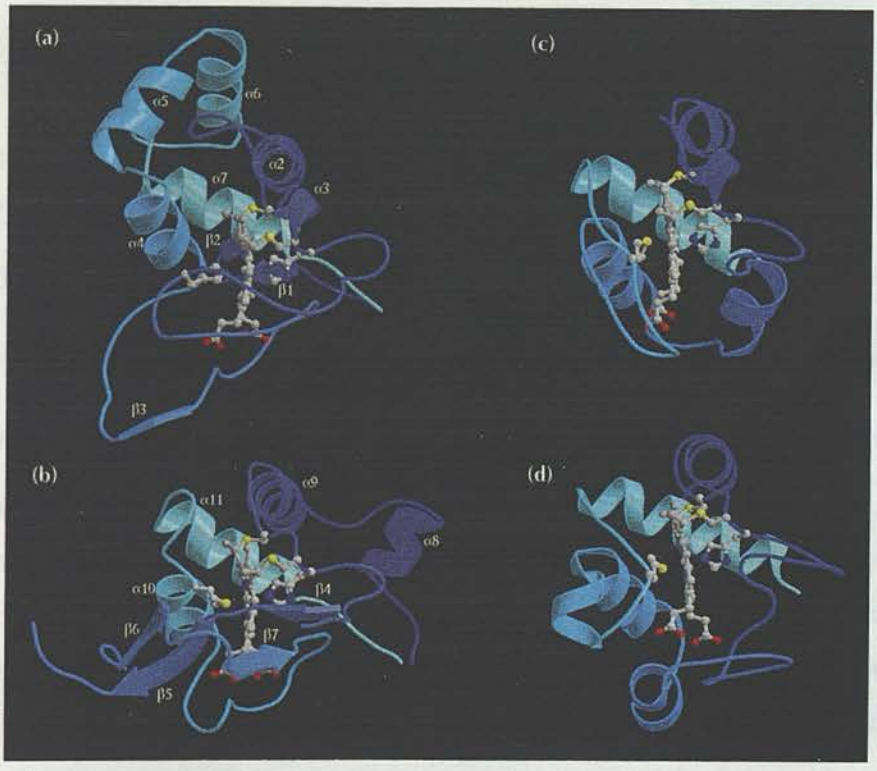
(a)
α5
α6
α2
α7
α3
α4
β2
β1
β3
(c)
(b)
α11
α9
α8
α10
β4
β6
β7
β5
(d)

loops back to the proximal side where the carbonyl of Pro 81 accepts a hydrogen bond from the back of His 55. The chain then loops back again to the distal side (Pro 108 H-bonds to His 71) before Trp 94, conserved in class I cytochromes, marks the start of the left side of the molecule, which includes α–helix 4, analogous to the left rear helix in class I cytochrome c. At the end of this helix resides Met 115, the presence of which will be discussed later in the Chapter. The N-terminal domain finishes with two non-class I helices at the top of the molecule (α5 and α6, see Figure 7.2) before the C-terminal helix (α7).

7.2.2 C-terminal haem domain of *P.aeruginosa* CCP

The C-terminal domain is comprised of residues 165-302. The domain has histidine (His 201) and methionine (Met 275) as haem iron ligands and has been ascribed the function of the high potential electron transferring domain by Fulop et al. (1995). The helices α9 and α11 correspond to the class I N and C-terminal helices respectively. The N-terminal helix (α9) contains the characteristic Gly (188) and Phe (192) , the C-terminal α-helix (α11) lying across the N-terminal helix at Gly 188 and containing an aromatic partner (Phe 295) for Phe 192. The haem is attached to Cys 197 and Cys 200 and has His 201 and Met 275 as ligands like a typical class I cytochrome c. Residues 223-228 are disordered and therefore not included in the final model (Figure 7.2) and although this region is a site of cleavage by *Pseudomonas* elastase, the molecules in the crystal were determined to be intact. This stretch will be discussed later in this Chapter in relation to the cleavage of the *P.denitrificans* CCP with subtilisin.

Other structural features of the *P.aeruginosa* enzyme will be discussed throughout this chapter as they influence the conclusions to the experimental work on *P.denitrificans* CCP. These include the location in the structure of His 261, analogous to the essential His 275 in the *P.denitrificans* enzyme. Also a metal-binding site has been identified in the structure, located between the two domains of the *Pseudomonas*

protein (Figure 7.2). This observation will be discussed in relation to putative Ca^{2+} binding sites identified in the *P.denitrificans* enzyme. Related to this is our laboratory's proposal of a Ca^{2+} located at the dimer interface of the *Paracoccus* enzyme (Gilmour et al.1995).

Now with the benefit of the *P.aeruginosa* CCP structure, the other bacterial peroxidase sequences can be utilised to provide further insights into the actual mode of action of this class of enzymes. Especially enlightening was identifying both conserved and non-conserved regions and individual residues throughout the family of bacterial peroxidases.

7.3 Sequence homology with *P.denitrificans* cytochrome c peroxidase

The primary sequence of cytochrome c peroxidase of *P.denitrificans* (Goodhew, van Beeumen and Pettigrew, unpublished results) is aligned in Figure 7.4 with that from *P.aeruginosa* , *R.capsulatus* and an open reading frame from *E.coli*. *R.capsulatus* CCP (van Beeumen, unpublished results) and *P.denitrificans* CCP are closely related (68% identity, as shown by the identity matrix in Figure 7.5) consistent with their placement together in the group of non-sulphur purple bacteria (reviewed in Moore & Pettigrew (1990)). This level of identity is higher than that between the cytochrome c_2 sequences of the two organisms (57%) suggesting stronger constraints on evolutionary change. The 60/61% identity for the comparisons of the *P.aeruginosa* enzyme with those of *R.capsulatus* and *P.denitrificans* (Figure 7.5) are again high figures in comparison with the low levels of similarity seen in the small cytochromes c and in S1 oligonucleotide rRNA mapping (Moore and Pettigrew, 1990).

The sequence of the CCP from *P.denitrificans* was used as a template for searching protein databases using the BLAST (Basic local alignment search tool) network service (Altschul et al.1990). The database survey retrieved homologous open reading frames from *Escherichia coli* (Sofia et al.1994) and from the translated MauG genes of *Methylobacterium extorquens* AM1 and *Methylophilus methylotrophus* W3A1-NS (Chistoserdov et al.1994b; Chistoserdov et al.1994a).

The *E.coli* encoded protein contains 465 residues and three Cys-X-Y-Cys-His

Figure 7.4 Sequence alignment of the cytochrome c peroxidases and a homologous open reading frame in *E.coli*

The amino acid sequences are for the cytochrome c peroxidases from (1)*Paracoccus denitrificans* (Goodhew, van Beeumen and Pettigrew, unpublished work) (2)*Rhodobacter capsulatus* (van Beeumen, unpublished work), (3)*Pseudomonas aeruginosa* (Ridout et al.1995). (4) is an open reading frame from the *Escherichia coli* chromosome (Sofia et al.1994). Conserved residues are shown in bold.

```
(4)                MKMVSRITAIGLAGVAICYLGLSGYVWYHDNKRSKQA
(4)DVQASAVSENNKVLGFLREKGCDYCHTPSAELPAYYYIPGAKQLMDYDIKL
(4)GYKSFNLEAVRAALLADKPVSQSDLNKIEWVMQYETMPPTRYTALHWAGKV

                10         20         30         40
(1)  <ETEAIDNGALREEAKGVFEAIPEKMTAIKQTEDNPEGVPLTAEKIELG
(2)        EDAALREEAKGLFEVIP      MQAPQLADNNTVTRDKIDLG
(3)          DALHDQASALFKPIP       EQVTELRGQPISEQQRELG
(4)SDEERAEILAWIAKQRAEYYASNDTAPEHRNEPVQPIPQKLPTDAQKVALG

    50         60         70         80         90
(1)KVLFFDPRMSSSGLISCQTCHNVGLGGVDGLPTSIGHGWQKGPRNAPTMLN
(2)AMLFFDPRMSKSGVFSCQSCHNVGLGGVDGLETSIGHGWQKGPRNAPTALN
(3)KKLFFDPRLSRSHVLSCNTCHNVGTGGADNVPTSVGHGWQKGPRNSPTVFN
(4)FALYHDPRLSADSTISCAHCHALNAGGVDGRKTSIGVGGAVGPINAPTVFN

  100        110        120        130        140        150
(1)AIFNAAQFWDGRAADLAEQAKGPVQAGVEMSN TPDQVVKTINSMPEYVEAF
(2)AVFNVAQFWDGRAPDLAAQAKGPVQAGVEMNN TPENLVATVQSMPGYVEAF
(3)AVFNAAQFWDGRAKDLGEQAKGPIQNSVEMHS TPQLVEQTLGSIPEYVDAF
(4)SVFNVEQFWDGRAATLQDQAGGPPLNPIEMASKSWDEIIAKLEKDPQLKTQF

           160        170        180        190        200
(1)KAAFPEEADPVTFDNFAAAIEQFEATLITPNSAFDRFLAGDDAAMTDQEKR
(2)AKAFPGQKDPISFDNFALAVEAFEATLITPNSKFDQWLMGADGAMSADEKA
(3)RKAFPKAGKPVSFDNMALAIEAYEATLVTPDSPFDLYLKGDDKALDAQQKK
(4)LEVYPQG   FSGENITDAIAEFEKTLITPDSPFDKWLRGDENALTAQQKK

          210        220        230        240        250
(1)GLQAFMETGCTACHYGVNFGGQDYHPFGLIAKPGAEVLPAGDTGRFEVT
(2)GLKLFIDTGCAACHNGINIGGNGYYPFGVVEKPGAEVLPAGDKGRFAVT
(3)GLKAFMDSGCSACHNGINLGGQAYFPFGLVKKPDASVLPSGDKGRFAVT
(4)GYQLFKDNKCATCHGGIILGGRSFEPLGLKKDFNFGEITAADIGRMNVT

           260        270        280        290        300
(1)RTTDDEYVFRAAPLRNVALTAPYFHSGVVWELAEAVKIMSSAQIGTELTDQQ
(2)ATADDEYVFRAGPLRNIALTAPYFHSGKVWDLREAVSVMANSQLGATLDDTQ
(3)KTQSDEYVFRAAPLRNVALTAPYFHSGQVWELKDAVAIMGNAQLGKQLAPDD
(4)KEERDKLRQKVPGLRNVALTAPYFHRGDVPTLDGAVKLMLRYQVGKELPQED

          310        320        330
(1)AEDITAFLGTLTGEQPVIDHPILPVRTGTTPLPTPM  P.denitrificans CCP
(2)VDQITAFLGTLTGEQPEVVHPILPVRSAQTPRPEHMN R.capsulatus CCP
(3)VENIVAFLHSLSGKQPRVEYPLLPASTETTPRPAE   P.aeruginosa CCP
(4)VDDIVAFLHSLNGVYTPYMQDKQ               E.coli ORF
```

Figure 7.5 Matrix of % identities of the sequences in Figures 7.4, 7.6
For the purposes of this figure Pad - *Paracoccus denitrificans*; Rhc - *Rhodobacter capsulatus*; Psa - *Pseudomonas aeruginosa*; Ec - *Escherichia coli*; Mm - *Methylophilus methlyotrophus*; Me *Methylobacter extorquens*.
In comparing sequences the total number of comparisons was obtained by summing:
(a) the number of core residues common to the whole set of sequences,
(b) the number of additional residues common to the pair under consideration,
(c) the number of gaps shared by a pair of sequences,
(d) the number of gaps where only one sequence differs from the other (gaps were scored as one point of comparison no matter what size).
The number of identities in a pair-wise comparison was obtained by summing:
(a) the number of identical residues,
(b) the number of identical gap regions.

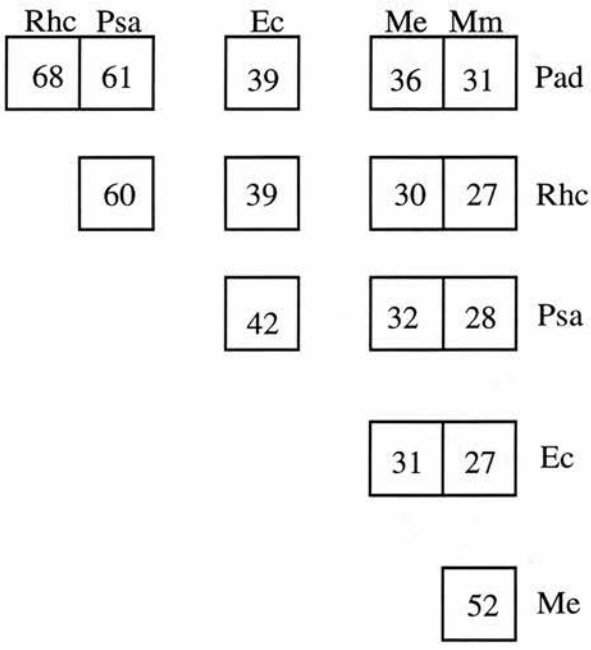
Rhc
Psa
Ec
Me
Mm
68
61
39
36
31
Pad
60
39
30
27
Rhc
42
32
28
Psa
31
27
Ec
52
Me

motifs indicative of a tri-haem c-type cytochrome. The primary sequences of the three bacterial cytochrome c peroxidases can be aligned and have approximately 39-42% identity with the *E. coli* protein around its two C-terminal haems (Figure 7.5). The *E.coli* sequence differs in having the additional stretch of N-terminal amino acids containing haem 1. It may be that this is a result of a gene fusion involving a small Class I cytochrome donor, a possibility which has precedents in the case of the caa_3 type oxidases (Sone and Yangita, 1982). Thus an interesting possible function for the third N-terminal domain of the *E.coli* protein is replacing the need for the separate cytochrome c electron donors of the other bacterial peroxidases. The intention of this laboratory is to express the enzyme using a recombinant DNA approach. The enzyme would be isolated and its properties compared to the other bacterial peroxidases. C-type cytochromes have only been expressed under anaerobic conditions in *E.coli* with nitrite or trimethylamine oxide as the sole electron acceptors (Iobbi-Nivol et al.1994) The presence of a cytochrome c peroxidase is therefore novel and hints at a ubiquitous distribution of this enzyme. This is further supported by the recent isolation of a di-haem cytochrome c peroxidase from the chemoautotroph *Nitrosomonas europaea* (Arciero and Hooper, 1994). The partial sequence of the *N.europaea* enzyme displays 43% identity to the corresponding regions of the *P.denitrificans* enzyme, but further sequence information is required to make a detailed comparison.

Although a case can be made for inclusion of the putative *E.coli* protein in a new class of bacterial cytochrome c peroxidases, the situation is less clear for the putative MauG proteins from *Methylobacterium extorquens* and *Methylophilus methylotrophus* . The primary sequences of the two MauG sequences can be aligned with *P.denitrificans* CCP (Figure 7.6) and share between 31-36% identity with the *Paracoccus* protein (Figure 7.5). Chistoserdov et al. (1994b) have suggested that the MauG protein is indeed a peroxidase but one for which the substrate is not cytochrome c but an intermediate in the synthesis of the prosthetic group of methylamine dehydrogenase - tryptophan tryptophylquinone (TTQ). The conclusion that the MauG proteins are members of a related but distinct family of enzymes is supported by a recent report of a MauG gene sequence in *P.denitrificans* itself (van der Palen et al.1995), which is more remote from the CCP sequences than are its MauG relatives

Figure 7.6 Sequence alignment of *P.denitrificans* CCP and homologous open reading frames from two methylotrophs

The amino acid sequences are from (1)*Paracoccus denitrificans* cytochrome c peroxidases (Goodhew, van Beeumen and Pettigrew, unpublished work). (2)*Methylobacterium extorquens* MauG open reading frame. (3)*Methylophilus methylotrophus* MauG open reading frame. Conserved residues are shown in bold. Boxed regions highlight haem-binding sites, N and C-terminal methionines (129 and 289 respectively, *P.denitrificans* CCP numbering) and essential histidine 275 (*P.denitrificans* CCP numbering).

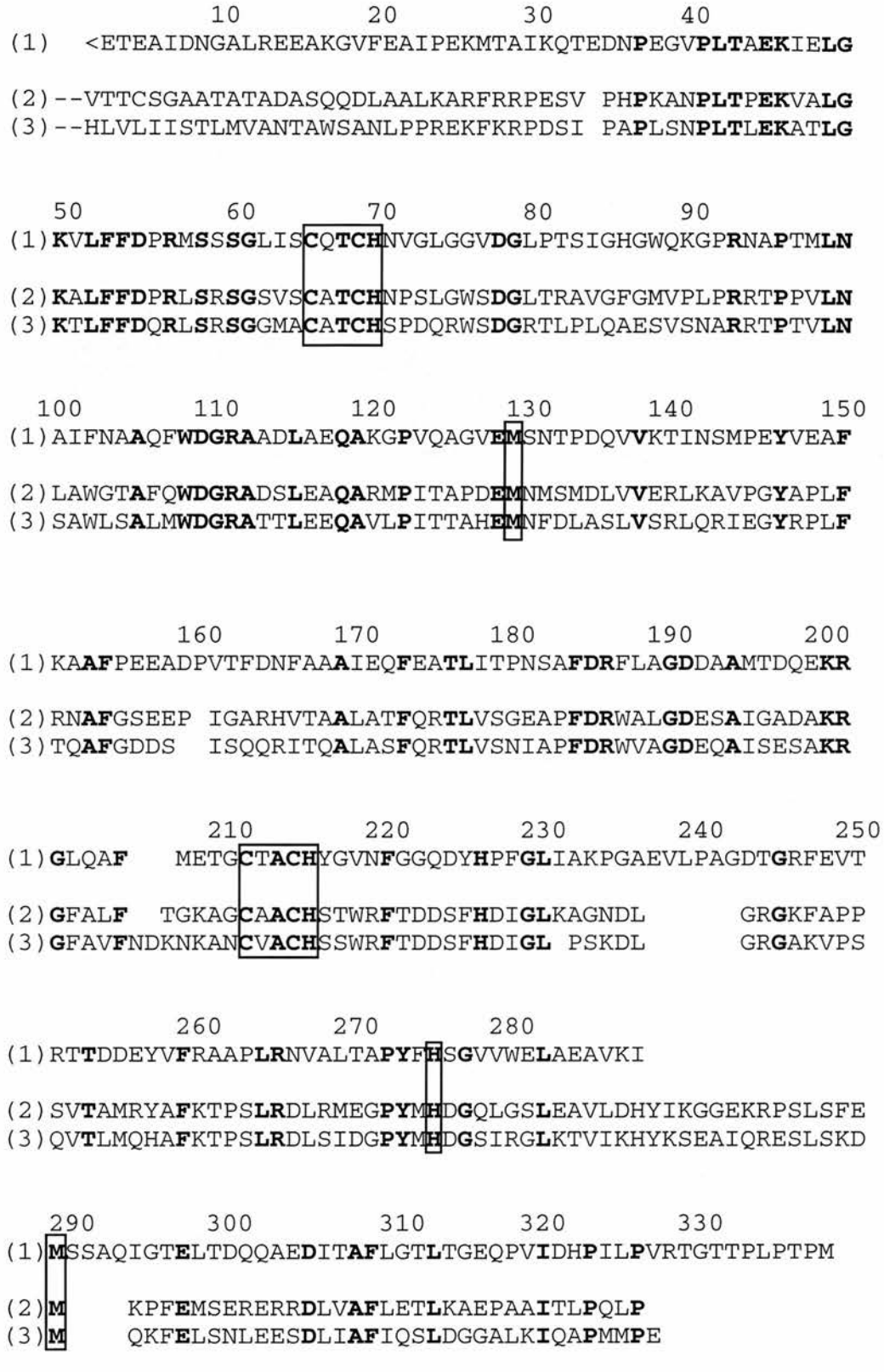

(1) *P.denitrificans* CCP
(2) *Methylobacterium extorquens* MauG
(3) *Methylophilus methylotrophus* MauG

from *M.extorquens* and *M.methylotrophus*.

Now that we are in possession of at least three bacterial peroxidase sequences and probably four if we include the *E.coli* open reading frame, we can return to the structure of the *P.aeruginosa* enzyme and try to identify particular residues and regions of the molecule that may have a role in the bacterial peroxidase mode of action. Although we have to remain cautious about the function of the MauG gene products, information from their sequences will identify conserved regions that suggest important roles in both sets of molecules.

7.4 Haem ligation and the function of the domains of CCP

With the defined pattern of key residues and secondary structures that characterise the Class I fold, Ellfolk et al. (1991) proposed two Class I domains containing the two haem groups in the *Pseudomonas* cytochrome c peroxidase. With the benefit of several homologous sequences and now the structure of one of those sequences we can confirm, adjust and extend many of the proposals of the Ellfolk paper. As the structure of only the oxidised form of *P.aeruginosa* CCP has been resolved, questions regarding the structure of the mixed-valence state and therefore the mode of action of bacterial peroxidases still remain.

The C-terminal haem domain of *P.aeruginosa* CCP was seen by Ellfolk et al.(1991) as being a conventional high potential, class I cytochrome c, coordinated by histidine 201 and methionine 275 and performing the electron transfer role in the enzyme. The class I features are conserved in all the bacterial peroxidases including the *Paracoccus* enzyme, the putative ligands being His 215 and Met 289 (*P.denitrificans* CCP numbering).

That the C-terminal domain is a Class I fold with methionine coordination is confirmed by the crystal structure of *P.aeruginosa* CCP in the oxidised state. We would expect this haem to be high potential and therefore to have the function of electron transfer. By default this leaves the N-terminal haem with the peroxidatic role. Ellfolk et al. (1991) proposed a model for the enzyme in which His 261 (His 275 in *P.denitrificans* CCP) from the C-terminal domain acted as the distal ligand for the N-terminal haem making it low potential in the oxidised enzyme and conferring

peroxidatic activity in the activated mixed-valence state (see Chapter 1, section 1.2.1.1). However the present study has shown His 275 not to be a haem ligand in oxidised *P.denitrificans* CCP and the *P.aeruginosa* CCP structure has also shown His 261 not to be a ligand in the oxidised enzyme. The actual role of this histidine, demonstrated in this thesis to be essential in the *Paracoccus* CCP, will be explored later in this chapter.

The crystal structure of *P.aeruginosa* CCP shows His 71 (His 85 in *Paracoccus*) to coordinate the N-terminal haem iron at the distal side. This was unexpected as it requires the residues immediately following the haem binding site to loop round to the distal side of the haem in an extended stretch of chain. In previous class I structures the molecules are constructed in two distinct halves with the right half containing the haem site and fifth iron ligand and the left half containing the sixth iron ligand. Thus the haem can be thought of as sitting in a crevice between the two halves with only a single linking region between the two. Also His 71, although conserved in the three known peroxidases, is not conserved in the *E.coli* open reading frame or the MauG translated genes (Figures 7.4, 7.5).

Methionine 115 (Met 129 in *Paracoccus*) is conserved throughout all seven known homologous sequences, including the bacterial peroxidases and the *E.coli* and MauG open reading frames. Even the MauG of *P.denitrificans*, the least homologous to the bacterial peroxidases, retains this methionine. The conservation of this methionine implies an essential role in the enzyme and in cytochromes c this would generally indicate coordination to the haem. In fact as far as we are aware from the literature, such a conserved methionine not involved in haem coordination would be unique. However, the crystal structure of *P.aeruginosa* CCP, shows Met 115 not to be coordinated to the N-terminal haem in the oxidised state of the enzyme. Also ^{1}H-NMR spectroscopy reveals the presence of only a single haem iron with methionine coordination in both the oxidised and mixed-valence states of the *Paracoccus* peroxidase (Prazeres et al.1993; Prazeres et al.1994).

In the model proposed by Fulop et al. (1995) the oxidised state of the enzyme has a low potential N-terminal haem, ligated by His 55 and His 71 and a high potential

haem ligated by His 201 and Met 275. The simplest model describing activation of the enzyme would be one in which His 71 (85 in *P.denitrificans* CCP) has dissociated from the N-terminal peroxidatic haem but remains close by as a distal catalytic ligand. As explained in Chapter I, section 1.3.1, the distal histidine in eukaryotic peroxidases promotes heterolytic cleavage of the O-O bond of hydrogen peroxide (Finzel et al.1984; Poulos et al.1993). However, as there are none of the likely catalytic residues near the proposed peroxidatic haem that one would expect by analogy with eukaryotic active sites a major conformational change may take place during formation of the active mixed-valence enzyme.

The bacterial cytochrome c peroxidase sequences show remarkable conservation in the region between residues 255-276 (*P.denitrificans* CCP numbering) (Figure 7.4) which in itself suggests a key functional role. Indeed one possibility is that the region which contains Arg 265, His 275 and Phe 274 (*Paracoccus* numbering) moves to form the distal side of a restructured peroxidatic site. Arg 265 may be the counterpart of the arginine which stabilises the developing charge on the 1O of the hydrogen peroxide in YCCP. Phe 274 may be the counterpart of the aromatic residue invariably adjacent to the distal histidine throughout the peroxidase family. It has been proposed that this aromatic residue acts as a barrier that restricts substrate access to the ferryl oxene intermediate and thus preventing ferryl oxygen transfer to the substrate in favour of oxidation of the substrate (Newmyer and Ortiz de Montellano, 1995).

Although proposed catalytic region is not α–helical in the X-ray structure of the oxidised form of *P.aeruginosa* CCP it is predicted to be α–helical (as in the analogous region in *P.denitrificans* CCP) (see Figure 7.7) and might adopt that conformation in the mixed-valence form. In response to the criticism that such major conformational changes would likely to be slow, it must be realised that the oxidised form that has been crystallised is almost certainly not part of the catalytic cycle and represents a dead-end conformation into which the protein relaxes, to protect the catalytic site in the absence of reductant. A possible weakness of this model is that it suggests no role for the conserved N-terminal methionine (129, *Paracoccus*

Figure 7.7 Putative active site region of bacterial cytochrome c peroxidases

The region containing His 275 from *P.denitrificans* CCP (van Beeumen and Pettigrew-unpublished results) is compared to the corresponding sequence in *P.aeruginosa* CCP (Ridout et al.1995) with conserved residues in bold. We have used a suite of eight secondary structure prediction programmes (PREDICT, E.Eliopoulos, Leeds University UK). One of the eight methods in PREDICT is that of Chou and Fasman (1974) and this coped well with predicting the secondary structures of a known Class I structure, tuna cytochrome c. Using the Chou and Fasman (1974) algorithm on the *P.denitrificans* CCP sequence an α-helix was predicted in the conserved region and is represented by α.

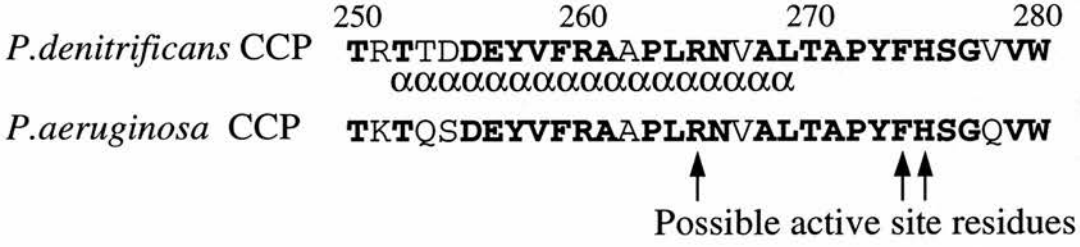
250
260
270
280
P.denitrificans CCP
TRTTDDEYVFRAAPLRNVALTAPYFHSGVVW
αααααααααααααααααα
P.aeruginosa CCP
TKTQSDEYVFRAAPLRNVALTAPYFHSGQVW
Possible active site residues

numbering) in the enzyme.

A more complicated model which incorporates a role for both methionines but also fits the available evidence is the 'haem switch' model. Although the simplest model incorporates electron entry at the N-terminal haem, followed by eventual transfer to the peroxidatic C-terminal haem, another possibility is that the initial entry of the electron is via the C-terminal haem. The structure of the *P.aeruginosa* CCP in the oxidised form, shows the conserved methionine 115 (129 in the *P.denitrificans* CCP) to be located on the distal side of the N-terminal haem at the end of α-helix 4 (Figure 7.2). This appears to be in an analogous position to the ligated methionine (275) in the C -terminal domain (Figures 7.2, 7.3). In the 'haem switch' model, reduction of the C-terminal haem would initiate a switch in haem properties so that internal electron transfer accompanied the movement of His 261 (275 in the *P.denitrificans* CCP) and other active site residues to form the distal side of the C-terminal haem, which would become the peroxidatic centre. In such a model the N-terminal haem would be ligated by the conserved Met 115 (129 in the *P.denitrificans* CCP) and would act as the storage point for the electron rather than a through route.

Because of the likelihood of substantial conformational change accompanying reduction of the enzyme, we will only have a reliable picture of the active site and the electron transfer routes when the crystallographic structure of the mixed-valence enzyme has been solved.

7.5 Nature and extent of modification of *P.denitrificans* CCP by DEPC

With 4μM protein and 20μM diethylpyrocarbonate the results of both spectrophotometric and radioactive labelling measurements are consistent with the modification of one mol histidine per mol protein. This correspondence between the two types of measurement also holds good over short time periods of modification when no development of the trough between 265 and 300 nm has yet occurred. Although the features of the trough between 265 and 300nm resemble that expected for O-ethoxyformylation of tyrosine (Burstein et al.1974), the extent of the absorbance change would imply a modification of at least one mol tyrosine per mol protein

(ε_{278nm} = 1.3 mM^{-1} cm^{-1}) and this is certainly not supported by measurement of radiolabelling. We therefore conclude that this spectral feature may not be associated with tyrosine modification. The feature is also present in the spectra of modified yeast CCP and similar features have been observed in other proteins modified with DEPC (Burstein et al.1974; Bhattacharyya et al.1992).

7.6 Modification of a single essential histidine

The good agreement between the proportional loss of activity and the modification of 1 mol of histidine indicates that a single histidine is being modified (rather than, for example, two residues each at a level of 50%). This is supported by the fact that one histidine is particularly susceptible to modification. Beyond 20 min of reaction, the slow loss of the ethoxyformyl groups from histidine exceeds any further modification by residual reagent. This loss of the ethoxyformyl group is associated with proportional recovery of the ability to form the active state of the enzyme. The broad trough between 265 and 300 nm persists and therefore, whatever its origin, it cannot be associated with activity changes.

In yeast CCP, one mol histidine is also readily modifiable at low concentrations of DEPC but in this case modification was not associated with loss of activity. This is consistent with the results of Bosshard et al. (1984) who found that three histidines could be modified with no loss of activity. Similarly in horseradish peroxidase two histidines were modified by DEPC but it is the more slowly modified that is essential (Bhattacharyya et al.1992). In the inactive oxidised state of the bacterial enzyme, the histidine is located near the surface of the molecule, at the domain interface and therefore is likely to be accessible to the reagent. However if the model presented above of a major conformation change occurring upon reduction of the high potential haem is correct, the histidine may reposition to the distal side of the peroxidatic haem and like its eukaryotic counterparts, be relatively inaccessible to modification.

7.7 The identification of the essential histidine as His 275

It was assumed that the two histidines which remain unmodified at high [DEPC] are the conserved proximal ligands to the two haem groups, thus leaving His 85 and His 275 as the only remaining conserved histidines. Therefore one or the other (or both) histidines was likely to be essential for activity. We were able to exploit a single bond cleavage by subtilisin in the native state, which released a C-terminal fragment containing the conserved His 275 and one other non-conserved histidine and an N-terminal fragment containing the conserved His 85 and one other non-conserved His. The nature of this cleavage site will be discussed later in this Chapter in relation to the structure of the *P.aeruginosa* CCP.

The great majority of the radioactivity due to ethoxyformylation was found to be associated with the C-terminal fragment (R251-M338), indicating that this fragment contained the modified histidine. Purification of the C-terminal fragment by molecular exclusion chromatography followed by tryptic digestion and peptide separation by reverse phase HPLC, allowed localisation of radioactive labelling in the tryptic peptide containing His 275 within 4h of modification.

In the course of this study quite variable ratios of radiolabel found in the peptide (R251-M338) to that in peptide (pE1-T250) were obtained. When labelled protein was left for 24h before subtilisin cleavage little radioactivity was lost from the protein despite the observed loss of ethoxyformylhistidine and the great majority of label was found in the peptide (pE1-T250) This retention of label on the protein no longer blocked enzyme activity.

There is no known precedent for such an intramolecular transfer of an ethoxyformyl group but we propose that it is consistent with attack on the ethoxyformylhistidine 275 by a lysine that is adjacent in the folded protein but resides in the N-terminal (pE1-T250) sequence. Ethoxyformyllysine is not susceptible to nucleophilic attack (Melchior and Fahrney, 1970). The conserved lysine 89 (75 in *P.aeruginosa* CCP) is a prime candidate for this role, as in the *P.aeruginosa* CCP structure it is situated at the opposite side of the domain interface from His 275 (261 in *P.aeruginosa* CCP) (Figure 7.1 and 7.2). However, without the protein coordinates the probability of this nucleophilic attack cannot be fully assessed. The proposal will

be tested by identification of the labelled residue in the peptide (pE1-T250).

7.8 The role of the essential histidine 275 in *P.denitrificans* CCP

This thesis has shown His 275 to be essential for activity. Consistent with this is its position in a highly conserved region in the cytochrome c peroxidase molecule (Figure 7.3 and 7.4). In the recent X-ray structure of the oxidised CCP from *P.aeruginosa* (Fulop et al.1995), His 261, the counterpart to His 275, is placed at the interface between the N and C-terminal domains (Figures 7.1 and 7.2). Figure 7.8, which is a copy of Figure 7(b) from Fulop et al. (1995) shows the histidine as part of a hydrogen bond network involving the haem propionates from both haems (Fulop et al.1995). Our finding that His 275 is the most modifiable histidine in the oxidised state would not have been consistent with the original role as haem ligand proposed by Ellfolk et al. (1991) but it is compatible with the position determined by crystallography. Fulop et al. (1995) propose that this histidine may form part of an electron transfer route between the two haem groups. Our finding that its modification abolishes activity would be consistent with disruption of this electron transfer route. However, Fulop et al. realise that proposals concerning the mixed-valence active enzyme based on the oxidised form must be regarded with scepticism.

The mechanism of the bacterial cytochrome c peroxidases might be expected to incorporate the features of a key distal histidine at the peroxidatic domain by analogy with the eukaryotic peroxidases (see Introduction Chapter I, section 1.3.1). Models proposed earlier in this Chapter suggest that major conformational changes may take place during formation of the active mixed-valence enzyme, to introduce His 275 (His 261 in *P.aeruginosa* CCP) and other catalytic residues to the distal side of a restructured peroxidatic site. Consistent with the identification of His 275 (*P.denitrificans* CCP numbering) as the distal catalytic histidine in bacterial peroxidases is the presence of a conserved Phe 274 adjacent to the histidine (see Figures 7.4 and 7.7) which is found in all crystal structures and sequence alignments from the peroxidase family.

Figure 7.8 Location of Histidine 261 at domain interface of CCP from *P.aeruginosa*

This figure is a copy of Figure 7(b) from Fulop et al. (1995). The N-terminal haem is shown at the top and C-terminal haem at bottom of page. The position of Histidine 261, the calcium ion and other side chains proposed by Fulop et al. (1995) to be involved in electron transfer between the two haems. One of the propionates of the C-terminal haem is hydrogen bonded to two bound water molecules.

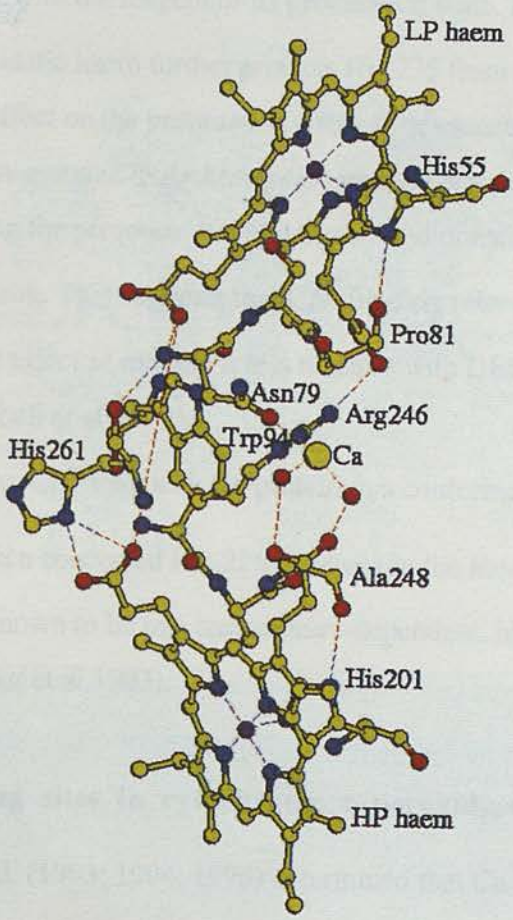
LP haem
His55
Pro81
Asn79
Arg246
Trp94
His261
Ca
Ala248
His201
HP haem

7.9 The susceptibility of His 275 to modification in different redox states

We had predicted, based on the model of Ellfolk et al. (1991) for the coordination structure of the enzyme, that His 275 would only become modifiable when it was released from haem coordination in the active mixed-valence form. In fact, His 275 is much more susceptible to modification in the oxidised form and this is now explicable in terms of the crystallographic structure which shows that it is not an iron ligand (Fulop et al.1995). The much lower susceptibility to modification in the mixed-valence states may be due to a changed environment of His 275 which affects either its accessibility to the reagent or its protonation state. The presence of CN^- bound at the peroxidatic haem further protects His 275 from modification. Again this may be due to an effect on the protonation state of the essential histidine. Such an effect has been demonstrated in *Arthromyces ramosus* peroxidase (Fukuyama et al.1995) by showing the presence of a hydrogen bond donated by the distal His 56 to CN^- bound to the iron. This suggests that CN^- binding raises the pK of the histidine and would have the effect of making it less reactive with DEPC (Holbrook and Ingram, 1973; Tudball et al.1972).

Alternatively, CN^- may lock the protein in a conformation corresponding to the active state and with a concealed His 275, whereas in the absence of CN^-, the mixed-valence protein is known to be in a temperature-dependent, high spin-low spin equilibrium (Gilmour et al.1993).

7.10 Ca^{2+} binding sites in cytochrome c peroxidase

Gilmour et al. (1993; 1994; 1995) determined that Ca^{2+} is required for the switch to the active high-spin state at the peroxidatic haem of *P.denitrificans* CCP and proposed that this Ca^{2+} is located at the dimer interface, at Ca^{2+} binding site II. The enzyme is proposed to be in a dimer-monomer equilibrium with the dimer as the active form. The crystal structure of cytochrome c peroxidase from *P.aeruginosa* revealed

the presence of a Ca^{2+} ion, located in the interface between the N and C-terminal domains (Figure 7.2) (Fulop et al.1995). As each monomer contains this Ca^{2+}, this may correspond to Ca^{2+} binding site I in the *P.denitrificans* CCP. Modification of the essential histidine 275 (*P.denitrificans* CCP numbering) has no effect on this site.

A Ca^{2+} binding motif has been identified in certain bacterial proteins which contains the consensus sequence GGXGXDXq where q is hydrophobic. In alkaline protease, for example (Baumann et al.1993), this sequence is situated at the end of a β-strand in a β-loop region and contributes one half of the coordination for a Ca^{2+}, the other half being provided by a second sequence of this type on a neighbouring β-loop region. Multiple Ca^{2+} binding sites are formed by stacks of these arrangements and the overall structure is described as a β-roll. In the bacterial peroxidases a reasonable match is found between residues 72-79 (*P.denitrificans* CCP numbering). Since there are no further sequences of this type detectable in the cytochrome c peroxidases, it is possible that Ca^{2+} is held at the interface of a dimer with each monomer contributing to the coordination.

Fascinatingly, in the recent structure from *P.aeruginosa* CCP, Fulop et al. (1995) determine that the protein molecules form dimers in solution and in the crystal (see Figure 7.9 which is a reprint of Figure 4(b) from Fulop et al.(1995)). Although Ca^{2+} is not reported at the dimer interface, residues 39-66 (*P.aeruginosa* CCP numbering) are determined to be involved in the subunit interactions. The putative half a Ca^{2+} binding motif in *P.aeruginosa* CCP spans residues 58-65 and forms a loop or reverse turn immediately following the N-terminal haem binding site. Without the protein coordinates it is difficult to assess but, from Figure 7.9, it is possible that both halves of the sequence motif from each monomer interact, to form a full Ca^{2+} coordination sphere. The reason for Ca^{2+} not being reported in this location by Fulop et al. (1995) could either be because the ion is present but not easily defined or that in

Figure 7.9 Structure of the dimer of CCP from *P.aeruginosa*
This figure is a scan of Figure 4(b) from Fulop et al. (1995) and shows the crystallographic dimer, looking down the twofold axis. The two haem porphyrin rings can be located by shading.

the *P.aeruginosa* CCP, as opposed to the *P.denitrificans* enzyme, the dimer is stabilised by forces other than Ca^{2+}.

If Ca^{2+} is present at the dimer interface in *P.denitrificans* CCP, the model presented in this thesis of modification of the essential histidine 275 disrupting Ca^{2+} binding to site II is interpretable. This model is consistent with the 'half-of-sites effect' for modification of an essential histidine. Under conditions where the dimer is the dominant species (such as high salt concentration), modification of only 0.5 mol histidine results in complete inactivation of the enzyme. This is in contrast to the monomeric enzyme in which complete inactivation requires modification of 1 mol histidine. Thus the molecules of the dimer show strong cooperativity, a feature already found for the binding of Ca^{2+} to site II (Gilmour et al.1995).

There is a certain similarity between the above model and the Ca^{2+} bound to lignin peroxidase (Poulos et al.1993). In this enzyme, serine 177 contributes its carbonyl and hydroxyl to the coordination of a Ca^{2+} and lies adjacent to the proximal haem ligand His 176. The remainder of the Ca^{2+} coordination sphere is formed by a type I reverse turn from Asp 194 to Ile 199. The role of the Ca^{2+} in the lignin peroxidase remains somewhat uncertain. The histidinate character of the proximal ligand is believed to be of importance in peroxidases in regulating the spin-state of the Fe and stabilising the the Fe III and Fe IV states. The positive charge of this nearby Ca^{2+} may act to favour the deprotonation of the histidine and therefore stabilise the anionic state. Ca^{2+} is also found in myeloperoxidase (Zeng and Fenna, 1992) and in horse radish peroxidase (Shiro et al.1986) but not in yeast cytochrome c peroxidase. However Miller et al. (1994) have mutated Trp 191 of YCCP to a smaller side chain (Gly) and found that they had created a cation binding site. The authors suggest that this site provides a shell of negative potential in the native protein to stabilise the Trp radical that forms compound I. Thus the same negatively charged site may have been adapted during evolution either to bind a cation or to stabilise a side chain radical.

7.11 Subtilisin cleavage of cytochrome c peroxidase

The crystal structure of *P.aeruginosa* CCP, made interpretable both the susceptibility to subtilisin cleavage in *P.denitrificans* CCP and the tight association of the resulting two peptides. Residues 223-228 in the *P.aeruginosa* CCP structure are disordered and were not include in the final model (Figure 7.2). This indicates the floppy and exposed nature of this surface loop and consequently the region is the target for proteolytic cleavage by *Pseudomonas* elastase, although the molecules are intact in the crystal. Residues 223-228 from *Pseudomonas* are in the analogous region to the stretch in the *P.denitrificans* enzyme that is the site for subtilisin cleavage. The enzyme cleaves between Threonine 250 and Arginine 251 in the *Paracoccus* CCP and this reflects a similar susceptibility to proteolytic cleavage.

The tight association of the two peptides resulting from subtilisin cleavage of the *P.denitrificans* enzyme is also evident from the structure of the *Pseudomonas* enzyme. Figure 7.2 shows the C-terminal tail extend into the N-terminal domain. Denaturation of the whole protein is required to release the C-terminal tail and thus the non-haem fragment.

Presumably upon reduction of the C-terminal haem, the cleaved protein cannot undergo the conformational change necessary for the formation of active enzyme. Pilot e.p.r. studies of the renatured di-haem peptide show the sole presence of the g_{max} 3.0 signal. This is consistent with the N-terminal domain containing the His-His ligated haem which is confirmed by the structure from the homologous CCP from *Pseudomonas*.

7.12 Conclusion

Cytochrome c peroxidase from *Paracoccus denitrificans* was modified with the histidine-specific reagent diethylpyrocarbonate. The reaction can be followed spectroscopically and, at low excess of reagent, one mol of histidine was modified in the oxidised enzyme. The agreement between the spectrophotometric measurement of histidine modification and radioactive incorporation using a radiolabelled reagent indicated little modification of other amino acids. Modification of this easily modifiable histidine was associated with loss of the enzyme's ability to form the active state. With

time, the modification reversed and the ability to form the active mixed-valence state was recovered. However the reversal of histidine modification observed spectrophotometrically was not matched by loss of radioactivity and a slow transfer of the ethoxyformyl group to a nearby lysine is proposed. The presence of CN^- bound to the active peroxidatic site of the enzyme completely protected the essential histidine from modification.

In its active form cytochrome c peroxidase is a dimer, with Ca^{2+} situated at the interface between the two monomers. Under conditions where the dimer is the dominant species modification of only 0.5 mol histidine abolishes enzyme activity.

Limited subtilisin treatment of the native enzyme resulted in cleavage at a single peptide bond. Although the two fragments remain tightly associated, the cleaved enzyme is inactive. Modification with radiolabelled diethylpyrocarbonate and subsequent subtilisin treatment, followed by tryptic digestion of a 9k fragment, showed that radioactivity was located in a peptide containing a single histidine 275.

With the benefit of homologous sequences we can determine that histidine 275 is fully conserved and is preceded by a remarkably unvaried region suggestive of functional importance. The recently determined X-ray structure of the oxidised state of CCP from *Pseudomonas aeruginosa* showed the conserved histidine to be at the interface of the N and C-terminal domain, near to the distal side of both haems. It is proposed that upon formation of the active mixed-valence enzyme a conformational change positions His 275 (*P.denitrificans* CCP numbering) to act as both a catalytic active site residue and a conduit for intramolecular electron transfer.

Bibliography

Aasa, R., Ellfolk, N., Ronnberg, M. and Vanngard, T. (1981) Electron paramagnetic resonance studies of Pseudomonas cytochrome c peroxidase. *Biochim.Biophys.Acta* 670: 170-175.

Almassy, R.J. and Dickerson, R.E. (1978) Pseudomonas cytochrome c551 at 2.0 A resolution: enlargement of the cytochrome c family. *Proc.Natl.Acad.Sci.U.S.A.* 75: 2674-2678.

Altschul, S.F., Gish, W., Miller, W., Myers, E.W. and Lipman, D.J. (1990) Basic local alignment search tool. *J.Mol.Biol.* 215: 403-410.

Arciero, D.M. and Hooper, A.B. (1994) A di-heme cytochrome c peroxidase from Nitrosomonas europaea catalytically active in both the oxidized and half-reduced states. *J.Biol.Chem.* 269: 11878-11886.

Avaeva, S.M. and Krasnova, V.I. (1975) . *Biorg.Khim.* 1: 1600.

Bates, R.G (1954) *Electrometric pH determination*,.Wiley, New York:pp208.

Baumann, U., Wu, S., Flaherty, K.M. and McKay, D.B (1993) Three dimensional structure of the alkaline protease of Pseudomonas aeruginosa - a two domain protein with a Ca2+ binding B-roll motif. *EMBO J.* 12: 3357-3364.

Berger, S.L. (1975) Diethyl pyrocarbonate: an examination of its properties in buffered solutions with a new assay technique. *Analytical Biochemistry* 67: 428-437.

Bhattacharyya, D.K., Bandyopadhyay, U. and Banerjee, R.K. (1992) Chemical and kinetic evidence for an essential histidine in horseradish peroxidase for iodide oxidation. *J.Biol.Chem.* 267: 9800-9804.

Blanke, S.R. and Hager, L.P. (1990) Chemical modification of chloroperoxidase with diethylpyrocarbonate. Evidence for the presence of an essential histidine residue. *J.Biol.Chem.* 265: 12454-12461.

Bosshard, H.R., Banziger, J., Hasler, T. and Poulos, T.L. (1984) The cytochrome c peroxidase-cytochrome c electron transfer complex. The role of histidine residues. *J.Biol.Chem.* 259: 5683-5690.

Bosshard, H.R., Anni, M. and Yonetani, T. (1991) *Peroxidases in Chemistry and Biology, Volume II*,.CRC Press, Boca Raton:pp51-84.

Burstein, Y., Walsh, K.A. and Neurath, H. (1974) Evidence of an essential histidine residue in thermolysin. *Biochemistry* 13: 205-210.

Chistoserdov, A.Y., Chistoserdova, L.V., McIntire, W.S. and Lidstrom, M.E. (1994a) Genetic organization of the mau gene cluster in Methylobacterium extorquens AM1: complete nucleotide sequence and generation and characteristics of mau mutants. *Journal of Bacteriology* 176: 4052-4065.

Chistoserdov, A.Y., McIntire, W.S., Mathews, F.S. and Lidstrom, M.E. (1994b) Organization of the methylamine utilization (mau) genes in Methylophilus methylotrophus W3A1-NS. *Journal of Bacteriology* 176: 4073-4080.

Chou, P.Y. and Fasman, G.D. (1974) Prediction of protein conformation. *Biochemistry* 13: 222-245.

Coulson, A.F., Erman, J.E. and Yonetani, T. (1971) Studies on cytochrome c peroxidase. XVII. Stoichiometry and mechanism of the reaction of compound ES with donors. *J.Biol.Chem.* 246: 917-924.

Ellfolk, N., Ronnberg, M., Aasa, R., Andreasson, L.E. and Vanngard, T. (1983) Properties and function of the two hemes in Pseudomonas cytochrome c peroxidase. *Biochim.Biophys.Acta* 743: 23-30.

Ellfolk, N., Ronnberg, M., Aasa, R., Andreasson, L.E. and Vanngard, T. (1984) Anion binding to resting and half-reduced Pseudomonas cytochrome c peroxidase. *Biochim.Biophys.Acta* 784: 62-67.

Ellfolk, N., Ronnberg, M. and Osterlund, K. (1991) Structural and functional features of Pseudomonas cytochrome c peroxidase. *Biochim.Biophys.Acta* 1080: 68-77.

Ellfolk, N., Ronnberg, M. and Soininen, R. (1973) Pseudomonas cytochrome c peroxidase. VII. Kinetics of the peroxidatic reaction mechanism. *Acta Chem.Scand.* 27: 2171-2178.

Ellfolk, N. and Soininen, R. (1970) Pseudomonas cytochrome c peroxidase. I. Purification procedure. *Acta Chem.Scand.* 24: 2126-2136.

Endo, S., Nagayama, K. and Wada, A. (1985) Comparison of protease susceptibility and thermal stability of cytochromes c. *J.Biomol Structure & Dynamics* 3: 409-421.

Erman, J.E., Vitello, L.B., Mauro, J.M. and Kraut, J. (1989) Detection of an oxyferryl porphyrin pi-cation-radical intermediate in the reaction between hydrogen peroxide and a mutant yeast cytochrome c peroxidase. Evidence for tryptophan-191 involvement in the radical site of compound I. *Biochemistry* 28: 7992-7995.

Erman, J.E., Vitello, L.B., Miller, M.A., Shaw, A., Brown, K.A. and Kraut, J. (1993) Histidine 52 is a critical residue for rapid formation of cytochrome c peroxidase compound I. *Biochemistry* 32: 9798-9806.

Falk, J.E. (1964) *Porphyrins and Metalloporphyrins*,.Elsevier, Amsterdam:pp240.

Finzel, B.C., Poulos, T.L. and Kraut, J. (1984) Crystal structure of yeast cytochrome c peroxidase refined at 1.7-A resolution. *J.Biol.Chem.* 259: 13027-13036.

Fishel, L.A., Farnum, M.F., Mauro, J.M., Miller, M.A., Kraut, J., Liu, Y.J., Tan, X.L. and Scholes, C.P. (1991) Compound I radical in site-directed mutants of cytochrome c peroxidase as probed by electron paramagnetic resonance and electron-nuclear double resonance. *Biochemistry* 19;30: 1986-1996.

Foote, N., Peterson, J., Gadsby, P.M., Greenwood, C. and Thomson, A.J. (1985) Redox-linked spin-state changes in the di-haem cytochrome c-551 peroxidase from Pseudomonas aeruginosa. *Biochem.J.* 230: 227-237.

Foote, N., Peterson, J., Gadsby, P.M.A.., Greenwood, C. and Thomson, A.J. (1984) A study of the oxidized form of *Pseudomonas aeruginosa* cytochrome c-551 peroxidase with the use of magnetic circular dichroism. *Biochem.J.* 223: 369-378.

Fukuyama, K., Kunishima, N., Amada, F., Kubota, T. and Matsubara, H. (1995) Crystal structures of Cyanide- and Triiodide-bound forms of Arthromyces ramosus Peroxidase at Different pH values. *J.Biol.Chem.* 270: 21884-21892.

Fulop, V., Ridout, C.J., Greenwood, C. and Hajdu, J. (1995) Crystal structure of the di-haem cytochrome c peroxidase from Pseudomonas aeruginosa. *Structure* 3: 1225-1233.

Gilmour, R., Goodhew, C.F., Pettigrew, G.W., Prazeres, S., Moura, I. and Moura, J.J. (1993) Spectroscopic characterization of cytochrome c peroxidase from Paracoccus denitrificans. *Biochem.J.* 294: 745-752.

Gilmour, R., Goodhew, C.F., Pettigrew, G.W., Prazeres, S., Moura, J.J. and Moura, I. (1994) The kinetics of the oxidation of cytochrome c by Paracoccus cytochrome c peroxidase. *Biochem.J.* 300: 907-914.

Gilmour, R., Prazeres, S., McGinnity, D.F., Goodhew, C.F., Moura, J.J.G., Moura, I. and Pettigrew, G.W. (1995) The binding of Ca^{++} to cytochrome c peroxidase from *Paracoccus denitrificans* - affinity and specificity of sites. *Eur.J.Biochem.* (In Press)

Goodhew, C.F., Brown, K.R and Pettigrew, G.W. (1986) Haem staining in gels. a useful tool in the study of bacterial c-type cytochromes. *Biochim.Biophys.Acta* 852: 288-294.

Goodhew, C.F., Wilson, I.B., Hunter, D.J. and Pettigrew, G.W. (1990) The cellular location and specificity of bacterial cytochrome c peroxidases. *Biochem.J.* 271: 707-712.

Greenwood, C., Foote, N., Peterson, J. and Thomson, A.J. (1984) The nature of species prepared by photolysis of half-reduced, fully reduced and fully reduced carbonmonoxy-cytochrome c-551 peroxidase from Pseudomonas aeruginosa. *Biochem.J.* 223: 379-391.

Halliwell, B. and Gutteridge, J.M.C. (1989) *Free radicals in biology and medicine*,.Oxford Science publications,

Hantgan, R.R. and Taniuchi, H. (1977) Formation of a biologically active ordered complex from two overlapping fragments of cytochrome c. *J.Biol.Chem.* 252: 1367-1374.

Haschke, R.H. and Friedhoff, J.M. (1978) Calcium-related properties of horseradish peroxidase. *Biochem.Biophys.Res.Commun.* 80: 1039-1042.

Hegyi, G., Premecz, G., Sain, B. and Muhlrad, A. (1974) Selective carbethoxylation of the histidine residues of actin by diethylpyrocarbonate. *Eur.J.Biochem.* 44: 7-12.

Henrissat, B., Saloheimo, M., Lavaitte, S. and Knowles, J.K. (1990) Structural homology among the peroxidase enzyme family revealed by hydrophobic cluster analysis. *Proteins* 8: 251-257.

Holbrook, J.J. and Ingram, V.A. (1973) Ionic properties of an essential histidine residue in pig heart lactate dehydrogenase. *Biochem.J.* 131: 729-738.

Iobbi-Nivol, C., Crooke, H., Griffiths, L., Grove, J., Hussain, H., Pommier, J., Mejean, V. and Cole, J.A. (1994) A reassessment of the range of c-type cytochromes synthesized by Escherichia coli K-12. *FEMS Microbiology Letters* 119: 89-94.

Kolthoff, I.M and Auerbach, C. (1952) .Studies on the System Iron-Ethylenediamine Tetraacetate. *J.Am.Chem.Soc.* 74: 1452-1456.

Laemmli, U.K. (1970) Cleavage of structural proteins during the assembly of the head of bacteriophage T4. *Nature* 227: 680-685.

Lenhoff, H.N. and Kaplan, N.O (1956). A cytochrome c peroxidase from Pseudomonas fluorescens *J.Biol.Chem.* 220: 967-982.

Mann, M. and Wilm, M. (1995) Electrospray mass spectrometry for protein characterization. *Trends Biochem.Sci.* 20: 219-224.

Mauro, J.M., Fishel, L.A., Hazzard, J.T., Meyer, T.E., Tollin, G., Cusanovich, M.A. and Kraut, J. (1988) Tryptophan-191----phenylalanine, a proximal-side mutation in yeast cytochrome c peroxidase that strongly affects the kinetics of ferrocytochrome c oxidation. *Biochemistry* 27: 6243-6256.

Melchior, W.B.,Jr. and Fahrney, D. (1970) Ethoxyformylation of proteins. Reaction of ethoxyformic anhydride with alpha-chymotrypsin, pepsin, and pancreatic ribonuclease at pH 4. *Biochemistry* 9: 251-258.

Miles, E.W. (1972) Modification of histidyl residues in proteins by diethylpyrocarbonate. *Meth.Enzymol.* 25: 44-55.

Miller, M.A., Han, G.W. and Kraut, J. (1994) A cation binding motif stabilizes the compound I radical of cytochrome c peroxidase. *Proc.Natl.Acad.Sci.U.S.A.* 91: 11118-11122.

Moore, G.R. and Pettigrew, G.W. (1990) *Cytochromes c - Evolutionary, Structural and Physiochemical Aspects*,.Springer-Verlag, Berlin:

More, C., Gayda, J.P. and Betrand, P. (1990) . *J.Mag.Res.* 90: 486-499.

Morihara, K., Tsuzuki, H., Oka, T., Inoue, H. and Ebata, M. (1965).Pseudomonas aeruginosa: Isolation,crystallization and preliminary characterization *J.Biol.Chem.* 240: 3295-3304.

Morris, D.L. and McKinley-McKee, J.S. (1972) The histidines in liver alcohol dehydrogenase. Chemical modification with diethylpyrocarbonate. *Eur.J.Biochem.* 29: 515-520.

Morrisey, J.H. (1981).Silver stain for proteins in polyacrylamide gels. A modified procedure with enhanced uniform sensitivity *Analytical Biochemistry* 117: 307-310.

Newmyer, S.L. and Ortiz de Montellano, P.R. (1995) Horseradish peroxidase His-42 --> Ala, His-42 --> Val, and Phe-41 --> Ala mutants. Histidine catalysis and control of substrate access to the heme iron. *J.Biol.Chem.* 270: 19430-19438.

Nozaki, M., Mizushima, H., Horio, T. and Okunuki, K. (1958) Futher studies on proteinase digestion of bakers yeast cytochrome c. *J.Biochem.* 45: 815-823.

Ovadi, J. and Keleti, T. (1969) Effect of diethylpyrocarbonate on the conformation and enzymic activity of D-glyceraldehyde-3-phosphate dehydrogenase. *Acta Biochimica et Biophysica Academiae Scientiarum Hungaricae* 4: 365-378.

Patterson, W.R. and Poulos, T.L. (1995) Crystal structure of recombinant pea cytosolic ascorbate peroxidase. *Biochemistry* 34: 4331-4341.

Pettigrew, G.W. (1991) The cytocrome c peroxidase of Paracoccus denitrificans. *Biochim.Biophys.Acta* 1058: 25-27.

Pettigrew, G.W. and Brown, K.R. (1988) Free and membrane-bound forms of bacterial cytochrome c4. *Biochem.J.* 252: 427-435.

Pettigrew, G.W. and Moore, G.R. (1987) *Cytochromes c - Biological Aspects*,.Springer-Verlag, Berlin:

Pettigrew, G.W. and Seilman, S. (1982) Purification and properties of a cross-linked complex between cytochrome c and cytochrome c peroxidase. *Biochem.J.* 201: 9-18.

Poulos, T.L., Edwards, S.L., Wariishi, H. and Gold, M.H. (1993) Crystallographic refinement of lignin peroxidase at 2 A. *J.Biol.Chem.* 268: 4429-4440.

Poulos, T.L. and Kraut, J. (1980) A hypothetical model of the cytochrome c peroxidase . cytochrome c electron transfer complex. *J.Biol.Chem.* 255: 10322-10330.

Prazeres, S., Moura, I., Gilmour, R., Pettigrew, G.W., Ravi, N. and Huynh, B.H. (1994) Redox and spin-state control of the activity of a diheme cytochrome c peroxidase - spectroscopic studies. In: La Mar, G.N. (Ed)*Nuclear Magnetic resonance of paramagnetic macromolecules*, Kluwer Academic, London: pp 141-163.

Prazeres, S., Moura, I., Moura, J.J.G., Gilmour, R., Goodhew, C.F. and Pettigrew, G.W. (1993) Control of the spin state of the peroxidatic heme by calcium ions in cytochrome c peroxidase from Paracoccus denitrificans: a 1H-NMR study. *Mag.Res.in Chem.* 31: S68-S72.

Prazeres, S., Moura, J.J.G., Moura, I., Gilmour, R., Goodhew, C.F., Pettigrew, G.W., Ravi, N. and Huynh, B.H. (1995) Mossbauer characterisation of Paracoccus denitrificans cytochrome c peroxidase - further evidence for redox and calcium-binding induced heme-heme interaction. *J.Biol.Chem.* 270: 24264-24269.

Ridout, C.J., James, R. and Greenwood, C. (1995) Nucleotide sequence encoding the di-haem cytochrome c_{551} peroxidase from *Pseudomonas aeruginosa*. *FEBS Lett.* 365: 152-154.

Ronnberg, M. (1987) Specific cleavage of Pseudomonas cytochrome-c peroxidase by elastase from Pseudomonas aeruginosa. *Biochim.Biophys.Acta* 916: 112-118.

Ronnberg, M., Araiso, T., Ellfolk, N. and Dunford, H.B. (1981a) The catalytic mechanism of Pseudomonas cytochrome c peroxidase. *Arch.Biochem.Biophys.* 207: 197-204.

Ronnberg, M., Araiso, T., Ellfolk, N. and Dunford, H.B. (1981b) The reaction between reduced azurin and oxidized cytochrome c peroxidase from Pseudomonas aeruginosa. *J.Biol.Chem.* 256: 2471-2474.

Ronnberg, M., Kalkkinen, N. and Ellfolk, N. (1989) The primary structure of Pseudomonas cytochrome c peroxidase. *FEBS Lett.* 250: 175-178.

Rosen, C.G., Gejvall, T. and Andersson, L.O. (1970) Reaction of diethyl pyrocarbonate with indole derivatives with special reference to the reaction with tryptophan residues in a protein. *Biochim.Biophys.Acta* 221: 207-213.

Sanders, S.A., Bray, R.C. and Smith, A.T. (1994) pH-dependent properties of a mutant horseradish peroxidase isoenzyme C in which Arg38 has been replaced with lysine. *Eur.J.Biochem.* 224: 1029-1037.

Shiro, Y., Kurono, M. and Morishima, I. (1986) Presence of endogenous calcium ion and its functional and structural regulation in horseradish peroxidase. *J.Biol.Chem.* 261: 9382-9390.

Sivaraja, M., Goodin, D.B., Smith, M. and Hoffman, B.M. (1989) Identification by ENDOR of Trp191 as the free-radical site in cytochrome c peroxidase compound ES. *Science* 245: 738-740.

Smith, A.T., Santama, N., Dacey, S., Edwards, M., Bray, R.C., Thorneley, R.N. and Burke, J.F. (1990) Expression of a synthetic gene for horseradish peroxidase C in Escherichia coli and folding and activation of the recombinant enzyme with Ca2+ and heme. *J.Biol.Chem.* 265: 13335-13343.

Sofia, H.J., Burland, V., Daniels, D.L., Plunkett, G. and Blattner, F.R. (1994) Analysis of the Escherichia coli genome. V. DNA sequence of the region from 76.0 to 81.5 minutes. *Nucleic Acids Research* 22: 2576-2586.

Soininen, R. and Ellfolk, N. (1975) Pseudomonas cytochrome c peroxidase. X. The effect of Pseudomonas neutral proteinase on the enzyme molecule. *Acta Chemica Scandinavica - Series B - Organic Chemistry & Biochemistry* 29: 134-136.

Sone, N. and Yangita, Y. (1982).A cytochrome aa_3-type terminal oxidase of a thermophilic bacterium: purification, properties and proton pumping *Biochim.Biophys.Acta* 682: 216-226.

Sundaramoorthy, M., Kishi, K., Gold, M.H. and Poulos, T.L. (1994) The crystal structure of manganese peroxidase from Phanerochaete chrysosporium at 2.06-A resolution. *J.Biol.Chem.* 269: 32759-32767.

Takano, T., Trus, B.L., Mandel, N., Mandel, G., Kallai, O.B. and Swanson, R. (1977) Tuna cytochrome c at 2.0 A resolution. II. Ferrocytochrome structure analysis. *J.Biol.Chem.* 252: 776-785.

Tudball, N., Bailey-Wood, R. and Thomas, P. (1972) The role of histidine residues in glutamate dehydrogenase. *Biochem.J.* 129: 419-425.

van der Palen, C.J., Slotboom, D.J., Jongejan, L., Reijnders, W.N., Harms, N., Duine, J.A. and van Spanning, R.J. (1995) Mutational analysis of mau genes involved in methylamine metabolism in Paracoccus denitrificans. *Eur.J.Biochem.* 230: 860-871.

Vincent, J.P., Schweitz, H. and Lazdunski, M. (1975) Structure-function relationships and site of action of apamin, a neurotoxic polypeptide of bee venom with an action on the central nervous system. *Biochemistry* 14: 2521-2525.

Vitello, L.B., Erman, J.E., Miller, M.A., Wang, J. and Kraut, J. (1993) Effect of arginine-48 replacement on the reaction between cytochrome c peroxidase and hydrogen peroxide. *Biochemistry* 32: 9807-9818.

Welinder, K.G., Mauro, J.M. and Norskov-Lauritsen, L. (1992) Structure of plant and fungal peroxidases. [Review]. *Biochem.Soc.Trans.* 20: 337-340.

Wilson, G.S. (1978) .Determination of oxidation-reduction potentials *Meth.Enzymol.* LIV: 396-409.

Wood, P.M. (1983) Why do c-type cytochromes exist? *FEBS Lett.* 164: 223-226.

Yamanaka, T., Mizushima, H., Nozaki, M., Horio, T. and Okunuki, K. (1959) Studies on cytochrome c. *J.Biochem.* 46: 121-132.

Zeng, J. and Fenna, R.E. (1992) X-ray crystal structure of canine myeloperoxidase at 3 A resolution. *J.Mol.Biol.* 226: 185-207.